9-6-2011 12:00 AM

# Geotechnique, Physico-chemical Behaviour and a New Erosion Model for Mine Tailings under Environmental Loading

Rozalina S. Dimitrova, *University of Western Ontario*

Supervisor: Dr. Ernest K. Yanful, *The University of Western Ontario*
A thesis submitted in partial fulfillment of the requirements for the Doctor of Philosophy degree in Civil and Environmental Engineering

# GEOTECHNIQUE, PHYSICO-CHEMICAL BEHAVIOUR AND A NEW EROSION MODEL FOR MINE TAILINGS UNDER ENVIRONMENTAL LOADING

(Spine title: Geotechnique, Physico-chemical Behaviour and a New Erosion Model for Mine Tailings under Environmental Loading)

(Thesis format: Integrated-Article)

by

Rozalina S. Dimitrova

Graduate Program in Civil and Environmental Engineering

A thesis submitted in partial fulfilment
of the requirements for the degree of
Doctor of Philosophy

School of Graduate and Postdoctoral Studies
The University of Western Ontario
London, Ontario, Canada

THE UNIVERSITY OF WESTERN ONTARIO
SCHOOL OF GRADUATE AND POSTDOCTORAL STUDIES

# CERTIFICATE OF EXAMINATION

Supervisor

______________________________
Dr. Ernest K. Yanful

Supervisory Committee

______________________________

______________________________

Examiners

______________________________
Dr. Tim Newson

______________________________
Dr. Jon Southen

______________________________
Dr. Patricia Corcoran

______________________________
Dr. Mamadou Fall

The thesis by

**Rozalina S. Dimitrova**

entitled:

**Geotechnique, Physico-chemical Behaviour and a New Erosion Model for Mine Tailings under Environmental Loading**

is accepted in partial fulfillment of the
requirements for the degree of
Doctor of Philosophy

Date______________________________

______________________________
Chair of the Thesis Examination Board

# ABSTRACT

Comprehensive geotechnical characterisation of mine tailings is required for the design, construction and safe operation of mine waste management facilities against the large number of potential failure risks. It is important that the characterization is carried out under the stress range and drainage conditions relevant to those encountered in the field.

The present research utilized mine tailings samples from a copper/nickel base-metal mine. Kaolinite and bentonite clays were added to the mine tailings in order to study the effect of clay percentage and clay mineralogy on the behaviour of saturated tailings/clay systems with varying composition. Slurries with moderate or high concentration of solids were prepared in the laboratory by mixing distilled water with mine tailings or artificial tailings/clay soils. Beds with different composition, thickness and age were sedimented from these slurries and tested under a stress range below 1 kPa, and under different degrees of drainage ranging from undrained to fully drained. The primary consolidation of the pure tailings beds was complete in approximately one hour and negligible volume changes occurred in the beds during secondary compression. The effect of adding kaolinite or bentonite to the tailings was to increase the time for primary consolidation of the mixed beds, but the rate of increase was greater when bentonite was used. The undrained shear strength of the beds was measured using an automated fall cone device at a depth interval of 1 cm below bed surface. It was found that the undrained strength increased, whereas the water content and void ratio decreased with depth within the beds. The factor controlling the undrained strength of the beds was the vertical effective stress, with the water content also having some secondary effect.

A specially built Tilting Tank was used to measure the shear strength of the beds under drained and partially drained conditions that were simulated by varying the loading rate. Bed failure within the Tank always occurred at a plane parallel to the surface of the bed and at a depth of 0.4 to 2.5 cm. Linear drained and partially drained shear strength envelopes with zero cohesion intercept were defined, with the partially drained (total) friction angle always remaining lower than the drained (effective) friction angle. The latter varied from 35.2° for the tailings/bentonite mixtures to 40.4° for the pure tailings, depending on the percentage and mineralogy of the clay fraction. It was found that adding clay to the mine tailings generally caused a decrease in the frictional resistance of the mixtures, with the effect being more pronounced for the bentonite additive. Time for consolidation did not influence the shear strength of the tailings and tailings/kaolinite mixtures, but produced an increase of 2.1° in the frictional resistance of the tailings/bentonite mixtures.

A critical stress for erosion as a function of depth was estimated for each bed using existing formulations for cohesive and noncohesive sediments and mixtures of both. A linear correlation between the undrained shear strength and the critical stress for erosion, with parameters dependent on the composition of the mixtures was proposed.

**KEYWORDS:** *mine tailings, sedimentation behaviour, shear strength, friction angle, consolidation stress, slope failure, drainage conditions, excess pore water pressure, clay fraction, tailings/clay mixtures, critical shear stress for erosion.*

## CO-AUTHORSHIP

The research work described in this thesis was carried out by Rozalina S. Dimitrova under the supervision of Prof. Ernest K. Yanful. Prof. Yanful provided significant contribution to the design of the equipment used in the laboratory work, as well as to the data analysis and interpretation. He also reviewed the individual chapters of the thesis and is a co-author of all publications derived from the research. The authorships details are summarized below.

**CHAPTER 3**

Undrained strength of deposited mine tailings beds: effect of water content, effective stress and time of consolidation.

Rozalina S. Dimitrova and Ernest K. Yanful

Geotechnical and Geological Engineering, Vol.29(5): 935-951.

**CHAPTER 4**

Effect of drainage conditions, thickness and age on the shear strength of deposited mine tailings beds in the very low stress range.

Rozalina S. Dimitrova and Ernest K. Yanful

Accepted by Canadian Geotechnical Journal

Presented at the 63rd Canadian Geotechnical Conference & 6th Canadian Permafrost Conference, Calgary, Alberta, 12-16 Sept. 2010.

**CHAPTER 5**

Factors affecting the shear strength of mine tailings/clay mixtures with varying clay content and clay mineralogy.

Rozalina S. Dimitrova and Ernest K. Yanful

Submitted to Engineering Geology Journal

**CHAPTER 6**

Relationship between erosional and mechanical strength of mine tailings and mine tailings/clay mixtures.

Rozalina S. Dimitrova and Ernest K. Yanful

Submitted to Canadian Journal of Earth Sciences

## ACKNOWLEDGEMENTS

This research project could not have been possible without the financial support by the Natural Sciences and Engineering Research Council of Canada (NSERC) in the form of an Individual Discovery Grant awarded to E.K. Yanful and a postgraduate scholarship awarded to Rozalina Dimitrova.

There are many people who deserve my gratitude for providing contributions and support over the years of research work. First and foremost, I would like to thank my supervisor, Dr. Ernest K. Yanful, for his valuable input, time, ideas, advice and comments on the draft of the manuscript. The mentorship and support provided by Dr. Yanful was tremendous and it was nothing short of a privilege to work with him on my doctoral research.

The skills and technical competence of the laboratory technicians was essential to the understanding and operating the equipment and data acquisition software central to my research. Sincere thanks to Wilbert Logan and Melodie Richards for their assistance.

The cooperation and input of Rob Levesque and Clayton Cook from the University Machine Shop during the design and development of the testing equipment was most valuable and deserves to be acknowledged.

I would also like to offer thanks to my fellow students who helped me with my research in a number of ways. Particular thanks to A. Geremew, L. Kachhwal, R. Ofori, and A. Tariq.

Last, but certainly not least, I would like to thank my family, Emil my husband, and my daughter, Monica, for their patience, understanding, support and encouragement. Thanks and I love you!

# TABLE OF CONTENTS

# LIST OF TABLES

# LIST OF FIGURES

# LIST OF APPENDICES

# NOMENCLATURE

| | |
|---|---|
| $a$ | Coefficient in Eq. (6.8) |
| $b$ | Coefficient in Eq. (6.8) |
| $c$ | Suspension concentration (by volume) |
| $c'$ | Effective cohesion |
| $Cc$ | Coefficient of curvature (gradation) |
| $c_T$ | Total cohesion |
| $C_u$ | Coefficient of uniformity |
| $c_u$ | Undrained shear strength |
| $d$ | Depth of cone penetration |
| $D_{50}$ | Sieve diameter that 50% of particles by weight pass through |
| $e$ | Void ratio |
| $e_{max}$ | Maximum void ratio |
| $e_{sk}$ | Skeleton (intergranular) void ratio |
| $g$ | Acceleration of gravity |
| $Gs$ | Specific gravity of soil solids |
| $h$ | Depth below bed surface (measured along the vertical) |
| $H_b$ | Thickness of deposited bed |
| $H_i$ | Initial height of suspension |
| $I_P$ | Plasticity index |
| $K$ | Cone factor (empirical constant that varies with the cone angle) |
| $k$ | Hydraulic conductivity (permeability) |
| $m$ | Coefficient in Eq. (6.3) |
| $n$ | Coefficient in Eq. (6.3) |
| $R$ | Correlation factor in regression analysis |
| $R_{e*}$ | Dimensionless boundary Reynolds number |
| $t_p$ | Time denoting the end of primary consolidation |
| $u_*$ | Shear velocity of fluid |
| $u_e$ | Excess pore water pressure |
| $u_t$ | Terminal settlings velocity of particles in suspension |
| $u_{t\infty}$ | Terminal settlings velocity of particles in infinite medium |
| $W$ | Cone weight |
| $w$ | Water content |
| $w_L$ | Liquid limit |
| $w_P$ | Plastic limit |
| $z$ | Depth below bed surface (measured normal to the slope) |
| $z_f$ | Depth from bed surface to the failure plane (measured normal to the slope) |

| | |
|---|---|
| $z_w$ | Depth of water above the tailings bed (measured normal to the slope) |
| $\beta$ | Angle of tilting |
| $\gamma'$ | Average buoyant unit weight of soil |
| $\gamma_{sat}$ | Average saturated unit weight of soil |
| $\gamma_w$ | Unit weight of water |
| $\varepsilon$ | Porosity of suspension |
| $\nu$ | Kinematic viscosity of fluid |
| $\rho$ | Density of fluid |
| $\rho_b$ | Wet bulk density |
| $\rho_s$ | Density of sediment |
| $\sigma'_n$ | Effective normal stress |
| $\sigma_{nf}$ | Total normal stress at the failure plane at failure |
| $\sigma'_{nf}$ | Effective normal stress at the failure plane at failure |
| $\sigma'_p$ | Preconsolidation stress |
| $\sigma'_v$ | Vertical effective stress |
| $\sigma_{v0}$ | Initial vertical total stress |
| $\sigma'_{v0}$ | Initial vertical effective stress |
| $\tau$ | Shear stress |
| $\tau_*$ | Dimensionless bed shear stress |
| $\tau_{*c}$ | Critical dimensionless bed shear stress (threshold) for erosion, Shields criterion |
| $\tau_c$ | Critical bed shear stress (threshold) for erosion |
| $\tau_f$ | Shear strength |
| $\phi'$ | Effective friction angle |
| $\phi_T$ | Total friction angle |

# CHAPTER 1. INTRODUCTION

## 1.1. Background of the research

Mining and extractive processes place their primary emphasis on the extraction of mineral commodities from the parent ore. The original rock is crushed and ground in mills in order to release the valuable constituents (Jewell 1998). Water and chemical reagents are added during this process to facilitate the recovery of the product mineral from the ore. The finely ground mill or mineral separation process residue that remains after the extraction of mineral values is termed tailings (Bussière 2007). Considering that the metal volume is low compared to the extracted volume of ore, tailings are produced in staggering quantity all over the world (Vick 1990). In Canada, INCO Limited's Copper Cliff tailings storage area near Sudbury, Ontario covers an area of about 5,500 acres and is the largest impoundment of acid-generating tailings (Martin and Tissington 1996). The facility has been in use since the 1940s and upon filling to its projected design capacity it will provide tailings storage for an estimated 800 million tons of tailings. Since the 1980s, because of growing public and technical awareness of mining impacts, disposal of tailings has been identified as the single most important source of environmental concern for many mining projects (Martin and Davies 2000; Bussière 2007).

In order to understand the fundamental nature of the tailings, one should have a basic knowledge of how they are generated and disposed. The milling process produces very sharp angular particles, typically in the sand and silt sizes, while the colloidal particles (size less than 100 μm) are generally lost when the excess water and fines are removed from the tailings (Pettibone and Kealy 1971). The final gradation of the tailings depends on both the mineral extraction method as well as the clay content in the orginal ore. For instance, copper tailings often consist almost exclusively of silicate particles produced by grinding of the parent rock, whereas the grain size distribution in the Florida phosphate tailings reflects the extremely high clay content of the original ore rather than particle breakdown due to grinding (Vick 1990). According to their gradation and plasticity tailings are divided into the following general categories (Vick 1990). The first category, soft-rock tailings, are derived from shale ores and although they may contain some sand-size particles, their behaviour is controlled by their high clay content. The second category, hard-rock tailings, which includes the lead-zinc, copper, gold-silver, molybdenum, and nickel tailings from sulphide-bearing ores, are mostly composed of sand and are generally coarse and nonplastic. On the basis of their sand/fines ratio tailings can be categorized as fine or coarse, with the former characterized by having little or no sand, and the latter containing a sizable coarse sand fraction. In addition to the above categorisation, tailings are often divided on the basis of gradation into sands and slimes. Sands represent the fraction of the whole tailings material that is greater than 0.075 mm (sieve #200), whereas slimes correspond to the fraction less than 0.075 mm.

The tailings, along with the spent process water, form a low-density slurry which is thickened by a dewatering process to a consistency at which they can be pumped to the tailings storage facility (Bussière 2007). The slurry is then distributed by spigots onto the exposed tailings surface ("subaerial" discharge method), or injected under water ("subaqueous" discharge method) in man-made or natural water bodies (Jewell 1998; Davé et al. 2003). Given that many metals occur as sulphide-rich ores, the mine tailings from such orebodies have the potential for oxidation and subsequent acid generation in the presence of oxygen. Furthermore, parent ores are often composed of other minerals that contain potentially toxic elements, such as antimony, arsenic, lead, chromium, cobalt, selenium and cadmium (Bussière 2007). Some chemical reagents used in the metal extraction process are also toxic in sufficient concentrations, e.g., the cyanide used to recover gold. Low pH conditions in the pond water promote liberation of those toxic elements, and if a breach develops in the confining embankment, tailings and associated contaminants can flow for considerable distances (Jewell 1998). The impact of such dam failure on public safety and the environment or from seepage of contaminants can be disastrous.

Disposal of tailings under water cover offers the advantage of controlling the oxidation process (and acid generation), by limiting the availability of dissolved oxygen through its low solubility and diffusivity in water compared to those in air (Davé et al. 1997). Following discharge of tailings into the tailings pond, tailings particles settle from suspension under quiescent conditions to form a deposited bed, which consolidates under self-weight. Sedimentation of tailings from suspension in pond water is a process of vertical settling, which produces loose to medium dense tailings deposits (Mian and Yanful 2007). Because of the looser state of deposition, tailings beds are generally more compressible than are natural soils of corresponding types. Consequently, primary consolidation for tailings sands and nonplastic slimes occurs rapidly, whereas the secondary compression is usually small and relatively insignificant from a practical standpoint (Vick 1990). The *in situ* density of the mine tailings beds is controlled by the grain size and clay content of the tailings and increases with depth within the deposit (Bussière 2007). Thus, lower void ratios usually correspond to greater depths within a deposit. Conversely, highest void ratios are usually associated with near-surface materials shortly after deposition.

Although a water cover significantly reduces oxygen ingress into tailings, some oxidation may still occur under the influence of wind action (Yanful and Verma 1999). For instance, wind-induced turbulence increases oxygen flux from the air into water thus increasing dissolved oxygen concentration. Wind-induced wave and water currents in the pond can also erode and resuspend particles from the tailings bed into the water column and because oxygen concentration is higher in the water cover than in pore water, suspended tailings are more prone to oxidation than bed tailings (Yanful and Verma 1999; Catalan and Yanful 2002).

In order to minimize their disposal costs, mine operators often use the coarser fraction of the tailings (sands) for the construction of embankments, while the finer tailings (slimes) are deposited in lagoons or ponds behind retaining tailings dams (Castro 2003). The challenge to mining companies is to design, construct and operate tailings management facilities in such a way that they will remain safe and cause minimal impact on the environment. Whether utilized in the construction of embankments or stored in tailings ponds, the engineering behaviour of tailings is controlled by both the geotechnical parameters of the material itself, and by the nature of the deposit. The principles of soil mechanics are applicable when characterizing tailings and their geotechnical behaviour, provided due recognition is given to the unique physico-chemical properties of the material, the processes during formation and consolidation of the tailings deposit, and the relevant stress range and drainage conditions (Jewell 1998).

In comparison to natural soils, tailings exhibit higher shear strength owing primarily to their high degree of particle angularity. Most tailings are cohesionless and show a zero effective cohesion intercept and an effective friction angle greater than 30° (Bussière 2007). The shear strength of tailings is significantly influenced by the stress range over which it is measured (Vick 1990). Therefore, it is recommended that strength testing on tailings is performed at stress levels representative of that of the tailings deposit.

A distinctive difference between tailings dams and water-retaining dams is that construction of the former is an ongoing process (Martin and Davies 2000). Tailings embankments are incrementally increased in height to accommodate the growing volume of wastes generated by the processing of ore. Over time, a wide range of drainage conditions may exist within the embankment and operators are encouraged to continuously monitor the pore water pressure within the structure (Blight 1998; Castro 2003). In the zones of the dam built with tailings sands, drained conditions are common because the sands are substantially more pervious than the fine tailings. After the tailings stored behind the embankment reach a level close to its top, a new embankment is built. Placement of new material may lead to development of excess pore water pressure within the starter embankment and consequently, if the rate of loading is fast enough, drainage conditions may become undrained or partially drained. Thus, the drained, partially drained or undrained strength of the tailings would govern the stability of the dam (Castro 2003).

With essentially all current tailings storage facilities being of considerable size, proper characterization of tailings for engineering evaluation becomes increasingly important for their safe operation. The main geoenvironmental concerns related to the disposal of hard-rock tailings include the geotechnical stability of tailings impoundments and the contamination of surface and groundwater by the mine effluents that could adversely affect the nearby ecosystems (Bussière 2007). During the evaluation of tailings, due consideration should be given to the prevailing *in situ* stress and drainage conditions.

## 1.2. Objectives of the research

The aim of the research described in this thesis has been to evaluate the engineering properties of saturated mine tailings and mine tailings/clay systems under a range of drainage conditions and in the stress range relevant to that encountered in the tailings management facilities. The specific tasks to be performed within the scope of the study are summarized below:

- To study the sedimentation and consolidation behaviour of slurries with varying concentration of solids, prepared from tailings and tailings/clay mixtures and distilled water, and to evaluate the effect of slurry solids concentration on the structure of the resulting deposit.
- To investigate the variation of the undrained strength, water content and void ratio with depth within deposited beds with different final thicknesses, sedimented from the above slurries, and to propose a correlation between the undrained shear strength and the vertical effective stress.
- To determine if time for consolidation affects the shear strength of the studied tailings and tailings/clay mixtures.

- To measure the shear strength of deposited tailings and tailings/clay beds under different drainage conditions by varying the rate of load application during shearing of the beds in a specially designed Tilting Tank.
- To define effective and total stress failure envelopes and corresponding strength parameters (effective and total friction angles and cohesion) for the studied tailings and artificial mixtures within the stress range of 0 to 1 kPa.
- To investigate the effect of clay content and clay mineralogy on the geotechnical properties of mine tailings, i.e., on their water content, density, void ratio, shear and erosional strength.
- To investigate the relationship between the bulk engineering properties (water content, wet bulk density, undrained shear strength) and the erosional strength of mine tailings and tailings/clay mixtures and propose a method for estimating the latter from knowledge of the former.

## 1.3. Originality of the research and major contributions

The evaluation of engineering properties of saturated mine tailings and tailings/clay systems described herein was performed through a comprehensive laboratory experimental program that spanned four years. The laboratory testing was complemented by theoretical analysis, statistical regression and empirical formulation. The mine tailings samples were obtained from the Clarabelle Copper Mine near Sudbury, Ontario. The site was specifically selected for our study because the Sudbury tailings area is among the largest waste management facilities in North America and accommodates about 10% of all tailings in Canada. The experimental methodology, employed in the described research, simulated the *in situ* sedimentation and consolidation of the tailings bed as closely as possible. Furthermore, testing was performed under drainage conditions similar to those in a tailings pond or tailings embankment, and over a stress range relevant to that encountered in most tailings management facilities. The specific contributions of the research are listed below:

- A novel Automated Fall Cone device, capable of measuring shear strengths about two orders of magnitude lower than the conventional geotechnical equipment, was designed and constructed. It was successfully utilized to measure the ultra low undrained shear strength of mine tailings and tailings/clay mixtures (as low as a few Pa) in the stress range below 1 kPa. The equipment was found to be easy to use and the obtained results showed good reproducibility. Its applicability to soils with various compositions was discussed and techniques to minimize drainage from tested samples were proposed.
- Undrained shear strength and water content profiles were obtained with depth below the surface of tailings and tailings/clay deposited beds. The factors affecting the undrained shear strength of the beds were identified and a correlation between the undrained shear strength and the vertical effective stress was established.
- The shear strength of normally consolidated deposited mine tailings and tailings/clay beds with varying final thicknesses was measured using a specially built Tilting Tank under different degrees of drainage. Drained and partially drained conditions were simulated by varying the tilting speed of the Tank and the evolution of the excess pore water pressure within the beds was monitored throughout each experiment.

- The mechanism of failure of the beds within the Tank was examined, the position of the failure plane was noted, and the angle of tilting at failure was used to calculate the drained and partially drained shear strength of the tailings and mixtures. Total and effective stress failure envelopes were defined over the stress range of 0 to 1 kPa.
- The effect of clay content and clay mineralogy on the fabric, water content, void ratio, density, undrained shear strength, and erosional strength of the deposited beds was determined and analysed.
- The erosional strength, expressed as critical shear stress for erosion, was defined for each bed as a function of depth. A linear correlation between the undrained shear strength and the critical shear stress for erosion, with parameters dependent on the composition of the mine/tailings clay mixtures was proposed.

## 1.4. Organisation of the thesis

This thesis is presented in integrated-article format and contains eight chapters and four appendices. Each article chapter incorporates a review of literature on the particular subject area and bibliography. Additional data pertinent to individual chapters is summarized in Appendices at the end of the thesis. The chapters are outlined as follows:

Chapter 1 provides an introduction to mine tailings with respect to their generation, transport and storage. It briefly touches on the processes during tailings bed formation and consolidation, summarizes the problems related to tailings disposal, and explains the importance of mine tailings characterization under the appropriate stress range and drainage conditions.

Chapter 2 contains a detailed review of the physico-chemical (e.g., grain size distribution, specific gravity, void ratio, plasticity, fabric and shear strength) and hydrodynamic (e.g., settling velocity) properties of mine tailings. The dependence of the shear strength of tailings on the drainage conditions and stress range is covered. Basic processes like settling, deposition, consolidation and erosion are described and the effect of the bulk sediment properties on these processes is discussed.

Chapter 3 describes the use of a novel Automated Fall Cone device to measure the undrained shear strength of deposited tailings beds with varying thicknesses and time for consolidation. A methodology to capture the variation of the geotechnical properties of tailings with depth within the deposit and to ensure undrained conditions during shear strength testing is proposed.

Chapter 4 outlines a method for determination of the shear strength of tailings beds under different drainage conditions using a specially constructed Tilting Tank. The use of the test results to obtain the drained (effective) and partially drained (total) strength envelopes of the tailings is described.

Chapter 5 presents an investigation of the effect of clay percentage and clay mineralogy on the shear strength of artificial mine tailings/clay mixtures under various degrees of drainage. The observed evolution of the excess pore water pressure within the tested beds is discussed with respect to clay content and mineralogy, and hypotheses for bed failure are proposed.

Chapter 6 outlines a study of the relationship between the erosional and mechanical strength of mine tailings and mine tailings/clay mixtures with varying percentage and mineralogy of the clay-size fraction.  A linear correlation between the undrained shear strength and the critical stress for erosion, with parameters dependent on the composition of the mixtures, is established.

Chapter 7 provides a summary of the main results obtained from the research program and outlines the conclusions derived from these results.

Chapter 8 presents authors' recommendations for future research on the subject.

Supplementary research data to Chapters 3, 4, 5 and 6 is organized and presented in Appendices A, B, C and D, respectively.

## 1.5. References

Blight GE (1998) Construction of tailings dams. In: Case studies on tailings management, International Council on Metals and the Environment (ICME), United Nations Environment Programme (UNEP), pp. 9-10.

Bussière B (2007) Colloquium 2004: Hydrogeotechnical properties of hard rock tailings from metal mines and emerging geoenvironmental disposal approaches. Canadian Geotechnical Journal, 44:1019-1052.

Castro G (2003) Evaluation of seismic stability of tailings dams. In: Proceedings of the 12th Panamerican Conference on Soil Mechanics and Geotechnical Engineering, Cambridge, Massachusetts, USA, 22-26 June 2003.

Catalan LJ, Yanful EK (2002) Sediment-Trap Measurements of Suspended Mine Tailings in Shallow Water Cover. Journal of Environmental Engineering, 128(1):19-30.

Davé NK, Krishnappan BG, Davies M, Reid I, Lanteigne L (2003) Erosion characteristics of underwater deposited mine tailings. Open presentations, Mining and the Environment International Conference, Laurentian University, Sudbury, Ontario, 25–28 May 2003.

Davé NK, Lim TP, Horne D, Boucher Y, Stuparyk R (1997) Water cover on reactive tailings and waste rock: laboratory studies of oxidation and metal release characteristics. In: Proceedings of the 4th International Conference on Acid Rock Drainage, 31 May – 6 June 1997, Vancouver, Vol. II, pp. 779–794.

Jewell RJ (1998) An introduction to tailings. In: International Council on Metals and the Environment (ICME), United Nations Environment Programme (UNEP), pp. 7-8.

Martin TE, Davies MP (2000) Trends in the stewardship of tailings dams. In: Proceedings of the 7th International Conference on Tailings and Mine Waste, Fort Collins, Colorado, USA, 23-26 January 2000. A.A. Balkema, Rotterdam, The Netherlands, pp. 393-407.

Martin TE, Tissington (1996) Design evolution of tailings dams at Inco Sudbury. In: Proceedings of the 3rd International Conference on Tailings and Mine Waste, Fort Collins, Colorado, USA, 16-19 January 1996. A.A. Balkema, Rotterdam, The Netherlands, Vol. I, pp. 49-58.

Mian MH, Yanful EK (2007) Erosion characteristics and resuspension of sub-aqueous mine tailings. Journal of Environmental Engineering and Science, 6:175–190.

Pettibone H, Kealy C (1971) Engineering properties of mine tailings. Journal of the Soil Mechanics and Foundations Division, 97(SM9):1207-1225.

Vick SG (1990) Planning, analysis, and design of tailings dams. 2nd edn. BiTech Publishers, Vancouver, B.C., Canada.

Yanful EK, Verma A (1999) Oxidation of flooded mine tailings due to resuspension. Canadian Geotechnical Journal, 36:826–845.

# CHAPTER 2. LITERATURE REVIEW

## 2.1. Characterization of mine tailings

The characterization of sedimentary deposits, occurring either naturally or as products of industrial operations, is fundamental for understanding their engineering behaviour (Zreik et al. 1995). Engineering applications that require sediment characterization include erosion resistance of deposited sediment beds needed to predict the sediment transport (e.g., Lick and McNeil 2001; Berlamont et al. 1993), design of water-covered tailings management facilities (Davé et al. 2003), and disposal and long term storage of tailings in a safe manner (Mian and Yanful 2007). Because tailings in any one category, i.e., soft-rock, hard-rock, coarse or fine, share the same broad physical characteristics, their engineering behaviour and disposal problems are somewhat similar (Vick 1990). The bulk parameters, classifying the sediment, can be used for preliminary estimates of the engineering properties of the material (e.g., erodibility and stability of sediment deposits) in the early stages of design (Carrier and Beckman 1984; Winterwerp and van Kesteren 2004).

### *2.1.1. Geotechnical properties*

This study is concerned with hard-rock tailings in particular, and therefore the focus of the subsequent review will be on their properties. Mine tailings from hard-rock metal mines are generally coarse-grained and are composed of clay-, silt- and fine sand-size particles of low plasticity (Bussière 2007). The solid phase of tailings is characterized by its grain size distribution, specific gravity, void ratio and plasticity, which are properties determined by the parent ore type and the milling process. The grain size distribution is the fundamental property of tailings that controls the permeability of the tailings body. Soil classifications distinguish between clay, silt, sand and gravel fractions (ASTM 1997). Often in the literature clay and silt fractions are considered together and referred to as the "mud" fraction, with diameter of the grains less than 0.063 mm (e.g., Mitchener and Torfs 1996; van Ledden et al. 2004; Jacobs et al. 2008). The clay-size particles, in relation to the chemical properties of the pore fluid, control the engineering behaviour of the soil (Mitchell and Soga 2005). In hard-rock tailings, however, even when clay-size particles are present in substantial proportions, they are derived from the crushed host rock rather than from clay (phyllosilicate) minerals. As a result, tailings slimes are nonplastic and do not exert much influence on the behaviour of the tailings as a whole (Vick 1990). Specific gravity of hard-rock tailings varies between 2.6 and 4.5 (Volpe 1979; Mittal and Morgenstern 1976; Benzaazoua et al. 2002; Wijewickreme et al. 2005), with higher (above 2.9) values usually resulting from the presence of sulphide minerals in the ore. The *in situ* void ratio of tailings depends primarily on two factors: particle size distribution and clay content. For most hard-rock tailings sands the *in situ* void ratio generally ranges from about 0.6 to 0.9 (Vick 1990). Slimes from these tailings of low to moderate plasticity show higher *in situ* void ratios ranging from about 0.7 to 1.3. Within a given tailings deposit, the void ratio generally decreases with depth due to the compressibility of the hydraulically deposited tailings. Because of their loose depositional state, high angularity, and gradation characteristics, both tailings sands and slimes are more compressible than most natural soils (Vick 1990).

The plasticity of the tailings is dictated by the size and the nature of the constituent clay particles, if present. The plasticity parameters (i.e., Atterberg limits), and in particular, the plastic limit ($w_P$) and the liquid limit ($w_L$) are very important in determining the engineering behaviour of the tailings. Atterberg limits tests performed on hard-rock mine tailings show only a slight plasticity, with $w_L$ usually below 40%, and $w_P$ between 0 and 15% (Mittal and Morgenstern 1976; Matyas et al. 1984). These plasticity parameters yield the water content, $w$, of a tailings sample. From the engineering perspective, the higher the water content of a soil the greater its compressibility and the lower the strength of the soil. The soil mechanical tests (e.g., the Casagrande's liquid limit test, the fall cone test) applied to determine the $w_P$ and $w_L$ can be regarded as undrained shear strength tests on remoulded samples, and therefore reflect the mechanical behaviour of the sediment as a function of its water content or void ratio (Winterwerp and van Kesteren 2004).

The sediment fabric contains information about the skeleton structure of the sediment, such as dispersed (granular) or flocculated. In fresh water suspension the repulsive forces between the negatively charged clay particles dominate and the particles will repel each other. In saline or brackish waters, e.g., in marine environments, the attractive forces dominate due to the presence of cations forming a cloud of positively charged ions around the clay particles resulting in the formation of aggregates (flocs). Other binding forces that promote particle agglomeration are chemical forces (e.g., hydrogen bonds, cementation, and coatings of organic materials) (van Rijn 1993).

### *2.1.2. Hydrodynamic properties*

An important hydrodynamic property of sediments (and mine tailings) deposited under water is their settling velocity as it allows evaluating the sediment behaviour in suspension. Whereas for noncohesive sediments the settling velocity may serve as an indication of their grain size distribution, this is not true for cohesive sediments due to the flocculation effects, affecting the shape, size and density of the particle aggregates (Berlamont et al. 1993). The settling velocity is strongly influenced by the suspension concentration (van Rijn 1993). In suspensions with very low-concentrations (less than 10% solids by volume), particles settle freely unencumbered by hydrodynamic influences of other particles (Major 2003). In dilute suspensions, particles settle according to the principles of Stokes' Law, in which buoyant particle weight is balanced by drag forces owing to slow fluid motion around the particle. Settling velocity is affected by particle size, density, and shape as well as by fluid properties, but particles that are hydraulically equivalent settle at the same rate. At a sufficient volume concentration of solids, however, changes in fluid density and viscosity, particle-to-particle interaction and upward flux of fluid caused by downward particle motion hinder particle settling (Davies 1968). As a result, the particle settling velocity is lower than that of a single particle of the same size settling in an infinite fluid. Settling velocity depends upon solids concentration and on particle size, density and distribution. When the concentration of solids exceeds 50% by volume, particle-to-particle contacts suppress segregation of particles in the suspension and all particles settle at approximately the same rate, a phenomenon referred to as *en masse* settling (Cheng 1980).

### *2.1.3. Depositional characteristics*

Tailings are almost always transported from the mill to the storage facility in a pipeline in the form of tailings-water slurry (pulp). The slurry is usually of high viscosity (0.2-0.6 Pa.s) and high concentration of solids, which ranges from about 15% to 55%, but is most commonly in the range of 40-50% by weight (Vick 1990). When subaqueous deposition is the preferred method of disposal, tailings particles tend to settle from suspension in standing water. The concentration of solids in the suspension strongly influences the degree of particle-size segregation within the resulting tailings deposit, with lower concentrations tending to promote a greater degree of segregation (Major 2003). Thus, particles in dilute suspensions (concentration less than 10% by volume) segregate rapidly according to particle size and density and produce a greatly segregated deposit. Hindered settling affects the settling characteristics of particles in suspensions with moderate concentrations (10 to 50% by volume). In these suspensions, the settling of the dense particles generates a counterflow that elutriates the lighter plastic particles. The resulting deposit is relatively unsorted with a capping layer of fines elutriated by escaping pore fluid. At sufficiently high concentrations (above 50%), particle segregation is suppressed and *en masse* settling is observed, resulting in an ungraded deposit (Cheng 1980).

During settling, the weight of the sediment mass near the bed/water interface is balanced by the force induced by the upward flow of pore water from the underlying sediment (Mehta et al. 1989). As the sediment particles continue to be brought closer together and the upward flux of pore water lessens, the weight of this near-surface sediment gradually turns into effective stress, which is transmitted by virtue of particle-to-particle contact. The development of effective stress marks the beginning of the primary consolidation, which continues until the excess pore water pressure is fully dissipated (Imai 1981). Primary consolidation occurs through compaction of the soil mass accompanied by migration of the pore water held in the pore spaces in an upward direction into the ambient water above the sediment deposit. The rate of consolidation is governed by the length and cross sectional area of the drainage path. The primary consolidation of coarser tailings occurs more rapidly than for fine tailings due to the higher hydraulic conductivity of the former (Bussière 2007). The *in situ* consolidation of tailings progresses in a vertical direction, often under a horizontally constrained condition, resulting in an effective horizontal stress less than the effective vertical stress. Anisotropic soil structure develops in response to such one-dimentional primary consolidation. Secondary compression begins after the primary consolidation ends and proceeds at constant effective stress, that is, after all the excess pore water pressure has dissipated (Holtz and Kovacs 1981). The mechanism of secondary compression involves sliding at interparticle contacts, expulsion of water from microfabric elements, and plastic rearrangement of soil skeleton (Mitchell and Soga 2005).

The effect of aging of cohesive sediment beds at constant effective stress was studied by Zreik et al. (1998b) who found that, at a particular depth and water content, the undrained shear strength increased with time after primary consolidation. The authors attributed the observed strength increase to thixotropy and hypothesized that particle rearrangement provided the main contribution to the time-dependent strength gain in remoulded cohesive soils. In granular soils, under the stress states commonly encountered in the field, excess pore pressure dissipates rapidly and deformation after completion of primary consolidation is almost negligible (Atkinson 2007). Therefore, it has been assumed that aging does not influence significantly the stress-strain response of these soils. More recently, however, the existence of time effect in sands has been recognized and investigated by researchers (e.g., Mitchell and Solymar 1984;

Schmertmann 1987, 1991; Mesri et al. 1990). Mitchell and Solymar (1984) presented evidence that even after all density changes were complete, freshly deposited or densified saturated sands could exhibit substantial time-dependent strength increase over periods from days to months. These authors hypothesized that the most probable mechanism for the observed phenomenon seemed to be the inter-particle cementation due to the formation of silica acid gel films of the particle surfaces. Mitchell and Solymar (1984) suggested that particle surface characteristics (e.g., particle shape) may also be important and contribute to the observed strength gain with time. An alternative explanation for the stiffness and strength increase with time was proposed by Schmertmann (1987, 1991). He suggested that, whether clay or sand, a dispersive particle reorientation, internal stresses redistribution and increased interlocking with time take place in all soils. Whereas cementation at interparticle contacts would lead to an increase in the cohesion intercept of the soil, the particle reorientation would result in a seemingly frictional strength gain with aging. Schmertmann (1991) provided extensive evidence that the observed laboratory and field strength increase with age involved primarily mechanical changes in the structure or fabric of a soil, and thus was due to an increase in the frictional rather than the cohesive component of the strength. This author also emphasised that the frictional strength mobilization with time was more pronounced at low strains. Mesri et al. (1990) discussed the possible causes for the substantial increase in stiffness with time under drained conditions and at constant vertical effective stress in freshly placed, consolidated, or densified clean sands. They ascribed these strength gains to the continued rearrangement of sand particles resulting in an enhanced macrointerlocking of sand grains and microinterlocking of grain surface roughness. Vick (1990) suggested that the deformation observed for some types of mine tailings under constant load after pore pressure dissipation, was due to continuing particle rearrangement and grain-to-grain slippage. The author pointed out, however, that secondary compression of tailings is usually small compared to primary consolidation (Vick 1990).

### 2.1.4. Shear strength dependence on drainage conditions and stress range

The shear strength is defined as the maximum resistance a soil has to shearing stresses and it can be determined experimentally by direct measurements of strength for a given set of laboratory and/or *in situ* soil conditions (Fang and Daniels 2006). When load is applied to a soil, the load is supported by an increase in the pore-fluid pressure until the pore-fluid can drain into regions of lower pressure. Hence, in the field the shear strength of the soil will depend on the rate of load application and on the permeability and drainage boundary conditions. When field conditions allow for full drainage, the soil particles are brought closer together, i.e., the soil is able to experience volume change throughout the shearing, and the response to loading is drained (Terzaghi et al. 1996). In contrast, undrained shear strength is mobilized when failure occurs before any dissipation of shearing-induced excess pore water pressure takes place. A zero volumetric strain is characteristic of the undrained loading, whereas during drained loading the excess pore water pressure is essentially zero. Undrained instability develops most readily in loose to moderately dense granular soils (e.g., silty sands or sands and gravels capped by or containing seams of impermeable sediment), which tend to behave in contractive manner during a loading event of short duration, such as an earthquake (Umehara et al. 1985; Youd et al. 2001). The tendency of the saturated soil to contract, which is not realized either because of low permeability or rapid shearing, produces a large positive pore water pressure with an associated decrease in effective stress (Terzaghi et al. 1996). Once the pore water pressure becomes equal to the effective stress, the soil loses all its strength and flows like a liquid, a phenomenon termed liquefaction (Holtz and Kovacs 1981).

Various criteria have been applied to determine whether a particular soil is prone to liquefaction or not. The so-called Chinese criteria, as defined by Seed and Idriss (1982), specify that liquefaction can only occur in a soil if all three of the following conditions are met:

- The clay content (particle size less than 5 μm) is lower than 15% by weight.
- The liquid limit is below 35%.
- The natural moisture content is greater than 0.9 times the liquid limit.

Depending on the initial void ratio, saturated granular soils may be in either of two states (Whitman 1985). Soils in State I are those that exhibit strain-softening response to loading (i.e., contractive behaviour), whereas soils in State II respond in a strain-hardening manner (i.e., dilative behaviour). The liquefaction resistance of dilative soils (moderately dense to dense granular materials under low confining stress) increases with increasing static shear stress (Youd et al. 2001). In contrast, the liquefaction resistance of contractive soils (loose soils and moderately dense soils under high confining stress) decreases with increased static shear stress. Under undrained conditions, State I soils can be triggered to collapse, either monotonically or cyclically, if the static shear stress is greater than the ultimate or steady-state shear strength of the soil. In this case, flow liquefaction occurs, where the soil deforms at a low constant residual shear stress. If the soil is in State II, flow liquefaction will generally not occur unless there is redistribution of void ratio within the soil, i.e., there must be local deviation from the undrained condition. Whitman (1985) describes two actual field situations, in which drainage conditions may shift from the undrained scenario. In the first situation, the granular soil layer is enclosed by much less pervious soils and is generally in an undrained state. If during a cyclic undrained loading, e.g., earthquake loading, a portion of the disturbed granular soil loses its shear strength (i.e., liquefies), thus causing a redistribution of void ratio within the remaining soil, then a phenomenon termed cyclic mobility can take place. Cyclic mobility entails development of high pore water pressures and large strains within the soil mass but proceeds with no loss in shear strength, and thus no flow of the soil is observed (Castro 1975). In the second situation, the high excess pore water pressures develop within cohesionless soil under cyclic loading, spread out into overlying soils, thus reducing their shear strength and causing cracking. The granular soil particles can then be carried upward into the cracks, the process resulting in loss of pore water pressure within the granular layer and shifting from undrained conditions. The above discussion aims to illustrate that in many cases (e.g., during and soon after earthquake loading), saturated granular soil elements in earth structures experience some degree of drainage, and consequently, volume and pore water pressure changes with time (Yamamoto et al. 2009; Vaid and Eliadorani 2000; Umehara et al. 1985). The rate of drainage is governed generally by the length of the drainage path and the permeability of the soil (Yamamoto et al. 2009). For example, drainage following an earthquake is due to the spatial variation of excess pore water pressure generated in the different zones of a soil structure during their dissipation (Vaid and Eliadorani 1998). Therefore, the commonly assumed undrained conditions cannot always be regarded as conservative. In fact, in most geotechnical problems associated with granular soils, only the initial loading can be regarded as undrained, with drainage commencing immediately. Lade (1992) showed that saturated granular soils (e.g., loose sands), which tend to compress during undrained shear, may become unstable (i.e., liquefy) under static loading at stress states located well below the effective strength failure envelope but above the instability line. The author postulated that the instability line, representing the lower boundary of the region of potential instability, could be obtained by connecting the tops of the undrained effective stress paths from a series of triaxial compression tests. Vaid and Eliadorani (1998) demonstrated that in saturated sand partial drainage may cause instability brought about by extremely small void ratio increases. These void ratio increases may be triggered by dynamic loading, such as an earthquake or wave action, or occur under static loading due to the redistribution of uneven pore water pressure in various regions of the earth structure. Based on comprehensive studies on two sands, Vaid and Chern (1985) showed that instability may occur at a mobilized friction angle considerably smaller than the undrained friction angle. The angle corresponding to the onset of instability has been found to be independent of the initial (prior to shear) state of sand defined by its void ratio and consolidation state. Liquefaction of loosely deposited beds of fine grained sand under partially drained conditions and dynamic wave loading has been investigated by Sassa and Sekiguchi (1999). They observed that the sand liquefied when the wave-induced excess pore water pressure at a given location within the deposit reached the value of the initial vertical effective stress at that location.

It seems, however, that there have been relatively few experimental studies that have dealt with the instability of mine tailings, in particular (e.g., Wijewickreme et al. 2005; Moriwaki et al. 1982; Ishihara et al. 1980; Poulos et al. 1985). Within the entire range of failures that have been observed at tailings impoundments, static liquefaction under undrained or partially drained conditions is likely the most common and, at the same time, the least understood (Davies et al. 2002). Undrained or partially drained response may result, for example, from the incremental raise of tailings embankments during the operation of the waste management facility or from the periodic deposition of tailings slurry in the tailings pond. Unless mechanically compacted, tailings are generally deposited in a loose state and therefore often exhibit contracting behaviour. The *in-situ* stress state is relatively "close" to the instability line and only a minor additional shear stress is sufficient to initiate a spontaneous liquefaction event. Below sloping surfaces (such as those in the tailings embankments), the *in-situ* stress conditions are even more unfavourable and the susceptibility of tailings material to liquefaction is further increased (Davies et al. 2002).

When mine tailings are brought to failure under drained conditions, their drained shear strength is mobilized. The drained shear strength of a soil can be expressed with the classic Mohr-Coulomb failure criterion, which represents stress conditions at failure for a material (Terzaghi et al. 1996) and is given by:

$$\tau_f = \sigma'_{nf} \tan\phi' + c' \tag{2.1}$$

where $\tau_f$ is the shear strength of the soil, $\sigma'_{nf}$ is the effective normal stress at the failure plane at failure, $\phi'$ is the drained (effective) friction angle, and $c'$ is the effective cohesion. In the Mohr-Coulomb theory of failure, the shear strength has two components: i) cohesive, which is due to the inherent strength of interparticle bonds or attractive forces between particles, and ii) frictional, which is produced by the frictional resistance to shearing movement.

As previously discussed, saturated loose tailings can liquefy under undrained or partially drained conditions. Liquefaction failure is characterized by a rapid rate of pore water pressure increase, loss of strength and development of large strains. The pore water pressure is an important consideration during undrained and partially drained shearing because it affects the normal effective stress on the tailings bed. If the tendency of a saturated soil is to contract upon shear, positive (i.e., in excess to hydrostatic) pore water pressure develops in undrained conditions, which counteracts and reduces the imposed effective stress. When the shearing-induced pore water pressure becomes equal to the normal effective stress on a given plane within a tailings deposit, the soil mass looses its integrity and bed failure occurs. Therefore, for undrained and partially drained conditions, the failure condition can be expressed with the excess pore water pressure/ effective normal stress ratio:

$$u_e / \sigma'_{nf} = 1.0 \tag{2.2}$$

where $u_e$ is the excess pore water pressure at the failure plane at failure.

Researchers have shown that consolidation stresses below 1 kPa are commonly observed in sediment deposits and mine tailings management facilities (e.g., Zreik et al. 1998a; Qui and Sego 2001). On the other hand, hard-rock tailings are often coarse-grained and noncohesive and the strength behaviour of such soils at low and high stress levels can be significantly different (Sture et al. 1998). Thus, a measurement of the soil strength over the stress range, appropriate to that encountered in the field is important (Fannin et al. 2005). However, within the stress range of 0 to 1 kPa, sediments and mine tailings also exhibit very low undrained shear strength, which often cannot be tested with conventional geotechnical equipment (Zreik et al. 1997; Zreik et al. 1998a). To overcome this problem, Zreik et al. (1995) developed a new fall cone device to measure the undrained strength of extremely weak soils without disturbance and at small depth intervals. A modified version of this device has been employed in the present study to measure the undrained strength of deposited mine tailings beds.

At the same density and stress level, mine tailings exhibit higher drained shear strength than natural soils, which is due primarily to their high degree of particle angularity. Most tailings are cohesionless and show a zero effective cohesion intercept and an effective friction angle 5° to 6° higher than that of natural soils of similar gradation (e.g., Mittal and Morgenstern 1975; Pettibone and Kealy 1971; Matyas et al. 1984; Vick 1990). The undrained (or partially drained) shear strength of tailings is determined in laboratory by tests, which produce total stress parameters, i.e., total friction angle and total cohesion. For the void ratios encountered in most tailings deposits, the total friction angle is in the range of 14° to 24° and the total cohesion, where present, does not exceed 75 kPa (Vick 1990). Zreik et al. (1997) demonstrated that the water content, effective stress and time for consolidation are the three most important parameters governing the strength behaviour of deposited sediment beds.

## 2.2. Erosional strength

The process of moving and removing sediment particles from their original source or resting place (e.g., river, lake or pond bed) is termed erosion (van Rijn 1993). The term resuspension applies when the bed sediment, which was eroded earlier and deposited subsequently, gets back into the water column either by current or wave action (Parchure et al. 2001). The same physical concepts used to describe natural sediment erosion and resuspension processes also apply to mine tailings. The sediments, whether naturally occurring or products of industrial operations, can be subdivided into cohesive or fine-grained sediments and noncohesive or coarse-grained sediments (Raudkivi 1998). The hydrodynamic behaviour of noncohesive sediments is controlled by the sediment particles' size, shape, specific gravity, and position in the matrix of surrounding particles (Dyer 1986). The process of erosion of cohesive sediments is much more complex as it incorporates the destruction of electrochemical bonds between sediment particles, related primarily to mineralogy (van Rijn 1993; Berlamont et al. 1993), and the natural structure or framework created through consolidation of the soil matrix (Ravisangar et al. 2005). Whether or not the sediments will be eroded depends on the magnitude of the hydrodynamic driving force and on the sediments erodibility, defined by the critical erosion shear stress and the erosion rate (Le Hir et al. 2007).

### *2.2.1. Critical stress for erosion*

As water flows over a sediment bed, as either steady flow or oscillatory flow under wave action, it exerts shear stress on the bed. If the rate of flow is increased, the bed shear stress also increases to a point at which the movement of the smallest and easiestto-move particles becomes noticeable (Roberts et al. 1998; Lick et al. 2004). The shear stress at which this movement occurs is referred to as the critical shear stress for erosion or erosion threshold (Soulsby 1997; Houwing 1999). These eroded particles then travel a relatively short distance until they come to rest in a new location. The initial motion tends to occur only at a few isolated spots but as the flow velocity and bed shear stress increase further, more particles are dislodged from the sediment surface and the erosion process becomes more sustained (Dyer 1986). Because of this gradual increase in erosion rate as a result of the applied bed shear stress, it is difficult to precisely define a critical stress at which sediment erosion is first initiated (Roberts et al. 1998). The instantaneous stress in any turbulent flow has magnitude that fluctuates about the mean bed shear stress and, at any given moment, exceeds the individual particle thresholds for some class of particles, determined by particle characteristics and position on the bed (Lavelle and Mofjeld 1987). Hence, under turbulent conditions, occasional transport can occur at all time-mean bed stress values, even down to very small ones. Although a single critical shear stress value below which no single grain is moving may not actually exist, its definition is necessary for practical design purposes (van Rijn 1993). Thus, the critical erosion threshold could be used to denote a point of significant erosion at which small, but measurable, rate of erosion occurs (Lavelle and Mofjeld 1987; Lick et al. 2004). It can be estimated if the fluid and bulk sediment properties are known (Lick and McNeil 2001).

### *2.2.2. Effect of bulk sediment properties*

In the case of noncohesive sediments, susceptibility to erosion can be estimated by knowing the size, shape and specific gravity of the grains, as well as the properties of the fluid, e.g., viscosity, temperature, specific weight (Dyer 1986). In order to characterize the ability of noncohesive sediments and earth materials to resist erosion, Annandale (1995) introduced an erodibility index which is a function of a several geological parameters of the sediment, including bulk compressive strength, particle diameter, shear strength of the interparticle bonds, grain shape and orientation relative to the flow. The physico-chemical properties affecting the erodibility of cohesive sediments include cohesion, clay content, type of clay mineral, water content, and organic matter (Grissinger 1966; Winterwerp and van Kesteren, 2004).

When a sediment bed contains appreciable amount of fine material (clay), cohesive forces between sediment particles become important and cause a distinct increase in the sediment's resistance against erosion (Grissinger 1966; van Rijn 1993). Depending on the mineralogy of the clay, this effect may be more or less pronounced. Sometimes only 10% clay is sufficient to assume control of the properties of the sediment (Raudkivi 1998). Kamphuis and Hall (1983) showed that the capability of a cohesive soil to resist erosion increases with clay content and plasticity. Also, the size of the eroded pieces tends to be larger for a soil with a low clay content (high silt and sand content).

Consolidation is an important factor governing the erodibility of sediments. For instance, freshly deposited sediment has a very loose fabric which can be easily eroded (van Rijn 1993). As the wet bulk density of the deposit increases as a result of consolidation, the critical shear stress for erosion and, respectively the erosion resistance, also increase (Grissinger 1966; Quaresma et al. 2004).

Fukuda and Lick (1980) found that a linear increase in sediment water content results in logarithmic increases in the entrainment rate of the sediment. The importance of the water content in the erosion process has also been emphasised by Aberle et al. (2004) who reported an increase in erosion resistance with a decrease in the sediment water content.

The ability of sediments to resist erosion is also affected by the shear strength of the soil. Kamphuis and Hall (1983) found that the critical shear stress for erosion increases linearly with unconfined compressive strength and with vane shear strength of consolidated clay samples. In an attempt to draw parallels between erosional and mechanical strength, Zreik et al. (1998c) found that at a given depth both the undrained and drained shear strength are approximately one order of magnitude higher than the erosional strength.

### *2.2.3. Effect of depositional properties*

A sediment bed deposited under water can be eroded through bottom currents and pressure fluctuations due to wind-induced turbulence and eddy motion (van Rijn 1993). Mehta et al. (1989) outlines two factors that control the erosion resistance of sediment beds: i) the magnitude of the bed shear stress, and ii) the nature of the deposit, which depends on the manner in which the deposit is formed. Parchure and Mehta (1985) divide sediment beds into two broad categories: i) beds with relative uniform properties over depth below bed surface, and ii) beds, which are stratified with respect to property variations with depth. The first category of sediment beds are formed eithier by deposition from slurries with high concentration of solids (above 50% by volume), or by remoulding previously formed beds, whereas the second category is created by allowing suspended sediments to deposit at low solids concentration (below 50% by volume) under quiescent conditions. Furthermore, a deposited bed may be soft, partially consolidated with a very high water content, or fully consolidated and more dense. Directly associated with the bed structure are two mechanisms of erosion (Parchure and Mehta 1985). Type I or depth-limited erosion is observed in deposited beds exhibiting shear strength increase with depth. Erosion of particles from the bed's surface is initiated once the critical threshold for erosion due to hydrodynamic forces is exceeded, and ceases when the applied bed shear stress reaches the bed shear strength at a certain eroded depth. Because of factors like sediment heterogeneity, consolidation, and tidal and wave oscillatory action, the variation of bed properties (e.g., density, shear strength) with depth causes sediment erosion to occur in discrete steps as the bed shear stress is increased (Mehta et al. 1989; Tolhurst et al. 2000; Banasiak and Verhoeven 2006). Type II or steady-state erosion is characteristic of beds with uniform properties over depth. The erosion rate is constant and controlled by the instantaneous difference between the bed shear stress and the critical shear stress, which remains unchanged with depth.

Sediment beds tend to erode through three modes of erosion: surface, bulk and mass erosion. Surface erosion occurs as wearing away the soil surface particles (or flocs), particle by particle (Krone 1999). If the applied shear stress is linearly increased with time the surface erosion rate also increases linearly until the pressure fluctuations and surface shear become sufficient to dislodge chunks of the bed surface. This mode in the erosion process is termed bulk erosion. Further increase in the bed shear stress would lead to mass erosion, which is in essence, an undrained bed failure (Mehta et al. 1989; Winterwerp and van Kesteren 2004).

Cohesive sediment beds typically erode through bulk erosion, whereas in noncohesive beds surface erosion is observed (Lick et al. 2004). Mass erosion may occur in both cohesive and noncohesive beds, if the applied bed shear stress is sufficiently large. Whether a sediment bed will erode in cohesive or noncohesive manner depends on two important parameters: cohesion and network structure (van Ledden et al. 2004). Cohesion is due to the clay-sized fraction of the sediment, which binds the sand matrix together. Depending on the type of clay, approximately 5-10% clay content by dry weight is sufficient for a natural bed to assume cohesive properties (Dyer 1986; Raudkivi 1998; Mitchener and Torfs 1996). The network structure of a sediment bed (i.e., sand, silt or clay dominated matrix) is determined by the relative proportions of sand-, silt- and clay-size particles (van Ledden et al. 2004).

Natural sediments as well as mine tailings, however, are often mixtures of cohesive and noncohesive material, and there is limited data concerning the erodibility of such mixtures (Le Hir et al. 2008; Jacobs et al. 2008). Among the critical parameters required for modeling the erodibility of mine tailings is the critical shear stress (threshold) for erosion and the present research has demonstrated that it may be evaluated on the basis of measurements of tailings bulk parameters (e.g., bulk density, water content, shear strength). Because the bulk properties of a soil can be determined relatively easily using the existing engineering standards (Roberts et al. 1998; Berlamont et al. 1993; Jacobs et al. 2008), being able to predict tailings erosion resistance from knowledge of these properties will greatly simplify data collection and evaluation when modelling the erosion and resuspension a given site.

## 2.3. References

Aberle J, Nikora V, Walters R (2004) Effects of bed material properties on cohesive sediment erosion. Marine Geology, 207:83-93.

Annandale GW (1995) Erodibility. Journal of Hydraulic Research, 33(4):471-494.

ASTM, Standard D 2487 (1997) Classification of soils for Engineering Purposes. Annual book of ASTM standards. American Society for Testing and Materials, Philadelphia, Pasadena, USA.

Atkinson J (2007) The mechanics of soils and foundations. 2nd edn. Taylor & Francis, New York, USA.

Banasiak R, Verhoeven R (2006) Quantification of the erosion resistance of undisturbed and remoulded cohesive sediments. Water, Air, and Soil Pollution, 6:381–391.

Benzaazoua M, Belem T, Bussière B (2002) Chemical factors that influence the performance of mine sulphidic paste backfill. Cement and Concrete Research, 32:1133-1144.

Berlamont J, Ockenden M, Toorman E, Winterwerp J (1993) The characterisation of cohesive sediment properties. Coastal Engineering, 21:105-128.

Bussière B (2007) Colloquium 2004: Hydrogeotechnical properties of hard rock tailings from metal mines and emerging geoenvironmental disposal approaches. Canadian Geotechnical Journal, 44:1019-1052.

Carrier WD, Beckman JF (1984) Correlations between index tests and the properties of remoulded clays. Géotechnique, 34(2):211-228.

Castro G (1975) Liquefaction and cyclic mobility of saturated sands. ASCE Journal of the Geotechnical Engineering Division, 101(6):551-569.

Cheng DCH (1980) Sedimentation of suspensions and storage stability. Chemistry and Industry, 10:407-414.

Davé NK, Krishnappan BG, Davies M, Reid I, Lanteigne L (2003) Erosion characteristics of underwater deposited mine tailings. Open presentations, Mining and the Environment International Conference, Laurentian University, Sudbury, Ontario, Canada, 25–28 May 2003.

Davies M, McRoberts E, Martin T (2002) Static liquefaction of tailings – fundamentals and case histories. In: Proceedings Tailings Dams 2002, ASDSO/USCOLD, Las Vegas, Nevada, USA.

Davies R (1968) The experimental study of the differential settling of particles in suspension at high concentrations. Powder Technology, 2(1):43-51.

Dyer KR (1986) Coastal and estuarine sediment dynamics. John Wiley & sons Ltd., Chichester, UK.

Fang HY, Daniels J (2006) Introductory Geotechnical Engineering: An Environmental Perspective. Taylor & Francis, New York, USA.

Fannin RJ, Eliadorani A, Wilkinson JMT (2005) Shear strength of cohesionless soils at low stress. Géotechnique, 55(6):467-478.

Fukuda MK, Lick W (1980) The entrainment of cohesive sediments in freshwater. Journal of Geophysical Research, 85(C5):2813–2824.

Grissinger EH (1966) Resistance of selected clay systems to erosion by water. Water Resources Research, 2(1):131-138.

Holtz R, Kovacs W (1981) An introduction to geotechnical engineering. Prentice-Hall Inc., Englewood Cliffs, New Jersey, USA.

Houwing EJ (1999) Determination of the critical erosion threshold of cohesive sediments on intertidal mudflats along the Dutch Wadden Sea Coast. Estuarine, Coastal and Shelf Science, 49:545–555.

Imai G (1981) Experimental studies on sedimentation mechanism and sediment formation of clay materials. Soils and Foundations, 21(1):7-20.

Ishihara K, Troncoso J, Kawase Y, Takahashi Y (1980) Cyclic strength characteristics of tailings materials. Soils and Foundations, 20(4):127–142.

Jacobs W, van Kesteren W, Winterwerp JC (2008) Strength of sediment mixtures as a function of sand content and clay mineralogy. In: Proceedings in Marine Science, Sediment and Ecohydraulics - INTERCOH 2005, Vol. 9, pp. 91-107.

Kamphuis JW, Hall KR (1983) Cohesive material erosion by unidirectional current. Journal of Hydraulic Engineering, 109(1):49-61.

Krone RB (1999) Effects of bed structure on erosion of cohesive sediments. Journal of Hydraulic Engineering, 125(12):1297-1301.

Lade PV (1992) Static instability and liquefaction of loose fine sandy slopes. Journal of Geotechnical Engineering, 118(1):51-71.

Lavelle JW, Mofjeld HO (1987) Do critical stresses for incipient motion and erosion really exist. Journal of Hydraulic Engineering, 113(3):370-385.

Le Hir P, Cann P, Waeles B, Jestin H (2008) Erodibility of natural sediments: experiments on sand/mud mixtures fro laboratory and field erosion tests. In: Proceedings in Marine Science, Sediment and Ecohydraulics – INTERCOH 2005, Vol. 9, pp. 137-153.

Le Hir P, Monbet Y, Orvain F (2007) Sediment erodibility in sediment transport modeling: Can we account for biota effects? Continental Shelf Research, 27:1116–1142.

Lick W, Jin L, Gailani J (2004) Initiation of movement of quartz particles. Journal of Hydraulic Engineering, 130(8):755-761.

Lick W, McNeil J (2001) Effects of sediment bulk properties on erosion rates. The Science of the Total Environment, 266:41-48.

Major JJ (2003) Hindered settling. In: Encyclopedia of Sediments and sedimentary rocks. Edited by Middleton GV, Kluwer Academic Publishers, Dordrecht, The Netherlands, pp. 358-360.

Matyas E, Welch D, Reades D (1984) Geotechnical parameters and behaviour of uranium tailings. Canadian Geotechnical Journal, 21:489-504.

Mehta AJ, Hayter EJ, Parker ER, Krone RB, Teeter AM (1989) Cohesive Sediment Transport. I: Process Description. Journal of Hydraulic Engineering, 115(8):1076-1093.

Mesri G, Feng TW, Benak JM (1990) Postdensification penetration resistance of clean sands. ASCE Journal of Geotechnical Engineering, 116(7):1095-1115.

Mian MH, Yanful EK (2007) Erosion characteristics and resuspension of sub-aqueous mine tailings. Journal of Environmental Engineering and Science, 6: 175–190.

Mitchell JK, Soga K (2005) Fundamentals of Soil Behavior, 3rd edn. John Wiley & Sons Inc., Hoboken, New Jersey, USA.

Mitchell JK, Solymar ZV (1984) Time-dependent strength gain in freshly deposited or densified sand. ASCE Journal of Geotechnical Engineering, 110(11):1559-1576.

Mitchener H, Torfs H (1996) Erosion of mud/sand mixtures. Coastal Engineering, 29:1-25.

Mittal H, Morgenstern N (1975) Parameters for the design of tailings dams. Canadian Geotechnical Journal, 12:235-261.

Mittal H, Morgenstern N (1976) Seepage Control in Tailings Dams. Canadian Geotechnical Journal, 13:277-293.

Moriwaki, Y., Akky, M.R., Ebeling, A.M., Idriss, I.M., Ladd, R.S. 1982. Cyclic strength and properties of tailings slimes. Dynamic Stability of Tailings Dams. Preprint 82-539, American Society of Civil Engineers (ASCE), New York.

Parchure TM, McAnally Jr. WH, Teeter AM (2001) Desktop method for estimating vessel-induced sediment suspension. Journal of Hydraulic Engineering, 127(7):577-587.

Parchure TM, Mehta AJ (1985) Erosion of soft cohesive sediment deposits. ASCE Journal of Hydraulic Engineering, 111(10):1308-1326.

Pettibone H, Kealy C (1971) Engineering properties of mine tailings. Journal of the Soil Mechanics and Foundations Division, 97(SM9):1207-1225.

Poulos SJ, Robinsky EI, Keller TO (1985) Liquefaction resistance of thickened tailings. ASCE Journal of Geotechnical Engineering, 111(12): 1380–1394.

Qiu Y, Sego D (2001) Laboratory properties of mine tailings. Canadian Geotechnical Journal, 38:183-190.

Quaresma VS, Amos CL, Flindt M (2004) The influences of biological activity and consolidation time on laboratory cohesive beds. Journal of Sedimentary Research, 74(2):184-190.

Raudkivi AJ (1998) Loose Boundary Hydraulics. A.A. Balkema, Rotterdam, The Netherlands.

Ravisangar V, Sturm TW, Amirtharajah A (2005) Influence of sediment structure on erosional strength and density of kaolinite sediment beds. Journal of Hydraulic Engineering, 131(5): 356–365.

Roberts J, Jepsen R, Gotthard D, Lick W (1998) Effects of particle size and bulk density on erosion of quartz particles. Journal of Hydraulic Engineering, 124(12):1261-1267.

Sassa S, Sekiguchi H (1999) Wave-induced liquefaction of beds of sand in a centrifuge. Géotechnique, 49(5):621-638.

Schmertman JH (1987) Time-dependent strength gain in freshly deposited or densified sand – discussion. ASCE Journal of Geotechnical Engineering, 113(2):173-175.

Schmertmann JH (1991) The mechanical aging of soils. ASCE Journal of Geotechnical Engineering, 117(9):1288-1330.

Seed HB, Idriss IM (1982) Ground motions and soil liquefaction during earthquakes. Earthquake Engineering Research Institure Monograph, Oakland, California.

Soulsby RL (1997) Dynamics of marine sands. Thomas Telford Publications, London, UK.

Sture S, Costes NC, Batiste SN, Lankton MR, AlShibli KA, Jeremic B, Swanson RA, Frank M (1998) Mechanics of granular materials at low effective stresses. Journal of Aerospace Engineering, 11(3):67-72.

Terzaghi K, Peck RB, Mesri G (1996) Soil mechanics in engineering practice. 3rd edn. John Wiley & Sons Inc., New York, USA.

Tolhurst TJ, Black KS, Paterson DM, Mitchener HJ, Termaat GR, Shayler SA (2000) A comparison and measurement standardisation of four in situ devices for determining the erosion shear stress of intertidal sediments. Continental Shelf Research, 20:1397-1418.

Umehara Y, Zen K, Kouji H (1985) Evaluation of soil liquefaction potentials in partially drained conditions. Soils and Foundations, 25(2):57-72.

Vaid YP, Chern JC (1985) Cyclic and monotonic undrained response of saturated sands. Advances in the Art of Testing Soils Under Cyclic Conditions, American Society of Civil Engineers Convention, Detroit, Michigan, USA, pp. 120–147.

Vaid YP, Eliadorani A (1998) Instability and liquefaction of granular soils under undrained and partially drained states. Canadian Geotechnical Journal, 35:1053-1062.

Vaid YP, Eliadorani A (2000) Undrained and drained (?) stress–strain response. Canadian Geotechnical Journal, 37:1126-1130.

Van Ledden M, van Kesteren WGM, Winterwerp JC (2004) A conceptual framework for the erosion behaviour of sand–mud mixtures. Continental Shelf Research, 24:1–11.

Van Rijn L (1993). Principles of Sediment Transport in Rivers, Estuaries and Coastal Seas. Aqua Publications, Amsterdam, The Netherlands.

Vick SG (1990) Planning, analysis, and design of tailings dams. 2nd edn. BiTech Publishers, Vancouver, B.C., Canada.

Volpe R (1979) Physical and engineering properties of copper tailings. In: Proceedings of Current Geotechnical Practice in Mine Waste Disposal. Edited by The Committee on Embankment Dams and Slopes of the Geotechnical Engineering Division. American Society of Civil Engineering, New York, USA, pp. 142-160.

Whitman RV (1985) On liquefaction. In: Proceedings of the 11th International Conference on Soil Mechanics and Foundation Engineering, A. A. Balkema Publishers, Rotterdam, The Netherlands, pp. 1923-1927.

Wijewickreme D, Sanin MV, Greenaway GR (2005) Cyclic shear response of fine-grained mine tailings. Canadian Geotechnical Journal, 42: 1408–1421.

Winterwerp JC, van Kesteren WGM (2004) Introduction to the physics of cohesive sediment in the marine environment. Elsevier B.V., 1000 AE, Amsterdam, The Netherlands.

Yamamoto Y, Hyodo M, Orense R (2009) Liquefaction resistance of sandy soils under partially drained condition. Journal of Geotechnical and Geoenvironmental Engineering, 135(8):1032-1043.

Youd TL, Idriss IM, Andrus RD, Arango I, Castro G, Christian JT, Dobry R, Finn WDL, Harder LF, Hynes ME, Ishihara K, Koester JP, Liao SSC, Marcuson WF, Martin GR, Mitchell JK, Moriwaki Y, Power MS, Robertson PK, Seed RB, Stoke KH (2001) Liquefaction resistance of soils: Summary report from 1996 NCEER and 1998 NCEER/NSF Workshop on evaluation of liquefaction resistance of soils. Journal of Geotechnical and Geoenvironmental Engineering, 127(10):817-833.

Zreik DA, Germaine JT, Ladd CC (1997) Undrained strength of ultra-weak cohesive soils: relationship between water content and effective stress. Soils and Foundations, 37(3):117-128.

Zreik DA, Germaine JT, Ladd CC (1998a) Failure envelope of cohesive soils in the ultra-low stress range. Soils and Foundations, 38(2):201-210.

Zreik DA, Germaine JT, Ladd CC (1998b) Effect of aging and stress history on the undrained strength of ultra-weak cohesive soils. Soils and Foundations, 38(4):31-39.

Zreik DA, Krishnappan BG, Germaine JT, Madsen OS, Ladd CC (1998c) Erosional and mechanical strengths of deposited cohesive sediments. Journal of Hydraulic Engineering, 124(11):1076-1085.

Zreik DA, Ladd CC, Germaine JT (1995) A new fall cone device for measuring the undrained strength of vey weak cohesive soils. Geotechnical Testing Journal, 18(4):472-482.

# CHAPTER 3. UNDRAINED STRENGTH OF DEPOSITED MINE TAILINGS BEDS: EFFECT OF WATER CONTENT, EFFECTIVE STRESS AND TIME OF CONSOLIDATION

## 3.1. Introduction

Mine tailings are ground rock material from which valuable minerals or metals have been extracted (Bussière 2007). Usually they are composed of sand- or silt-size particles ranging between 2 and 80 μm. The quantity of tailings that must be managed by mines annually is enormous as the metal volume is low compared to the extracted volume of the ore, especially for the large lower grade deposits. The large quantity, combined with the fact that many tailings are potentially acid generating and pose an environmental hazard due to their potential for future acidification caused by sulphide minerals (e.g., pyrrhotite, chalcopyrite) oxidation, can explain why the problem with tailings disposal is considered one of the major issues faced by the mining industry worldwide. Inadequate disposal of sulfide-bearing tailings often causes severe contamination of surface streams and groundwater reservoirs, due to oxidation of the inherent sulfide phases and the subsequent generation of leachate characterized by high acidity and elevated concentration of hazardous elements (Komnitsas et al. 2004). To ensure that contamination from mine effluents does not occur, mine operators employ measures to prevent, control or mitigate the problem (Bussière 2007). This is commonly done through limiting the availability of one or more components of the sulfide oxidation reactions; these being oxygen, water and sulfide minerals. The introduction of a low hydraulic conductivity cover made of geomaterials and/or natural soils is one possible option (Bussière 2007). The subaqueous disposal of limestone-treated tailings is another effective approach to reduce sulfide mineral oxidation, acid generation, and subsequent release of dissolved metals to the environment (Yanful and Verma 1999; Catalan and Yanful 2002; Samad and Yanful 2005). This method takes advantage of the low oxygen solubility and diffusivity in water (Catalan and Yanful 2002) and creates a barrier minimizing the exposure of the tailings mass to the atmospheric oxygen.

Once produced, tailings are transported in the form of a slurry to an impoundment, surrounded by dykes retaining both the solid tailings and the mill effluent (Bussière 2007). Often the dykes used to create the tailings storage reservoir are built of the tailings themselves. Hydraulic transportation by pipeline to the disposal site is among the cheapest forms of solids transportation and thus, the method is used extensively in the mining industry (Blight and Bentel 1983). When disposal of tailings under water cover is the preferred management method, the tailings slurry is deposited subaqueously at one or more points of deposition, located along the length of the impoundment dyke. The slurry runs down the beach with decreasing velocity as the flow moves away from the deposition point. Because coarser particles in the slurry settle faster than finer ones, a gradation of particle size down the beach occurs, with coarser material adjacent to the points of deposition and progressively finer material being deposited with increasing distance from these points (Vick 1990). During deposition the tailings slurry undergoes three simultaneously occurring stages of behaviour: suspension, sedimentation and consolidation (Imai 1981; Been and Sills 1981; Pane and Schiffman 1985; Toorman 1996, 1999). In the suspension stage the settlement rate is approximately constant and the speed of fall of particles is determined by the local particle shape and density. When the solids concentration is low, either dispersed soil particles or particle flocs settle freely, with flocs formation depending on the sediment type (cohesive or non-cohesive) and the salt concentration in the water (Imai 1981). Hindered settling is observed when the solids concentration is high and it is characterized by mutual collisions between particles or aggregates (Kynch 1952). The sediment in the stage of consolidation behaves like a soil and the traditional consolidation theories, e.g., Terzaghi's theory (Terzaghi 1942) or Gibson's finite strain theory (Gibson et al. 1967, 1981), are applicable. It is worth noting here that the Terzaghi's theory of consolidation is based on a number of important assumptions that limit its validity. For instance, it has been assumed that the consolidation strains are small, the coefficient of permeability remains constant during consolidation, and the relationship between the void ratio (or vertical strain) and vertical effective stress is linear and independent of time (Terzaghi et al. 1996). In soft soils, because of the linear small strain approximation, Terzaghi's theory has the potential to seriously underestimate the excess pore water pressure in a soil layer and as a result, the shear strength will be overestimated and a potentially unsafe desigh could emerge (Gibson et al. 1981). Furthermore, the softer the soil the greater the underestimation of the exess pore water pressure. Some researchers (e.g., Caldwell et al. 1984; Priscu et al. 1999) propose to model the self-weight consolidation of the soft fine fraction of tailings using a finite strain sedimentation/consolidation theory (Gibson et al. 1967, 1981). This theory allows for nonlinear, time dependent simulation of slurry deposition and consolidation in the tailings pond. In the transitional zone between suspension and consolidation, i.e., the sedimentation stage, the settlement rate is decreasing and large concentration gradients with depth exist. The skeleton is extremely compressible and strains are comparatively large. A major difficulty faced by researchers attempting the development of a unified theory describing the effective stress principle in all three stages was to solve the effective stress discontinuity at the interface between suspension and the consolidating bed. Pane and Schiffman (1985) introduced an effective stress modifier or interaction coefficient $\beta(e)$, which is a function of the void ratio. In the suspension stage, the particles are so distant that their interaction or contact is negligible and $\beta(e)$ is equal to zero implying a zero effective stress. The consolidation stage is characterized with fully active effective stress transmitted by virtue of particle-to-particle contact and thus, $\beta(e)$ is equal to unity. In the transition between suspension and consolidation $\beta(e)$ is set to vary between zero and unity. Using the Pane and Schiffman (1985) solution, Azevedo et al. (1994) conducted a numerical analysis of the sedimentation/consolidation behaviour of red mud and found a good agreement between the analytically calculated effective stress distribution and laboratory and field measurements. Toorman (1996, 1999) proposed another general equation giving the evolution of particle concentration distribution over the depth of a quiescent fluid column based on solving the mass balance equation of the solid phase. According to the author, the formulation can be applied to predict the sedimentation and consolidation behaviour of both noncohesive and cohesive sediments. The validity of the constitutive laws adopted in the discussed models, however, needs to be established using reliable experimental data, which sometimes may be difficult to obtain for the following reasons. Firstly, the quick evolution of the material at the beginning of the test requires performing multiple measurements in very small time intervals; and secondly, the interpretation of the very low effective stresses calls for a measurement accuracy of a few Pascals for both stresses and pressures (Alexis et al. 2004). A laboratory experimental device capable of meeting both requirements of speed and accuracy was described by Alexis et al. (2004), along with a bench for the study of settling and consolidation behaviour of soils in formation stage. The development of effective stress marks the beginning of primary consolidation under the influence of the sediment self-weight (Imai 1981). The process ends when the excess pore water pressure has completely dissipated and at this stage a consolidated bed is formed (Imai 1981; Mehta et al. 1982). Secondary consolidation, resulting from plastic deformation of the bed under a constant overburden, occurs with no changes in effective stress and may continue long after primary consolidation ends.

Sediment beds can exhibit either relatively uniform properties over depth, or be stratified with respect to property variations (Parchure and Mehta 1985). The former are usually formed by remoulding previously deposited beds (e.g., following an undrained bed failure), whereas the latter are created by allowing suspended sediments to settle under low flow velocity conditions. The nature of the mine tailings depositional process gives rise to a considerable vertical anisotropy of tailings deposits (Vick 1990). The tailings beds are frequently layered, with percent fines (less than 0.075 mm) varying as much as 10-20% over several inches in thickness. Because of their layered nature, tailings deposits exhibit significant variation in their engineering properties with depth, which causes sediment erosion to occur in discrete steps and layers as the shear stress is increased (Tolhurst et al. 2000). To account for bed anisotropy with depth, many comprehensive numerical erosion models require the bed to be discretized into layers, which allows the bed properties to vary from layer to layer (Mehta et al. 1989). If these models are to be used to predict the erosional resistance of the tailings, knowledge of the strength and density variation with depth in the deposited tailings bed is required.

Bussière (2007) notes that mine tailings exhibit some unique geotechnical properties, which are at least partly responsible for the main environmental problems associated with tailings disposal facilities. The characterization of mine tailings deposits is fundamental for understanding their consolidation and strength behaviour (Zreik et al. 1995) and thus, to further improve the erosion resistance of tailings beds, the stability of the impoundment dykes, the effectiveness of the disposal and long term storage facilities, etc (Zreik et al. 1997; Qui and Sego 2001; Shamsai et al. 2007). Transportation of the tailings in a slurry condition produces tailings mass with initially low in-situ density, high water content and porosity and low mechanical strength (Bussière 2007). The consolidation and strength behaviour of the tailings must be considered during the design of the tailings storage facility in order to evaluate their potential application as a construction material for the dykes of the impoundment; as well as during the operation to estimate the settlement and erosion resistance of the tailings bed. In geotechnical practice different tests can be used to evaluate the shear strength of soils, among which are triaxial (consolidated-drained, CD, and consolidated-undrained, CU) and direct shear tests. However, the stress range in the majority of tailings management facilities is extremely low and varies between 0.5 and 100 kPa (Qui and Sego 2001). Within this range, the sediment and mine tailings deposits exhibit very low shear strength that often cannot be measured using conventional geotechnical techniques (Qui and Sego 2001; Zreik et al. 1995; Zreik et al. 1998). The mechanical properties of freshly deposited Boston Blue Clay sediment beds, and in particular the relationship between water content, effective stress and undrained strength, were studied by Zreik et al. (1997) using a new fall cone device, capable of measuring shear strengths about two orders of magnitude lower than the traditional Swedish fall cone. These authors postulated that the water content, effective stress and time for consolidation are the three most important parameters governing the strength behaviour of cohesive sediments. Mine tailings, however, often differ from naturally occurring cohesive sediments in their physical properties and strength behaviour. For example, most tailings are non-cohesive sandy soils and behave like loose or dense sands rather than like clays. Although previous studies of the geotechnical properties of mine tailings were reported in the literature (e.g., Mittal and Morgenstern 1975; Volpe 1979; Qui and Sego 2001; Shamsai et al. 2007; Newson et al. 1996), they either provided bulk average strength and water content values without capturing the variation of these parameters with depth within the tailings deposit or worked with higher than 1 kPa vertical effective stresses. The objective of the present work was to bridge this gap in the existing knowledge by investigating the variability with depth of the strength properties of mine tailings beds deposited from concentrated slurries and consolidated over different times. The stress range of interest was selected to be below 1.5 kPa.

## 3.2. Testing Materials and Procedures

### *3.2.1. Tailings beds preparation*

Samples of mine tailings were obtained fresh from the mill at the Clarabelle Copper Mine, Sudbury, Ontario. The tailings source (Clarabelle Mine) has been specifically selected for our study because the Sudbury tailings area is one of the largest tailings disposal sites in North America and accommodates about 10% of all tailings in Canada (Shaw et al. 1998). Upon closure, the estimated amount of tailings is expected to reach 720 million tonnes. The original samples were received in the form of tailings/water slurry and were oven dried at a temperature of 105°C, and subsequently pulverized to produce dry tailings powder. Since the oven dried tailings mass exhibited very low cohesiveness, the pulverization required minimum effort and could be done with a spoon. It was believed that it did not cause any particle crushing, and hence, did not alter the initial particle size of the tailings. The grain size distribution curve of the tailings is shown in Figure 3.1 and their index properties are summarized in Table 3.1. Following the plastic limit test procedure defined by ASTM Standard D4318-93 (ASTM 1997b), the tailings were found to be nonplastic and cohesionless. Using the Unified Soil Classification System (ASTM 1997a), they were classified as silty sand with 4% clay-size fraction (less than 2 μm). It should be noted here that with 50% of the tailings particles finer than 0.12 mm diameter ($D_{50}$ of 0.12 mm), the selected tailings material may appear quite coarse; however, this is not unusual for copper tailings (Vick 1990). Such coarse tailings are also representative of the material stored at the Sudbury tailings management facility as shown by Shaw et al. (1998) and McGregor et al. (1998). Additionally, in their study on tailings resuspension, Adu-Wusu et al. (2001) used uranium tailings from the Quirke tailings pond at Elliot Lake, Northern Ontario, for which they reported a $D_{50}$ between 0.10 and 0.17 mm at 7 out of the 9 tailings sampling stations. Therefore, while our results may not apply to every hard rock mine tailings, they provide useful information to many sites that store copper and other tailings types. The mineralogical composition of the Sudbury ore and tailings is well studied and publicised (e.g., Shaw et al. 1998; McGregor et al. 1998). Primary minerals found in the tailings are pentlandite, chalcopyrite, pyrrhotite, quartz, feldspar, chlorite, biotite, amphibole and carbonates plus minor pyroxene, apatite, magnetite, ilmenite, marcasite, galena and pyrite. The tailings powder was mixed with a controlled amount of distilled water in a tailings to water ratio of 1:1.8 to obtain a suspension with 180% water content. Tailings beds with varying thicknesses were deposited from the above suspension using different initial suspension heights. The volume of slurry required to obtain a sediment bed with the desired final thickness was poured into a glass sedimentation cylinder with a diameter of 14.2 cm. The beds were left to consolidate under their self-weight for a period of minimum 3 days. From the results of the sedimentation experiments presented further down in this chapter, the 3 days were deemed sufficient to ensure that the primary consolidation process was complete before testing. All tests were performed at an ambient temperature of 22°±1°C.

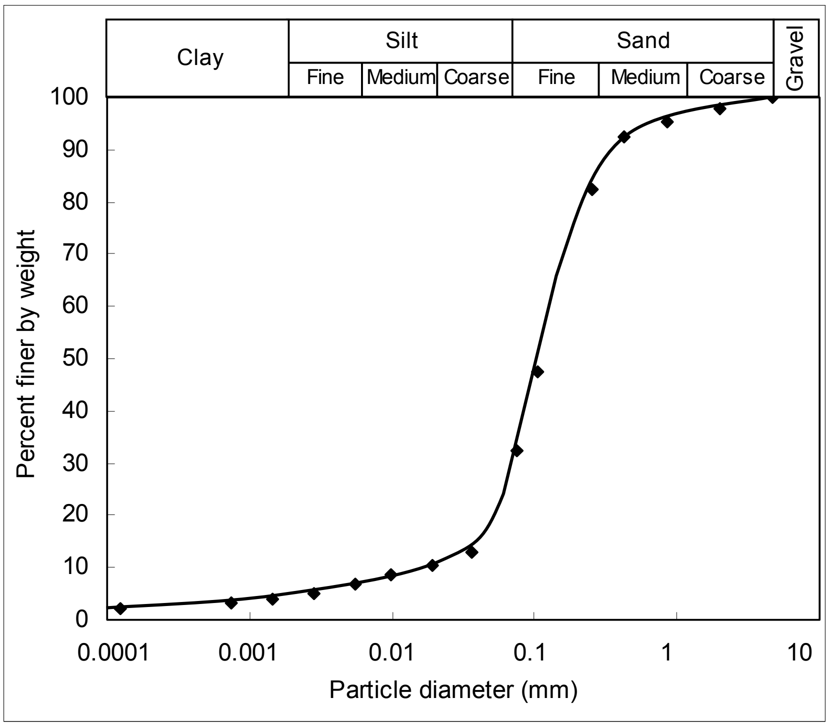


**Figure 3.1.** Grain size distribution curve of the tailings used.

| Parameter | Value |
|---|---|
| Uniformity Coefficient ($C_u$) | 7.89 |
| Coefficient of Gradation ($Cc$) | 1.97 |
| Specific Gravity ($Gs$) | 2.99 |

**Table 3.1.** Index properties of Clarabelle Mine tailings.

### 3.2.2. *Undrained shear strength testing*

Just before the beginning of the undrained shear strength testing the water above the tailings bed was pumped out with a mini pump. The selected pumping rate was the slowest allowed by the mini pump (0.384 L/min) and was believed to cause minimum bed disturbance, i.e., no visible particles dislodgement from the bed surface occurred during pumping. The thin water film remaining on the top of the beds was carefully removed by absorption with paper towels and the exposed surface was tested immediately. The undrained shear strength testing was performed using an Automated fall cone device, first introduced by Zreik et al. (1995) and modified slightly for the present study, as shown in Figure 3.2. The major advantage offered by the device was a counterweight system that allowed the use of cones having a very small effective weight and, thus, measuring undrained shear strengths down to 1.5 Pa. The cone was first positioned at the surface of the soil specimen and allowed to penetrate the soil under its own weight for a specified period of time (5 s). The undrained shear strength, $c_u$, was then calculated from the equation (Hansbo 1957):

$$c_u = \frac{KW}{d^2} \tag{3.1}$$

where *K* is an empirical constant that varies with the cone angle (i.e., cone factor), *W* is the cone weight, and *d* is the depth of cone penetration.

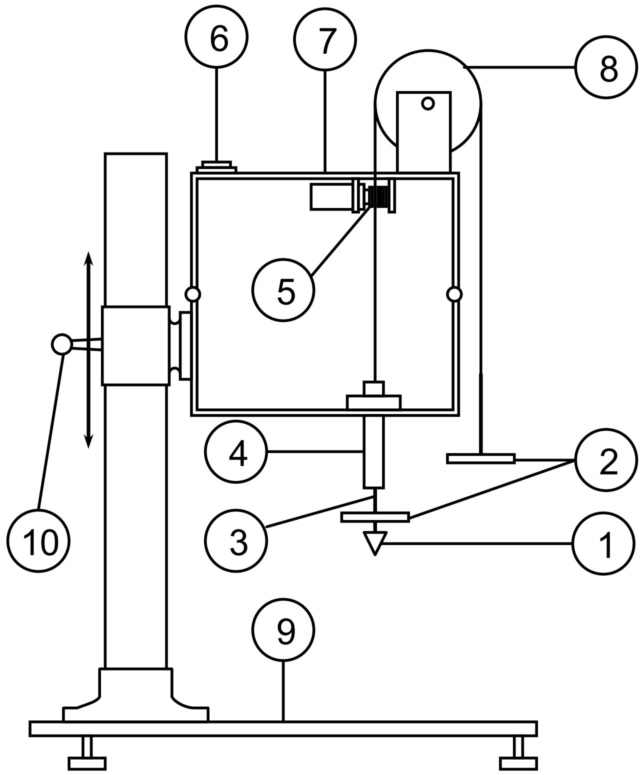


**Figure 3.2.** The Automated fall cone device: 1 cone tip; 2 weight trays; 3 LVDT core; 4 LVDT; 5 electric clamp; 6 level bulb; 7 cone box; 8 pulley; 9 aluminum plate; 10 vertical adjustment handle.

Between 10 and 15 cone drops were used on the tailings bed's surface and the corresponding shear strength values were calculated. The obtained average shear strength value was considered representative of the tested 1 cm thick tailings layer. The mechanical removal of the water film remaining on the surface of the tailings beds resulted in some initial partial desaturation of the top layer, which in turn led to unusually shallow depth of cone penetration in the first 4-5 fall cone drops in comparison with the subsequent drops on the same surface. The loss of water in the top layer, however, was compensated for quickly (within 5 min) through upward drainage from the underlying layers, thus restoring full saturation and from that moment on, the depth of cone penetration in the following 10 cone drops remained almost constant. To minimize the experimental error in the undrained shear strength measurements caused by the initial desaturation of the top layer, the results of the first 4-5 cone drops on the bed's surface were disregarded and only the results of the next 10 measurements were used. Upon completion of the fall cone test, the tested layer was carefully removed with a spatula and set aside for moisture content determination. The exposed surface of the underlying layer was immediately covered with damp paper towels to minimize evaporation and maintain the layer's moisture content. Usually the next fall cone test began within 5 min from the end of the previous one, as this was the time required to perform the water content measurements. Four water content measurements were made for each layer and then averaged. In all performed tests, the average deviation of the shear strength data from their mean value was less than 15%, whereas for the moisture content data it remained within 5%. Obtained average shear strength and average moisture content were attributed to the middle of the tested layer. The above procedure was repeated for each 1 cm thick soil layer within the tested sediment bed. Tests were performed with 60° and 90° apex angle cones weighing between 10 and 200 g. The light-weight cones were used on the weaker beds and layers, usually beds at early formation stage (3 days) and/or surface layers; whereas heavier cones were selected to measure the shear strength of beds at more advanced formation stage (> 3 days) and subsurface layers. At each surface, the cone weight was chosen to yield a penetration depth of 0.3 to 0.6 cm, where the lower limit was set to ensure that the strength value obtained was representative of the entire layer depth (1 cm), whereas the upper limit was imposed to prevent disturbance of the underlying layer. A zone of influence of the cone penetration was defined to have a conical shape with a height equal to the depth of cone penetration and a diameter of three times the diameter of cone imprint on the soil surface (Houlsby 1982). Thus, for the maximum depth of cone penetration (0.6 cm) the calculated diameter of the zone of influence was 2.0 and 3.6 cm for the cones with 60° and 90° apex angle, respectively. When the 60° apex angle cone was used and to ensure that the shear strength measurements were not affected by the test dish walls or previous tests, cone drops were located at a minimum distance of 3 cm from the walls and 2 cm from each other, measured between the cone imprint on the soil surface. For the 90° apex angle cone, these distances were adjusted to 4 cm from the walls as well as from each other.

## 3.3. Results and Discussion

### *3.3.1. Validity of the testing methods*

The tailings used in the present study contained an appreciable (32%) amount of fines (less than 0.075 mm). For soils containing more than 12% fines, the Unified Soil Classification System (ASTM 1997a) prescribes that they are classified according to their plasticity characteristics (liquid and plastic limits) in addition to their gradation. In general, liquid and plastic limits tests are performed on the fraction passing the No. 40 sieve for all soils including gravels, sands, and fine grained soils (Bowles 1986). Current procedures for determining the liquid limits include a variety of methods primarily based on either the Casagrande type devices or on the fall cone apparatus (Farrell 1997; Leroueil and Le Bihan 1996). Many researchers believe that the fall cone test is much more reliable than the conventional liquid limit test, gives excellent repeatability and is easy to perform (e.g., Feng 2000; Prakash and Sridharan 2006). It has been shown that the liquid limits determined by the Casagrande and the fall cone methods show good agreement for liquid limit values up to about 100%, which is the approximate maximum value in most natural soils (Wasti and Bezirci 1985; Leroueil and Le Bihan 1996; Sridharan and Prakash 2000). The theoretical background of the fall cone tests was first developed by Hansbo (1957) who proposed Eq. (3.1) to express the relationship between the undrained shear strength, $c_u$, and the cone penetration. The experimental work by Hansbo (1957) showed an approximately linear relationship between the logarithm of the depth of cone penetration and the logarithm of $c_u$. The approximately linear relationship between the water content and the logarithm of $c_u$ is well established (e.g., Wood and Wroth 1978; Sharma and Bora 2003) and if it is adopted, then it can be shown that the relationship between the water content and the logarithm of depth of cone penetration is also linear (Farrell 1997). The latter conclusion provides the theoretical grounds for the fall cone tests, which already have been adopted as a standard liquid limit test in several European countries, e.g., Great Britain (BS 1377-2 1990) and Sweden (SS 027120 1990), and in the province of Quebec, Canada (CAN/BNQ 2501-092 2006). The preceding discussion aimed at demonstrating the applicability of Eq. (3.1) to the fraction passing the No. 40 sieve of all soils, including the coarse grained ones. For the studied tailings, the fraction passing the No. 40 sieve is about 93%, therefore the authors believe that this percentage is sufficiently high to justify using Eq. (3.1) in the calculation of $c_u$.

The fall cone device (and its modifications) is not only used for liquid limit determination but also for directly measuring the undrained shear strength of a soil, since it is, in fact, an undrained strength test (Farrell 1997; Feng 2000; Sridharan and Prakash

2000; Prakash and Sridharan 2006). The undrained shear strength, $c_u$ is determined from Eq. (3.1) as a function of the depth of cone penetration. Wasti and Bezirci (1985) compared the undrained shear strength values obtained from fall cone tests with those from a laboratory vane test for four natural and artificial soils and concluded that the agreement between the two sets of strength data is quite satisfactory. Sridharan and Prakash (2000) performed a detailed study of the controlling mechanism that is operative during the cone penetration test in a number of soils ranging from fine sands to clays. The undrained shear strength of a soil has two components, namely undrained cohesion and undrained friction. Whereas the undrained cohesion arises out of viscous diffuse double layer, the undrained friction is due to the interparticle attractive forces (i.e., soil fabric). Depending on the clay content and clay mineralogy, one of these components essentially controls the undrained strength behaviour of the soil (Sridharan and Prakash 1999, 2000). For less plastic and nonplastic soils with low clay content, the cone penetration method measures the undrained strength mainly contributed by undrained friction. Another factor that influences the undrained shear strength mobilized during the fall cone test is the rate of load application. When the liquid limit decreases to below 30%, the permeability of the soil becomes relatively high, leading to a partially drained condition during the Casagrande test, but in the cone test it is still in an undrained condition due to the fast rate of loading (Feng 2002).

### *3.3.2. Settling behaviour and consolidation*

The settling behaviour of Clarabelle mine tailings slurries, prepared at 180% water content, was observed by performing sedimentation experiments in 1000 cm$^3$ graduated cylinders with a diameter of 6 cm. The initial slurry heights were selected to correspond to those used in the preparation of the actual deposited sediment beds, that was between 33.2 and 6.2 cm. Figure 3.3 shows sedimentation curves for five slurries with various initial heights plotted on a logarithmic time scale.

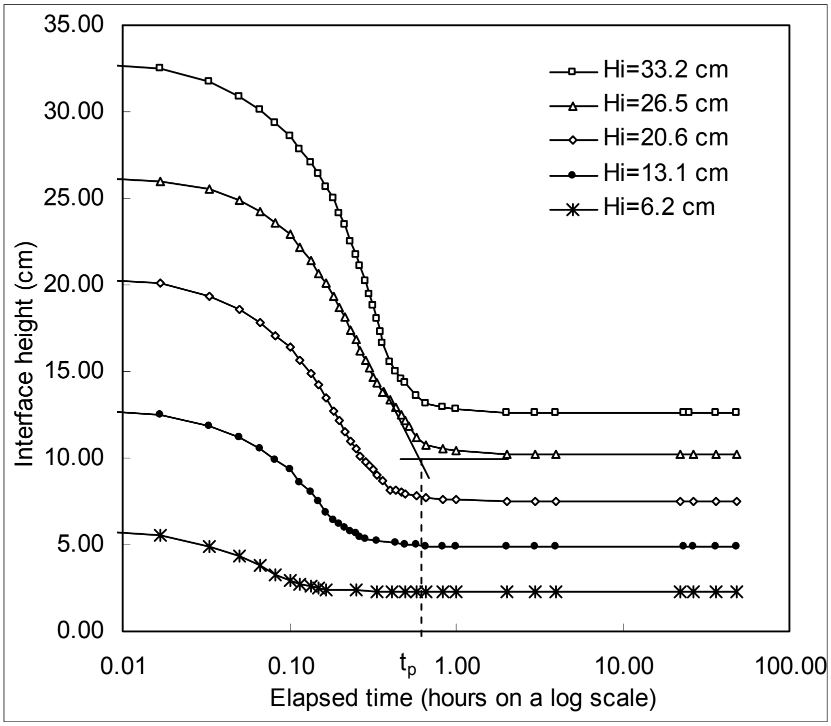


**Figure 3.3.** Interface height versus time for mine tailings slurries with various heights prepared at 180% water content.

As soon as the mixing of the slurry was terminated, the coarser particles settled quickly to the bottom of the cylinder initiating the formation of a deposited sediment bed. Zones of hindered settling and consolidation were immediately formed. For all slurry heights, the bed reached 90% of its final thickness within the first 3 minutes of the test. Concurrently, a well defined interface formed quickly between the finer particles and the clear water, which advanced to the bottom of the cylinder with decreasing speed. Referring to Figure 3.3, an abrupt change in the slope of the plots is evident at about 0.12

to 0.17 hours from the beginning of the test and marks the end of the settling phase and the beginning of the primary consolidation phase. The primary consolidation of the newly formed bed continued for about one hour for all tested deposited beds. During this stage the self weight of the tailings is initially carried by the pore water, which results in the development of excess pore water pressure. After some elapsed time, the excess pore water pressure dissipates via expulsion of pore water and the load from the tailings self weight is transferred to the soil skeleton as effective stress. Another change in the slope of the curves delineates the end of the primary consolidation and the beginning of the secondary compression phase. Recalling that the studied tailings are a noncohesive coarse grained soil, a short time for primary consolidation is expected because of their high hydraulic conductivity and rapid draining characteristics. Secondary compression occurs after complete dissipation of the excess pore water pressure, i.e., at constant effective stress, when some deformation of the bed takes place because of the plastic readjustment of soil fabric. The time, $t_p$, corresponding to the end of primary consolidation and beginning of secondary compression was determined from the intersection of the lines tangent to the last two segments of the plot. The method involving determination of $t_p$ from the sedimentation curves (interface height versus logarithm of time) has been previously described in the literature, e.g., Imai (1981), Zreik et al. (1997). Although it is not based on direct pore water pressure measurements, the results of Alexis et al. (2004) for example, show that there is a good agreement between the time for primary consolidation estimated from the interface height versus logarithm of time plots, and that determined from excess pore water pressure measurements. Once the primary consolidation of the deposited bed was complete, no further decrease of the bed thickness was observed, which led to the conclusion that volume changes during the secondary compression phase were negligible as expected for a coarse grained soil. The end of primary consolidation and the lack of subsequent volume changes prompted the termination of the sedimentation experiments after elapsed 48 hours from the beginning of tests.

The tailings beds used in the present study were deposited from slurries with moderate concentrations of solids (16% by volume), characterized by a high percentage of coarse particles (68%) with an irregular shape, typical for hard-rock tailings. The visual inspection showed that the beds comprised two portions: a relatively uniform lower and thicker layer of coarser particles and a capping layer of fines. This capping layer had a thickness of 0.5 – 1.0 cm and differed from the rest of the bed in a way that it had a lighter colour and finer texture. Thus, at the end of settling and primary consolidation phases, two interfaces were observed in the sedimentation column: one between the tailings beds and the clear water, and a second between the capping layer of finer particles and the remaining bed. It was believed that the tailings beds formed according to the following settling mechanism, for slurries with moderate to high solid concentrations. The segregation of particles in sediment beds deposited from unflocculated slurries is strongly affected by slurry solids concentration in addition to particle size and shape (Davies 1968). Particles segregate and settle according to their size at low concentrations, whereas at higher concentrations, particle segregation and settling are modified by hydrodynamic interactions among particles. In slurries with moderate to high concentrations, hindered settling is observed and Stokes' law cannot be used to predict the settling velocities. Coarser particles (more than 0.075 mm) settle with minimum to no segregation, unlike finer particles (less than 0.075 mm), which undergo considerable segregation during settling (Imai 1981). The segregation of particles during settling is suppressed if a wide range of particle sizes are present in the solid phase and if the particle shape is irregular (Davies 1968). Settling of larger particles displaces fluid and causes counterflow through the pore spaces of the larger particle matrix. This counterflow of draining water elutriates the finer particles up through the pores and permits them to concentrate at the surface of the bed. Sediment deposits formed by settling from slurries with moderate to high concentrations are relatively unsorted and capped by a thin layer of elutriated fines. The capping layer of fines, with its low permeability, offers the benefit of minimizing drainage from the underlying coarser layers and thus, ensures that desaturation of the bed does not occur prior to the subequent testing. The initial slurry concentration, used in this study, was chosen in order to yield a deposit capped by a layer of fines.

The settling of tailings particles from tailings/water slurries takes place in a cylinder of finite dimensions that has some effect on the sedimenting velocity. This effect is related to the size of solids relative to the container, *d/D*, and is more relevant for dilute systems (concentration less than 10% by volume) where particle-particle and particle-wall hydrodynamic interaction effects could be of the same order (Di Felice and Parodi 1996; Chong et al. 1979). The sedimentation velocity of concentrated multiparticle suspensions is well described by the empirical Richardson and Zaki (1954) equation for hindered settling:

$$\frac{u_t}{u_{t\infty}} = k\,\varepsilon^n \tag{3.2}$$

where $u_t$ is the terminal settlings velocity of particles in suspension, $u_{t\infty}$ is the terminal settling velocity of particles in infinite medium; *k* and *n* are empirical parameters; $\varepsilon$ = 1-*c*, is the porosity of the suspension, where *c* is the suspension concentration by volume.

For sedimentation in viscous flow, Richardson and Zaki (1954) report parameter *k* always equal to unity, and propose correlation of *n* with *d/D* which takes the form:

$$n = 4.65 + 19.5d / D \tag{3.3}$$

In the present study, when the geometric mean particle size is used, the ratio *d/D* is equal to 0.002 and the slurry porosity, $\varepsilon$, is 0.84. The parameter, *n* is calculated from Eq. (3.3) as 4.689, and the ratio, $u_t / u_{t\infty}$ between the terminal settling velocity of particles in suspension and in infinite medium (Eq. 3.2) is equal to 0.442. To investigate the effect of the side walls of the container on $u_t / u_{t\infty}$, the diameter of the settling cylinder was hypothetically increased to 600 mm, and the above calculations were repeated. It was found that the ten fold increase in container size resulted in only 0.4% increase in $u_t / u_{t\infty}$ ratio. Therefore, it was concluded that the wall effect had negligible influence on the settling velocity of the tailings particles in the suspensions used. Furthermore, the wall effects at high concentrations predicted by the Richardson and Zaki (1954) equation (Eq. 3.2) were not confirmed by successive work, as for example that of Chong et al. (1979) and Di Felice and Parodi (1996). These two studies demonstrated that for concentrated systems (suspension porosity up to around 0.95), the wall hardly affects the parameter, *n* at all, and its value remains roughly constant between 4.6 and 4.9. Similarly, they found *k* also to be independent from *d/D*.

### *3.3.3. Compression curves*

Similar to cohesive sediments, the consolidation of noncohesive sediments occurs through compaction of the soil mass accompanied by drainage of the pore water held in the pore spaces. Drainage is through the bed surface, into the ambient water. The rate of consolidation is governed by the length and cross sectional area of the drainage path. Whereas in cohesive sediments, the drainage path length is long and the area is small, in noncohesive sediments, due to their high permeability, the path length is short and drainage occurs through larger pore spaces. Thus, in noncohesive sediments drainage is faster leading to shorter time for consolidation. The dissipation of the excess pore water pressure under pressure gradient starts at the surface of the bed and proceeds to its bottom where the drainage path is longest. In the work of Jeeravipoolvarn et al. (2009), it has been demonstrated that when tailings contain a high percentage of sand (82% and above), it acts as an internal surcharge within the soil matrix and causes faster rate of compression. The tailings/water slurry behaves like a normal soil and significant excess pore water pressure dissipation starts immediately after pouring the slurry into the sedimentation column. The finite strain consolidation theory (Gibson et al. 1967, 1981) can successfuly be applied to predict the consolidation behaviour of such tailings. The high sand content also minimizes the segregation of the soil matrix and subdues the time-dependent effects of thixotropy and creep. Consequently, volume decrease by creep compression does not appear significant and thixotropic strength gain is not observed (Jeeravipoolvarn et al. 2009).

The variation of the water content (and void ratio) with depth below surface for Clarabelle mine tailings beds aged at 3 and 12 days is shown in Figures 3.4a and b. All beds were deposited from a 180% -water content slurry and their final thickness varied between 3.3 and 10.1 cm.

a)

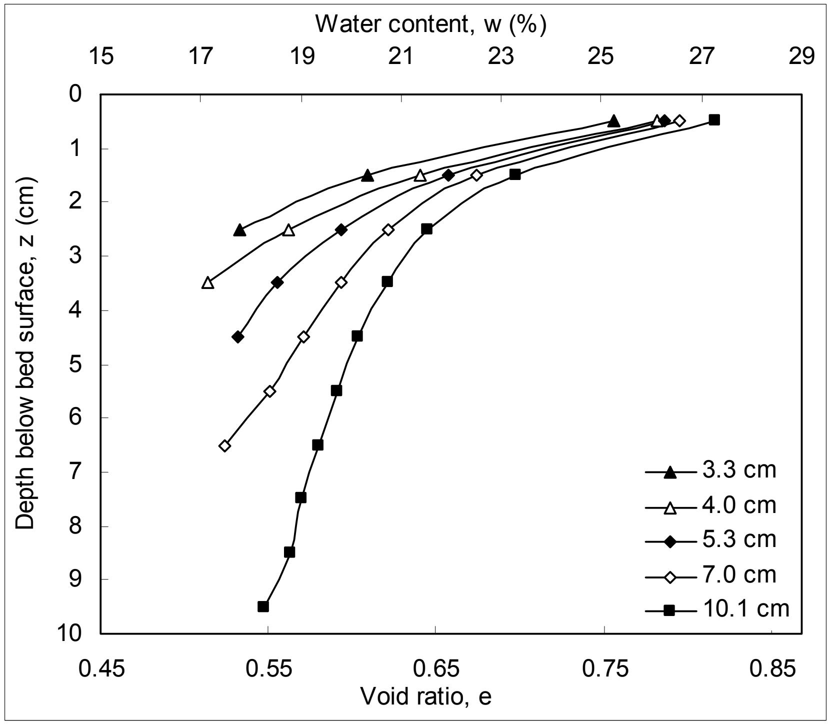


b)

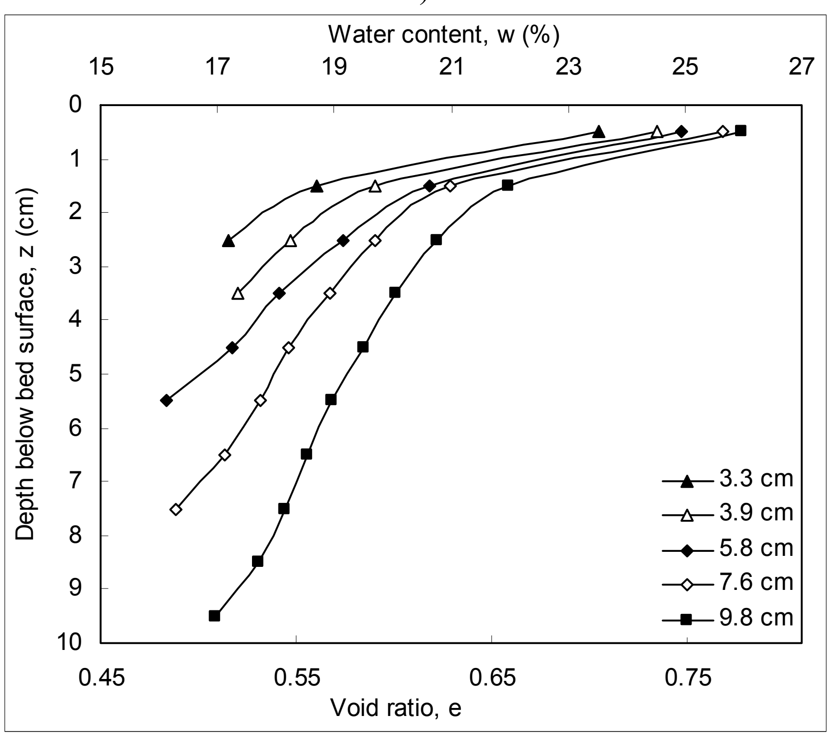


**Figure 3.4.** Water content profiles of mine tailings beds with different thicknesses consolidated for: (a) 3 days; and (b) 12 days.

Referring to Figure 3.4a and b, the void ratio varies between 0.48 and 0.78, which compares well with the void ratio of 0.6 - 0.8 reported by Volpe (1979) for copper sandy tailings and by Jeeravipoolvarn et al. (2009) for tailings/sand mixtures. For all tested beds, the top 1 cm-thick layer exhibits the highest water content and void ratio, with both quantities decreasing with depth below the bed surface. The rate of water content decrease with depth is highest within the top layer and relatively constant further down. This is believed to be caused by some particle segregation during the sedimentation phase, whereby the finest clay and silt particles settle according to the mechanism described in the previous section and form the top layer of the bed. Thus, the composition of this top layer differs from the rest of the bed in such a way that it contains a higher concentration of fines, thereby resulting in higher void ratio and water content. Beneath the capping fine grained layer, the variation in the void ratio with depth is not appreciable and the plots are steeper, which supports the hypothesis of relatively limited particle sorting within that portion of the tailings bed. Whereas the difference between the void ratio of the capping layer and the remaining bed can be attributed to particle segregation, the variation in the void ratio within the relatively homogeneous coarse layer can be attributed to self-weight consolidation of the bed (Sridharan and Prakash 2003). Although the data presented in Figures 3.4a and b refer to 3 and 12 days old beds, tests were also performed with beds aged 6, 18 and 46 days. Little variation in the water content profiles of the beds was noted regardless of the beds' age and thickness. For example, for the 9 - 10 cm beds, there was only about 2% decrease in the water content of the 46 days old compared to the 3 days old beds, which could be attributed to the secondary compression but might also be due to experimental variations. Accurate interpretation of the water content profiles, however, was hindered by the fact that the removal of the water film remaining on the surface of the beds was mechanical (by hand and paper towels) and could not ensure completely uniform pre-testing conditions.

Figures 3.5a and b present the respective variation of the vertical effective stress with water content for the same beds shown in Figures 3.4a and b.

a)

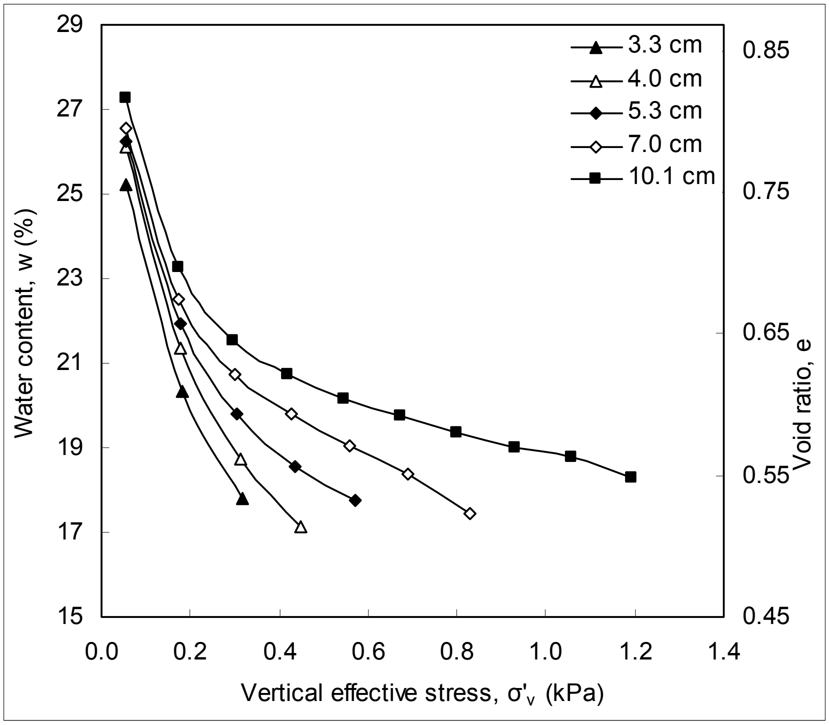


b)

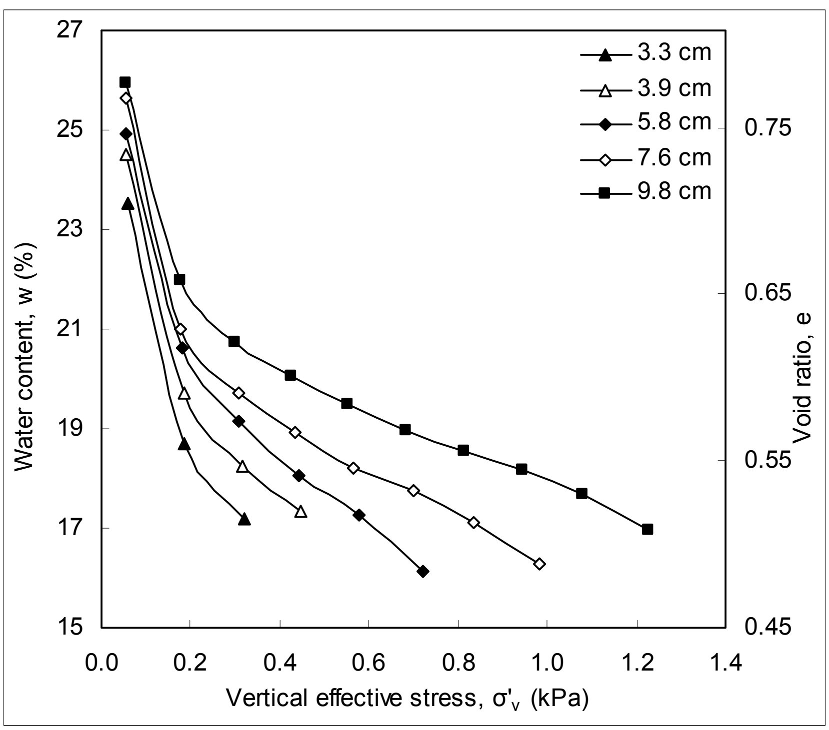


**Figure 3.5.** Variation of vertical effective stress with water content for mine tailings beds with different thicknesses consolidated for: (a) 3 days; and (b) 12 days.

During the calculation of the vertical effective stress, $\sigma'_v$, it was assumed that primary consolidation of the bed was complete and hence, excess pore pressure was dissipated prior to testing. The pore pressure at any given point in the tailings bed, therefore, was considered equal to the hydrostatic pressure at that point. This assumption was based on the results of sedimentation experiments performed with beds deposited in the same manner (Figure 3.3), which showed that primary consolidation of all tested beds was complete within less than an hour.

Another important assumption that was made is that the soil is fully saturated and remains so for the duration of the test. Additionally, although the first series of fall cone tests were actually performed on the surface of the bed, the obtained results were attributed to the middle rather than to the top of the first 1 cm-thick layer and thus, all presented plots start with a greater than zero $\sigma'_v$ value.

As can be seen in Figures 3.5a and b, in all beds as the water content and void ratio decrease with depth below bed surface, the vertical effective stress increases. Referring to Figures 3.5a and b, presented data suggest that the relationship between the void ratio and vertical effective stress is not unique for the studied mine tailings and that it varies from bed to bed depending on bed thickness and age. For example, at 12 days of age (Figure 3.5b), a void ratio of 0.6 corresponds to effective stresses of 0.15 and 0.43 kPa for the 3.3 and 9.8 cm thick beds, respectively. Similarly, at 3 days (Figure 3.5a), the same void ratio of 0.6 corresponds to effective stresses of 0.19 and 0.51 kPa for the 3.3 and 10.1 cm-thick beds, respectively. This observation is in agreement with the results of other researchers, suggesting that multiple compression curves exist when sediment beds are tested in the very low effective stress range (Imai 1981; Elder and Sills 1985; Zreik et al. 1997). The formation of sedimented beds from slurries is a complex process, influenced by the initial rate of bed deposition as well as by consolidation. Elder and Sills (1985) investigated specifically the effect of deposition rate on the final density of the sedimented bed and concluded that the slower the deposition rate, the more open the fabric of the bed, i.e., the higher the void ratio at a given effective stress. Considering that in the present study, the beds with higher final thickness were formed more slowly than the thinner beds (Figure 3.3), this might explain why at a given depth the thinner beds exhibited lower water content and void ratio than the thicker ones. Another possible explanation for the observed multiple compression curves may be in the experimental procedure. Despite measures employed by the authors to maintain full saturation of the tailings beds throughout the tests (e.g., rapid testing, covering the surface of the beds with damp towels between tests), due to the material's high permeability, some drainage and consequently, desaturation probably still occurred. Thus, the beds of different thicknesses would appear to have different water contents and void ratios at a given effective stress.

### *3.3.4. Undrained shear strength*

Undrained shear strength tests were performed on tailings beds with thicknesses between 3.3 and 10.1 cm consolidated for 3, 6, 12, 18, and 46 days. All beds were deposited from slurries with water content of 180%. Figures 3.6 to 3.8 present the results obtained for 3 and 12 days old beds as these results have been considered representative of the trends identified for the newly formed (3 days) and consolidated (12 days) beds.

a)

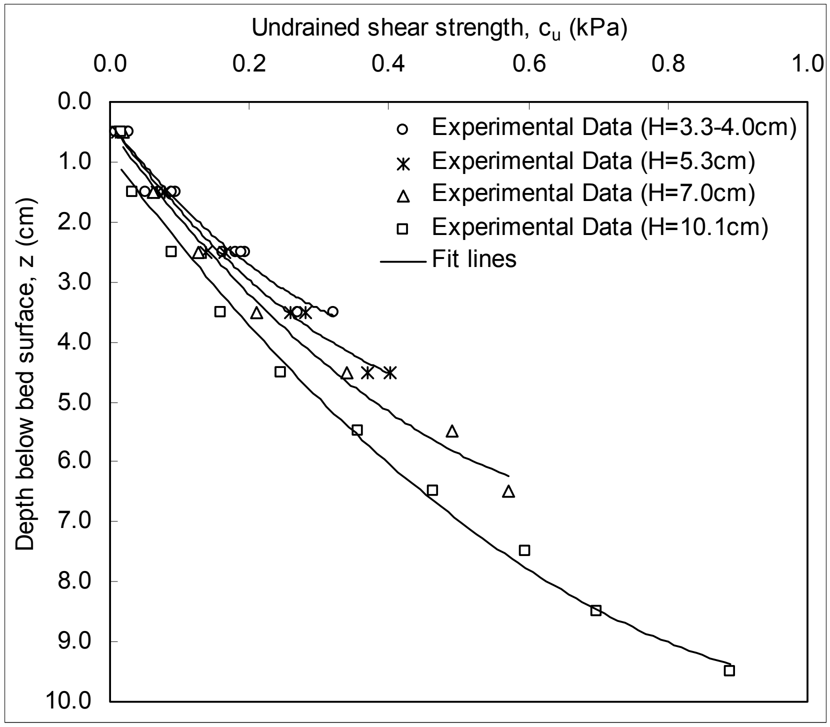


b)

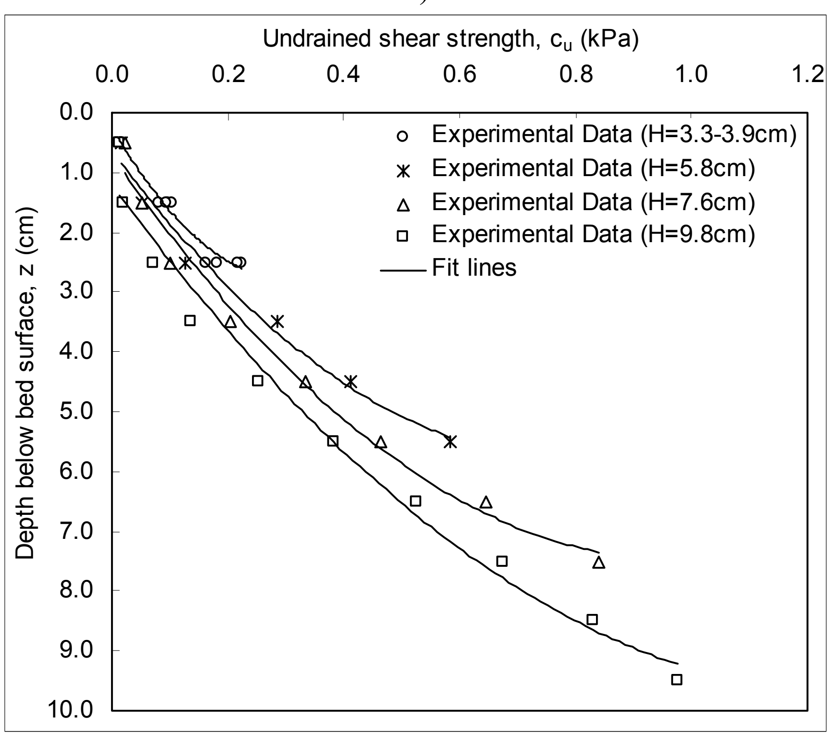


**Figure 3.6.** Undrained shear strength profiles of mine tailings beds with different thicknesses consolidated for: (a) 3 days; and (b) 12 days.

a)

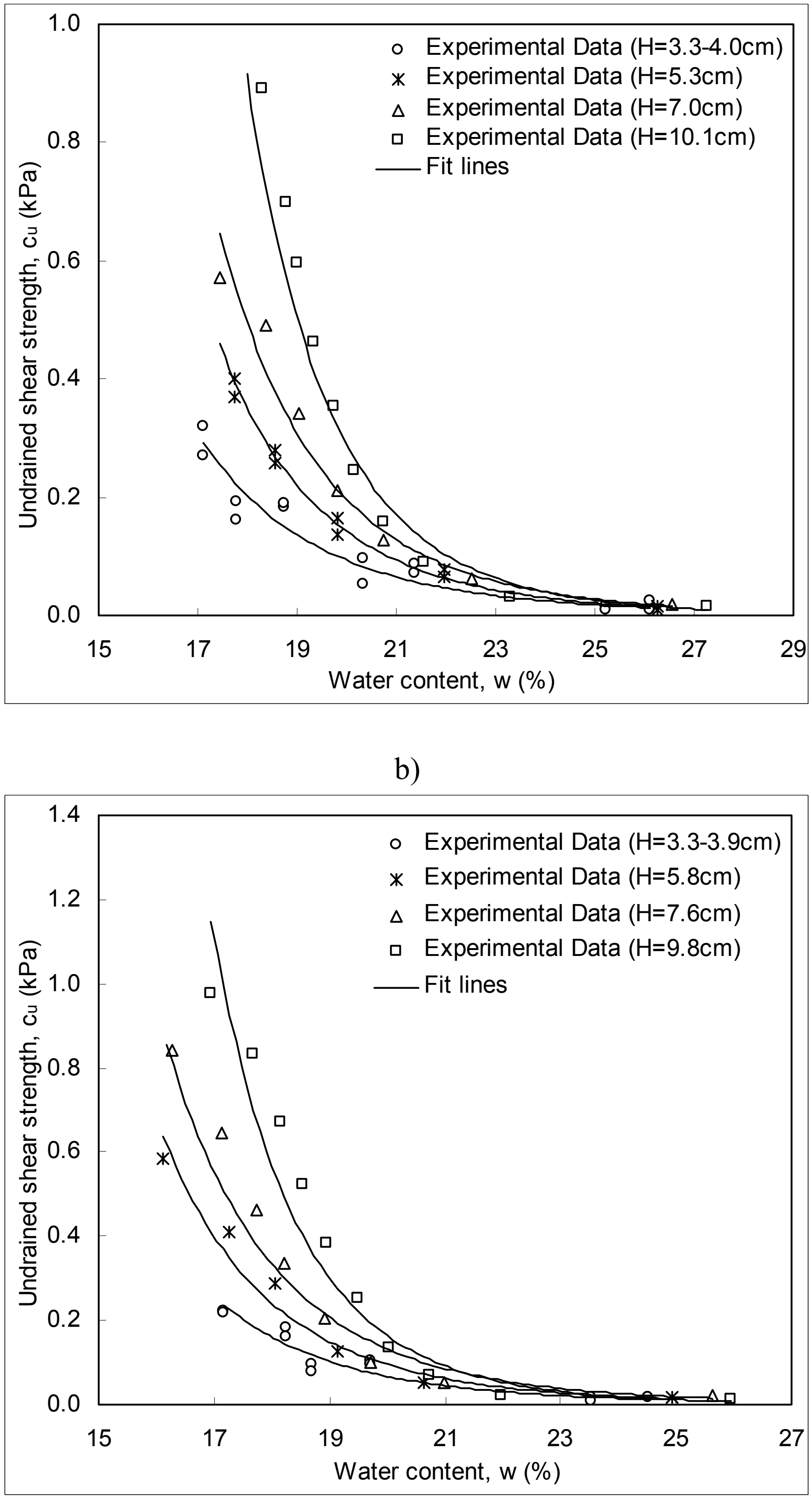


b)



**Figure 3.7.** Variation of undrained shear strength with water content for mine tailings beds with different thicknesses consolidated for: (a) 3 days; and (b) 12 days.

a)

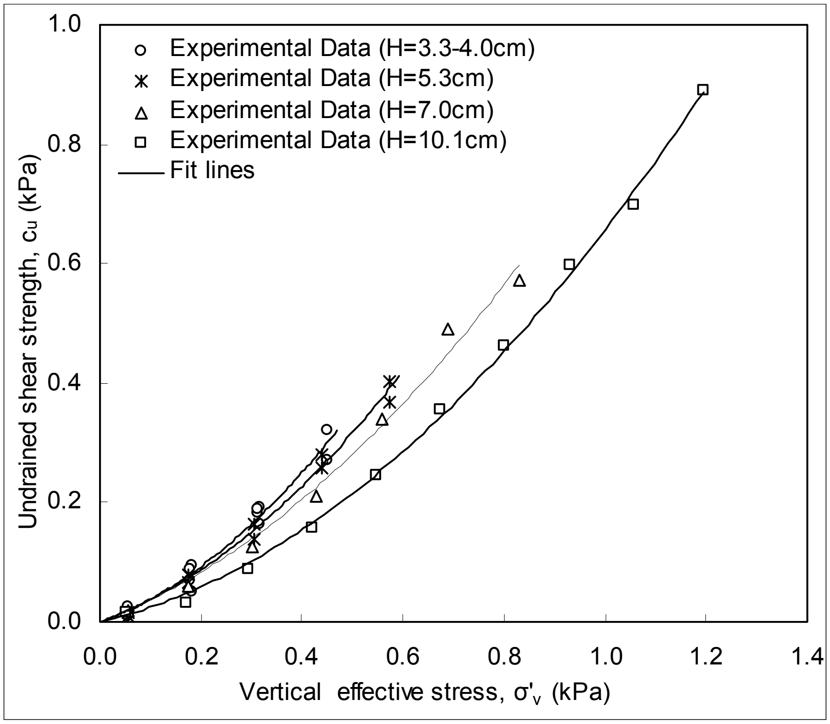


b)

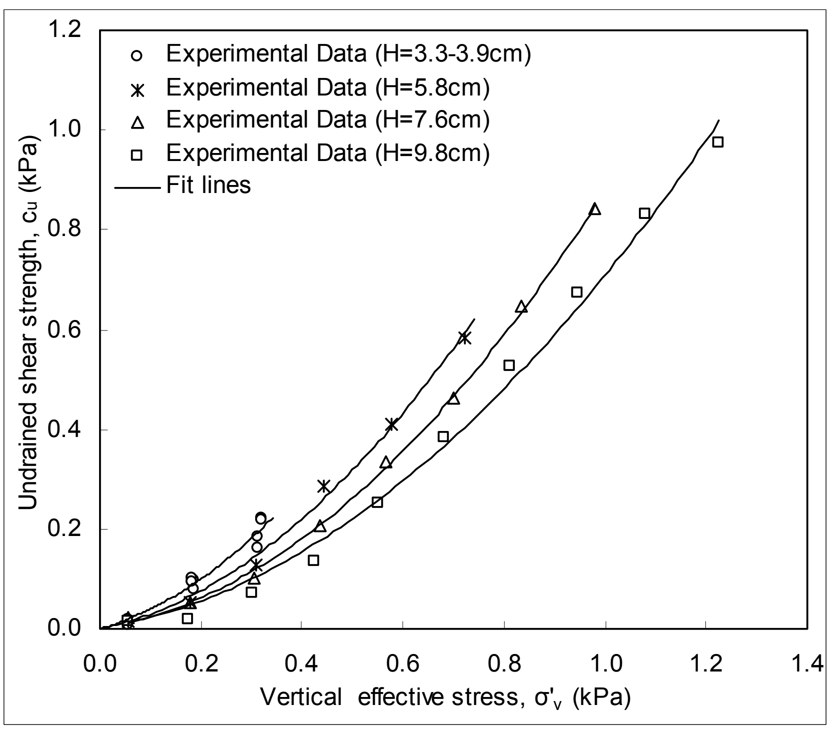


**Figure 3.8.** Undrained shear strength versus vertical effective stress for mine tailings beds with different thicknesses consolidated for: (a) 3 days; and (b) 12 days.

Figures 3.6a and b show the variation of the undrained shear strength, $c_u$, with depth below surface of the tailings bed. The experimental data points for the thinner beds, i.e., 3.3 and 4.0 cm (Figure 3.6a) and 3.3 and 3.9 cm (Figure 3.6b) were combined for easier reading of the plots and fitted with a single second order polynomial trend line. The experimental data points obtained for beds of all thicknesses were fitted with individual trend lines of the same type. The *R*-squared (correlation factor) values for the fit lines fall between 0.96 and 0.99. From Figures 3.6a and b it can be seen that the undrained shear strength, $c_u$, increases with depth below the surface for all tested beds consolidated for 3 and 12 days. This trend can be easily explained with the corresponding water content decrease with depth (Figures 3.4a and b) and effective stress increase with water content decrease (Figures 3.5a and b). Moreover, the $c_u$ profiles of the tested beds are very similar regardless of the bed thickness and age. At a particular depth, the largest shear strength is observed in the thinner beds, whereas the lowest is recorded in the thicker ones, which is consistent with the results obtained by Zreik et al. (1997) for cohesive Boston Blue Clay deposited beds.

In Figures 3.7a and b the undrained shear strength is plotted as a function of the water content. The experimental data points were fitted with power-law trend lines with *R*-squared values falling between 0.91 and 0.99. The plot at 3 days (Figure 3.7a) shows that at a water content of approximately 25% and above, the shear strength becomes independent of the bed thickness, whereas for lower water content values it is larger for the thicker beds compared to the thinner ones. Similarly, for the beds consolidated for 12 days the water content at which the shear strength plots for the beds of various thicknesses converge is 23% (Figure 3.7b).

Figures 3.8a and b represent the relationship between the undrained shear strength and vertical effective stress for the tested mine tailings beds. Polynomial trend lines with *R*-squared values of above 0.97 were used to successfully fit the obtained experimental results. Referring to Figures 3.8a and b, at the same magnitude of the vertical effective stress the undrained shear strength increases with decreasing bed thickness. This trend is consistent with the lower water content observed for the thinner beds in comparison with the thicker ones at the same effective stress. In addition, when approaching the lowest vertical effective stress, the plots corresponding to beds with different thicknesses converge about 0.16 and 0.1 kPa for the 3 and 12 days old beds, respectively. In contrast, at higher effective stress range a large variation in the undrained strength of beds with various thicknesses is notable, probably because of the higher differences between the water contents recorded at the same vertical effective stresses within this range.

Similar experimental results were obtained for mine tailings beds aged at 6, 18 and 46 days. A common trend identified for beds of all ages is that the water content at a given depth decreases with decreasing bed thickness, whereas the undrained shear strength decreases with increasing bed thickness. As discussed in the previous section, the variation of the water content at a given depth in the beds with different thicknesses might be due to either bed deposition rate or drainage during testing. Undrained shear strength at the same depth would also vary as a consequence of the water content changes.

### *3.3.5. Dependence of the undrained shear strength on water content and effective stress*

Zreik et al. (1997) postulated that for newly formed Boston Blue Clay beds (3 days) the strength is more sensitive to variations in the water content than in the effective stress, while the opposite trend is evident for the beds at later stages of formation (6 days). To investigate the validity of the findings of Zreik et al. (1997) with respect to mine tailings, the undrained shear strength values of all tested beds at a given age were plotted as a function of water content (Figures 3.9a and b) and vertical effective stress (Figures 3.10a and b) without consideration of specific bed heights.

a)

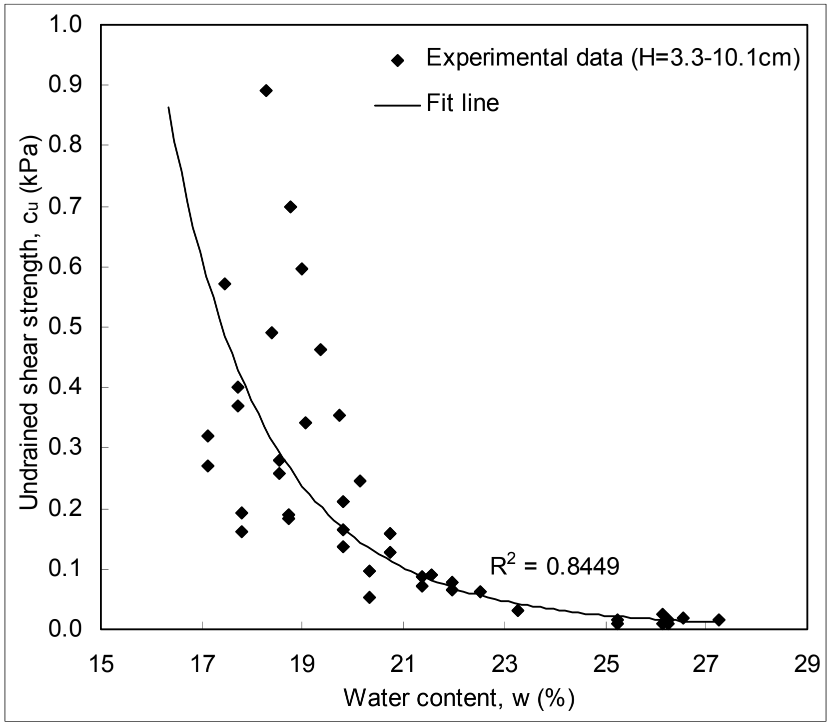


b)

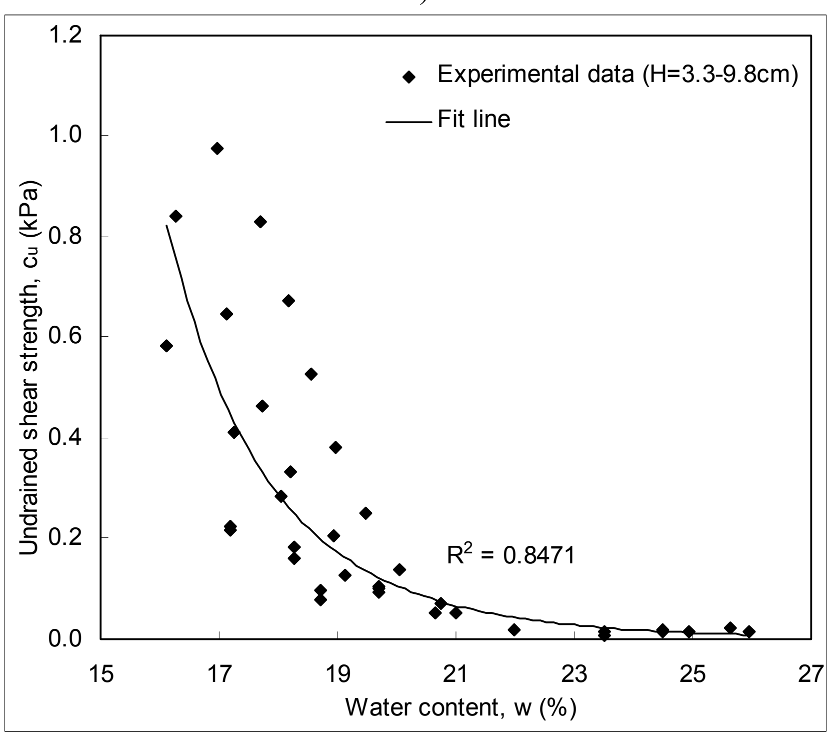


**Figure 3.9.** Variation of undrained shear strength with water content for mine tailings beds consolidated for: (a) 3 days; and (b) 12 days.

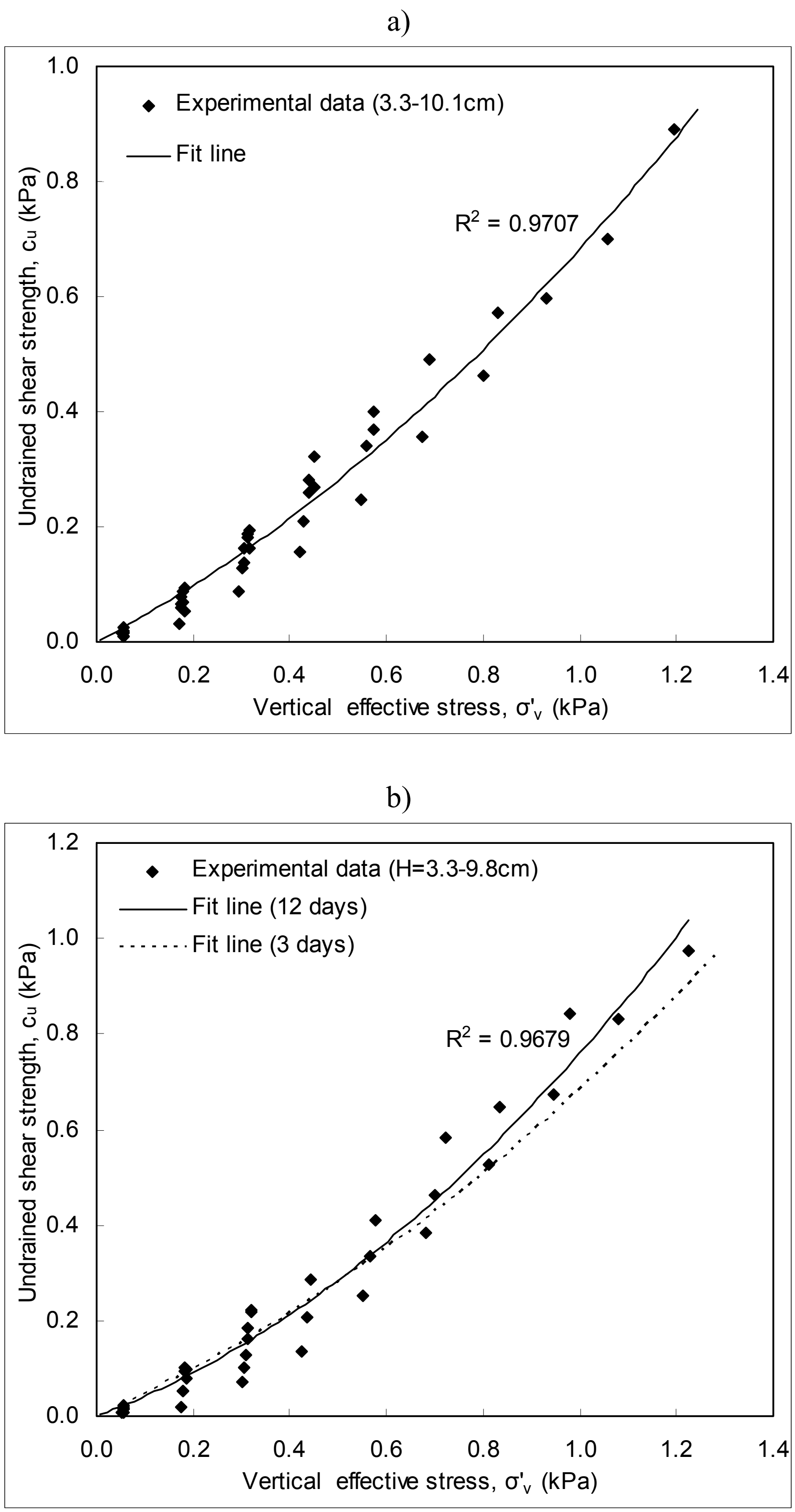


**Figure 3.10.** Variation of undrained shear strength with vertical effective stress for mine tailings beds consolidated for: (a) 3 days; and (b) 12 days.

Referring to Figures 3.9a and b, it can be seen that there is a substantial scatter of experimental data for beds of both ages allowing for a fit with relatively low correlation factor, that is 0.84 and 0.85 for the 3 and 12 days old beds, respectively. In contrast, when the undrained shear strength was plotted as a function of the vertical effective stress as shown in Figures 3.10a and b, the experimental data produced a very small scatter. A second order polynomial fit line was used to fit both the 3 and 12 days old beds data points with a high correlation factor of 0.97. The equations of the fit lines for the 3 and 12 days old beds, respectively, are:

a) $c_u(kPa) = 0.24\sigma'^{\,2}_v + 0.44\sigma'_v$ (3.4)

b) $c_u(kPa) = 0.39\sigma'^{\,2}_v + 0.37\sigma'_v$ (3.5)

Obtained results demonstrate that for the tested mine tailings beds the undrained shear strength is primarily a function of the vertical effective stress regardless of the time for consolidation. Although, the strength is clearly dependent on the water content as well, that is, decreases with water content increase, this dependence is secondary and there is no direct correlation between the undrained shear strength and the water content. The above discussed dependence of the undrained shear strength on the vertical effective stress extends to the relatively homogeneous thick coarse grained layer within the bed. The authors believe, however, that the capping layer of fines behaves differently from the rest of the bed. Within this layer, the undrained shear strength is controlled by the water content, as a function of the soil fabric, rather than by the vertical effective stress, which is a function of the bed thickness. This hypothesis is supported by the observation that at the highest water contents (i.e., above 25% and 23% for the 3 and 12 days old beds, respectively), measured in the capping layer of the beds, the undrained shear strength becomes independent of the bed thickness (Figures 3.7a and b). Also, as evident from Figures 3.9a and b, at these high water contents the experimental data show minimum scatter confirming the dependence of $c_u$ on $w$.

Based on field vane test results, Skempton (1957) established an empirical correlation relating the undrained shear strength of normally consolidated clays, $c_u$, to the effective preconsolidation pressure, $\sigma'_p$, and the Plasticity index , $I_P$:

$$c_u/\sigma'_p = 0.11 + 0.0037(I_P) \tag{3.6}$$

For inorganic soft clays and silts, independent of plasticity index and overconsolidation ratio, Mesri (1975) suggested the following relationship between the undrained shear strength mobilized on the failure surface in the field, $c_u(mob)$, and the effective preconsolidation pressure of the layer where the failure occurred, $\sigma'_p$, obtained from the standard oedometer test:

$$c_u(mob)/\sigma'_p = 0.22 \tag{3.7}$$

The above relationship (Eq. 3.7) was derived on the basis of the results from laboratory triaxial compression tests on inorganic clayey soils, showing that:

$$c_u(TC)/\sigma'_p = 0.31 \tag{3.8}$$

where $c_u(TC)$ is the undrained shear strength measured during triaxial compression.

Mesri (1989, 2001) pointed out that the undrained shear strength from the laboratory tests is not equal to the undrained shear strength that is mobilized in full-scale field failure situations and must be corrected with a factor accounting for the variations in the time-to-failure during triaxial testing and in the field. Keeping in mind that for a normally consolidated soil $\sigma'_p = \sigma'_v$, all the Eqs. (3.6), (3.7) and (3.8) suggest a linear relationship between the undrained shear strength and the vertical effective stress for inorganic clays and silts. In contrast to natural soils, even at relatively low applied stress, stresses at the point-to-point contacts of the angular tailings grains are very high, producing particle crushing (Vick 1990). The result is often curvature of the strength envelope, especially at low applied stresses. In illustration, Vick (1990) reported a zero cohesion intercept and a particularly pronounced envelope curvature for loose tailings sand in the stress range of 0 to 143 kPa. The undrained shear strength testing using the fall cone implicitly accounts for the excess pore pressured generated by rapidly applied shear stress and the obtained undrained cohesion and friction angle are total stress parameters. As shown in Figures 3.10a and b, zero cohesion and curved undrained (total) strength envelopes were obtained for the studied mine tailings. It is worth noting here, that any deviation from the assumed fully saturated conditions during the fall cone testing would affect the relationship between the vertical effective stress and the undrained shear strength. Thus, the ratio $c_u/\sigma'_p$ woud appear unusually high and the undrained strength envelope would be curved. The observed non-linear relationship between $c_u$ and $\sigma'_v$ in the present study may be due to multiple factors, i.e., particle crushing, drainage during testing or a combination of both.

Referring to Figure 3.10b, it can be seen that the fit line for 3 days old beds is slightly lower than that for the 12 days whereby the difference between 3 and 12 days lines becomes more pronounced at higher vertical effective stresses. This suggests that for the tested mine tailings beds, time of consolidation has little effect on the undrained shear strength. Such observation can be explained by revisiting the results form the sedimentation experiments (Figure 3.3). Since the observed volume changes during secondary compression were negligible, it can be concluded that almost no additional particle rearrangement occurs during this phase resulting in minimum or no strength gain with time for consolidation.

In a study of the behaviour of deposited Boston Blue Clay sediment beds, Zreik et al. (1997) also noted a consistent trend of strength gain with time which they attributed to thixotropy. Thixotropy is the property of certain clays to regain, if kept in undisturbed state, part of the strength lost due to remoulding, at constant water content (Ranjan and Rao 2000). The phenomenon of thixotropy is explained with the tendency of cohesive soils to regain their chemical equilibrium, with the reorientation of water molecules in the adsorbed water layer. The tested mine tailings, however, represent a coarse grained, noncohesive soil, and therefore a thixotropic strength gain effect should not be expected. Indeed, if the undrained shear strength of beds aged at 3 days is compared to the strength of those aged at 12 days at constant water content (for example at 20%) and the same vertical effective stress, the following results are obtained. For the 3-4 cm and 5-6 cm-thick beds, the undrained shear strength is slightly lower in the 12 days in comparison to the 3 days old beds. The beds with thickness 7-8 cm demonstrate almost identical shear strengths at 3 and 12 days, whereas the thickest beds (9-10 cm) show larger undrained strength at 12 days (Figures 3.9a and b, and Figures 3.10a and b). These results indicate that the undrained shear strength of the deposited mine tailings beds is mainly determined by the bed thickness as it governs the vertical effective stress. The effect of the water content is also notable, although secondary to the bed thickness, whereas the effect of consolidation time is minimal.

Newson et al. (1996) performed a field study of the consolidation behaviour of gold tailings beds deposited from 165% water content slurries in large water tanks and allowed the tailings to consolidate and evaporate for a period of time. After the bed consolidation was complete, the authors measured the undrained shear strength with depth within the deposit using a vane shear strength apparatus. Newson et al. (1996) found that at a depth of 10 cm below the surface of a tailings bed a few months old, $c_u$ was about 5 kPa. In comparison, the present investigation found that $c_u$ at a depth of 10 cm below the surface was 0.89 and 0.98 kPa for the 3 and 12 days old beds, respectively. Although lower, these $c_u$ values are of the same order of magnitude as the ones reported by Newson et al. (1996). The higher $c_u$ measured by Newson et al. (1996) is most probably due to the fact that evaporation from the bed surface was allowed and this resulted in the formation of a tailings crust on the surface. Different experimental conditions in the work by Newson et al. (1996) could also have contributed to the slightly higher $c_u$ values.

The selection of correct strength parameters has been long recognized as a major factor critical to reliable slope stability or erosion resistance analysis. Undrained shear strength, $c_u$ is used in the analysis when the engineering loading is assumed to take place so rapidly that there is no time for the induced excess pore water pressure to dissipate or for consolidation to occur during the loading period (Holtz and Kovacs 1981). For these situations, the critical condition occurs when the induced pore pressure is the maximum but before consolidation has had time to take place. Once consolidation begins the void ratio and the water content decrease and the shear strength increases so the embankment or tailings bed becomes safer with time. Seneviratne et al. (1996) note that knowledge of the $c_u$-profile of a tailings deposit can be very beneficial during the construction of tailings embankment dams, when surface access for machinery is required to place tailings cover layers. The erosional resistance of deposited tailings beds during bed formation stage, either immediately following tailings disposal in the pond, or after a storm event that has caused some erosion of the sediment bed, can also be inferred on the basis of $c_u$. Furthermore, zoning the strength parameters to account for tailings anisotropy with depth is also required to improve the accuracy of the analysis (Seneviratne et al. 1996). The present work provides a representation of the variation of $c_u$ with depth below surface and investigates the effect of time for consolidation on $c_u$. The results may be used to select geotechnical parameters for the design and management of tailings disposal facilities.

## 3.4. Summary and Conclusions

Mine tailings sediment beds were deposited from slurries prepared at water content of 180% and with initial heights of approximately 3 to 27 cm. The final bed thickness varied between 3.3 and 10.1 cm. The beds were consolidated for 3, 6, 12, 18 and 46 days. Sedimentation experiments were run on tailings/water suspensions with initial heights between 6.2 and 33.2 cm. Obtained results showed that the primary consolidation of the deposited sediment beds was complete in about one hour. No measurable volume changes were recorded during the secondary compression phase as would be expected for a coarse grained soil. All beds were tested at depth intervals of 1 cm using the automated fall cone device to obtain the undrained shear strength variation with depth below the surface of the bed. At each interval four specimens were taken to determine the average water content within the tested layer. It was found that for effective stress below 1.19 kPa, the undrained shear strength of the tested beds varied between 0.008 and 0.975 kPa and the water content between 17 and 27%. The test results showed that the primary factor governing the undrained shear strength variation within a sediment bed was the vertical effective stress, whereas the water content had measurable but secondary effect. It was proposed to use a second order polynomial function to express the correlation between the undrained shear strength and the vertical effective stress. Time for aging did not seem to influence the observed undrained shear strength which was explained by the lack of thixotropic hardening with time in the coarse grained and cohesionless mine tailings. For all tested beds, the water content decreased and the undrained shear strength increased with depth below surface. At a given depth, the undrained shear strength decreased with increasing bed thickness.

## 3.5. Acknowledgements

This work was supported by funding from the Natural Sciences and Engineering Research Council of Canada (NSERC) in the form of an Individual Discovery Grant awarded to E.K. Yanful and a postgraduate scholarship awarded to Rozalina Dimitrova.

## 3.6. References

Adu-Wusu C, Yanful EK, Mian MH (2001) Field evidence of resuspension in a mine tailings pond. Canadian Geotechnical Journal, 38:796–808.

Alexis A, Le Bras G, Thomas P (2004) Experimental bench for study of settling-consolidation soil formation. Geotechnical Testing Journal, 27(6):557-567.

ASTM, Standard D 2487 (1997a) Classification of soils for Engineering Purposes. Annual book of ASTM standards. American Society for Testing and Materials, Philadelphia, Pasadena, USA.

ASTM, Standard D 4318-93 (1997b) Standard test methods for liquid limit, plastic limit, and plasticity index of soils. Annual book of ASTM standards. American Society for Testing and Materials, Philadelphia, Pasadena, USA.

Azevedo RF, De Campos TM, Alves MCM, Villar LF (1994) Sedimentation and consolidation of a neutralized red mud. In: Macari EJ, Frost JD, Pumarada LF (eds) Geoenvironmental issues facing the Americas, American Society of Civil Engineers, New York, USA, pp. 111-114.

Been K, Sills GC (1981) Self-weight consolidation of soft soils: an experimental and theoretical study. Gèotechnique, 31(4):519-535.

Blight G, Bentel G (1983) The behaviour of mine tailings during hydraulic deposition. Journal of the South African Institute of Mining and Metallurgy, 83(4):73-86.

Bowles JE (1986) Engineering properties of soils and their measurement, 3rd edn. McGraw-Hill Inc., New York, USA.

British Standards Institution, Standard BS 1377-2 (1990) Methods of test for soils for civil engineering purposes, Part 2: Classification tests. British Standards Institution, London, UK.

Bussière B (2007) Colloquium 2004: Hydrogeotechnical properties of hard rock tailings from metal mines and emerging geoenvironmental disposal approaches. Canadian Geotechnical Journal, 44:1019-1052.

Caldwell JA, Ferguson K, Schiffman RL, Van Zyl D (1984) Application of finite strain consolidation theory for engineering design and environmental planning of mine tailings impoundments. In: Sedimentation/Consolidation Models – Predictions and Validation, eds. Yong RW and Townsend FC, ASCE, pp. 581-606.

Canadian Standards Association and Bureau de normalisation du Quebec, Standard CAN/ BNQ 2501-092 (2006) Soils - Determination of Liquid Limit by the Fall Cone Penetrometer and Determination of Plastic Limit. Bureau de normalisation du Quebec, Quebec, Canada.

Catalan LJ, Yanful EK (2002) Sediment-trap measurements of suspended mine tailings in shallow water cover. Journal of Environmental Engineering, 128(1):19-30.

Chong YS, Ratkowsky DA, Epstein N (1979) Effect of particle shape on hindered settling in creeping flow. Powder Technology, 23:55-66.

Davies R (1968) The experimental study of the differential settling of particles in suspension at high concentrations. Powder Technology, 2(1):43-51.

Di Felice R, Parodi E (1996) Wall effects on the sedimentation velocity of suspensions in viscous flow. AlChE Journal, 42(4): 927-931.

Elder DMcG, Sills GC (1985) Thickening and consolidation of sediment due to self weight. In: Moudgil BM, Somasundaran P (eds) Flocculation, sedimentation and consolidation. Proceeding of the Engineering Foundation Conference, Sea Island, Georgia, USA, February 1985. Engineering Foundation, pp. 349-362.

Farrell E (1997) ETC 5 Fall-cone study. Ground Engineering, 30(1):33-36.

Feng TW (2000) Fall-cone penetration and water content relationship of clays. Gèotechnique, 50(2):181-187.

Feng TW (2002) Discussion of "Percussion and cone methods of determining the liquid limit of soils: controlling mechanisms." by A. Sridharan and K. Prakash. Geotechnical Testing Journal, 25(1):104-105.

Gibson RE, England GL, Hussey MJL (1967) The theory of one-dimensional consolidation of saturated clays: I. Finite non-linear consolidation of thin homogeneous layers. Geotechnique, 17(3):261-273.

Gibson RE, Schiffman RL, Cargill KW (1981) The theory of one-dimensional consolidation of saturated clays: II. Finite nonlinear consolidation of thick homogeneous layers. Canadian Geotechnical Journal, 18(2):280-293.

Hansbo S (1957) A new approach to determination of the shear strength of clay by the fall cone test. In: Proceedings of the Royal Swedish Geotechnical Institute, Stockholm, Sweden, Publication No.14, pp. 7-47.

Holtz R, Kovacs W (1981) An introduction to geotechnical engineering. Prentice-Hall Inc., Englewood Cliffs, New Jersey, USA.

Houlsby GT (1982) Theoretical analysis of the Fall Cone Test. Gèotechnique, 32(2):111-118.

Imai G (1981) Experimental studies on sedimentation mechanism and sediment formation of clay materials. Soils and Foundations, 21(1):7-20.

Jeeravipoolvarn S, Scott JD, Chalaturnyk RJ (2009) 10 m standpipe tests on oil sand tailings: long-term experimental results and prediction. Canadian Geotechnical Journal, 46:975-888.

Komnitsas K, Bartzas G, Paspaliaris I (2004) Efficiency of limestone and red mud barriers: laboratory column studies. Minerals Engineering, 17(2):183-194.

Kynch GL (1952) A theory of sedimentation. Transactions of the Faraday Society, 48:166-176.

Leroueil S, Le Bihan JP (1996) Liquid limits and fall cones. Canadian Geotechnical Journal, 33:793-798.

McGregor RG, Blowes DW, Jambor JL, Robertson WD (1998) Mobilization and attenuation of heavy metals within a nickel mine tailings impoundment near Sudbury, Ontario, Canada. Environmental Geology, 36(3/4):305-319.

Mehta AJ, Hayter EJ, Parker ER, Krone RB, Teeter AM (1989) Cohesive Sediment Transport. I: Process Description. Journal of Hydraulic Engineering, 115(8):1076-1093.

Mehta AJ, Parchure TM, Dixit JG, Ariathurai R (1982) Resuspension potential of deposited cohesive sediment beds. In: Kennedy VS (ed) Estuarine comparisons, Academic Press, New York, USA, pp. 591–609.

Mesri G (1975) Discussion of “New design procedure for stability of soft clays.” by Ladd CC and Foott R. ASCE Journal of the Geotechnical Engineering Division, 101:409-412.

Mesri G (1989) A reevaluation of $s_{u(mob)} = 0.22\sigma'_p$ using laboratory shear tests. Canadian Geotechnical Journal, 26(1):163-164.

Mesri G (2001) Undrained shear strength of soft clays from push cone penetration test. Gèotechnique, 51(2):167-168.

Mittal H, Morgenstern N (1975) Parameters for the design of tailings dams. Canadian Geotechnical Journal, 12:235-261.

Newson T, Fujiyasu Y, Fahey M (1996) A field study of the consolidation behaviour of saline gold tailings. In: Proceedings of 3rd International conference on Tailings and Mine Waste, Fort Collins, Colorado, USA, 16-19 January 1996. A. A. Balkema, Roterdam, The Netherlands, pp. 179-188.

Pane V, Schiffman RL (1985) A note on sedimentation and consolidation. Gèotechnique, 35(1):69-72.

Prachure TM, Mehta AJ (1985) Erosion of soft cohesive sediment deposits. ASCE Journal of Hydraulic Engineering, 111(10):1308-1326.

Prakash K, Sridharan A (2006) Critical appraisal of the cone penetration method of determining soil plasticity. Canadian Geotechnical Journal, 43: 884-888.

Priscu C, Mitri HS, Kiera H, Jacobsz SW (1999) Evaluation of mine tailings dams behaviour – A case study. . In: Proceedings of 6th International conference on Tailings and Mine Waste, Fort Collins, Colorado, USA, 24-27 January 1999. A. A. Balkema, Roterdam, The Netherlands, pp. 325-334.

Qiu Y, Sego D (2001) Laboratory properties of mine tailings. Canadian Geotechnical Journal, 38:183-190.

Ranjan G, Rao A (2000) Basic and Applied soil mechanics, 2nd edn. New Age International (P) Publishers, New Delhi, India

Richardson JF, Zaki WN (1954) Sedimentation and Fluidisation: Part I. Transactions of the Institute of Chemical Engineers, 32:82-100.

Samad MA, Yanful EK (2005) A design approach for selecting the optimum water cover depth for subaqueous disposal of sulphide mine tailings. Canadian Geotechnical Journal, 42:207-228.

Seneviratne N, Fahey M, Newson T, Fujiyasu Y (1996) Numerical modelling of consolidation and evaporation of slurried mine tailings. International Journal for Numerical and Analytical Methods in Geomechanics, 20:647-671.

Shamsai A, Pak A, Bateni S, Ayatollahi S (2007) Geotechnical Characteristics of Copper Mine Tailings: A Case Study. Geotechnical and Geological Engineering, 25:591-602.

Sharma B, Bora PK (2003) Plastic limit, liquid limit and undrained shear strength of soil – reappraisal. Journal of Geotechnical and Geoenvironmental Engineering, 129(8):774-777.

Shaw SC, Groat LA, Jambor JL, Blowes DW, Hanton-Fong CJ, Stuparyk RA (1998) Mineralogical study of base metal tailings with various sulfide contents, oxidized in laboratory columns and field lysimeters. Environmental Geology, 33(2/3):209-217.

Skempton AW (1957) Discussion of "The Planning and Design of the New Hong Kong Airport". In: Proceedings of the Institure of Civil Engineers, Vol. 7, pp. 305-307.

Sridharan A, Prakash K (1999) Mechanisms controlling the undrained shear strength behaviour of clays. Canadian Geotechnical Journal, 36(6):1030-1038.

Sridharan A, Prakash K (2000) Percussion and cone methods of determining the liquid limits of soils: controlling mechanisms. Geotechnical Testing Journal, 23(2): 236-244.

Sridharan A, Prakash K (2003) Self weight consolidation: compressibility behaviour of segregated and homogeneous fine grained sediments. Marine Georesources and Geotechnology, 21:73-80.

Swedish Standards Commission, Standard SS 027120 (1990) Geotechnical tests — cone liquid limit. Swedish Standards Commission, Stockholm, Sweden.

Terzaghi K (1942) Theoretical soil mechanics. John Wiley and Sons Inc., New York, USA.

Terzaghi K, Peck R, Mesri G (1996) Soil mecanics in engineering practice. 3rd edn., John Wiley and Sons Inc., New York, USA.

Tolhurst T, Black K, Paterson D, Mitchener H, Termaat G, Shayler S (2000) A comparison and measurement standardisation of four in situ devices for determining the erosion shear stress of intertidal sediments. Continental Shelf Research, 20:1397-1418.

Toorman EA (1996) Sedimentation and self-weight consolidation: general unifying theory. Géotechnique, 46(1):103-113.

Toorman EA (1999) Sedimentation and self-weight consolidation: constitutive equations and numerical modelling. Gèotechnique, 49(6):709-726.

Vick SG (1990) Planning, analysis, and design of tailings dams. 2nd edn. BiTech Publishers, Vancouver, B.C., Canada.

Volpe R (1979) Physical and engineering properties of copper tailings. In: Proceedings of Current Geotechnical Practice in Mine Waste Disposal. Edited by The Committee on Embankment Dams and Slopes of the Geotechnical Engineering Division. American Society of Civil Engineering, New York, USA, pp. 142-160.

Wasti Y, Bezirci MH (1985) Determination of the consistency limits of soils by the fall cone test. Canadian Geotechnical Journal, 23: 241-246.

Wood DM, Wroth CP (1978) The use of cone penetrometer to determine the plastic limit of soils. Ground Engineering, 11(3):37.

Yanful EK, Verma A (1999) Oxidation of flooded mine tailings due to resuspension. Canadian Geotechnical Journal, 36:826–845.

Zreik DA, Germaine JT, Ladd CC (1997) Undrained strength of ultra-weak cohesive soils: relationship between water content and effective stress. Soils and Foundations, 37(3):117-128.

Zreik DA, Germaine JT, Ladd CC (1998) Effect of aging and stress history on the undrained strength of ultra-weak cohesive soils. Soils and Foundations, 38(4):31-39.

Zreik DA, Ladd CC, Germaine JT (1995) A new fall cone device for measuring the undrained strength of vey weak cohesive soils. Geotechnical Testing Journal, 18(4):472-482.

# CHAPTER 4. EFFECT OF DRAINAGE CONDITIONS, THICKNESS AND AGE ON THE SHEAR STRENGTH OF DEPOSITED MINE TAILINGS BEDS IN THE VERY LOW STRESS RANGE

## 4.1. Introduction

Tailings are a waste product of mining and milling operations. Despite the similarities in grain size distribution curves between tailings and naturally occurring sand-silt mixtures, the former differ significantly from the latter in mechanical properties (Abadjiev 1985; Sarsby 2000). Being man-made materials, mine tailings are often more uniform than natural soils and exhibit lower density, higher angle of internal friction and smaller cohesion. For instance, researchers (e.g., Mittal and Morgenstern 1975; Pettibone and Kealy 1971; Matyas et al. 1984) have observed that the effective friction angle of mine tailings is 5° to 6° higher than that of natural soils of similar gradation, which they have attributed to the high angularity of tailings particles.

Most of the experimental programs on mine tailings reported in the literature were carried out on specimens consolidated under stresses well above 1 kPa (e.g., Pettibone and Kealy 1971; Matyas et al. 1984; Tibana et al. 2002). Zreik et al. (1998), however, noted that ultra low consolidation stresses are commonly observed when assessing the stability of mine tailings, bottom sediments or dredged material. Qui and Sego (2001) reported that the operative consolidation stresses in tailings management facilities can be as low as 0.5 kPa. Sture et al. (1998) observed significant difference between the strength behaviour of cohesionless granular soil at low and high stress levels. Fannin et al. (2005) emphasised that a characterisation of soil strength over the stress range, appropriate to that encountered in the field, would provide confidence in stability analysis of earth structures. Vick (1990) pointed out that the most important factor influencing the strength of mine tailings was the stress range over which it is measured. While the literature offers a few examples of studies on the strength properties of natural soils in the ultra low stress range (e.g., Zreik et al. 1998; Sture et al. 1998; Fannin et al. (2005) none of these works have dealt with mine tailings, in particular. Accordingly, the objective of this experimental program is to provide an assessment of the shear strength of non-cohesive mine tailings in the range of effective stress appropriate to mine waste management facilities.

Performing stability or erosion resistance analysis of mine tailings also requires comprehensive understanding of their behaviour under applied loading. Traditionally, the response of a saturated soil element to an imposed stress or strain increment is considered to lie between two extremes, namely, the fully drained and the undrained response (Vaid and Eliadorani 2000). Drainage conditions other than the extremes of zero drainage (undrained) and complete drainage (drained) are referred to as "partially drained". In some cases, the partial drainage scenario may constitute a more damaging response than either of the conventional drained or undrained loading conditions. Vaid and Eliadorani (1998) experimentally demonstrated that partial drainage may render saturated sand unstable that would otherwise be stable in a completely undrained state. Instability is defined as a condition that occurs when a soil element, subjected to even a small effective stress perturbation, can no longer sustain the current stress state imposed on it and a runaway deformation results (Vaid and Eliadorani 1998). With respect to mine tailings facilities, there are many rapid loading scenarios, besides seismic loading, which may trigger undrained or partially drained response. Examples are the incremental rise of tailings embankments during the operation of the waste management facility, as well as the periodic placement of tailings slurry in the tailings pond. The former can lead to relatively rapid increase in stress levels and undrained or partially drained conditions in susceptible materials, while the latter can cause temporary changes to the amount of saturated tailings in a given section of the impoundment. In loose tailings, both events can increase instability and cause limited or full-scale liquefaction due to rapid reductions in effective stress. For instance, liquefaction of mine tailings upon rapidly applied static loading was observed by Highter and Vallee (1980) who concluded that the liquefaction potential of studied mine tailings was controlled by their initial void ratio and consolidation stress. Ulrich and Fourie (2003) performed undrained triaxial and oedometer tests on saturated and unsaturated specimens from a tailings dam in South Africa, and identified a potential for sudden collapse of unsaturated tailings upon wetting.

To the present authors' knowledge, a thorough investigation of the strength behaviour of deposited mine tailings beds in the ultra low stress range has not been performed yet. An accurate estimation of the strength of mine tailings within this stress range is important as the obtained results can be easily incorporated into the existing slope stability or erosion resistance methods of analyses. The testing procedure, employed in the described study, aimed to simulate the in-situ drainage conditions in a tailings pond as closely as possible. Several drained and partially drained experiments were performed in order to investigate the effect of drainage conditions, bed thickness and aging on the strength characteristics of mill tailings subjected to consolidation stresses below 1 kPa. The failure mechanism of the tailings beds under the influence of gravitational forces was described and discussed.

## 4.2. Testing Materials and Procedures

### *4.2.1. Tailings beds preparation*

The mine tailings used in the present study were received from the Clarabelle Copper Mine, Sudbury Ontario in the form of tailings/water slurry. Shaw et al. (1998) identified the primary minerals in the Sudbury ore and tailings as pentlandite, chalcopyrite, pyrrhotite, quartz, feldspar, chlorite, biotite, amphibole and carbonates, plus minor pyroxene, apatite, magnetite, ilmenite, marcasite, galena and pyrite. The grain size distribution curve (Figure 3.1) indicated that the tailings were composed of 68% coarse (more than 0.075 mm) and 32% fine fraction (less than 0.075 mm), of which only 4% was clay-sized material (less than 2 μm).

The low content of clay-sized particles rendered the tailings non-cohesive and non-plastic and they were classified as silty sand based on the Unified Soil Classification System (ASTM 1997a). The liquid limit of the tailings was in the range of 12 - 15%, according to ASTM Standard D4318-93 (ASTM 1997b). Tailings/water slurries with 50% concentration of solids (by volume) were prepared by mixing dry tailings powder with distilled water. The desired volume of slurry was then poured into an acrylic tank, 45 cm long, 22.5 cm wide and 12.5 cm high. Tailings beds with final thicknesses between 1 and 10.3 cm were deposited from these slurries and were left to consolidate under self-weight for a minimum period of 3 days. The beds with final thicknesses between 1 and 7.2 cm were used in the shear strength experiments, whereas the ones with thicknesses between 8.6 and 10.3 cm were prepared during the sedimentation/consolidation tests. Since the initial concentration of the suspension was kept constant at 50% (by volume), slurries with different initial heights (between 2 and 12.4 cm) were used to prepare the above mentioned beds. The minimum consolidation time of 3 days was proven sufficient to ensure that primary consolidation of the beds was complete. The reason for using higher bed thicknesses in the sedimentation experiments was to obtain additional assurance that if the primary consolidation of the thicker beds was complete within 3 days than, given the shorter drainage paths, it would also be complete in the thinner ones. Thus, all tailings beds deposited in this manner were normally and fully consolidated. The deposited mine tailings beds were tested at 3, 6, 12, 18 and 46 days. Upon completion of each test, the content of the Tank was carefully remixed to produce tailings/water slurry identical to the one from which the tailings bed was deposited. The slurry was then reused, with small amounts of tailings powder or water added to account for losses, to obtain the tailings bed for the next experiment. This experimental procedure ensured that tailings and fluid properties remained as constant as possible for all beds of a particular final thickness, which minimized experimental variability. During the experimental cycle the ambient temperature in the laboratory was kept constant at 22°±1°C.

### *4.2.2. Shear strength testing*

The shear strength of the sedimented tailings beds under drained and partially drained conditions was obtained using the Tilting Tank shown in Figure 4.1a. The conceptual design of similar tanks was previously described by Zreik et al. (1998) and

Kamhawi and Arthur (1992), however, the equipment used in the present study was modified from the previous design.

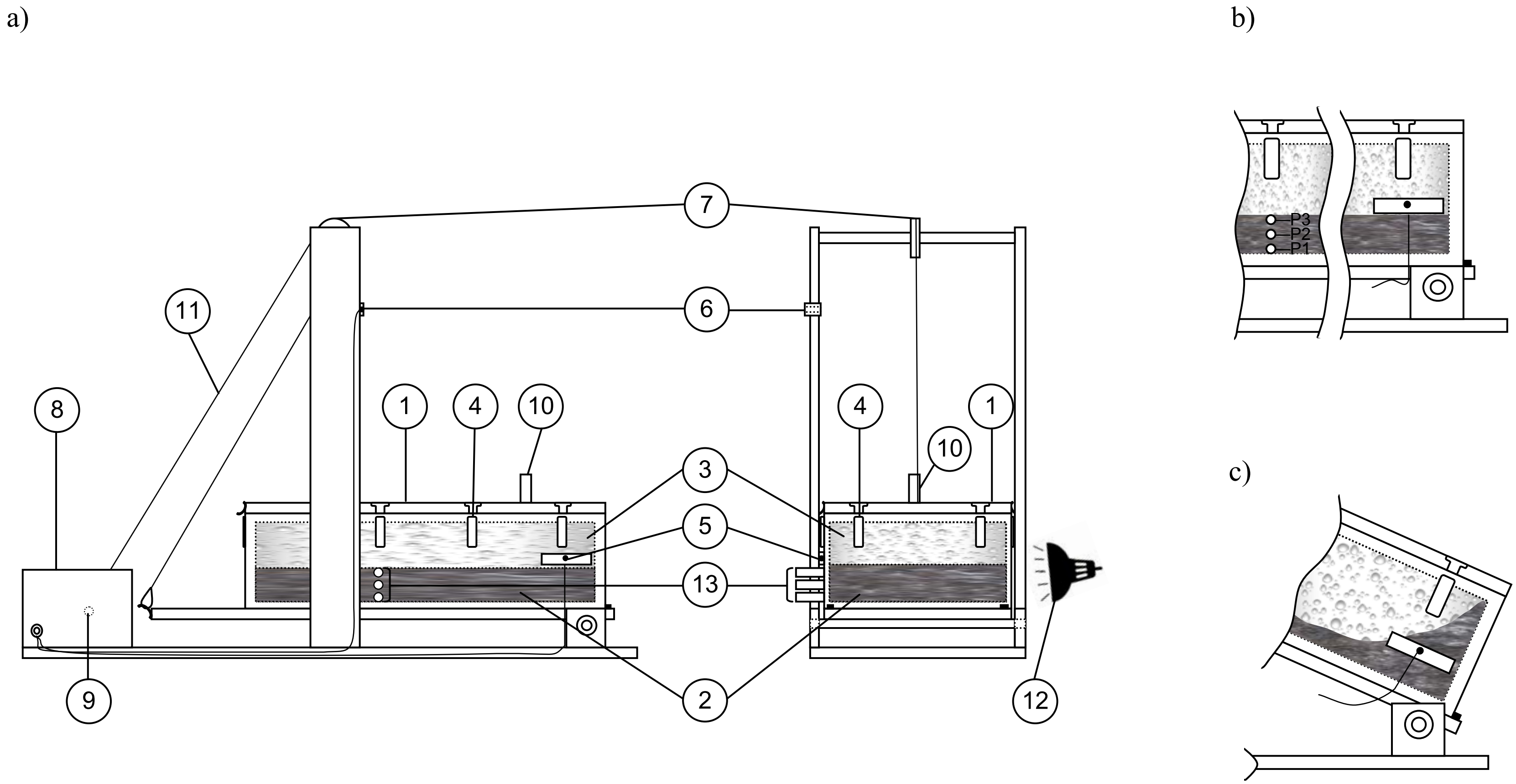


**Figure 4.1.** (a) The Tilting Tank: 1 acrylic tank; 2 deposited tailings bed; 3 water; 4 clamps; 5 photosensor; 6 back-up photosensor; 7 pulley; 8 DC motor; 9 motor shaft; 10 water spout; 11 cable; 12 light source; 13 pore water pressure measuring ports; (b) Tailings bed and photosensor at the onset of tilting; (c) Tailings bed and photosensor at failure.

Prior to each test the Tank was filled to the top with distilled water using a mini pump. A sufficiently slow pumping rate (0.384 L/min) was selected to ensure minimum disturbance of the bed during the filling process. At this time, the tailings bed deposited in the Tank was at least 3 days old, fully consolidated and had developed certain strength. Filling the Tank with water did not cause any visible particle dislodgment from the surface of the bed and the overlying water remained clear throughout the process. Furthermore, adding water to the top of the Tank did not change the effective stress distribution within the bed and, hence, the authors believe that this procedure did not introduce any significant changes in the properties of the deposited bed and allowed comparison between beds of different final thicknesses. After filling the Tank, the cover was sealed in place using the clamps positioned on all four walls of the Tank (Figure 4.1a). The cover was equipped with two openings: a water spout, connecting the Tank to a constant head flask; and an air vent allowing the air trapped within the Tank during the filling process to escape (not shown in Figure 4.1a). The Tank was then placed on a tilting platform and tilted at one side by means of the pulley and DC motor system (Figure 4.1a) until failure of the deposited bed occurred. Failure was identified as sliding of a portion of the bed under the influence of gravity forces to the bottom of the Tank and it was detected by a cadmium sulphide photosensor that, at failure, automatically broke the electric circuit, preventing further tilting. The portable photosensor was placed in a protective rubber sleeve and mounted on a small acrylic block. Prior to tilting, it was positioned at approximately 1 cm above the bed surface and held in place on the outside wall of the Tank using adhesive tape as shown in Figure 4.1b. A light source (desk lamp) on the side of the Tank opposite the photosensor ensured that the sensor remained illuminated (and the electric circuit open) throughout the tilting. From the onset of tilting up until bed failure, the light from the source was able to penetrate the relatively clear water above the bed and reach the photosensor (Figure 4.1b). Upon bed failure, the soil above the failure plane slid to the bottom of the Tank and accumulated there, thus impeding the light from reaching the photosensor and triggering a circuit break which terminated tilting (Figure 4.1c). The tilting angle, at which failure occurred, was measured with an electronic digital protractor (AN451-101 Electronic Digital Protractor) and recorded.

Pore water pressure (PWP) changes with time within the tested beds were monitored using pressure transducers (VIATRAN 245) at three ports numbered P1, P2 and P3 and positioned in a vertical array at elevations 0.5, 3.5 and 7.0 cm from the bottom of the Tank, respectively, and at 17 cm horizontal distance from the left side wall (Figure 4.1a). The diameter of the pressure tube at the pressure connection was 8 mm. The selected Viatran 245 pressure transducer is a high accuracy transducer and measures from 3 psi to 5000 psi (0.2 to 345 bar) with standard accuracy of ≤ ±0.06% FSO (full scale output). During the tilting experiments, the PWP within the bed was continuously measured and recorded at 5 sec intervals, by means of a data logger (SCIEMETRIC INSTRUMENTS LLSYS). The design of the Tilting Tank allowed for a maximum angle of tilting of 50° and if it was reached, a back-up cadmium sulphide photosensor was triggered; activating a relay switch that automatically broke the electric circuit.

Two tilting modes were employed during the experimental program: i) slow tilting at an average speed of 0.07°/min, and ii) rapid tilting at a speed of 1.61°/min. The DC motor was manufactured to run at a constant speed (1 rpm, corresponding to an angle of tilting 1.61°/min), which was used during rapid tilting. The slow tilting was achieved by adding a timer (DELTA D6DI) to the experimental setup, that switched the motor on for 10 s every 4 min. A thin sand layer was glued to the acrylic base of the Tank to prevent slippage along the bottom of tailings/Tank interface. Once bed failure had occurred as a result of tilting, the thickness of the soil layer still remaining at the bottom of the Tank was measured with a ruler placed along the outer wall of the box. This value was subtracted from the total bed thickness prior to tilting and the location of the failure plane relative to the bed surface was determined.

The infinite slope theory was adopted to analyse the stability of the tested tailings beds. In this analysis, the thickness of the unstable material is considered small compared to the overall thickness of the bed and the failure surface is assumed parallel to the slope (Lambe and Whitman 1969). These assumptions are in agreement with the observed failure mode of the tested beds. In all calculations, the bed was also assumed to be homogeneous. At the onset of tilting and under the assumption of zero excess pore pressure, the normal effective and shear stress at the base of a tailings layer inclined at an angle $\beta$ from the horizontal are given by:

$$\sigma'_n = \gamma' h \cos^2 \beta = \gamma' z \cos \beta \tag{4.1}$$

$$\sigma_t = \tau = \gamma' h \sin \beta \cos \beta = \gamma' z \sin \beta \tag{4.2}$$

where $\sigma'_n$ is the effective normal stress at the base of the layer in kPa, $\sigma_t = \tau$ is the shear stress at the base of the layer in kPa, $\gamma'$ is the average buoyant unit weight of the tailings bed in kN/m$^3$, $h$ is the depth below bed surface along the vertical in m, $z$ is the depth below bed surface along the normal in m, and $\beta$ is the measured angle of tilting in degrees.

Under drained conditions, at failure the shear stress at the base of the failure plane is equal to the strength of the tailings beds, i.e., $\tau = \tau_f$, and also $\sigma'_n = \sigma'_{nf}$. Zreik et al. (1998) showed that, at failure, the effective normal and shear stress at the failure plane can be calculated using the effective vertical stress before tilting, at a depth corresponding to the depth of the failure plane, and from the failure angle as follows:

$$\sigma'_{nf} = \sigma'_{v0} \cos\beta \qquad (4.3)$$

$$\tau_f = \sigma'_{nf} \tan\phi' = \sigma'_{v0} \sin\beta \qquad (4.4)$$

where $\sigma'_{nf}$ is the effective normal stress at the failure plane at failure in kPa, $\tau_f$ is the shear strength of the tailings bed in kPa, $\phi'$ is the drained (effective) friction angle in degrees, and $\sigma'_{v0}$ is the vertical effective stress at a depth corresponding to the depth of the failure plane at the start of tilting in kPa.

At the onset of tilting, the vertical effective stress at a depth corresponding to the depth of the failure plane can be computed using the average buoyant unit weight of the tailings bed and the thickness of the soil layer above the failure plane:

$$\sigma'_{v0} = \gamma' z_f \qquad (4.5)$$

where $z_f$ is the depth from bed surface to the failure plane along the normal to the slope in m.

At failure, the total normal stress and shear strength at the failure plane can be determined from:

$$\sigma_{nf} = \sigma_{v0} \cos \beta \tag{4.6}$$

$$\tau_f = \sigma_{nf} \tan \phi_T = \sigma_{v0} \sin \beta \tag{4.7}$$

where $\sigma_{nf}$ is the total normal stress at the failure plane at failure in kPa, $\tau_f$ is the shear strength of the tailings bed in kPa, $\phi_T$ is the total friction angle in degrees, and $\sigma_{v0}$ is the vertical total stress at a depth corresponding to the depth of the failure plane at the start of tilting in kPa.

The vertical total stress at a depth corresponding to the depth of the failure plane at the start of tilting is given by:

$$\sigma_{v0} = \gamma_{sat} z_f + \gamma_w z_w \tag{4.8}$$

where $\gamma_{sat}$ is the average saturated unit weight of the tailings bed in kN/m$^3$, $\gamma_w$ is the unit weight of water in kN/m$^3$, and $z_w$ is the depth of the water above the tailings bed in m.

## 4.3. Results and Discussion

### *4.3.1. Settling behaviour and consolidation*

The tailings beds used in this research were sedimented from slurries with 50% concentration of solids (by volume). Previous studies have shown that gravitational settling and segregation of particles in suspensions are strongly affected by suspension concentration (e.g., Davies 1968; Cheng 1980). At sufficient volume concentration of solids (above 50%), changes in fluid density and viscosity, particle interactions and counterflow of fluid caused by downward particle motion result in hindered settling. All particles in the suspension settle at approximately the same rate, a phenomenon termed *en masse* settling (Cheng 1980). The counterflow caused by the displaced fluid consists of nearly pure water and fractionation in the resulting sediment deposit is negligible. The concentration at which this mode of sedimentation dominates suspension behaviour varies with particle sorting, size and shape. In general, the more irregularly shaped or better sorted the sediment solids, the lower the concentrations at which this mode of sedimentation occurs (Davies 1968). Therefore, the authors believed that the high suspension concentration coupled with the irregular shape of particles, typical for hard rock tailings, and the wide range of gradation, present in the studied tailings material, were sufficient to suppress particle segregation during bed deposition from tailings/water suspensions. Furthermore, visual inspection showed uniform texture and colour of the deposited tailings beds, without any indication of particle size variations with depth.

Pore water pressure (PWP) changes with time at the bottom of the tailings beds were monitored during bed formation, i.e., from the moment the tailings/water slurry was poured into the Tilting Tank until the excess PWP was fully dissipated. It was found that the PWP at the bottom of the beds (port P1) returned to its hydrostatic value within 1 - 1½ hour from the beginning of each experiment, i.e., the excess PWP generated during the settling and primary consolidation phases of bed formation was fully dissipated by the end of that period (Figure 4.2).

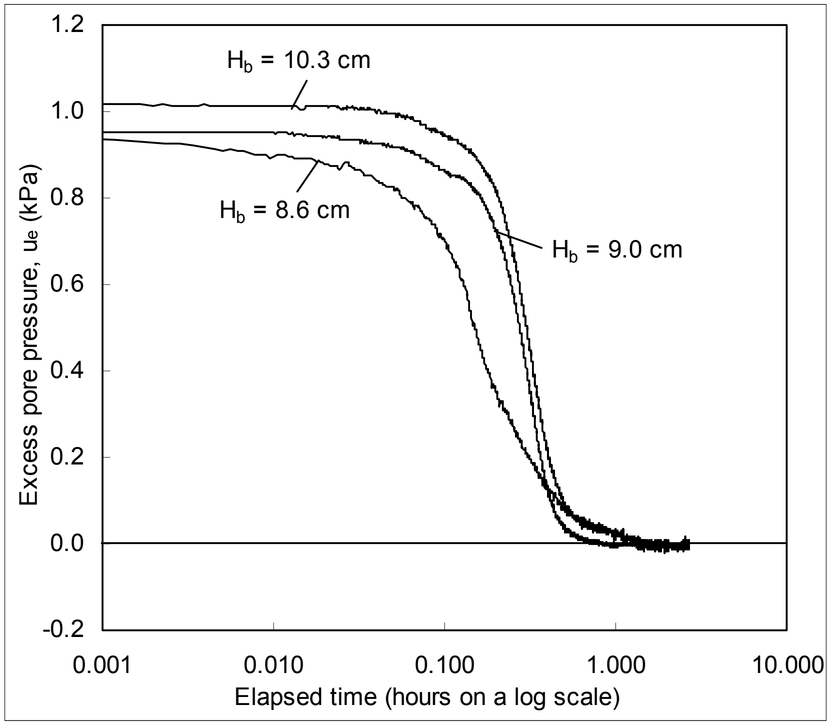


**Figure 4.2.** Excess pore water pressure variation with time at the bottom of tailings beds during sedimentation and consolidation.

Given that the tested mine tailings represented coarse grained silty sand and were, as such, a fast draining material, a relatively short time for full dissipation of excess PWP was expected. Indeed, Matyas et al. (1984) also observed rapid dissipation of excess PWP during the construction of a test embankment comprised of sandy tailings fill. In the previous Chapter 3 we also indirectly determined that the primary consolidation of all tested beds was complete in approximately 60 to 90 min. Measured PWP confirmed this inference. Sedimentation experiments helped determine the time required to complete the primary consolidation of tailings beds of final thicknesses 8.6 - 10.3 cm. Since the tested 10.3 cm-thick beds had the longest drainage path, as measured from the bottom of the beds to their surface, it was deemed appropriate to assume that, because of their shorter drainage paths, the primary consolidation of the thinner beds would also be complete within this time frame.

### *4.3.2. Slow tilting experiments*

During tilting, excess PWP is generated within the tailings beds under the influence of gravitational forces. The magnitude of the excess PWP at a given horizontal plane within the bed depends on the angle of tilting, $\beta$, and on the location (depth), $z$, of that plane relative to the surface of the bed. The upper free surface of the bed represents an unconfined boundary through which the excess PWP built up as a result of tilting tends to dissipate due to drainage, with accompanying volume changes. The response of mine tailings beds to applied loading can be considered fully drained only if the total and the effective stress paths are parallel, i.e., $d\sigma = d\sigma'$ and the excess pore water pressure, $du_e = 0$ at all times. When the "slow" tilting mode was selected, the loading rate was slow enough that, irrespective of the depth below the bed's surface, the shear-induced excess PWP remained at least an order of magnitude lower that the normal effective stress at the same horizon. Figures 4.3a to c show the variation of the excess PWP with time and angle of tilting at three elevations (ports P1, P2 and P3) in a 3-day old tailings bed with a final thickness of 7.2 cm during slow tilting.

a)

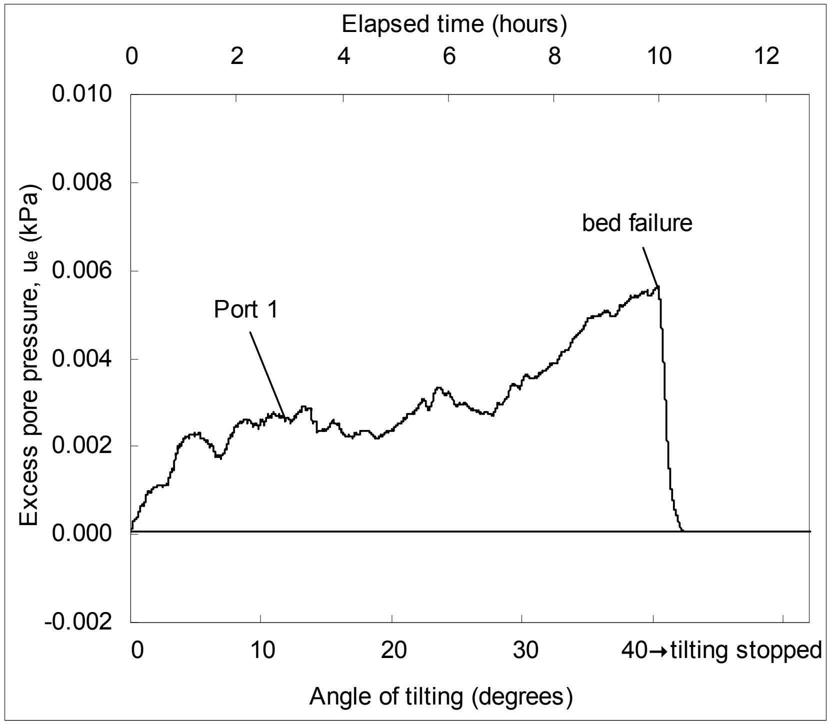
Elapsed time (hours)
0
2
4
6
8
10
12
0.010
0.008
0.006
0.004
0.002
0.000
-0.002
Excess pore pressure, $u_e$ (kPa)
bed failure
Port 1
0
10
20
30
40→tilting stopped
Angle of tilting (degrees)

b)

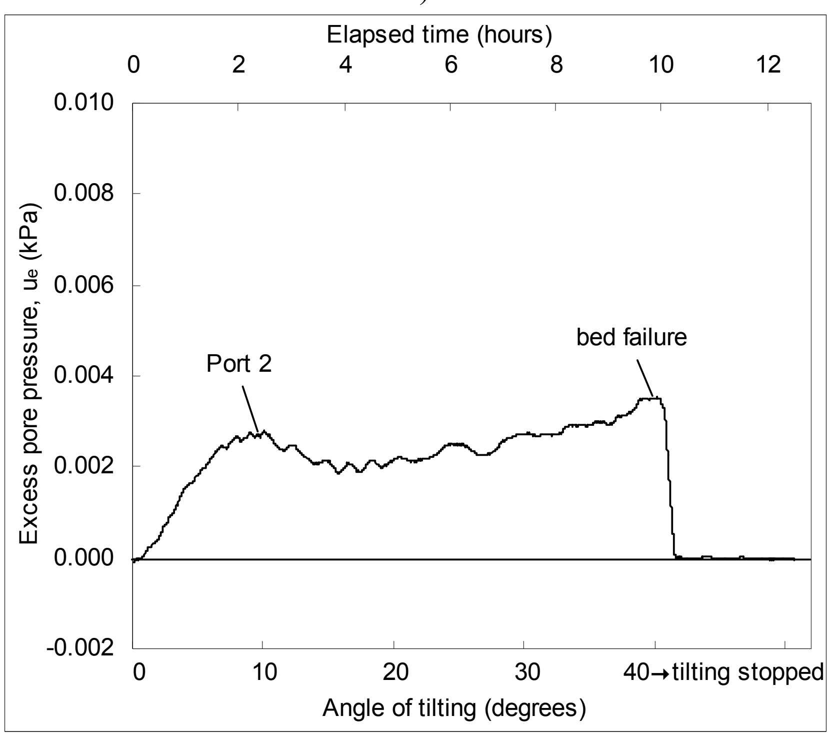
Elapsed time (hours)
0
2
4
6
8
10
12
0.010
0.008
0.006
0.004
0.002
0.000
-0.002
Excess pore pressure, $u_e$ (kPa)
bed failure
Port 2
0
10
20
30
40→tilting stopped
Angle of tilting (degrees)

c)

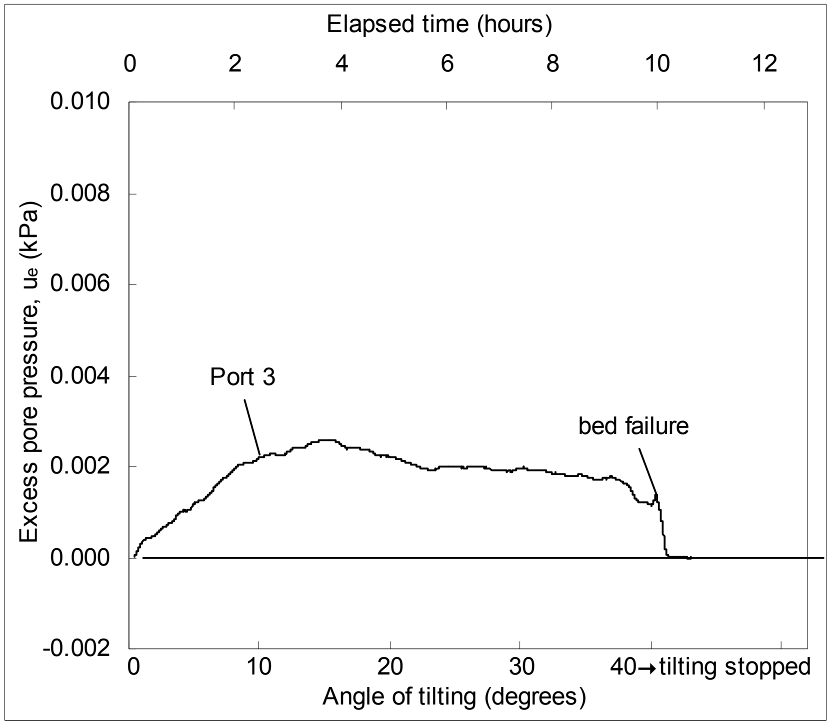


**Figure 4.3.** Excess pore water pressure variation with time during slow tilting of 7.2 cm–thick tailings bed consolidated for 3 days at: (a) Port P1; (b) Port P2; (c) Port P3.

The initial void ratio of the tailings bed was estimated as 0.67. As evident from Figure 4.3a, at port P1, positioned at the bottom of the tailings bed, the excess PWP, $u_e$, generally increased from the onset of tilting until the angle of bed failure of 40°. Two short periods of $u_e$ decrease were observed throughout the experiment: one from 13° to 20° that lasted about 1.3 hours (78 min), and a second one from 24° to 28° that continued for about 0.7 hours (42 min). During these two periods, the rate of excess PWP dissipation due to drainage was higher than the rate of excess PWP generation. The opposite trend was observed during the remaining time of the test, when the rate of excess PWP generation dominated over the rate of dissipation, resulting in a net $u_e$ increase with time (Figure 4.3a). At 40° angle of tilting, slope failure and sliding of a portion of the bed occurred in the Tank along a failure plane located at approximately 0.5 cm from the surface of the bed. As soon as the sliding soil reached the bottom of the Tank, the photosensor on the side wall was activated preventing further titling. After the tilting ceased at 40°, the $u_e$ generated prior to and during failure, immediately began to dissipate. Full excess PWP dissipation was complete within approximately 0.33 hours (20 min) from the end of tilting, and $u_e$ returned to a zero value.

A different pattern of $u_e$ variation with time was observed at port P2, located approximately in the middle of the bed (Figure 4.3b). Within the first two hours of the experiment and up to about 10° angle of tilt, $u_e$ continuously increased and reached 76% of the maximum $u_e$-value recorded during the test. Further tilting to 16° over the next hour was accompanied by slow dissipation of $u_e$, following which the excess PWP began to gradually increase again until slope failure at 40°. Dissipation of $u_e$, generated in response to tilting, started immediately after the cessation of tilting, and $u_e$ returned to a zero value within 0.17 hours (10 min).

A less significant excess PWP generation during slow tilting was measured at port P3, located immediately below the bed's surface (Figure 4.3c). Up to about 16° angle of tilt, $u_e$ steadily increased and reached about 70% of the maximum $u_e$-value recorded at port P2, and only about 43% of the maximum $u_e$-value recorded at port P1 during the same experiment. Beyond a tilt angle of 16°, a slight and relatively constant $u_e$ dissipation was observed which continued until failure at 40°. A minor peak in the

$u_e$ versus time plot was registered at the time of failure, following which the excess PWP returned to zero within 0.06 hours (4 min) of cessation of tilting.

In Figure 4.4, profiles of $u_e$ with depth below the bed surface were plotted on a semi-logarithmic scale at tilting angles of 10°, 30° and 40°, with the last profile showing the excess PWP distribution in the tested tailings bed at failure. A line representing the variation of $\sigma'_n$ with depth below the bed's surface was also plotted for purposes of comparison.

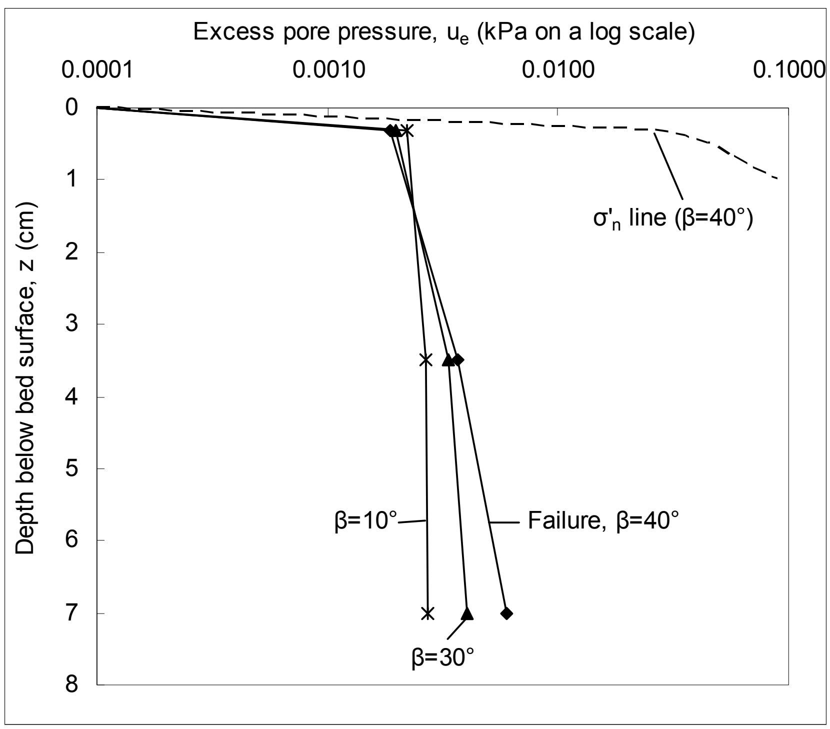


**Figure 4.4.** Profiles of the excess pore pressure versus depth below bed surface during slow tilting of 7.2 cm–thick tailings bed, consolidated for 3 days at three angles of tilting.

Figure 4.4 shows that at 10° angle of tilt, the spatial distribution of $u_e$ in the bed was relatively uniform. In contrast, the data points obtained for 30° angle show a slightly lower $u_e$ value close to the surface, and relatively constant $u_e$ in the middle and at the bottom of the bed. To explain that uneven $u_e$ distribution within the bed, we propose the hypothesis that drainage through the surface of the bed caused some excess PWP dissipation, which was more pronounced at shallow horizons, compared to the bottom of the bed, because of the shorter drainage path at small depths. During tilting beyond 30°, the excess PWP dissipation progressed in downward direction until, at failure, it affected the entire bed, as can be seen from the sloping profile at 40° angle of tilt. It is worth noting here, that the $u_e$ values at all horizons remained far from the $\sigma'_n$-line at all times during the experiment. Comparison between $\sigma'_n$ values and $u_e$ data points, obtained at 40° angle of tilt, showed that at 0.3 cm depth below the bed surface (P3), $u_e$ constituted about 7% of $\sigma'_n$, whereas at 3.5 cm (P2) and 7.0 cm (P1) depths, $u_e$ reached only 1% of $\sigma'_n$. Based on this observation, it is hypothesized that the excess PWP generated in the tailings bed during slow tilting did not affect significantly the shear strength of the bed and, hence, it was safe to assume that bed shearing occurred under drained conditions. It is concluded that slope failure took place when the shear stress at the failure plane exceeded the shear strength of the tailings at the same depth.

### *4.3.3. Rapid tilting experiments*

During rapid tilting, the magnitude of the excess pore water pressure generated in the tailings beds, in response to applied loading, was significantly larger compared to slow tilting. The distribution of excess PWP in a 7.2-cm thick tailings bed, aged 3 days during rapid tilting, may be seen in Figures 4.5a to c, where the $u_e$ values recorded at the three measuring ports (P1, P2 and P3) are plotted versus time and angle of tilting.

a)

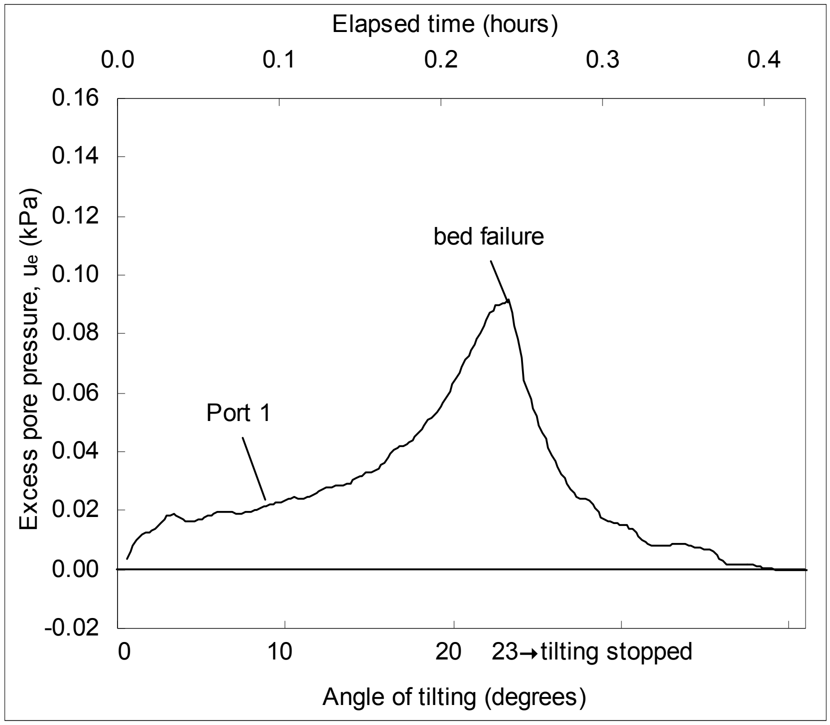

b)

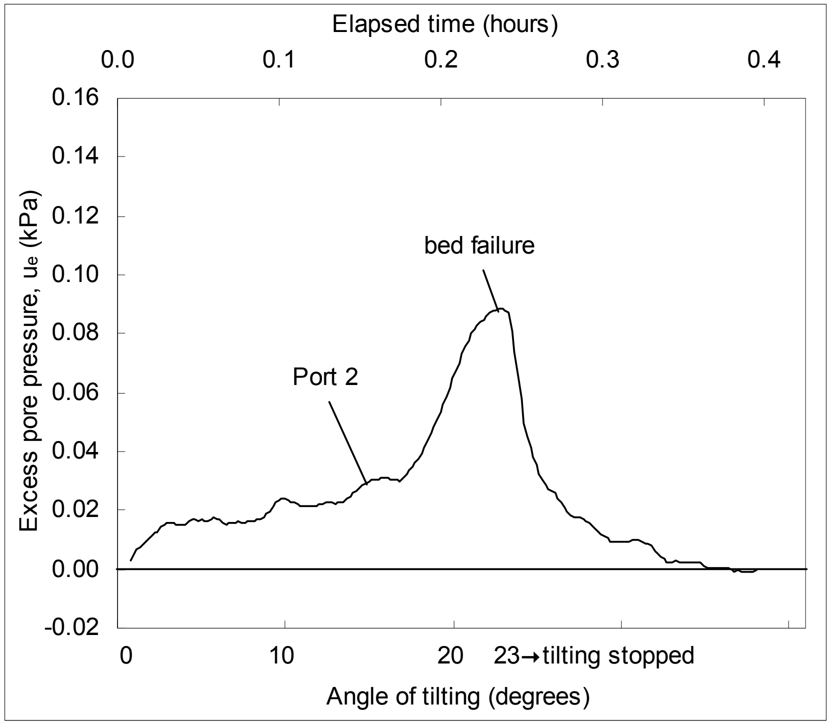


c)

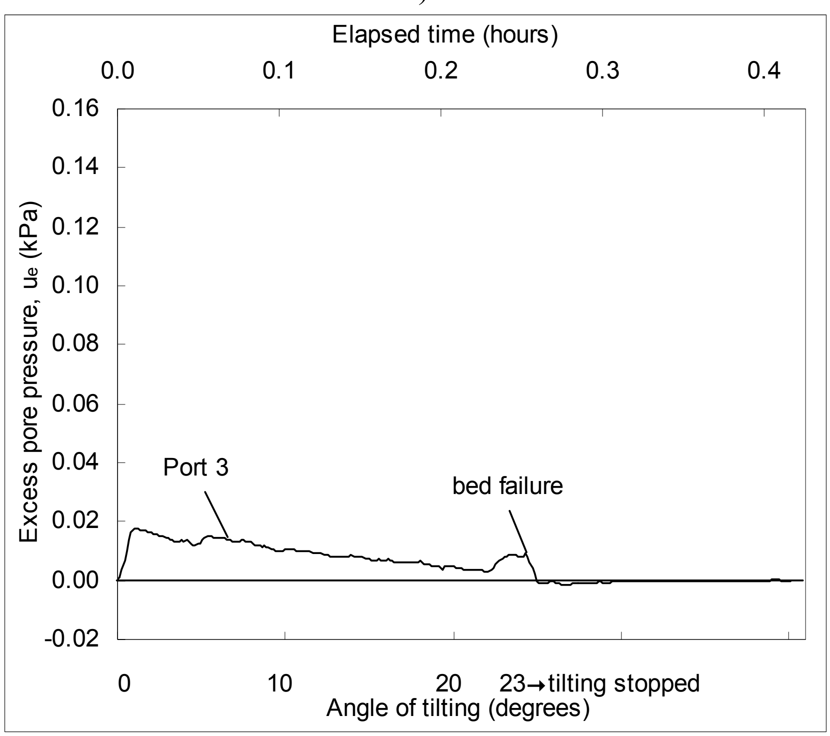


**Figure 4.5.** Excess pore water pressure variation with time during rapid tilting of 7.2 cm–thick tailings bed, consolidated for 3 days at: (a) Port P1; (b) Port P2; (c) Port P3.

At port P1 at the bottom of the bed, $u_e$ increased continuously until an angle of tilting of 23°, which was reached at approximately 0.24 hours (14 min) from the onset of tilting (Figure 4.5a). At 23° angle of tilt, failure of the slope occurred within the Tank along a failure plane located at about 0.6 cm from the surface of the bed. Following the failure event, the photosensor on the side of the Tank was activated and tilting ceased. Upon cessation of tilting, $u_e$ dissipated rapidly and within 0.16 hours (10 min) reached a zero value, i.e., returned to the hydrostatic pressure. It is inferred that, although some partial drainage most probably occurred at that horizon throughout tilting, the rate of excess pore water pressure generation remained generally higher than the dissipation rate due to drainage.

Essentially, the same pattern of $u_e$ variation in response to tilting was recorded at port P2 in the middle of the bed (Figure 4.5b). At this horizon also, the rate of excess PWP generation dominated the rate of dissipation, which led to a continuous $u_e$ increase from the onset of tilting to slope failure at 23°. After the tilting of the Tank ceased, $u_e$ returned to a zero value within 0.09 hours (5 min), which period was even shorter than the one recorded at port P1. The faster dissipation of the excess PWP at port P2 compared to P1 was probably due to the closer proximity of port P2 to the drainage boundary, i.e., the surface of the bed.

At port P3 immediately below the surface of the bed, a rapid initial increase in $u_e$ was recorded that lasted from the onset of tilting until about 0.02 hours (1.3 min), i.e., the time corresponding to 1.5° angle of tilt (Figure 4.5c). Past 0.02 hours, the rate of

$u_e$ dissipation due to partial drainage became higher than the rate of pressure generation, probably because of the short drainage path to the bed's surface and the high permeability of tailings. It was believed that the pressure dissipation proceeded in the upward direction into the ambient water above the bed and was driven by the pressure gradient induced by the non uniform excess PWP build up. The net result was a decrease in the magnitude of $u_e$ at that depth within the bed, which continued until the failure of the slope at 23°. At that point, a visible peak in $u_e$ was recorded by the transducer at P3. As evident from Figure 4.5c, after the tilting ceased, $u_e$ decreased to a slightly negative value and then returned to zero within only 0.05 hours (3 min).

The generation of excess PWP within tailings beds during rapid tilting ultimately led to tailings liquefaction and bed failure. The stages in the excess PWP development within a 7.2 cm-thick bed in response to tilting can be more clearly seen in Figure 4.6, where $u_e$-profiles with depth below surface are shown for 5°, 15° and 23° angles of tilt. The plot at 23° angle of tilt corresponds to the actual bed failure within the Tank. For comparison, a line representing the variation of $\sigma'_n$ with depth below the bed surface is also presented in Figure 4.6.

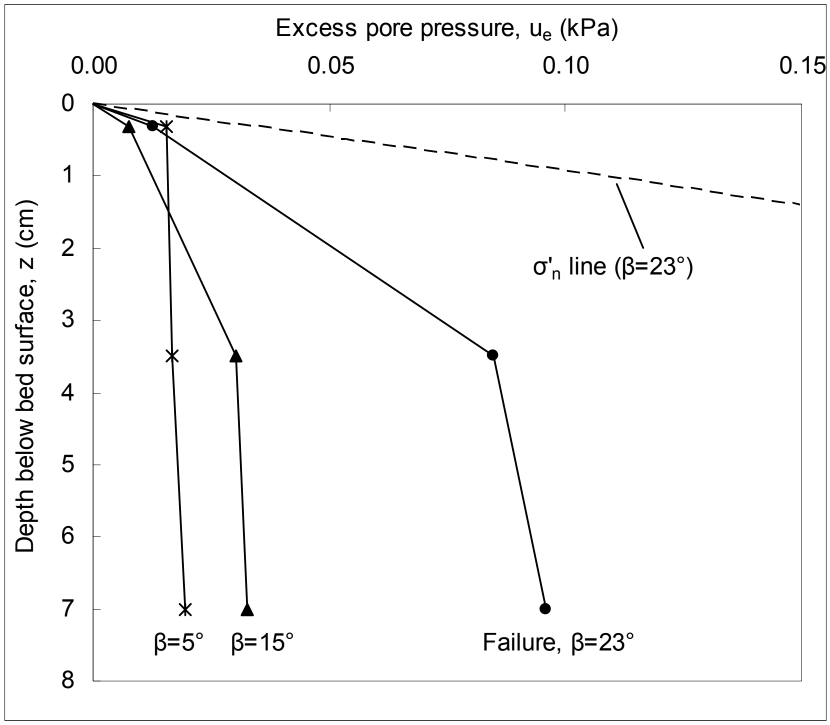


**Figure 4.6.** Profiles of the excess pore pressure versus depth below bed surface during rapid tilting of 7.2 cm–thick tailings bed, consolidated for 3 days at three angles of tilting.

Referring to Figure 4.6, it can be seen that at a tilt angle $\beta = 5^\circ$, the $u_e$ values at the top (P3), in the middle (P2) and at the bottom (P1) of the tailings bed are all very close, indicating uniform spatial distribution of excess PWP within the bed. This observation suggests that no hydraulic gradient exists within the tailings bed at $\beta = 5^\circ$. The profile at $\beta = 15^\circ$ shows that immediately below the bed surface (port P3), the rate of $u_e$ dissipation becomes greater than the rate of generation, resulting in a net decrease in measured $u_e$ values. The spatial distribution of excess PWP within the tailings bed at this angle of tilt is no longer uniform and hydraulic gradient begins to develop, which becomes the driving force behind the $u_e$ dissipation. At failure ($\beta = 23^\circ$), the $u_e$ data points at the bottom of the bed (port P1) and in the middle of the bed (port P2) are well away from the $\sigma'_n$-line. The maximum $u_e$ values recorded at the bottom and in the middle of the bed are 0.096 and 0.085 kPa, respectively. These values constitute approximately 23% and 13% of $\sigma'_n$ at these horizons, respectively. As evident from the $u_e$-profiles shown in Figure 4.6, during the test the generated excess PWP at the bottom and in the middle of the tailings bed remained much lower than the effective normal stresses at the same depths (e.g., the minimum difference between $u_e$ and $\sigma'_n$ was 0.29 kPa and 0.65 kPa, respectively), which was probably the reason why soil sliding did not occur along the base or in the middle of the bed. Recall that in all tilting experiments, drainage was allowed to occur only at the bed surface (z = 0). A close examination of the data in Figure 4.6 shows that immediately below the bed surface (port P3), the excess PWP remained very close to, although still below the effective normal stress, $\sigma'_n$, throughout the test. This could explain why tailings liquefaction and bed failure were observed at a failure plane located very close to that horizon (i.e., at 0.6 cm below the bed surface). We hypothesize that at the depth of the failure plane, because of the longer drainage path, the rate of excess PWP dissipation throughout the tests was slightly lower compared to the one measured at port P3. At a titling angle $\beta = 23^{\circ}$, the excess PWP reached the $\sigma'_n$ value at this horizon, which led to tailings liquefaction, and ultimately, to slope failure.

### *4.3.4. Failure modes*

In both rapid and slow tilting tests, initial slope failure occurred as a sheet along a failure plane parallel to the bottom of the Tank and located approximately 0.4 to 1.5 cm below the surface of the bed. Indeed, the conventional slope stability methods of analysis indicate that the most critical failure surface for a cohesionless slope is parallel to the slope surface (Lade 1992). During failure, the soil layer above the failure plane showed full loss of integrity and the entire soil mass slowly moved like a dense liquid to the bottom of the Tank. The failing soil appeared to liquefy and traveled down the slope like a wave leaving behind a rippled surface. Such behaviour can be explained with the following hypothesis. At failure, the soil structure in the vicinity of the failure plane begins to break down, the compressibility of the soil increases significantly and, consequently the PWP increases. The PWP increase propagates in an upward direction with associated reduction in effective stress, causing a loss of shear strength within the entire soil mass above that plane. Whitman (1985) terms this type of flow failure "disintegrative failure". When disintegrative failure occurs, the soil mass deforms continuously under constant static shear stress and large displacements are observed. In loose materials, such as the tested mine tailings, this phenomenon takes place under low to moderate shear stresses, e.g., beneath sloping ground. It is worth noting here, that for beds of the same thickness and age, the drained failure of the slope (slow tilting) usually occurred at angles of tilting, $\beta$, almost two times higher than in the partially drained tests (rapid tilting).

#### *4.3.5. Drained shear strength failure envelope*

In Subsection 4.3.1, we demonstrated that the primary consolidation of deposited mine tailings beds was complete within one and a half hours and, therefore, all beds (consolidated 3 or more days) tested in the present experimental program were believed to be fully consolidated. The consolidation time was defined as the time that elapsed between pouring the slurry into the Tank and the beginning of tilting. The tilting of the Tank containing the deposited tailings bed results in gravity components of the bed self weight tending to move the tailings mass from the higher to the lower wall. These forces produce shear stress throughout the soil mass and if it exceeds the shearing resistance of the tailings on any possible failure surface, sliding will occur. The shearing resistance depends on the shear strength of the tailings, which in the presented experimental program, can be considered either partially drained or drained depending on the mode of tilting. PWP measurements performed on 7.2 cm-thick tailings beds showed that, if slow tilting was employed, the excess PWP within the beds remained an order of magnitude lower than the normal effective stress at the respective depths. It was assumed that in beds with smaller final thickness, due to the shorter drainage paths, the excess PWP developed during slow tilting would dissipate even faster compared to the 7.2 cm-thick beds, resulting in similar or lower magnitude of the residual excess PWP in the beds. It is believed that during slow tilting, the generated excess pore water pressure had no significant effect on the strength of the tailings bed, the behaviour of which suggested drained loading and response. Therefore, the measured bed shear strength during slow tilting was considered "drained" and the recorded angle of failure was related to the effective stress parameters. The Mohr-Coulomb failure criterion, expressed as $\tau_f = \sigma'_{nf} \tan\phi'$, was applied to obtain the drained shear strength envelope of the studied mine tailings beds.

Deposited mine tailings beds with final thickness between 1 and 7.2 cm were also tested using the "slow" tilting mode at consolidation times of 3 and 12 days. The obtained drained shear strength results were plotted as a function of the normal effective stress at the failure plane (Figures 4.7a and b). The stress paths followed by the effective normal and shear stresses at the depth of the failure plane from the onset of the tilting to failure of the slope are also shown in Figures 4.7a and b.

a)

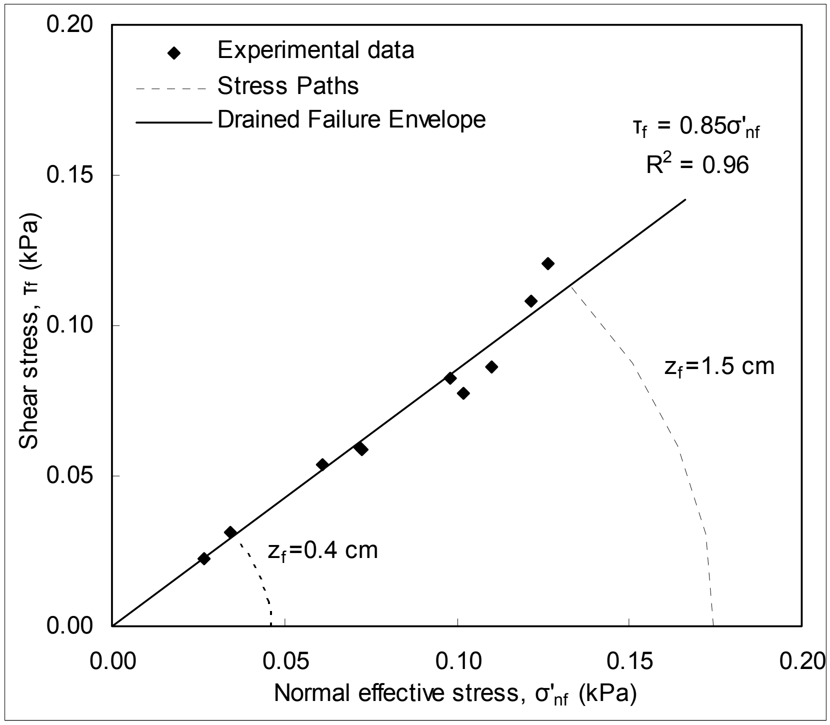


b)

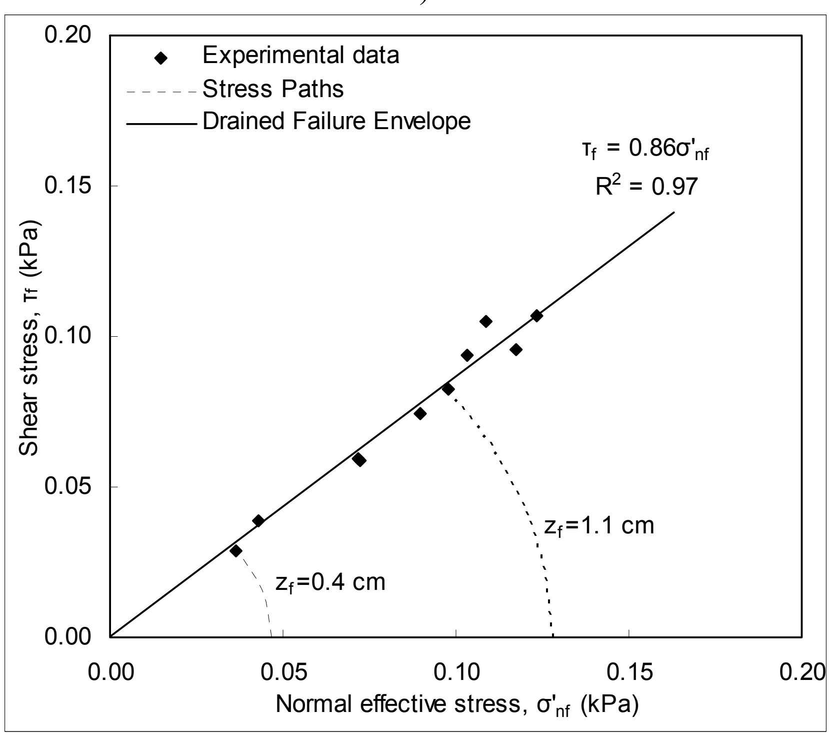


**Figure 4.7.** Drained failure envelope and effective stress paths for tailings beds of various thicknesses consolidated for: (a) 3 days; (b) 12 days.

Referring to Figures 4.7a and b, the stress states lying on the stress paths were obtained from Eqs. (4.3) and (4.4) and by varying the angle of tilting, $\beta$ , from zero to the angle of failure. Thus, at an angle of tilting, $\beta$ , equal to zero, the normal effective stress at the depth of the failure plane $\sigma'_n$ equals the vertical effective stress, $\sigma'_{v0}$ at the same depth. Respectively, when $\beta$ is set to be equal to the angle of tilting at failure, $\sigma'_n$ is equal to the normal effective stress at failure, $\sigma'_{nf}$ and the corresponding shear stress, $\tau$ is equal to the drained shear strength, $\tau_f$ of the tailings bed. At the onset of tilting, the vertical effective stress at a depth corresponding to the depth of the failure plane (Eq. 4.5) within beds of various final thicknesses was between 0.05 and 0.17 kPa. For each set of experimental data, a best fit line was drawn through the experimental data points and through the origin assuming a zero cohesion intercept. Based on the fact that the tested Clarabelle mine tailings were coarse grained and the tested beds were normally consolidated, the assumption was deemed reasonable. The *R*-squared (correlation coefficient) values for the fitted lines fall within 0.96 - 0.97. From Figures 4.7a and b, the slope of the fit line is 0.85 and 0.86 for the 3 and 12-day old beds, respectively. These slopes correspond to effective friction angle, $\phi'$ of 40.4° and 40.8°, for the 3 and 12-days old beds, respectively. Effective (drained) friction angle between 30° and 42° and close to zero cohesion, $c'$ have been reported in the literature for initially saturated hard rock mine tailings (Rassam 2002; Masengo and Julien 2003; Pettibone and Kealy 1971; Abadjiev 1985). When compared to values for natural sands or silts, it appears that $\phi'$ of the tested mine tailings is slightly higher. For example, naturally occurring silty sands at the same dry density as the tested tailings show an effective friction angle, $\phi'$ of about

34°-35° (Holtz and Kovacs 1981). Therefore, $\phi'$ of the tailings is approximately 5° to 6° higher than that of natural soils, which researchers have attributed to the more pronounced particle angularity of tailings (Pettibone and Kealy 1971; Mittal and Morgenstern 1975; Sarsby 2000).

Several authors have observed that the mechanical strength of granular soils increases with time for consolidation (e.g., Mitchell and Solymar 1984; Schmertmann 1987, 1991; Mesri et al. 1990). In saturated sands, for instance, the time-dependent strength increase after completion of primary consolidation can become pronounced after a period of only a few days (Mitchell and Solymar 1984). It has been suggested that the strength increase in granular soils is frictional in nature and is due to dispersive particle reorientation, internal stresses redistribution and increased interlocking with time (Schmertmann 1987, 1991). To investigate whether aging under constant effective stress had any effect on the mechanical strength of the tested mine tailings, drained strength experiments were performed also with tailings beds aged at 6, 18 and 46 days and the respective effective friction angles, $\phi'$ were determined. Obtained results consistently yielded a zero cohesion intercept for all tested beds, suggesting that cohesion due to cementation at the interparticle contacts did not develop as a result of aging. Furthermore, the effective friction angle, $\phi'$, showed only a minor increase with time for consolidation, i.e., from 40.4° at 3 days to 42.1° at 46 days. It was unclear whether this increase was due to a small frictional strength gain with time or to variation in the experimental conditions and hence, it was concluded that the shear strength of the tested mine tailings was relatively independent of the age of the deposited tailings beds.

### 4.3.6. Partially drained shear strength envelope

In contrast to slow tilting, rapid tilting caused a build up of excess PWP within the tailings bed with 7.2 cm final thickness; this pressure was of the same order of magnitude as the normal effective stress at the respective depths within the bed (Figures 4.5a to c). As discussed in Subsection 4.3.3, some of the excess PWP dissipated via drainage through the bed surface, resulting in partially drained shearing conditions. The two phenomena of excess pore pressure generation and dissipation took place simultaneously. Bed failure under these conditions was caused by the residual excess pore pressure becoming equal to the effective normal stress at a given plane, termed failure plane. Therefore, for partially drained shear strength tests, the excess pore water pressure/ effective normal stress ratio, $u_e / \sigma'_n = 1.0$ was adopted as a failure criterion and the angle of tilt, $\beta$, at which the failure criterion was satisfied was considered a failure angle. At the time of failure, the tailings mass above the failure plane suffered such a substantial reduction in shear strength that it seemed to flow like a liquid. In other words, bed failure through tailings liquefaction could be defined as the state where $\sigma'_{nf} = \sigma'_n - u_e = 0$ and the horizon where this condition was reached was the failure plane. However, since the exact depth of the failure plane could not be anticipated prior to testing, it was not possible to position any of the pore pressure transducers at this horizon and thus, obtain the actual value of $u_e$ at the moment of failure. Although, the $u_e$-profile at the angle of failure (Figure 4.6) suggested that positive (above hydrostatic) excess PWP developed within the entire bed, its exact magnitude at the location of the failure plane remained unknown and therefore, the reported partially drained strength envelope was a total stress envelope.

In Figures 4.8a and b, the partially drained shear strength results from testing of 3 and 12 days old beds of various final thicknesses were plotted as a function of the normal total stress at the failure plane.

a)

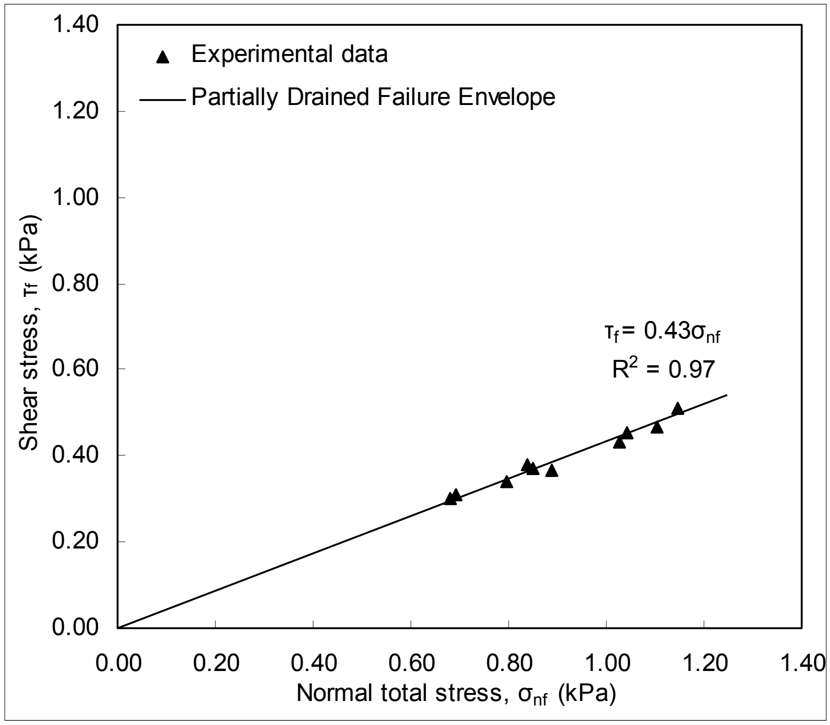


b)

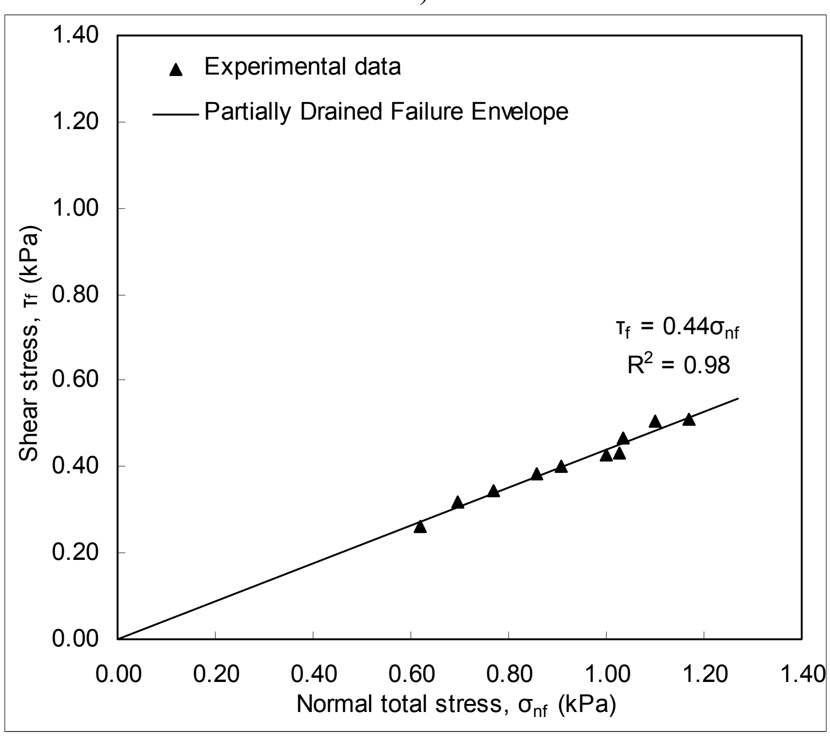


**Figure 4.8.** Partially drained failure envelope for tailings beds of various thicknesses consolidated for: (a) 3 days; (b) 12 days.

At the onset of tilting, the vertical total stress at the depth of the failure plane was calculated from Eq. (4.8) and varied between 0.61 and 1.16 kPa. Passing through the origin straight lines with *R*-squared values 0.97 and 0.98 for the 3 and 12 days old beds, respectively, were used to successfully fit the two sets of experimental data. Referring to Figures 4.8a and b, the total friction angle, $\phi_T$ for the beds aged at 3 and 12 days, was computed from the slopes of the fit lines as 23.3° and 23.8°, respectively. Such $\phi_T$ values fall within the same range as the ones reported in the literature for saturated hard rock mine tailings tested under undrained conditions, these being between 14° and 25° (Volpe 1979; Wahler 1974). Similarly to the effective friction angle, $\phi'$, the observed total friction angle, $\phi_T$ of the tailings appeared higher than of natural soils due to the more pronounced particle angularity caused by crushing the ore in the mill.

Little variation in the total stress failure envelopes and corresponding total (undrained) friction angles, $\phi_T$ was found when tailings beds aged at 3, 6, 12, 18 and 46 days were tested. For example, $\phi_T$ was determined to be 23.3° and 24.2° for the 3 and 46 days old beds, respectively, which suggested that, similarly to the drained strength, the partially drained strength of the tailings beds was also relatively insensitive to variations in time for consolidation.

### *4.3.7. Comparative evaluation of drained and partially drained shear strength results*

Figures 4.9a and b show a comparison between drained and partially drained shear strength results obtained using the Tilting Tank for 3 and 12 days old deposited beds, respectively. Recall that the drained strength envelope is essentially an effective strength envelope, whereas the partially drained envelope is a total stress envelope.

a)

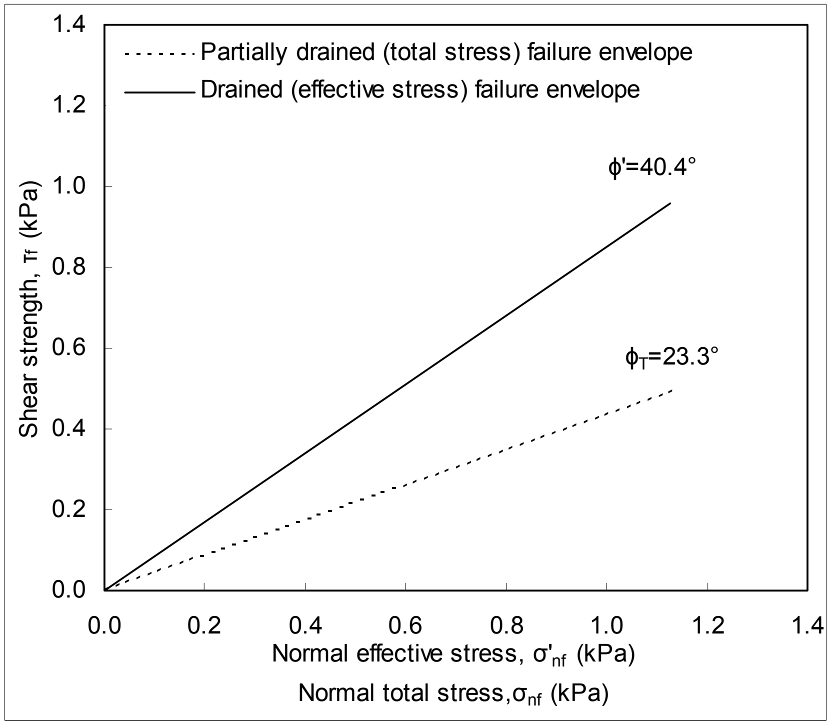


b)

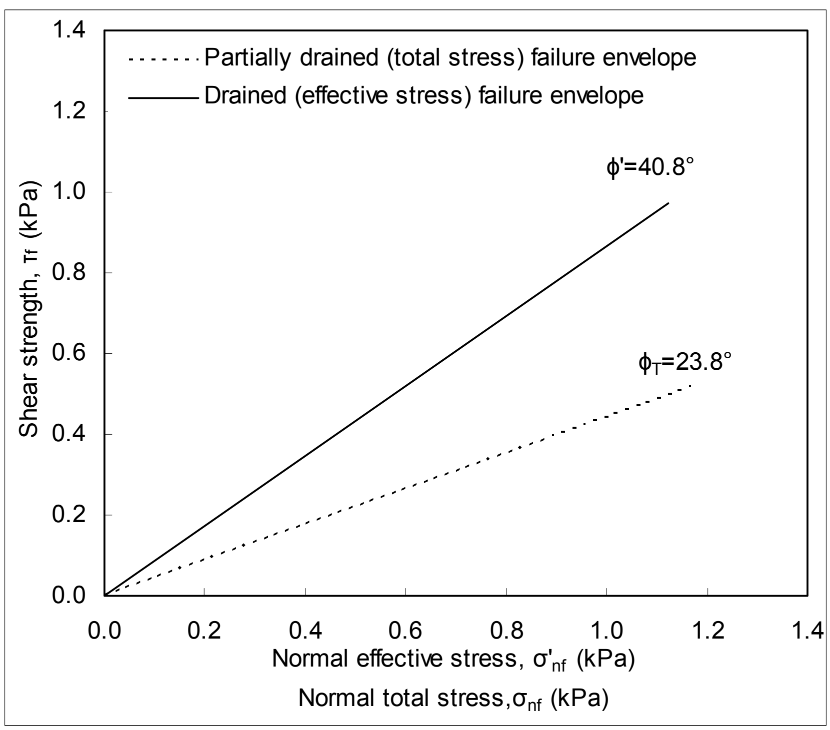


**Figure 4.9.** Comparison between drained and partially drained shear strength for tailings beds consolidated for: (a) 3 days; (b) 12 days.

As expected for a normally consolidated soil, the drained shear strength was higher than the partially drained strength over the entire stress range for all tested beds. This was due to the positive excess pore pressures generated during the rapid partially drained shearing in the Tilting Tank, which caused a reduction in the normal effective stress. The calculated total friction angle, $\phi_T$ was about 1.7 times lower than the effective friction angle, $\phi'$ .

The relatively small size of the tank (compared to that of a tailings pond, for example) could potentially produce scale effects on the shear strength of the tailings (both drained and partially drained), which effects would originate from two main sources: i) the limited length of the tank; and, ii) the side walls of the tank. The former would prevent the failing soil layer from behaving as an infinite slope due to the resistance of the soil that accumulates at the bottom end of the tank during failure and exerts an additional passive force, which would increase the resistance of the tailings to failure. The latter would increase the shear strength of the failing tailings layer due to mobilized shear resistance along the side walls of the tank. Both effects would increase the measured failure angle and, hence, the shear strength of the tailings. Zreik et al. (1998) assessed the effect of the size and geometry of the container on the shear strength of Boston Blue Clay deposited beds and concluded that the recorded failure angles most likely remained unaffected by the length of the tank. These authors also found that the effect of the shearing resistance along the side walls of the tank was negligible because the acrylic plastic-to-soil resistance was much smaller than the soil-to-soil resistance along the failure plane. On the basis of the results obtained by Zreik et al. (1998), the authors of the present paper concluded that tailings strengthening due to scale effects was not significant and the measured in the laboratory shear strength should be comparable to that in the field.

## 4.4. Summary and Conclusions

Mine tailings beds with final thicknesses between 1 and 7.2 cm were deposited from tailings/ water slurries with high concentration of solids (50% by volume) and left to consolidate for a period of at least 3 days. The slurry concentration was chosen in order to suppress segregation of particles during settling and to ensure that the obtained tailings deposit was relatively homogeneous and with minimum property variation with depth. Primary consolidation of the deposited tailings beds was complete within 1 - 1½ hour from the beginning of sedimentation. Obtained normally consolidated beds were tested at ages of 3, 6, 12, 18 and 46 days using a specially built Tilting Tank that closely simulated in-situ drainage conditions in a tailings pond. The effect of drainage conditions on the shear strength of the tailings beds was evaluated in a series of experiments involving tailings beds of various thicknesses and ages using two tilting modes. A slow titling speed of 0.07°/min was applied to measure the drained shear strength of the tested beds, whereas rapid tilting at 1.61°/min was adopted to induce tailings shearing under partially drained conditions. The principal findings of the research are summarized below.

The PWP measurements at three elevations within 7.2 cm-thick tailings bed demonstrated that measurable excess PWP built up within the beds during partially drained shearing, whereas during drained shearing, the excess PWP remained an order of magnitude lower than the normal effective stress at the respective depths. It was observed that slope failure always occurred along a failure plane parallel to the bottom of the Tank and located at 0.4 to 1.5 cm from the bed surface. At the time of failure, the structure of the failing layer was completely destroyed and the liquefied soil moved slowly like a wave to the bottom of the Tank. This behaviour was attributed to rapid generation of excess PWP at failure, leading to a substantial normal effective stress reduction and tailings liquefaction. Drained and an partially drained shear strength envelopes were successfully defined at a normal stress range from 0 to approximately 1.0 kPa, which was much lower than the stresses utilized in conventional geotechnical testing equipment. It was found that both drained and partially drained failure envelopes were linear within the tested stress range with zero cohesion intercept, as expected for a normally consolidated sandy soil. For beds tested at ages 3 and 12 days, the effective friction angle, $\phi'$ fell between 40.4° and 40.8°, whereas the total friction angle, $\phi_T$ was determined to be 1.7 times lower than $\phi'$ and ranged from 23.3° to 23.8°. Experimental results demonstrated little variation in both drained and partially drained shear strength with bed age.

## 4.5. Acknowledgements

This work was supported by funding from the Natural Sciences and Engineering Research Council of Canada (NSERC) in the form of an Individual Discovery Grant awarded to E.K. Yanful and a postgraduate scholarship awarded to R.S. Dimitrova.

## 4.6. References

Abadjiev C (1985) Estimation of the physical characteristics of deposited tailings in the tailings dam of nonferrous metallurgy. In: Proceedings of the 11th International Conference on Soil Mechanics and Foundation Engineering, San Francisco, California, USA, 12-16 August 1985. A. A. Balkema, Rotterdam, The Netherlands, pp. 1231-1234.

ASTM, Standard D 2487 (1997a) Classification of soils for Engineering Purposes. ASTM. Annual book of ASTM standards. American Society for Testing and Materials, Philadelphia, Pasadena, USA.

ASTM, Standard D4318-93 (1997b) Standard test methods for liquid limit, plastic limit, and plasticity index of soils. Annual book of ASTM standards. American Society for Testing and Materials, Philadelphia, Pasadena, USA.

Cheng DCH (1980) Sedimentation of suspensions and storage stability. Chemistry and Industry, 10:407-414.

Davies R (1968) The experimental study of the differential settling of particles in suspension at high concentrations. Powder Technology, 2(1):43-51.

Fannin RJ, Eliadorani A, Wilkinson JMT (2005) Shear strength of cohesionless soils at low stress. Géotechnique, 55(6):467-478.

Highter WH, Vallee RP (1980) The liquefaction of different mine tailings under stress controlled loading. Engineering Geology, 16:147-150.

Holtz R, Kovacs W (1981) An introduction to geotechnical engineering. Prentice-Hall, Inc., Englewood Cliffs, New Jersey, USA.

Kamhawi KZR, Arthur JRF (1992) The shear strength of two reconstituted clays at very low stress levels. Report, University College of London, London, UK.

Lade PV (1992) Static instability and liquefaction of loose fine sandy slopes. Journal of Geotechnical Engineering, 118(1):51-71.

Lambe T, Whitman R (1969) Soil mechanics. John Wiley & Sons, New York, USA.

Masengo E, Julien M (2003) Risks associated with construction on submerged tailings beaches. In: Proceedings of the 10th International conference on Tailings and Mine Waste, Vail, Colorado, USA, 12-15 October 2003. Swets & Zeitlinger, Lisse, The Netherlands, pp. 159-169.

Matyas E, Welch D, Reades D (1984) Geotechnical parameters and behaviour of uranium tailings. Canadian Geotechnical Journal, 21:489-504.

Mesri G, Feng TW, Benak JM (1990) Postdensification penetration resistance of clean sands. ASCE Journal of Geotechnical Engineering, 116(7):1095-1115.

Mitchell JK, Solymar ZV (1984) Time-dependent strength gain in freshly deposited or densified sand. ASCE Journal of Geotechnical Engineering, 110(11):1559-1576.

Mittal H, Morgenstern N (1975) Parameters for the design of tailings dams. Canadian Geotechnical Journal, 12:235-261.

Pettibone H, Kealy C (1971) Engineering properties of mine tailings. Journal of the Soil Mechanics and Foundations Division, 97(SM9):1207-1225.

Qiu Y, Sego D (2001) Laboratory properties of mine tailings. Canadian Geotechnical Journal, 38:183-190.

Rassam D (2002) Variation of evaporative and shear strength parameters along a tailings delta. Canadian Geotechnical Journal, 39:32-45.

Sarsby R (2000) Environmental geotechnics. Tomas Telford Publishing, London, UK.

Schmertman JH (1987) Time-dependent strength gain in freshly deposited or densified sand–discussion. ASCE Journal of Geotechnical Engineering, 113(2):173-175.

Schmertmann JH (1991) The mechanical aging of soils. ASCE Journal of Geotechnical Engineering, 117(9):1288-1330.

Shaw SC, Groat LA, Jambor JL, Blowes DW, Hanton-Fong CJ, Stuparyk RA (1998) Mineralogical study of base metal tailings with various sulfide contents, oxidized in laboratory columns and field lysimeters. Environmental Geology, 33(2/3):209-217.

Sture S, Costes NC, Batiste SN, Lankton MR, AlShibli KA, Jeremic B, Swanson RA, Frank M (1998) Mechanics of granular materials at low effective stresses. Journal of Aerospace Engineering, 11(3):67-72.

Tibana S, de Campos T, Bernardes G (2002) A brief discussion of the behaviour of a loose iron tailing material under undrained triaxial loading. In: Proceedings of the 9th International Conference on Tailings and Mine Waste, Fort Collins, Colorado, USA, 27-30 January 2002, Swets & Zeitlinger, Lisse, The Netherlands, pp. 325-330.

Ulrich BF, Fourie AB (2003) Assessment of the potential for static liquefaction of a tailings dam using laboratory and field testing. In: Proceedings of the 10th International conference on Tailings and Mine Waste, Vail, Colorado, USA, 12-15 October 2003. Swets & Zeitlinger, Lisse, The Netherlands, pp. 137-147.

Vaid YP, Eliadorani A (1998) Instability and liquefaction of granular soils under undrained and partially drained states. Canadian Geotechnical Journal, 35:1053-1062.

Vaid YP, Eliadorani A (2000) Undrained and drained (?) stress–strain response. Canadian Geotechnical Journal, 37:1126-1130.

Vick SG (1990) Planning, analysis, and design of tailings dams. 2nd edn. BiTech Publishers, Vancouver, B.C., Canada.

Volpe R (1979) Physical and engineering properties of copper tailings. In: Proceedings of Current Geotechnical Practice in Mine Waste Disposal. Edited by The Committee on Embankment Dams and Slopes of the Geotechnical Engineering Division. American Society of Civil Engineering, New York, USA, pp. 142-160.

Wahler WA 1974. Evaluation of mill tailings disposal practices and potential dam stability problems in Southwestern United States. Bureau of Mines Open File Report, U.S. Bureau of Mines, OFR50(1)-75-OFR50(5)-75.

Whitman RV (1985) On liquefaction. In: Proceedings of the 11th International Conference on Soil Mechanics and Foundation Engineering, San Francisco, California, USA, 12-16 August 1985. A. A. Balkema, Rotterdam, The Netherlands, pp. 1923-1927.

Zreik DA, Germaine JT, Ladd CC (1998) Failure envelope of cohesive soils in the ultra-low stress range. Soils and Foundations, 38(2):201-210.

# CHAPTER 5. FACTORS AFFECTING THE SHEAR STRENGTH OF MINE TAILINGS/CLAY MIXTURES WITH VARYING CLAY CONTENT AND CLAY MINERALOGY

## 5.1. Introduction

Tailings are the waste product generated during the recovery of mineral commodities from ore. In the conventional hard-rock milling process, the crude ore is crushed and then ground in mills to a particle size of less than 0.1 mm in order to allow the extraction of the valuable metals (Jewell 1998). The milling of ore-bearing, hard silicate rocks produces very sharp angular particles typically in the sand and silt size range whereas the colloidal particles are generally lost when the excess water and fines are removed from the mill tailings. As a result, the percentage of clay-size particles (less than 2 μm) in base metal tailings usually does not exceed 10-15% by weight, which is confirmed by the literature examples given in Table 5.1.

| No. samples analyzed | Description of material used | $G_s$ | $D_{50}$ (mm) | % clay-size particles by weight | Source | Clay mineralogy | Reference |
|---|---|---|---|---|---|---|---|
| 4 | Hard-rock mine sulphide tailings | 2.9-3.8 | 0.016-0.040 | 5-9 | Canada | Unknown | Benzaazoua et al. (2002) |
| 3 | Hard-rock mine tailings (low plasticity silts, ML) | - | 0.028-0.038 | 4-6 | Unknown | Unknown | Aubertin et al. (1998) |
| 1 | Gold mine tailings | 2.6 | 0.01 | 2-4 | Kirkland Lake, ON | Unknown | Amaratunga and Yaschyshyn (1997) |
| 6 | Hard-rock mine sulphide tailings (sand with minor layers of silt) | - | - | 0 | Sudbury, ON | C, B | Shaw et al. (1998) |
| 4 | Hard-rock mine tailings (fine to medium grained, well graded sand) | - | 0.08-0.18 | 0 | Sudbury, ON | C, B | McGregor et al. (1998) |
| 9 | Hard-rock mine tailings | - | 0.016 | 7-10 | Eastern Canada | - | Fall et al. (2009) |
| 10 | Hard-rock mine tailings, low plasticity silts, ML) | - | 0.012 | 3-5 | North-eastern Cuba | S | Rodríguez (2006) |
| 3 | Mine tailings, silt and fine sand | - | 0.017 | 10 | Val-d'Or, Quebec | Ms, C | Ouangrawa et al. (2009) |
| 4 | Hard-rock tailings from base and precious metal mines | - | 0.023-0.037 | 4-8 | Abitibi, Quebec | C, Mc,T | Benzaazoua et al. (2000) |
| 9 | Hard rock tailings | 2.80-3.35 | 0.05-0.26 | 2-3 | USA, Canada | C | Pettibone and Kealy (1971) |
| 27 | Copper-gold and copper-gold-zinc tailings | 2.8-4.5 | - | 6-14 | BC, Canada | - | Wijewickreme et al. (2005) |

**Table 5.1.** Characteristics of mine tailings samples used in published research work. C – Chlorite; B – Biotite; K - Kaolinite, S – Serpentine, Ms – Muscovite, Mc – Mica, T – Talc.

The tailings, along with the spent process water, form a slurry, which is then pumped to a tailings storage facility. Although the solid fraction of this slurry behaves like a soil, the tailings are different from most naturally occurring soils in several respects (Jewell 1998). The ores, typically containing some base, rare or precious metals, are often sulphide-rich and extraction of these metals results in the generation of large quantities of sulphide-rich tailings. In the presence of oxygen and water, these tailings have the potential to oxidise and generate acid. Elevated acidity leads to solubilisation and subsequent release of toxic heavy metals such as Pb, Cu, Zn, As, Ni, Co and Cd. Acidic waters can cause discoloration and turbidity in the mining effluent, but it is the dissolved metals that can cause a decrease in aquatic life, bioaccumulation of metals, and reduction in the groundwater quality. Some chemical reagents such as cyanide used to recover precious metals are also toxic in sufficient concentrations. The density and strength of a body of tailings are initially low and increase relatively slowly with time (Jewell 1998; Wilson et al. 2006). If a breach develops in the confining embankment, low strength tailings can flow for considerable distances and the impact from such failure or from seepage of contaminants on public safety and the environment can be disastrous. Another notable difference between mine tailings and natural soils is the wide range of specific gravity values observed in the former due to the presence of heavy metals in the tailings (Pettibone and Kealy 1971; Rankine et al. 2006). Whereas for most natural soils the specific gravity typically varies between 2.65 and 3.0, for mine tailings it can fall anywhere between 2.6 and 4.5 (Table 5.1). Larger range of void ratios in mine tailings in comparison to natural sandy soils has also been observed (Mittal and Morgenstern 1975). Mine tailings also exhibit close to zero cohesion and 5° to 6° higher friction angles than most natural soils of similar gradation, which researches have attributed to the angularity of tailings particles (Pettibone and Kealy 1971; Rodríguez 2006; Rankine et al. 2006). For instance, Rankine et al. (2006) compared the estimated friction angle of mine tailings using existing empirical relations for granular soils with the actual effective peak friction angles measured in the laboratory. The authors observed that the measured drained friction angles were substantially higher than the estimated and concluded that empirical relations developed for granular soils cannot be applied successfully to mine tailings.

The literature offers many examples of utilizing mine tailings as engineering material. Because the tailings provide a convenient and economic source of borrow material, mining companies often use the coarse fraction for construction of engineered tailings dams (e.g., Penman 1998) or as a hydraulic backfill (e.g., Amaratunga and Yaschyshyn 1997; Benzaazoua et al. 2002; Rankine et al. 2006) whereas the fine fraction is disposed of in tailings ponds. If the physical and chemical properties of the whole tailings fraction are modified in a way so that they can be utilized in an environmentally safe manner for surface or underground applications, this would reduce their accumulation in the tailings pond and even possibly eliminate the need for tailings impoundments altogether. Additional benefits would include the reduction of costs associated with constructing, managing and reclaiming tailings ponds and the removal of constraints placed upon fine grinding as an effective means of valuable minerals liberation (Amaratunga and Yaschyshyn 1997). Researchers have proposed the incorporation of acid-generating tailings containing at least 20% paricles with size less than 20 μm into paste backfill as a viable means of preventing sulphide mineral oxidation and subsequent release of toxic metals in the environment (Benzaazoua et al. 2004). The use of desulphurised tailings as construction material for an engineered cover to prevent acid mine drainage (AMD) has been considered as well (Benzaazoua et al. 2000; Bois et al. 2004; Demers et al. 2009). The feasibility of using bentonite/ mine tailings paste mixtures as a barrier (liner or cover) material for mine waste containment facilities has also been investigated (Fall et al. 2009; Wilson et al. 2006). Such mixtures would offer the benefit of reducing the amount of waste to be managed by mining operators as well as the cost of surface tailings management and can potentially also be used in municipal landfills (Fall et al. 2009).

Whether disposed in tailings ponds or used in constructing containment walls, there are many geotechnical issues involved in tailings management, including the rate of sedimentation of the tailings, their consolidation behaviour, erodibility and compaction characteristics (Fahey and Newson 1997). From the geotechnical point of view, the basic tailings characteristics are specific gravity, particle size distribution, mineralogy of the clay-size fraction, strength, density and hydraulic conductivity. These properties are often used as input parameters in various models of tailings behaviour (e.g., Holtz and Kovacs 1981; Aubertin et al. 1998) and when evaluating the stability and long term performance of tailings embankments and cover systems (Wilson et al. 2006). For example, the stability and resistance of tailings dams against erosion strongly depends upon the strength of the tailings used in their construction and upon the type of loading (static or dynamic), whereas the rate at which seepage from a tailings embankment occurs is governed by the permeability of the tailings (Bell 1999). Those properties that are related to the constitution and general nature of tailings are referred to as intrinsic variables. An example of intrinsic variable is the critical state friction angle, which is commonly taken as a unique value for a given granular soil, regardless of the initial relative density of the sample and initial confining stress (Salgado et al. 2000). In tailings sands and other soils with rotund particles, for which particle orientation during shearing does not occur, the critical shear strength is equal to the residual strength. Other intrinsic variables are the particle shape and size distribution, particle surface characteristics, and mineralogy. Many researchers have shown that the engineering behaviour of tailings, and soils in general, is strongly influenced by both the percent clay-size particles (less than 2 μm) present and the clay mineralogy (e.g., Kenney 1967; Mittal and Morgenstern 1975; Stark and Eid 1994; Raudkivi 1998; Al-Shayea 2001; Di Maio et al. 2004; Tiwari and Marui 2005). With increasing clay-size fraction, the soil becomes more plastic, its swelling and shrinkage potential increases and so does its compressibility. In contrast, the permeability and angle of internal friction of the soil mass decrease (e.g., Mitchell and Soga 2005; Stark and Eid 1994; Al-Shayea 2001; Tiwari and Marui 2005). Only 10% of clay is sufficient to assume control of the properties of a soil (Raudkivi 1998). Clay mineralogy controls the size, shape and surface characteristics of the clay particles and thus determines the engineering properties of the soil (Mitchell and Soga 2005). For instance, volume change behaviour of artificial mixtures and natural soils reconstituted using distilled water is strongly influenced by the clay mineral composition and, in particular, by the percentage of smectite (Di Maio et al. 2004). The effect of smectite content is stress-dependent, i.e., it is most pronounced at low axial stresses and decreases with the stress level increase. Furthermore, the influence of the salt concentration of the pore water solution is close to negligible for mixtures containing kaolinite as primary clay mineral, and increases with increasing percentage of montmorillonite in the samples. Thus, compressibility of bentonite reconstituted with concentrated salt solutions becomes close to that of commercial kaolin, irrespective of the pore water solution. Fahey and

Newson (1997) noted that even a relatively small percentage of montmorillonite can severely affect the sedimentation rate, consolidation behaviour, permeability and strength of mine tailings. Stark and Eid (1994) found that the drained residual strength of soils was related to both the type of clay mineral and percentage of clay-size particles. They proposed to use the liquid limits as an identificator of clay mineralogy and defined a relationship between the liquid limit, clay-size fraction and the residual shear strength of the soil. Tiwari and Marui (2005) proposed a correlation method based on mineralogical composition for the estimation of the residual friction angle of soils with various proportions of clay and non-clay minerals. Lupini et al. (1981) noted that the clay fraction may not be sufficient to determine the residual strength of a soil and the proportion of platy to rotund particles present should also be considered. Thus, depending on clay fraction and the proportion of platy to rotund particles, three residual shearing modes are likely to take place. A turbulent shearing mode is observed in soils with clay fraction below 25% and a high proportion of rotund particles or with platy particles of high interparticle friction, in which preferred orientation of platy particles does not occur. A sliding mode is characteristic of soils with clay fraction above 50% in which a low strength shear surface of strongly oriented low friction platy particles forms. In soils with clay fraction in the intermediate range, i.e., between 25% and 50% both turbulent and sliding shear modes take place.

The present paper studies the various factors that control the shear strength of artificially prepared mine tailings/clay mixtures with various clay content and clay mineralogy. Considered are the effect of mixture composition, rate of load application, drainage conditions and time for consolidation under constant effective stress. As discussed above, the importance of clay content and clay mineralogy as parameters influencing the behaviour of soils has been well established and widely publicised. The originality of the present work lies in the experimental methods used to measure the extremely low mechanical strength of freshly deposited mixed tailings/clay beds in their undisturbed, structured state closely simulating conditions in a tailings pond. Performance of the shear strength measurements under different rates of loading and degrees of drainage also contributes to the novelty of the research. Although test results were obtained using specific mine tailings and clay additives, and therefore may not be generalized for all mine tailings and clay minerals, they can facilitate the interpretation of the behaviour of other saturated tailings with varying clay mineral composition or other tailings/clay mixtures.

## 5.2. Testing materials and Procedures

### *5.2.1. Tailings beds preparation*

The original mine tailings used in the present study were received in the form of tailings/water slurry from the Clarabelle Copper Mine located in Sudbury, Ontario, and were obtained from the processing of the Sudbury Basin ore. The mineralogical composition of the Sudbury Basin ore, as given in Agar (1991), is: pentlandite (3%), chalcopyrite (3.7%), pyrrhotite (20%), quartz (16%), feldspar (14%), chlorite (21%), biotite (11%), amphibole (10%) and carbonates (2%). The primary minerals found in the tailings are: pentlandite, chalcopyrite, pyrrhotite, quartz, feldspar, chlorite, biotite, amphibole, carbonates plus minor pyroxene, apatite, magnetite, ilmenite, marcasite, galena and pyrite (Shaw et al. 1998; McGregor et al.1998). Reported studies (Agar 1991;

Shaw et al. 1998; McGregor et al. 1998) have also indicated that the predominant clay minerals in the Sudbury tailings are chlorite and biotite. These clay minerals are traditionally not reactive and possess low cohesive strength. Artificial mine tailings/clay mixtures were prepared in the laboratory by mixing the original non-cohesive and non-plastic silty sand tailings with various amounts of dry kaolin (Fisher Scientific Chemical) or bentonite powder (Baroid Quick-Gel Fast Mixing High Viscosity Bentonite). The primary clay mineral in the selected commercial kaolin was kaolinite, whereas the bentonite was composed of Na-montmorillonite. The total clay content in the obtained mixed soil samples was 8, 12 or 16% (by weight), with the upper boundary selected to correspond to the maximum clay percentage found in most tailings in Canada. Kaolinite (the main constituent in kaolin) was chosen as an additive because it is a common clay mineral and, in terms of physico-chemical properties, it exhibits characteristics close to those of chlorite (Mitchell and Soga 2005), the dominant clay mineral present in the original tailings. Kaolinite possesses low plasticity and cohesion, low compressibility and limited surface activity and thus, it is not likely to react with the pore-water solution in the course of testing. This makes it a suitable candidate for additive, since the present study was also concerned with the effect of clay content on the geotechnical properties of tailings/clay mixtures. Another part of the study aimed at investigating the effect of clay mineralogy on the engineering behaviour of mine tailings. Researchers have shown that for reconstituted samples prepared using distilled water, the percentage of smectite has the highest influence on the geotechnical properties of soils, such as shear strength, compressibility, void ratio and hydraulic conductivity (Di Maio et al. 2004). Na-montmorillonite with its thin particles exhibits very high specific surface (50-800 $m^2/g$), combined with high plasticity and cohesion. The high shrink/swell potential of Na-montmorillonite makes soils containing this mineral extremely compressible (Holeman 1965). Since even a small quantity of Na-montmorillonite can have a major effect on engineering properties of mine tailings, it was used as a second additive in the present study.

The characteristics of the original tailings (denoted T) and soil mixtures prepared in the laboratory with increased amounts of clay-size material (denoted M) are summarized in Table 5.2.

| Sample ID | Clay (%) | Silt (%) | Sand (%) | Clay mineralogy | $G_s$ | $w_L$ (%) | $w_P$ (%) | $I_P$ (%) | Casagrande classification |
|---|---|---|---|---|---|---|---|---|---|
| T1 | 4 | 28 | 68 | C, B | 2.986 | 12-15 | NP | - | SM |
| M2 | 8 | 27 | 65 | C, B, K | 2.968 | 15-16 | NP | - | SM |
| M3 | 12 | 26 | 62 | C, B, K | 2.955 | 16-17 | NP | - | SM |
| M4 | 16 | 25 | 59 | C, B, K | 2.949 | 18-20 | NP | - | SM |
| M5 | 8 | 27 | 65 | C, B, Na-M | 2.913 | 26 | 21 | 5 | SM-SC |

**Table 5.2.** Composition and physical properties of mine tailings and artificial mixtures. C – Chlorite; B – Biotite; K – Kaolinite; M – Montmorillonite; $w_L$- liquid limit; $w_P$ - plastic limit; $I_P$- plasticity index.

Grain size distribution curves of the dry tailings mass and the artificial tailings/clay mixtures are presented in Figure 5.1.

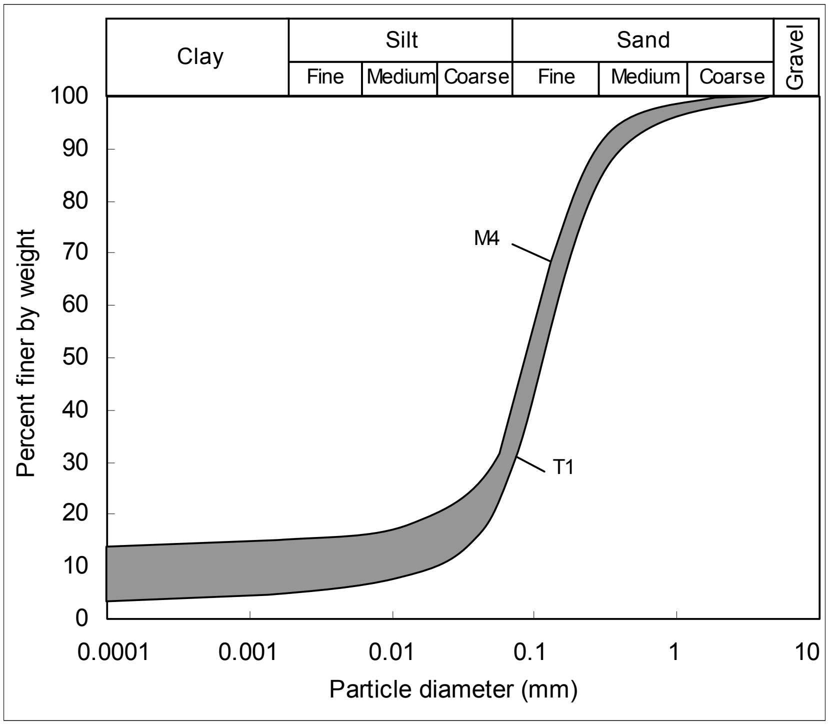


**Figure 5.1.** Grain size distribution curves of the original mine tailings and artificial tailings/clay mixtures.

As shown in Figure 5.1, the original tailings material (T1) was composed of 68% coarse (more than 0.075 mm) and 32% fine fraction (less than 0.075 mm), of which only 4% was clay-size material (less than 2 μm). The grain size distribution curve of the T1 tailings gave the lower boundary of the range of curves describing the particle size distribution of the mixtures used in the present study. As clay (kaolin or bentonite) was added to the tailings, the total clay content of the mixtures was brought up to 16% while keeping a constant sand/silt ratio. The mixture with the highest total clay content was M4 and it gave the upper boundary of the range of curves for all tested soil specimens. The grain size distribution curves of the mixtures with clay content intermediate between T1 and M4 fell in the shaded area in Figure 5.1 between the M4 and T1 curves.

Distilled water was added to the tailings/clay mixtures to obtain slurries with high concentration of solids (50% by volume). The slurries were thoroughly mixed with an electrical mixer (ARROW 1750) for about ten minutes after which they were poured directly into an acrylic tank (L = 45 cm, W = 22.5 cm, H = 12.5 cm) and left to consolidate under self-weight for a minimum period of 3 days. This minimum consolidation time was proven sufficient to ensure that primary consolidation of the beds was complete as explained in greater detail later in this paper. Distilled water was used in the slurry preparation to minimize chemical interactions in the tailings-clay-water system, whereas the specific slurry concentration was chosen to obtain deposits with relatively homogeneous properties over depth. Deposited mixed tailings/clay beds with final thickness between 1 and 11 cm were prepared using slurries of the same concentration (50% by volume) but with various initial heights. All sedimented tailings beds were normally consolidated and were tested at consolidation times of 3 and 12 days. During the experiments, the ambient temperature in the laboratory was kept constant at 22°±1°C.

### *5.2.2. Shear strength testing*

The shear strength of the sedimented mixed beds under drained and partially drained conditions was obtained using the Tilting tank, previously described in Chapter 4, Section 4.2, Subsection 4.2.2. The acrylic tank with the deposited tailings bed was first filled with water, sealed and then tilted on one side by the means of a pulley and a motor system. The angle of tilting at which failure of the tested bed occurred was measured and recorded. Bed failure was defined as sliding of a portion of the bed to the bottom of the Tank as a result of tilting and it was detected by a photosensor mounted on the sidewall of the Tank. The evolution of excess pore water pressure (PWP) with time within the beds was monitored and recorded using pressure transducers (VIATRAN 245) at three ports numbered P1, P2 and P3 and positioned in a vertical array at elevations 0.5, 3.5 and 7.0 cm from the bottom of the Tank, respectively. Two tilting modes were employed during the experimental program: i) slow tilting at an average speed of 0.07°/min, and ii) rapid tilting at a speed of 1.61°/min. Further details on sample preparation procedure and used equipment can be found in Chapter 4, Section 4.2, Subsections 4.2.1 and 4.2.2.

Observed failure patterns during shearing suggested that infinite slope theory may be adopted to analyse the stability of the tested beds. In this type of analysis, the thickness of the unstable material is small compared to the overall thickness of the bed and the failure surface is parallel to the slope (Lambe and Whitman 1969). For drained conditions and under the assumption of zero excess pore pressures, at failure, the normal effective and shear stress at the failure plane are given by:

$$\sigma'_{nf} = \sigma'_{v0} \cos\beta \tag{5.1}$$

$$\tau_f = \sigma'_{nf} \tan\phi' = \sigma'_{v0} \sin\beta \tag{5.2}$$

where $\sigma'_{nf}$ is the effective normal stress at the failure plane at failure in kPa, $\tau_f$ is the shear strength of the tailings bed in kPa, $\phi'$ is the drained (effective) friction angle in degrees, $\sigma'_{v0}$ is the vertical effective stress at a depth corresponding to the depth of the failure plane at the start of tilting in kPa, and $\beta$ is the measured angle of tilting in degrees.

At the onset of tilting, the vertical effective stress at a depth corresponding to the depth of the failure plane can be computed from the average buoyant unit weight of the tailings/clay bed and the thickness of the soil layer above the failure plane:

$$\sigma'_{v0} = \gamma' z_f \tag{5.3}$$

where $\gamma'$ is the average buoyant unit weight of the tailings bed in kN/m$^3$, and $z_f$ is the depth from bed surface to the failure plane along the normal to the slope in m.

At failure, the total normal stress and shear strength at the failure plane can be determined from:

$$\sigma_{nf} = \sigma_{v0} \cos \beta \tag{5.4}$$

$$\tau_f = \sigma_{nf} \tan \phi_T = \sigma_{v0} \sin \beta \tag{5.5}$$

where $\sigma_{nf}$ is the total normal stress at the failure plane at failure in kPa, $\tau_f$ is the shear strength of the tailings bed in kPa, $\phi_T$ is the total friction angle in degrees, and $\sigma_{v0}$ is the vertical total stress at a depth corresponding to the depth of the failure plane at the start of tilting in kPa.

The vertical total stress at the depth of the failure plane at the start of tilting is given by:

$$\sigma_{v0} = \gamma_{sat} z_f + \gamma_w z_w \tag{5.6}$$

where $\gamma_{sat}$ is the average saturated unit weight of the tailings bed in kN/m$^3$, $\gamma_w$ is the unit weight of water in kN/m$^3$, and $z_w$ is the depth of the water above the tailings bed in m.

## 5.3. Results and Discussion

### *5.3.1. Physico-chemical properties of the tailings/clay mixtures*

As the data presented in Table 5.2 suggest, increasing the amount of clay in the tailings/clay mixtures produces a corresponding increase in their liquid limit ($w_L$) while reducing their specific gravity ($G_s$). This can be expected since the water in the soils is almost entirely associated with the clay-size fraction and thus, increasing the clay content of the mixtures would also increase their water content at the liquid limit (Mitchell and Soga 2005). When the added clay is highly expansive, as is the case with bentonite, a large amount of water is absorbed as interlayer water, which is effectively immobilized within the soil matrix thereby leading to high water content of tailings/clay mixture at both the liquid and plastic limits. Furthermore, pure kaolinite and Na-montmorillonite both have specific gravities (2.61 and 2.51, respectively) that are lower than that of the pure tailings (2.99) and, therefore, adding clay would result in lowering the $G_s$ of the entire mixture (Fang and Daniels 2006). Mixing the tailings with up to 12% kaolinite did not result in development of plasticity, whereas addition of only 4% bentonite (Na-montmorillonite) gave the samples some low but measurable plasticity. Futhermore, whereas the tailings/kaolinite mixtures remained inactive, the activity of the tailings/bentonite mixture was calculated as 0.625

### 5.3.2. Excess Pore Water Pressure (PWP) measurements

#### *5.3.2.1. Sedimentation and consolidation*

The high concentration of solids in the slurries used in the preparation of the mixed tailings/clay beds ensured relatively constant particle gradation in the bed profile. This was also confirmed by visual observations which showed uniform texture and colour of the beds. The void ratio, *e*, of the sedimented beds generally increased with increasing percentage clay in the mixture in the following order T1<M2<M3<M4<M5. Thus, the average bed *e* was approximately 0.67 for T1, 0.69 for M2, 0.71 for M3, 0.74 for M4, and 1.34 for M5. These results indicate that kaolinite had a much smaller effect on bed *e* than bentonite, which may be explained by the highly expansive character of bentonite as indicated in literature. For instance, Di Maio et al. (2004) demonstrated that with respect to compression and swelling, at the low stress range (between 10 and 100 kPa) the void ratio and compression behaviour of kaolinite was similar to that of pure sand, while bentonite exhibited 5 to 8 times higher void ratio and much higher compressibility than sand.

Figure 5.2 shows the PWP variation with time at the bottom of three mixed tailings/clay beds prepared from mixtures T1, M4 and M5 (Table 5.2), during bed formation and primary consolidation, i.e., from the moment the tailings/clay/water slurry was poured into the Tank until the excess PWP was fully dissipated.

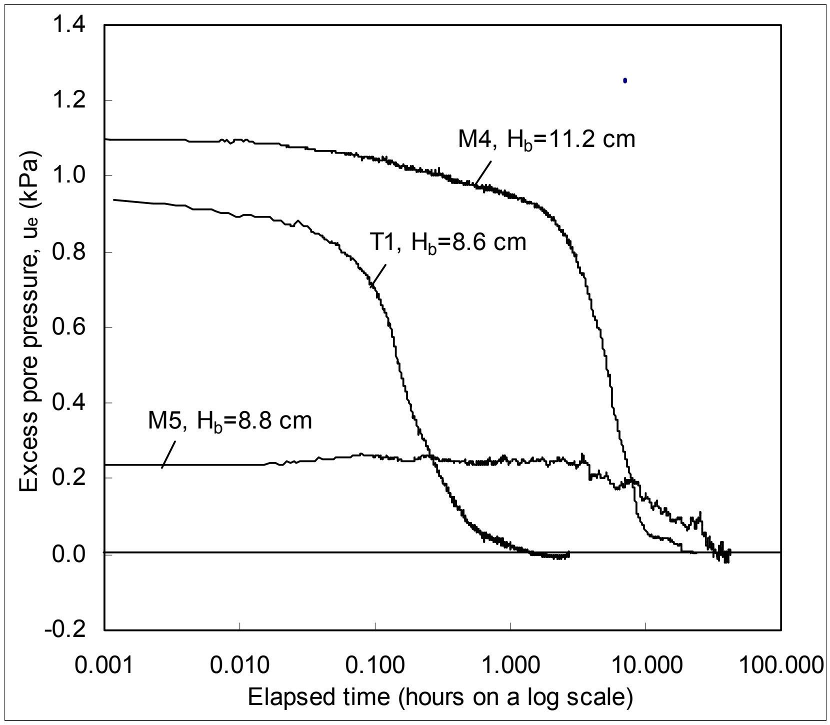


**Figure 5.2.** Excess pore water pressure variation with time at the bottom of three tailings/clay beds during sedimentation and consolidation.

It was found that in the T1 bed with 4% clay content and clay fraction comprising only inactive clay minerals (chlorite and biotite), the PWP at the bottom of the bed returned to its hydrostatic value within 1 - 1½ hour from the beginning of the sedimentation/consolidation experiment. In the M4 bed with the highest clay content (16%) of all investigated mixtures and clay fraction comprising inactive minerals (chlorite, biotite and kaolinite) it took approximately 24 hours for the excess PWP generated during the settling and primary consolidation phases of bed formation to fully dissipate (Figure 5.2). In the M5 bed with intermediate clay content (8%) composed of equal percentage of active (Na-montmorillonite) and inactive (chlorite, biotite) clay minerals, it took nearly 42 hours for the excess PWP to dissipate.

It can be seen from Figure 5.2 that the shape of the plots for beds deposited from T1 and M4 mixtures is generally similar suggesting similar sedimentation/consolidation behaviour of these two artificial soils, whereas the plot for the bed prepared from M5 mixture is entirely different. In both T1 and M4 beds the excess pore pressure dissipation began immediately after the slurry was poured into the container. Recalling that the T1 mixture (the original tailings) represented coarse grained silty sand and, as such, was a fast draining material, a relatively short time for full dissipation of excess PWP was expected. Increasing the total clay content from 4 to 16% by adding kaolinite resulted in significantly longer sedimentation phase in the bed with the highest clay content (M4), the end of which phase was delineated by the first change in the slope of the plots (compare T1 and M4 plots in Figure 5.2). While in the T1 bed (4% clay content) the settling phase continued for approximately 0.12 hours from the beginning of the test, in the M4 bed (16% clay content) it extended to 1.7 hours. Although not immediately obvious because of the logarithmic time scale in Figure 5.2, an examination of the slope of the second portion of the T1 and M4 plots suggests that in the T1 bed the primary consolidation occurred faster (approximately 0.4 to 0.6 hours) compared to the M4 bed (7.3 hours). This can be attributed to increased drainage path length in the latter bed due to the higher percentage of platy clay particles in the M4 mixture coupled with slightly greater bed thickness. In Figure 5.2, the plot for the M5 bed shows that after the slurry is poured into the container, initially there is no change in the excess pore water pressure. The authors believe that this portion of the plot corresponds to a period of gellation (or floc formation) when no settling takes place, which continues for about 0.02 hours. Although distilled water rather than electrolyte was used in the preparation of the tailings/bentonite slurries, according to the manufacturer's data sheet (Baroid 2011), the utilized Baroid Quick-Gel Fast Mixing High Viscosity Bentonite is capable of imparting gellation even in fresh water suspensions. Since Baroid Quick-Gel Fast Mixing High Viscosity Bentonite is manufactured to be used primarily as a drilling fluid, the observed flocculation was most probably triggered by the soluble salts, which are always present in the drilling fluids in sufficient concentration to cause at least a mild degree of flocculation (Darley and Gray 1988). At the end of flocculation (i.e., at about 0.02 hours), the flocs gradually begin to settle and form a layer of sediment on the bottom of the container. The onset of the settling stage is marked by initial rise in the excess pore water pressure, after which the PWP slowly begins to decrease (Figure 5.2). Throughout the settling stage, the bottom sediment grows while the settling zone becomes thinner and finally vanishes at about 3.7 hours from the beginning of the test. A distinct change in the slope of the plot for the M5 bed at about 3.7 hours delineates the beginning of the primary consolidation phase during which the sediment deposit undergoes self-weight consolidation and reduction in water content. Equilibrium condition is reached at the end of primary consolidation, i.e., at about 42 hours from the beginning of the test when all excess PWP becomes fully dissipated.

Overall, the sedimentation/consolidation behaviour of the beds prepared from T1 and M4 mixtures was similar, a finding that is consistent with the results of other researchers. For instance, Jacobs et al. (2007) reported that adding kaolinite to sand increased the void ratio but did not significantly change the permeability and compressibility of the sand/clay mixtures, whereas adding bentonite also resulted in more loose packing of the bed (higher void ratio) but led to a significant decrease in the permeability of the mixtures. Al-Shayea (2001) also observed significant reduction in the hydraulic conductivity of sand/clay mixtures with the addition of expansive smectite clay which effect was more pronounced at low clay contents (up to about 10%). He attributed the effect to the fact that at low clay content, pore spaces are larger, thus allowing more freedom for clay particles to freely expand and effectively block the relatively larger drainage paths. Al-Shayea (2001) found that the coefficient of permeability (hydraulic conductivity), $k$, for sand/clay mixtures with 10% clay content was five to six orders of magnitude lower than that of pure sand. The substantial difference in the behaviour of tailings/bentonite beds could be explained by the following hypothesis. As the highly expanding bentonite (Na-montmorillonite) absorbs water and swells, it reduces the pore spaces and blocks the drainage paths leading to the reduction in the overall hydraulic conductivity of the mixture and longer time for drainage and excess pore water pressure dissipation. Adding kaolinite to the tailings has a similar effect of reducing the pore spaces and decreasing the hydraulic conductivity of the beds but is much less effective than bentonite. Furthermore, in their study of the mechanisms controlling the permeability of clays, Mesri and Olson (1971) suggested that the reduction in the coefficient of permeability at constant void ratio, from kaolinite to montmorillonite is largely the result of a reduction in the size of individual flow channels and an increase in the tortuosity of the flow paths. The smaller the particle size the smaller the size of the individual flow channels, all other variables being constant. Thus at the same void ratio, kaolinite, which has the largest particles of all clay minerals is 200,000 time more pervious than montmorillonite, which has the smallest particles (Mesri and Olson 1971).

The results of the sedimentation/consolidation experiments demonstrated that the primary consolidation of all beds was complete in less than two days and, thus, all beds used in the experimental program were considered fully consolidated prior to the shear strength testing.

*5.3.2.2. Slow tilting experiments*

The tilting of the Tank results in generation of excess pore water pressure (PWP) within the tested mixed tailings/clay beds, the magnitude of which at a given horizon depends on the tilting speed, angle of tilting, $\beta$, and depth, $z$, of that horizon below the bed surface. When the tilting speed is sufficiently slow, the generated excess PWP is so small that, for practical purposes, the response of the bed can be considered drained. A drained response to an applied loading is characterised by parallel total and effective stress paths, i.e., $d\sigma = d\sigma'$, and zero (or close to zero) excess PWP, $du_e = 0$ at all times.

Figures 5.3a to c show the evolution of the excess pore water pressure with time and angle of tilting at the three measuring ports (P1, P2 and P3) within beds prepared of mixtures T1, M2, and M5. The beds were 7.2 to 7.8 cm thick and consolidated for 3 days prior to testing.

a)

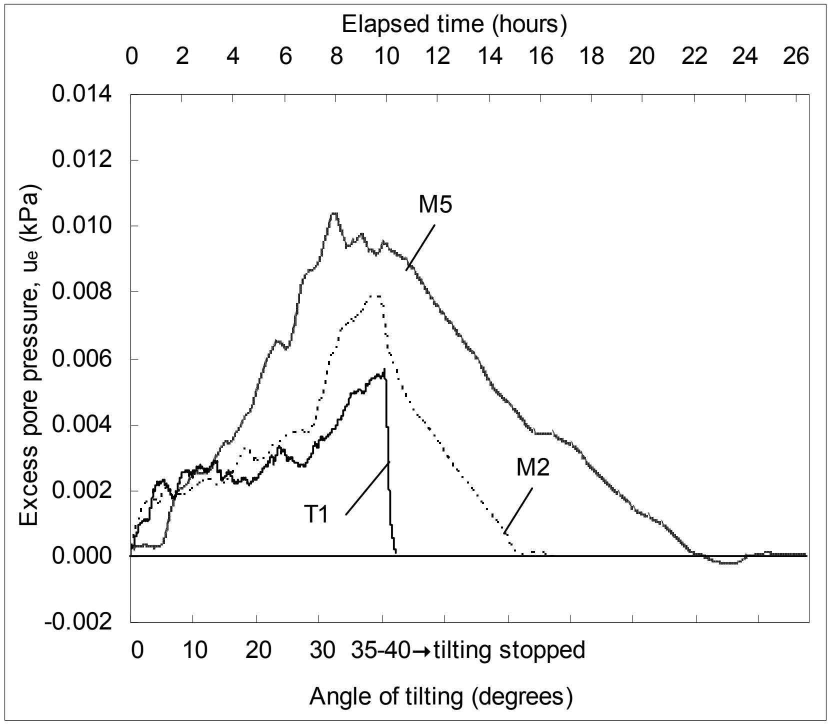
Elapsed time (hours)
0 2 4 6 8 10 12 14 16 18 20 22 24 26
0.014
0.012
0.010
0.008
0.006
0.004
0.002
0.000
-0.002
Excess pore pressure, ue (kPa)
M5
M2
T1
0 10 20 30 35-40→tilting stopped
Angle of tilting (degrees)

b)

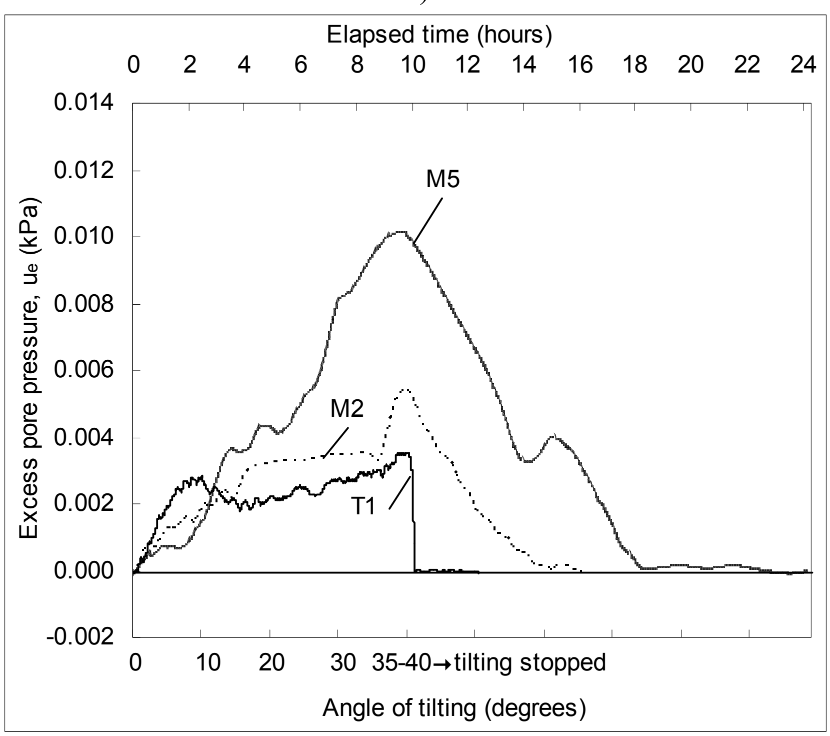
Elapsed time (hours)
0 2 4 6 8 10 12 14 16 18 20 22 24
0.014
0.012
0.010
0.008
0.006
0.004
0.002
0.000
-0.002
Excess pore pressure, ue (kPa)
M5
M2
T1
0 10 20 30 35-40→tilting stopped
Angle of tilting (degrees)

c)

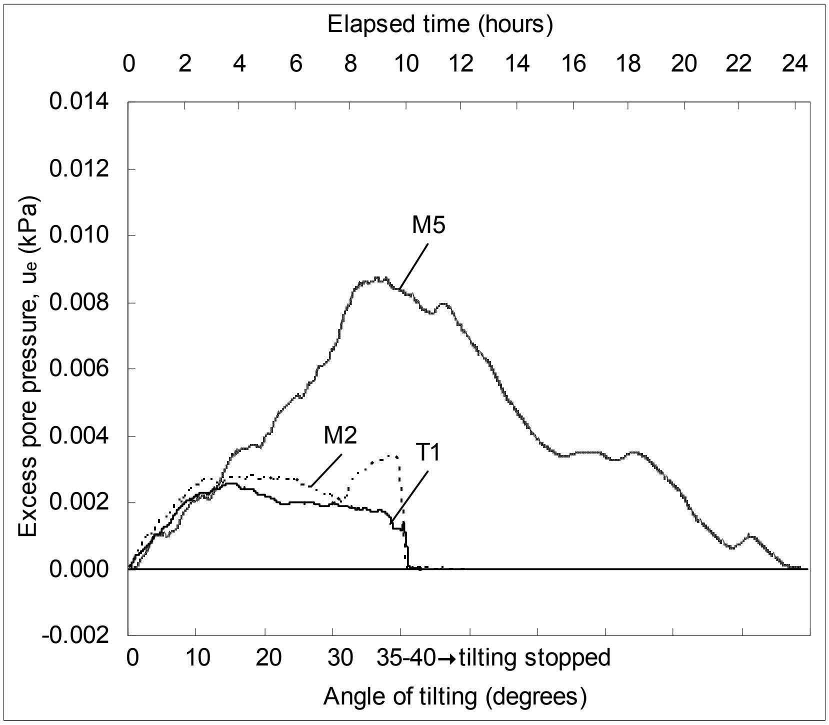


**Figure 5.3.** Excess pore water pressure variation with time during slow tilting of mixed tailings/clay beds consolidated for 3 days at: (a) Port P1; (b) Port P2; (c) Port P3.

Referring to Figure 5.3a, at port P1 located at the bottom of the beds, the excess PWP, $u_e$, within each bed increased continuously throughout the tilting test and reached its maximum value at time corresponding to the failure of the slope within the tank. It is interesting to note, that for the bed prepared from the M5 mixture, the excess PWP buildup did not start immediately from the beginning of the test but with some 30 minutes offset (approximately 5°). Bed failure through sliding of a portion of the bed to the bottom of the Tank under the influence of gravitational forces was recorded at different angles of tilting for the beds prepared from various mixtures. These angles were 40.4°, 39.6° and 35.2° for the beds deposited from the T1, M2 and M5 mixtures, respectively. As soon as the sliding soil reached the bottom of the Tank, the photosensor on the side wall was activated thus preventing further tilting. Upon cessation of tilting, the generated $u_e$ immediately began to dissipate, which process continued for about 0.3, 7.1 and 17.6 hours for the beds prepared from T1, M2 and M5 mixtures, respectively.

For the M5 bed, the recorded $u_e$ variation with time at port P2 (Figure 5.3b), located approximately in the middle of the bed, closely resembled that at port P1. However, the pattern of $u_e$ evolution at port P2 observed in T1 and M2 beds was different from that at port P1 within the same beds. For instance, in the M2 bed, $u_e$ steadily increased until about 20° angle of tilting after which point the slope of the curve flattened suggesting that the rate of pore water pressure generation became almost equal to the rate of pressure dissipation. This trend persisted to approximately 35° angle of tilting, beyond which $u_e$ began to rapidly increase again until bed failure at 39.6°. In the T1 bed, the rate of $u_e$ generation dominated over the rate of dissipation up until about 10° angle of tilt. Tilting from 10° to 16° resulted in the opposite trend and the net excess pore water pressure decreased over this period. Past 16° angle, $u_e$ began to gradually increase again until slope failure at 40.4°. In all beds, dissipation of the excess pore water pressure started right after the cessation of tilting and continued for about 0.2, 6.3 and 15.4 hours for the beds prepared from T1, M2 and M5 mixtures, respectively.

Referring to Figure 5.3c, in the bed prepared from M5 mixture, the $u_e$ evolution at port P3 located immediately below bed surface followed that in ports P1 and P2. The excess PWP within this bed steadily increased throughout the slow tilting and reached its maximum value at failure of the bed slope at 35.2°. It is worth noting here that at all three ports (P1, P2 and P3), the maximum $u_e$ values reached during the slow tilting experiments, were very close to each other, suggesting that excess PWP dissipation through drainage did not occur at any horizon within this bed. In contrast, the $u_e$ variation with time at port P3 within the beds prepared from M2 and T1 mixtures significantly differed from that recorded at ports P1 and P2 for the same beds. For instance, the maximum $u_e$ value reached at P3 within the T1 bed was 32% of that at P1 for the same bed. Within the M2 bed, the maximum $u_e$ reached at P3 was about 43% of that at port P1. The slope of the $u_e$-plot versus time and angle of tilting for the T1 bed clearly shows that the rate of excess PWP dissipation was greater than the rate of pressure dissipation from 16° to about 40° angle of tilting (Figure 5.3c). In the M2 bed, the shape of the plot at P3 suggests that the rate of pressure dissipation was close to or greater than the rate of pressure generation between approximately 12° and 32° angle of tilting. A peak in $u_e$ versus time and angle of tilting plots was registered in both M2 and T1 beds at failure, with the peak in the M2 bed being much more pronounced than that in the T1 bed.

In Figures 5.4a and b, profiles of $u_e$ with depth below surface of M2 and M5 beds, consolidated for 3 days, were plotted on a semi-logarithmic scale at various angle of tilting. A line representing the variation of the normal effective stress, $\sigma'_n$, with depth below the bed surface was also drawn for comparison.

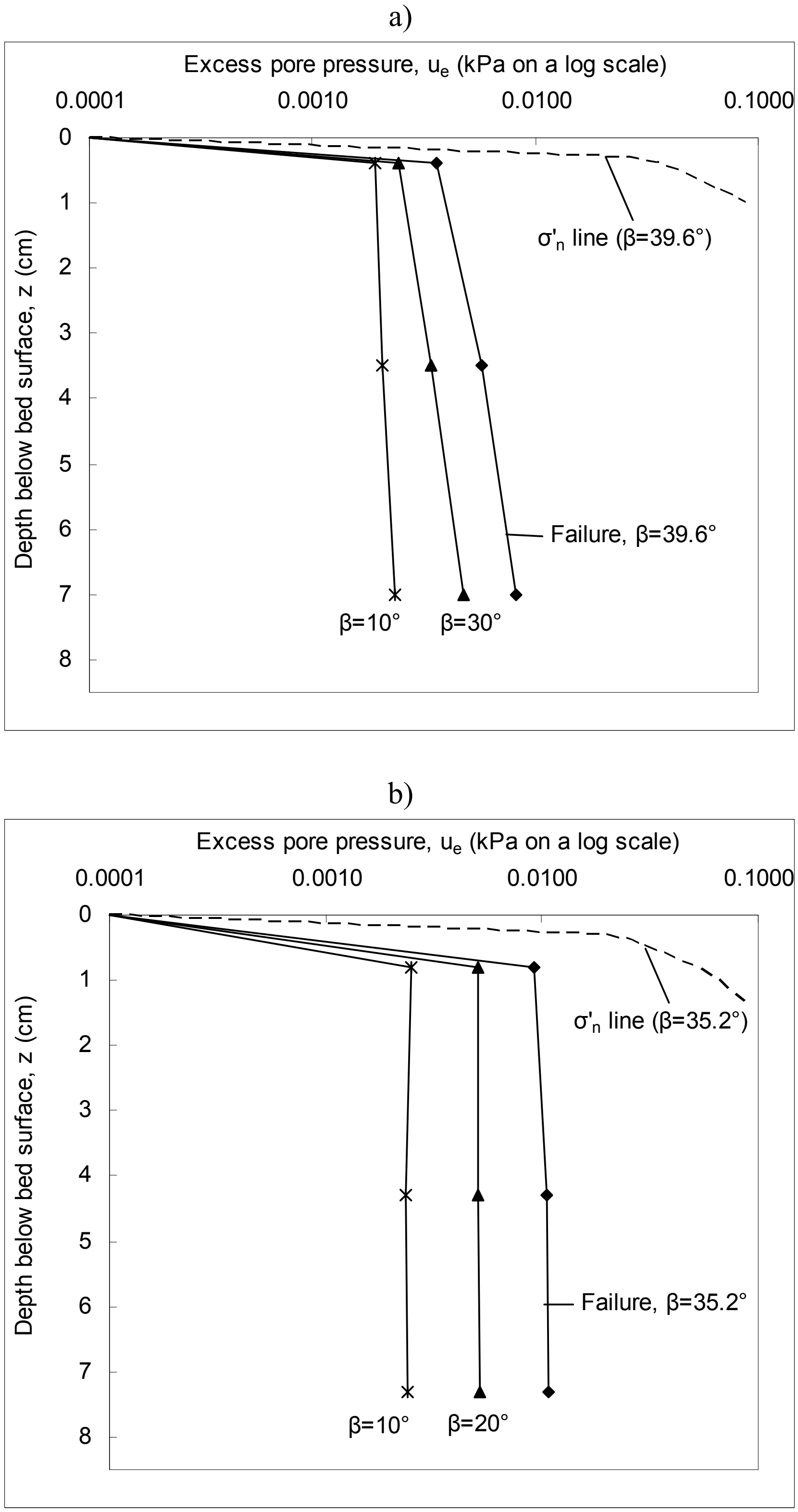


**Figure 5.4.** Profiles of the excess pore pressure versus depth below bed surface during slow tilting in 3 days-old tailings beds prepared from: (a) M2, and (b) M5 mixtures.

In the previous chapter (Section 4.3, Subsection 4.3.2) we demonstrated that the spatial distribution of $u_e$ within the T1 tailings bed during slow tilting was nonuniform, showing lower $u_e$ values at port P3 compared to those at P1 and P2. We attributed the observed nonuniform $u_e$ distribution to drainage through bed surface, which accelerated with the angle of tilting and became greatest at failure of the slope. Thus, at 10° angle of tilting, drainage was present only in the shallow horizons and resulted in lowering the $u_e$ values at port P3 in comparison with those at P1 and P2. With increasing angle of tilting, the excess PWP dissipation progressed in downward direction to the lower horizons and reduced the $u_e$ values at port P2 as well. At failure, the drainage affected the entire bed.

A similar pattern of $u_e$ evolution during slow tilting was evident in the bed prepared from M2 mixture (Figure 5.4a) suggesting that adding 4% kaolinite to the mine tailings did not alter significantly the permeability of the latter. This was not the case with the M5 beds, though. Referring to Figure 5.4b, it can be seen that the plots at 10°, 20°, and 35.2° are nearly straight vertical lines implying a relatively uniform $u_e$ distribution within the M5 bed at all angles of tilting. These results suggest that almost no drainage occurred in this bed during slow titling and confirm that adding bentonite to the tailings introduced a major modification in the permeability of the tailings. The most important finding from the slow tilting experiments, however, is that in all beds, the $u_e$ values at each horizon remained at least an order of magnitude lower than the $\sigma'_n$ values at the same horizon. This observation led to the conclusion that the excess pore water pressure generated during slow tilting did not significantly affect the strength of the beds, and consequently bed failure occurred under drained conditions when the shear stress at the failure plane exceeded the shear strength of the bed at this depth.

*5.3.2.3. Rapid tilting experiments*

During rapid tilting, the excess pore water pressure generated in the mixed tailings/clay beds was much more substantial than during slow tilting and thus, affected the shear strength of the tested beds. The response of the beds to loading could no longer be considered fully drained and since volume change during tilting was not prevented and drainage through the bed surface was allowed, shearing occurred under partially drained conditions. Figures 5.5a to c show the evolution of excess PWP within beds prepared of T1, M2 and M5 mixtures at the three measuring ports during rapid tilting. The final thickness of the beds varied between 7.2 to 7.8 cm and they were consolidated for 3 days prior to testing.

a)

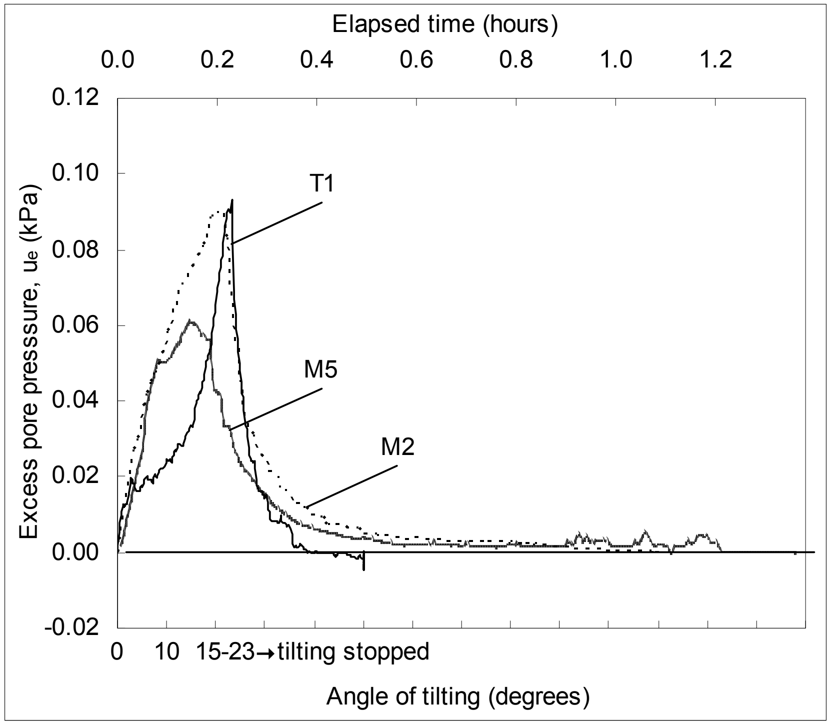
Elapsed time (hours)
0.0
0.2
0.4
0.6
0.8
1.0
1.2
Excess pore presssure, $u_e$ (kPa)
0.12
0.10
0.08
0.06
0.04
0.02
0.00
-0.02
T1
M5
M2
0
10
15-23→tilting stopped
Angle of tilting (degrees)

b)

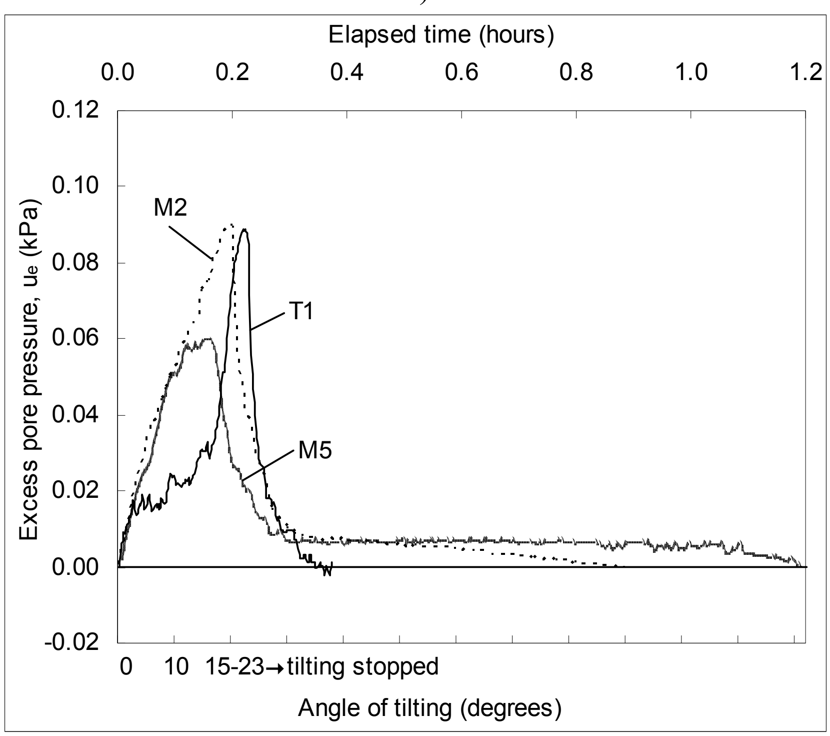
Elapsed time (hours)
0.0
0.2
0.4
0.6
0.8
1.0
1.2
Excess pore pressure, $u_e$ (kPa)
0.12
0.10
0.08
0.06
0.04
0.02
0.00
-0.02
M2
T1
M5
0
10
15-23→tilting stopped
Angle of tilting (degrees)

c)

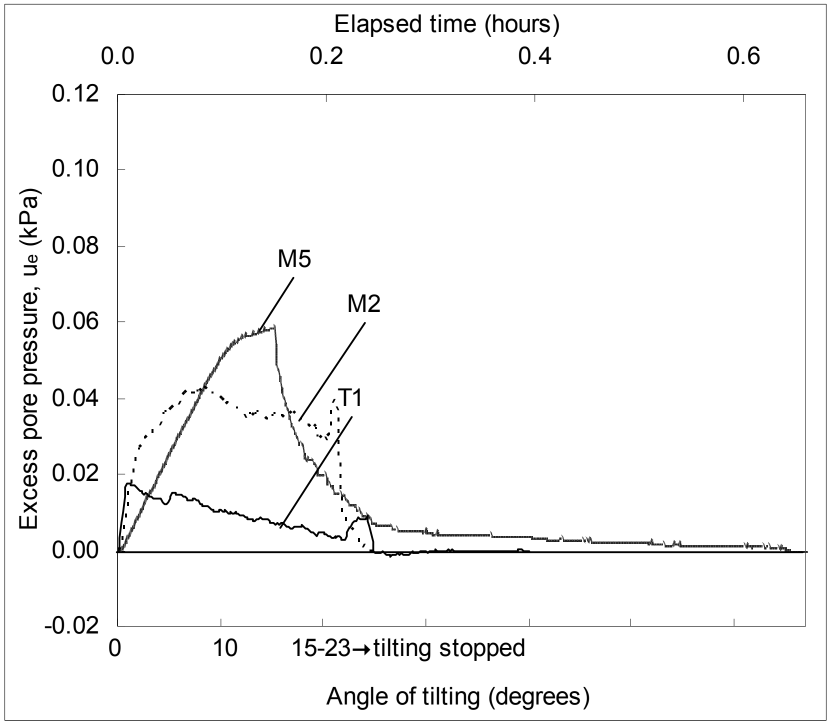


**Figure 5.5.** Excess pore water pressure variation with time during rapid tilting of mixed tailings/clay beds consolidated for 3 days at: (a) Port P1; (b) Port P2; (c) Port P3.

Figure 5.5a shows that, at port P1, $u_e$ increased continuously during rapid tilting until failure of the slope, which occurred at 23.3°, 21.2° and 15.2° in the beds prepared of T1, M2 and M5 mixtures, respectively. The failure event activated the photosensor on the side wall of the Tank, which broke the electrical circuit and prevented further tilting. Upon cessation of tilting, $u_e$ immediately began to dissipate and returned to zero within 0.16, 0.89 and 1.20 hours in the T1, M2 and M5 beds, respectively. The maximum $u_e$ value reached during the experiment on the M5 bed was about 60-65% of that reached within the T1 and M2 beds.

A similar pattern of $u_e$ evolution with time and angle of tilting was recorded at P2 in all tested beds (Figure 5.5b). Similar to P1, the maximum $u_e$ for the bed prepared from M5 mixture was about 66-71% of that reached within the T1 and M2 beds.

At port P3 (immediately below the bed surface), the plots for the M2 and T1 beds suggest that partial drainage occurred in both beds at this horizon, which caused some excess PWP pressure dissipation (Figure 5.5c). The rate of $u_e$ dissipation dominated over the rate of pressure generation from about 2° angle of tilting to slope failure in the T1 bed, and from 8° to 20° angle in the M2 bed. It is believed that drainage in these beds proceeded in an upward direction through the bed surface into the ambient water and was driven by the pressure gradient brought about by the nonuniform excess PWP distribution. A distinct peak in $u_e$ was recorded in the T1 and M2 beds at failure. Beyond this point, the tilting ceased and the excess PWP returned to zero. In the bed prepared from the M5 mixture $u_e$ steadily increased during rapid tilting towards a maximum value, which was reached at failure. It is interesting to note, that the maximum $u_e$ values recorded within the M2 and T1 beds constituted about 75% and 21%, respectively, of the maximum value reached in the M5 bed, probably because of the lack of drainage in the latter bed.

The excess PWP buildup within the mixed tailings/clay beds in response to the rapid tilting ultimately led to liquefaction of the mixture and bed failure. The phases in the development of excess PWP can be seen more clearly in Figures 5.6a and b, where

$u_e$-profiles with depth below the surface of M2 and M5 beds are plotted for various angles of tilting. The figures also show the variation of $\sigma'_n$ within the same beds.

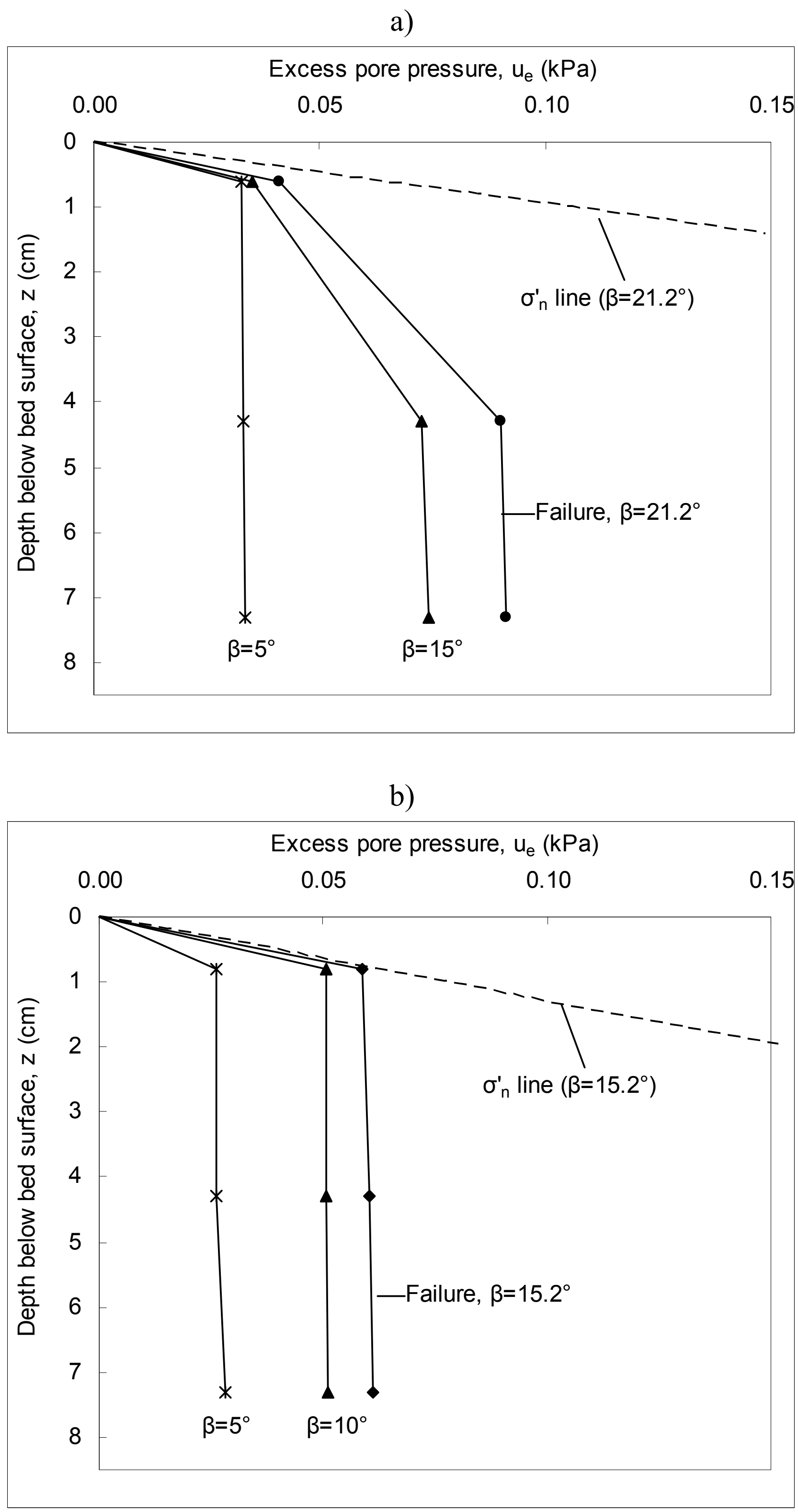


**Figure 5.6.** Profiles of the excess pore pressure versus depth below bed surface during rapid tilting in 3 days-old tailings beds prepared from: (a) M2, and (b) M5 mixtures.

Referring to Figure 5.6a, in the M2 bed the distribution of $u_e$ at 5° angle of tilting is nearly uniform, which is evident from the close $u_e$ values measured at ports P1, P2 and P3. The plot at 15° angle of tilting shows $u_e$ value at port P3 significantly lower than those at P1 and P2, indicating that excess PWP dissipation through drainage has occurred at this shallow horizon. The nonuniform distribution of $u_e$ within the bed brought about hydraulic gradient that became the driving force for subsequent drainage in the upward direction. The plot at failure ($\beta = 21.2^\circ$) also indicates the presence of drainage. As shown in Figure 5.6a, the generated excess PWP at the bottom (P1) and in the middle (P2) of the beds remained lower than the $\sigma'_n$ value at these horizons during the experiment and reached a maximum of 10 to 20% of the $\sigma'_n$ at failure. In contrast, at port P3 $u_e$ moved close to the $\sigma'_n$ line throughout rapid tilting and, at failure, was about 65% of $\sigma'_n$ at the same depth. This could explain why the failure plane within the beds was always located close to the P3 elevation, i.e., at 0.4 to 2.0 cm below bed surface. In the M5 bed , the distribution of excess PWP remained relatively uniform during rapid tilting until failure as seen from the nearly vertical $u_e$ profiles obtained at 5°, 10° and 15.2° angles of tilting (Figure 5.6b). These results suggest that drainage from the bed was minimal and that the rate of excess pore pressure generation far exceeded the rate of dissipation at all times during the experiment. Failure in all investigated beds occurred when the excess PWP generated in response to tilting reached the $\sigma'_n$ value at a given horizon at which point the soil mixture liquefied leading ultimately to slope failure along this plane.

### 5.3.3. Failure modes

During tilting the gravity components of the bed self weight produce shear stress throughout the soil mass and, if it exceeds the shearing resistance of the mixtures on any possible failure surface, sliding will occur. In both slow and rapid tilting experiments, failure of the slope was observed as a sheet along a failure plane parallel to the bottom of the Tank. In the beds prepared from tailings and kaolinite mixtures (M2, M3, and M4) the failure plane was located approximately 0.5 to 2.0 cm from the surface of the beds, whereas in those prepared from the tailings and bentonite mixture (M5) the depth of the failure plane was slightly greater, i.e., 0.9 to 2.5 cm below bed surface. Failure happened quickly over a period of 5-6 seconds in the beds prepared from T1 and M2 mixtures and even faster (1-2 sec) in the beds prepared from M3, M4 and M5 mixtures. During failure, the soil mass above the failure plane liquefied and travelled down the slope like a wave to the bottom of the Tank. The authors propose the following hypothesis to explain the failure mechanism of the studied mixtures. At failure, a rapid excess PWP buildup occurs at the failure plane, which excess pressure propagates in upward direction and causes a complete loss of shear strength in the soil mass above that plane. For beds of the same thickness and age, failure under drained conditions (slow tilting) occurred at an angle of tilting approximately two times higher than under partially drained conditions (rapid tilting).

### 5.3.4. Shear strength

As demonstrated in Subsection 5.3.2.1, the longest time for completion of primary consolidation was observed in the M5 beds and it was approximately 42 hours. The beds used in the shear strength experiments were consolidated at least 3 days (72 hours) prior to testing and were, therefore, believed to be fully consolidated. The consolidation time was defined as the time that elapsed from pouring the slurry into the tank and the beginning of the tilting. Measurements of excess PWP during tilting experiments showed that negligible excess PWP was generated if a slow tilting mode was selected, whereas a more substantial excess PWP buildup occurred during the rapid tilting. It was believed that during slow tilting soil shearing occurred under drained conditions and the measured bed shear strength was also "drained". In contrast, rapid tilting resulted in partially drained shearing and this mode was chosen to evaluate the effect of rate of loading on the shear strength of the deposited mixed tailings/clay beds. Accordingly, the recorded angle of failure during slow tilting was considered effective friction angle, whereby the friction angle measured during rapid tilting was related to the total stress parameters at failure (Eqs. 5.4 and 5.5).

#### *5.3.4.1. Drained shear strength*

In granular soils of low plasticity, where particle orientation is not a factor, residual shear strength, equal to the critical state strength, is mobilized during drained slope failure. Critical state is defined as constant shear stress and volume with increasing shear strain. The large shear displacements at failure reduce the shearing resistance to the residual condition along the entire slip surface (Mesri and Shahien 2003). The residual shear strength depends on many factors, among which the most important are: clay content and mineralogy, particle shape and size distribution, pore-water chemistry, and rate of shear displacement (Kenney 1967; Lupini et al. 1981; Skempton 1985; Stark and Eid 1994; Stark et al. 2005). The studied mine tailings/clay mixtures with clay content of

16% or below were most likely to exhibit a turbulent shearing mode as defined by Lupini et al. (1981). In this mode, soil shearing occurs through rolling and translation of the coarse particles. The residual shear strength is high, no preferred particle orientation occurs and the residual friction angle depends primarily on the shape and packing of the rotund particles and is relatively independent of the applied stress (Lupini et al. 1981; Stark et al. 2005). The Mohr-Coulomb shear strength criterion, representing stress state at failure, was applied to determine the drained (effective) residual shear strength envelope of the studied tailings/clay beds under drained conditions. For a normally consolidated soil this criterion can be expressed with the following relationship:

$$\tau_f = \sigma'_{nf} \tan\phi' \tag{5.7}$$

The Mohr-Coulomb failure criterion (Eq. 5.7) yields a linear failure envelope passing through the origin and assuming a zero cohesion intercept. Tiwari and Marui (2005) studied more than 35 mixtures of smectite, kaolinite and quartz in different proportions and with liquid limit between 26 and 120%. They found that, for the majority of mixtures, the drained residual failure envelope was linear and the cohesion intercept ranged between 0 and10 kPa. Stark and Eid (1994) also concluded that the drained failure envelope of soils with clay-size fraction less than 45% and liquid limit below 120% was essentially linear. Since all tailings/clay mixtures used in the present study satisfied both conditions for clay-size fraction lower than 45% and liquid limit below 120%, it was believed that a straight line would accurately describe the drained residual failure envelope of the tested soils. The assumption of zero cohesion was based on the following facts: i) the tested tailings/clay mixtures were coarse grained for all investigated clay contents; ii) all tailings/clay deposited beds were prepared in the laboratory, i.e., were reconstituted, and iii) all beds were normally consolidated under self-weight.

The drained shear strength results for beds prepared from T1, M2, M3 and M4 mixtures and consolidated for 3 days were plotted as a function of the normal effective stress at the failure plane as shown in Figures 5.7a and b. These figures present data obtained for tailings/clay mixtures in which the percentage of added clay is varied but the clay mineralogy is kept constant, and as such illustrate the effect of clay content on the shear strength of the tested artificial soils.

a)

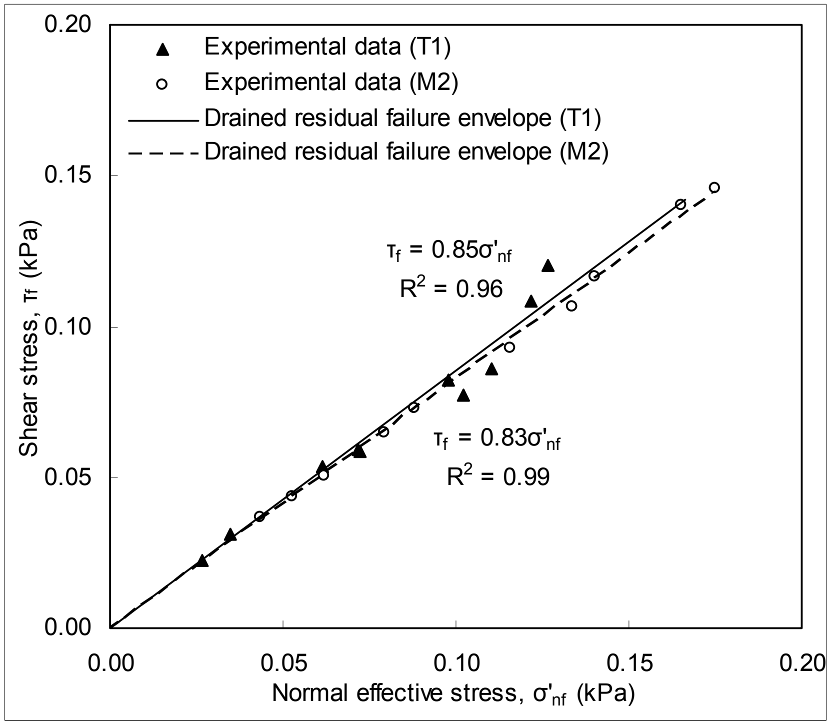


b)

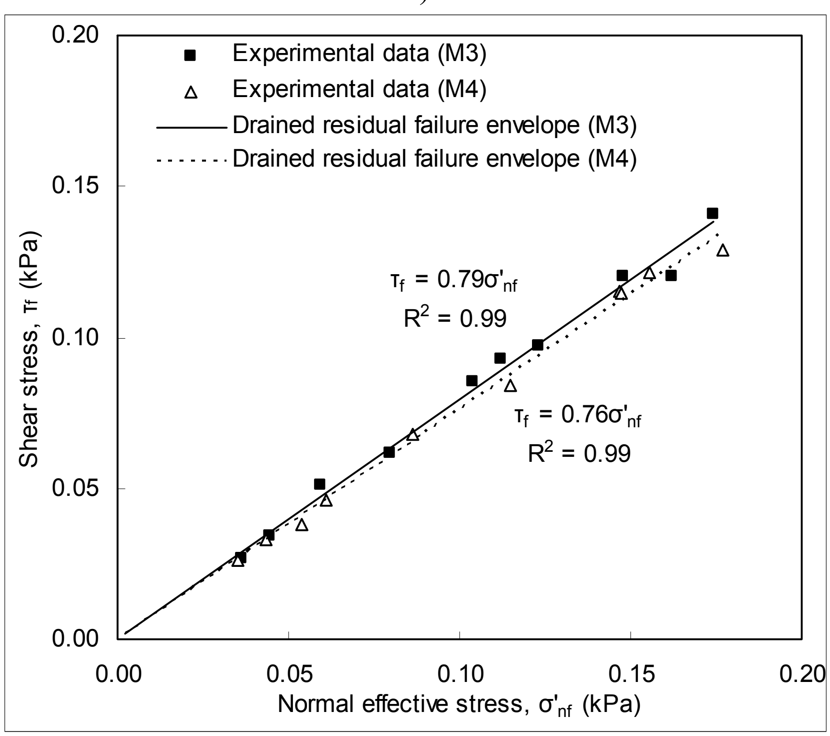


**Figure 5.7.** Drained failure envelopes for beds prepared from: (a) T1 and M2, and (b) M3 and M4 mixtures and consolidated for 3 days.

At the onset of tilting, the vertical effective stress at a depth corresponding to the depth of the failure plane (Eq. 5.3) varied between 0.03 and 0.23 kPa. Assuming a zero cohesion intercept, a straight line passing through the origin was used to fit the experimental data points with a high degree of confidence based on the high *R*-squared (correlation) factors between 0.96 and 0.99. Referring to Figures 5.7a and b, the slopes of the fitted lines fall between 0.76 and 0.85 and decrease with increasing clay (kaolinite) content in the order T1>M2>M3>M4. These results imply that in the effective stress range of interest, i.e., between 0 and 0.18 kPa, the drained shear strength of the investigated tailings/clay mixed beds also decreases with clay content increase.

The effect of clay mineralogy on the drained residual shear strength of mine tailings/clay mixtures can be seen in Figure 5.8, where results from drained shear strength testing of mixed beds with the same percentage (4%) of added clay but different clay mineralogy (i.e., kaolinite versus bentonite) are compared.

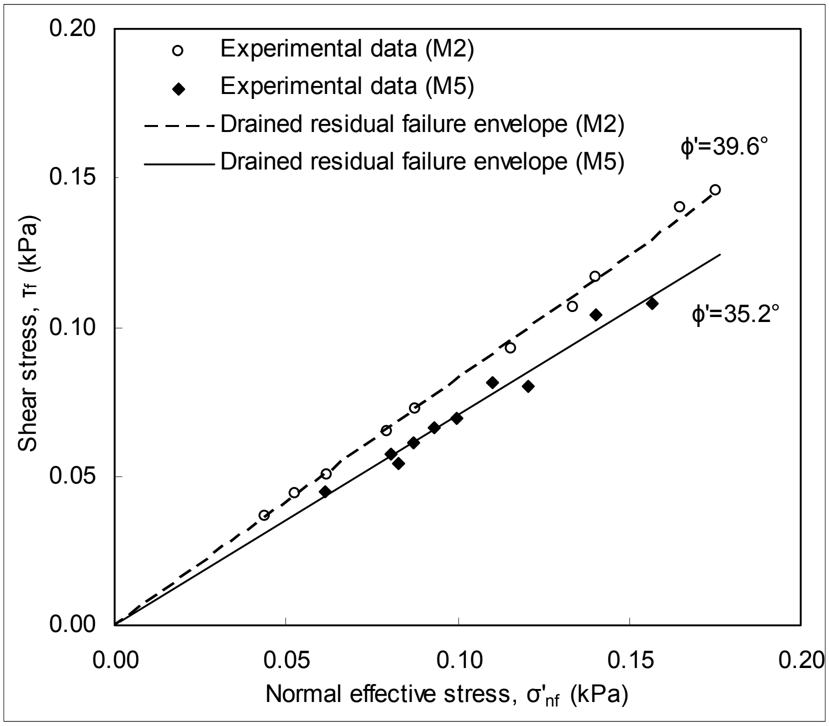


**Figure 5.8.** Drained failure envelopes for beds prepared from M2 and M5 mixtures and consolidated for 3 days.

As seen in Figure 5.8, adding either kaolinite or bentonite to the original mine tailings resulted in a decrease in the effective friction angle and respectively, the drained shear strength of the tailings. Adding bentonite, however, had much greater effect and thus, only 4% added bentonite brought about a reduction in the effective friction angle of the tailings from 40.4° to 35.2°, i.e., in about 5°. For comparison, adding the same percentage (4%) of kaolinite reduced the effective friction angle of the tailings to 39.6°, i.e., in less than 1°.

Similar observations of decreasing effective friction angle (and shear strength) of sandy soils with increasing clay content were reported by Kenney (1967), Stark and Eid (1994), Al-Shayea (2001) and Tiwari and Marui (2005). The results presented by Al-

Shayea (2001) show that when the clay (smectite) content in a sand/clay mixture is increased from 0 to about 4%, the peak effective friction angle is reduced by about 5° degrees, which finding is consistent with the results of the present study. An effective friction angle of 35.6° and a cohesion of zero were reported by Rodríguez (2006) who performed undrained triaxial tests on tailings samples containing 3-5% clay by weight, which is close to the clay content of the beds used in the present study. Tiwari and Marui (2005) demonstrated that although adding kaolinite or bentonite to sand both resulted in a decrease in the residual friction angle, the magnitude of the decrease was much higher for sand/bentonite samples than for sand and kaolinite. For instance, mixtures with approximately 20% kaolinite showed the same residual friction angle as mixtures with only 4% bentonite.

Ishihara et al. (1980) suggested that relative density is not a suitable index for the characterization of the mechanical behaviour of silty sands and that void ratio should be used instead. Kuerbis et al. (1988) noted that the void ratio of a silty sand bed deposited from slurry depends upon the fines (silt and/or clay) content and introduced the concept of sand skeleton void ratio to explain the undrained behaviour of silty sand tailings with varying fines content under cyclic loading. The skeleton void ratio, $e_{sk}$, is the void ratio corresponding to a fines content for which the fines completely separate adjacent sand particles and it can be determined from the following relationship:

$$e_{sk} = \frac{1+e}{1-f} - 1 \tag{5.8}$$

where $e$ is the overall void ratio of soil, and $f = \frac{Weight\ of\ fines}{Weight\ of\ solids}$ is the fines fraction of the soil. Thus, when $e_{sk}$ calculated for a given sand/fines mixture (Eq. 5.8) is greater than the maximum void ratio for clean sand, $e_{\max}$, it appears that the soil matrix can reach a void ratio higher than it could achieve in the absence of fines. In this case, the sand particles are no longer in contact, i.e., they are floating in the fines matrix, and the mechanical behaviour of the soil is controlled by the fines matrix. In contrast, when $e_{sk} < e_{\max}$, the fines simply occupy the void spaces in the sand skeleton and the mechanical behaviour is controlled essentially by the sand matrix. Kuerbis et al. (1988) determined that the threshold for transition between sand dominated and fines dominated matrix occurred at about 20% fines fraction, depending on the gradation and mean particle size of the sand. The artificial tailings/clay mixtures, used in the present study, had relatively high percentage of fines, i.e., from 32% in the original tailings to 41% in the M4 samples with 12% added kaolinite. Additionally, for the investigated mixed tailings/clay beds the skeleton void ratio, $e_{sk}$, calculated using Eq. (5.8) was found to vary between 1.46 and 2.60, i.e., was always greater than the maximum void ratio of the pure tailings sand, $e_{\max} = 1.01$. For this comparison, $e_{\max}$ was determined following ASTM standard D4253-00 (ASTM 2006) on the sand fraction of the original tailings (i.e., the fraction greater than 0.075 mm). Therefore, it was concluded that the quantity of fine material (silt and clay) in the original mine tailings was sufficient to fully occupy the voids between larger sand particles and they were floating within the fines matrix. Adding clay to the mine tailings led to a further increase in the distance between the sand grains, which was reflected in a corresponding increase in the void ratio of the deposited beds. It should be noted here that there is also a tendency for clay particles to coat granular particles thus preventing direct interparticle contact of the granular particles. The decrease in the particle-to-particle contact between sand grains caused a decrease in the frictional resistance of the beds and hence in the measured drained residual friction angle.

*5.3.4.2. Partially drained shear strength*

The rapid tilting of the Tank resulted in excess PWP buildup, which at the horizons where the measuring ports were located within the beds, was found to be of the same order of magnitude as the normal effective stress (Figures 5.5a to c). As discussed in Subsection 5.3.2.3, during rapid tilting shearing occurred under partially drained conditions with the two phenomena of excess pore water pressure generation and dissipation taking place simultaneously. The authors suggest the following hypothesis to explain failure of the beds within the Tank. During rapid tilting experiments the magnitude of the residual (net) excess pore water pressure, $u_e$, at shallow depths was generally close to that of the normal effective stress, $\sigma'_n$, at these depths. At a certain angle of tilting and depth, $u_e$ became equal to $\sigma'_n$ causing complete loss of shear strength within the soil mass at that horizon and failure of the slope along that plane. Thus, for the partially drained condition, the ratio $u_e / \sigma'_n = 1.0$ was adopted as a failure criterion and the angle of tilting, $\beta$, at which the failure criterion was satisfied was considered the failure angle. However, because the exact location of the failure plane could not be predicted in advance, it was not possible to position any of the PWP transducers at this exact depth and to measure the $u_e$-value at failure. Therefore, the recorded angle of tilting at failure was reported as a total friction angle, $\phi_T$ and the obtained partially drained failure envelope as total stress envelope.

In Figures 5.9a and b, the partially drained shear strength results from testing of beds prepared from mixtures T1, M2, M3 and M4 and consolidated for 3 days are plotted as a function of the normal total stress at the failure plane. These figures serve as an illustration of the effect of clay content on the total strength envelope (and total friction angle) of the mine tailings/clay mixtures.

a)

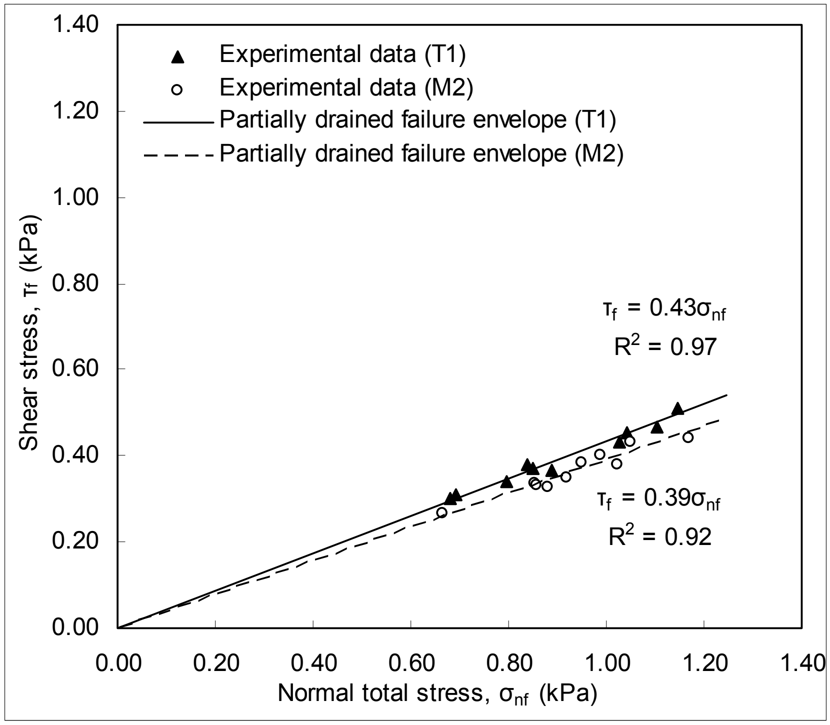


b)

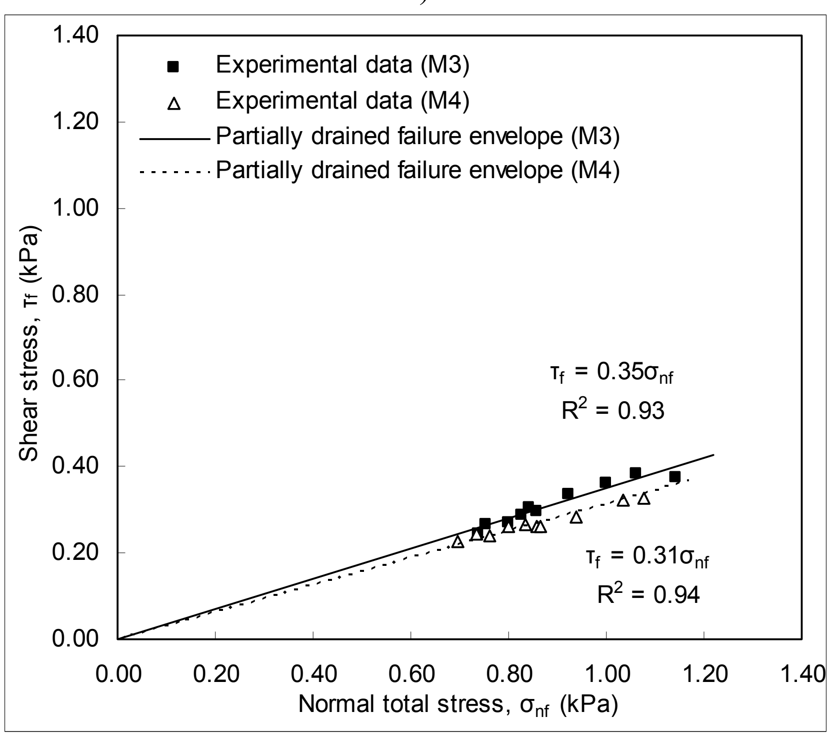


**Figure 5.9.** Partially drained failure envelopes for beds prepared from: (a) T1 and M2, and (b) M3 and M4 mixtures and consolidated for 3 days.

At the onset of tilting, the vertical total stress at the depth of the failure plane was calculated from Eq. (5.6) and found to vary between 0.72 and 1.25 kPa. Straight lines, passing through the origin and with *R*-squared values between 0.92 and 0.97, were used to successfully fit the four sets of experimental data. A shown in Figures 5.9a and b, the slopes of the failure envelopes decrease with increasing clay content in the mixed tailings/clay beds, from 0.43 for the T1 bed to 0.31 for the M4 bed. These results suggest that, similar to the drained strength, the effect of increasing clay content the content of clay-size particles in the mixed mine tailings/clay beds was to decrease the partially drained strength of the beds.

At the same total clay content, the effect of clay mineralogy on the partially drained strength of mine tailings/clay mixtures can be seen in Figure 5.10, where the measured partially drained shear strengths of the M2 and M5 beds are plotted as a function of the normal total stress at failure.

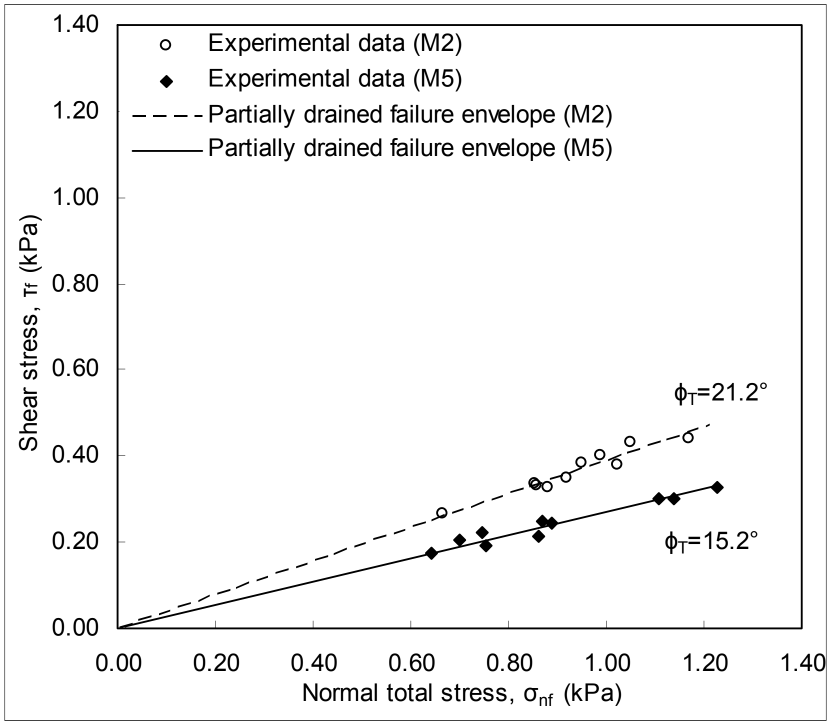


**Figure 5.10.** Partially drained failure envelopes for beds prepared from M2 and M5 mixtures and consolidated for 3 days.

Adding clay (kaolinite or bentonite) to the mine tailings generally decreased the total friction angle of the mixture but the magnitude of that decrease was greater for the tailings/bentonite samples than for the tailings/kaolinite ones. For instance, adding 4% kaolinite to the tailings reduced the total friction angle by 2.1°, i.e., from 23.3° in the original tailings to 21.2° for the M2 mixture, while adding the same percentage of bentonite caused a decrease of 8.1° in the total friction angle. It is hypothesised that two factors contributed to the observed decrease in the total friction angle with clay content increase. The first factor is related to the reduced interparticle contact between coarse sand particles caused by the presence of fine material and was discussed in Subsection 5.3.4.1. The second factor concerns the drainage conditions during rapid tilting. Because the investigated mixed beds exhibited different permeability and void ratios, the degree of drainage during the tilting experiments was also different. Observed excess PWP profiles (Figures 5.6a and b) and consolidation times (Figure 5.2) confirm this hypothesis and imply that the permeability of the mixed beds decreased in the order T1>M2>M3>M4>M5, as would be expected. It was assumed, therefore, that drainage during rapid tilting decreased in the same order, i.e., highest degree of drainage was present in the T1 bed and lowest in the M5 bed. Reduced drainage in the latter bed caused a more rapid buildup of excess PWP, which, along with the reduced interparticle contact between tailings sand particles, led to earlier failure of this bed.

*5.3.4.3. Effect of aging*

To investigate whether bed aging under constant effective stress had any effect on the mechanical strength of the mixed mine tailings/clay beds, drained and partially drained strength experiments were performed at 3 days and 12 days consolidation times and the respective effective and total friction angles were determined. Figures 5.11a and b show a comparison between the observed drained residual failure envelopes of the beds prepared from mine tailings/kaolinite mixtures and consolidated for 3 and 12 days.

a)

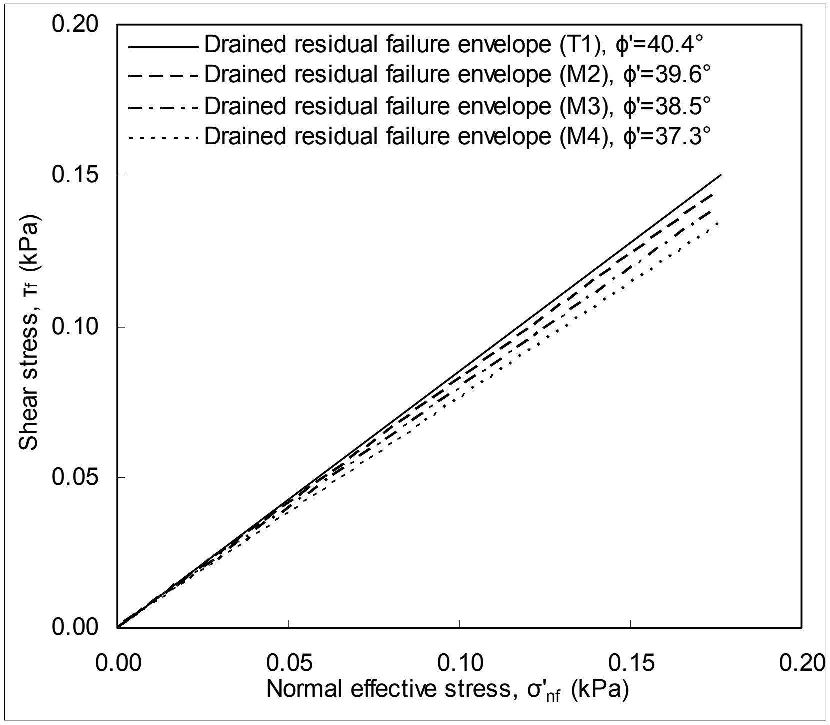


b)

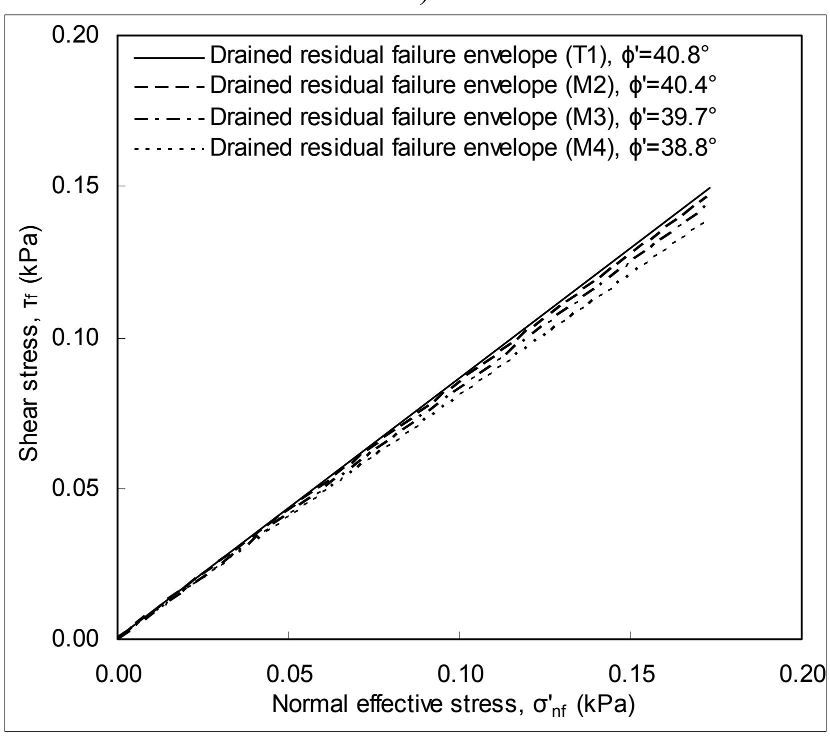


**Figure 5.11.** Drained failure envelopes for beds prepared from T1, M2, M3 and M4 mixtures and consolidated for: (a) 3 days; and (b) 12 days.

Referring to Figure 5.11a, at a consolidation time of 3 days, the slopes of the drained failure envelopes correspond to effective friction angles, $\phi'$ of 37.3, 38.5, 39.6 and 40.4°, for the M4, M3, M2 and T1 beds, respectively. In comparison, when the time for consolidation was increased to 12 days, the effective friction angles in the respective beds demonstrated only a small (0.4° to 1.5°) increase (Figure 5.11b). Such a minor increase could be either caused by a variation in the experimental conditions or by a minor strength gain with time. Since the exact cause of the strength increase remained unclear, it was concluded that $\phi'$ of the deposited tailings/kaolinite beds was relatively independent of the bed age.

Similar plots to those in Figures 5.11a and b, but showing partially drained failure envelopes of mixed tailings/kaolinite beds consolidated for 3 and 12 days are shown in Figures 5.12a and b.

a)

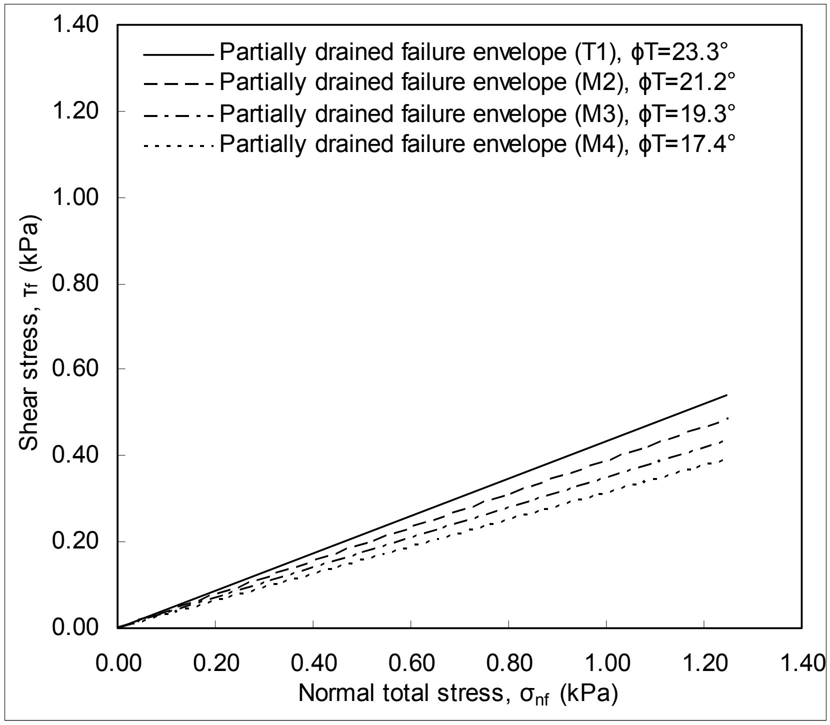


b)

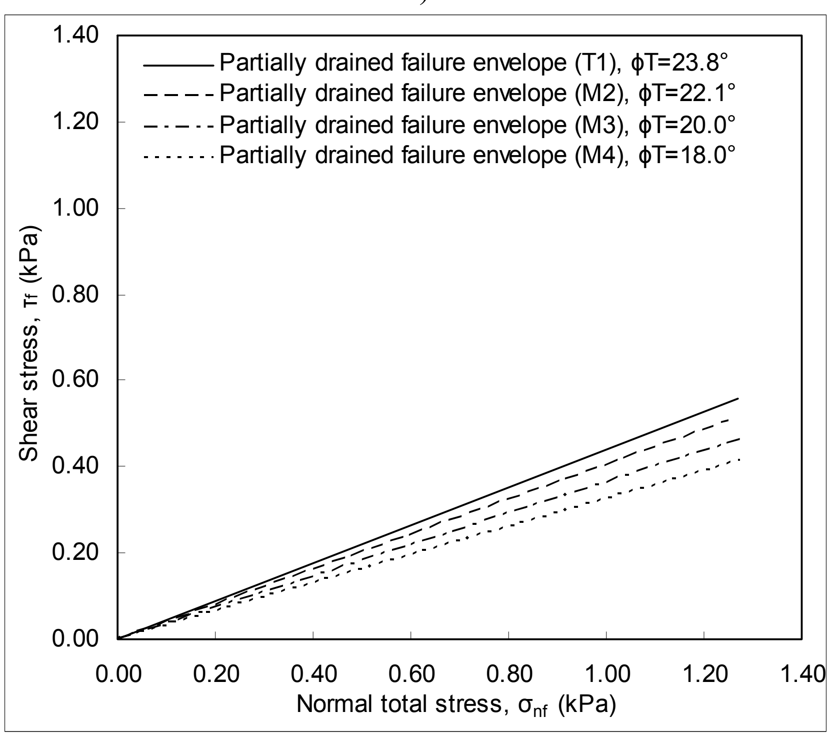


**Figure 5.12.** Partially drained failure envelopes for beds prepared from T1, M2, M3 and M4 mixtures and consolidated for: (a) 3 days; and (b) 12 days.

As evident from Figure 5.12a, the slopes of the obtained partially drained (total stress) failure envelopes correspond to total friction angles, $\phi_T$ of 17.4°, 19.3°, 21.2° and 23.3° for the 3 days old beds prepared from M4, M3, M2 and T1 mixtures, respectively. At consolidation time of 12 days (Figure 5.12b), computed $\phi_T$ was less than 1° higher, suggesting a negligible increase in the partially drained shear strength with time for consolidation. On the basis of the experimental results presented in Figures 5.11a and b and Figures 5.12a and b, it can be concluded that increasing the clay content of the original mine tailings by adding up to 12% kaolinite did not modify the time-dependent strength behaviour of the tailings.

To investigate the effect of adding bentonite to the mine tailings, drained and partially drained shear strength experiments were conducted with beds prepared from the M5 mixture and consolidated for 3 or 12 days and the obtained results are shown in Figures 5.13a and b.

a)

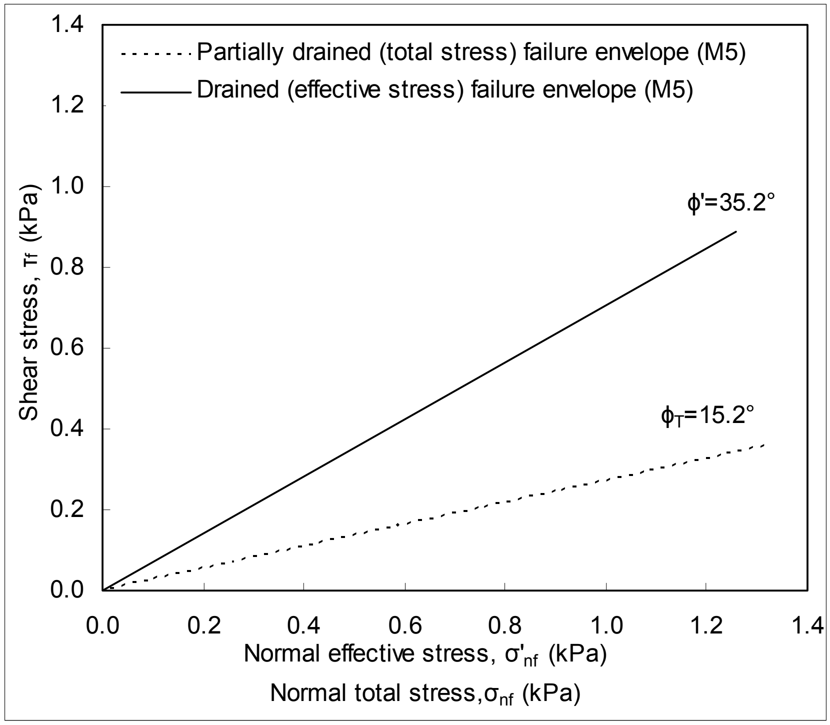


b)

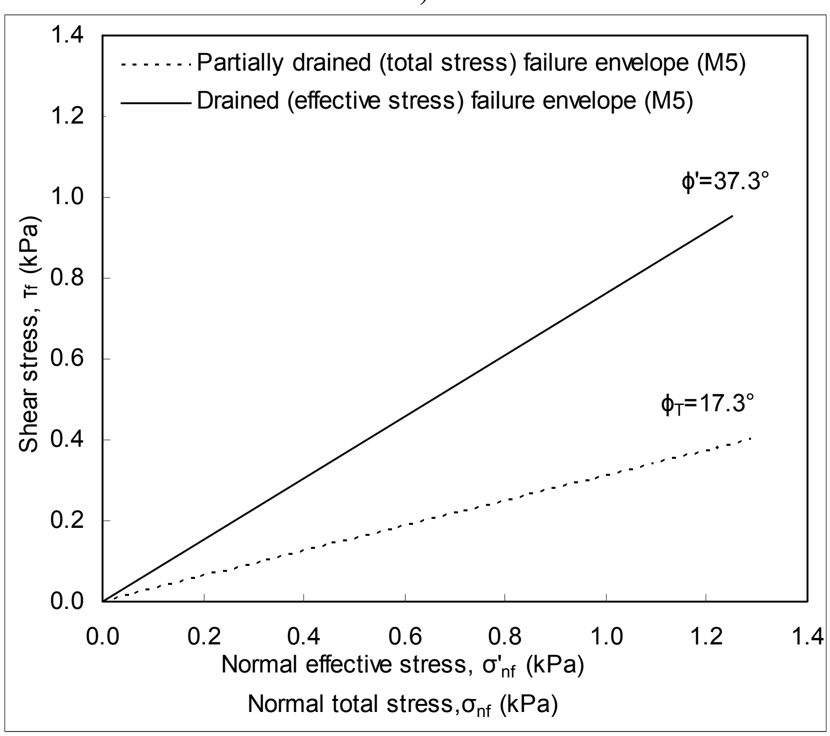


**Figure 5.13.** Drained and partially drained failure envelopes of beds prepared from M5 mixture and consolidated for: (a) 3 days; and (b) 12 days.

As can be seen from Figures 5.13a and b, the tailings/bentonite beds with 4% added bentonite (M5) exhibited a more pronounced strength gain with time in comparison to the tailings/kaolinite beds with the same percentage of added clay (M2), that is, an increase of 2.1° for both drained and partially drained strength. A possible explanation for the observed strength gain with time in the M5 beds is given below. As discussed in Subsection 5.3.2.1., the utilized bentonite showed a tendency to flocculate even in slurries prepared with distilled water. Thus, during sedimentation of the tailings/bentonite beds, flocs develop in the suspension and settle under the influence of their self-weight. A load-bearing skeleton consisting of sand and silt grains, clay aggregates (flocs) and pores begins to develop marking the onset of primary consolidation. The fabric of the resulting sediment deposit depends on the applied effective stress (Imai 1981), and under very low stresses such as those induced by self weight consolidation, the tailings/bentonite beds exhibit more open and flocculated fabric with higher void ratio than the tailings/kaolinite beds. In tailings/bentonite beds, as additional material settles on the top, the weaker flocs in the forming deposit break up, pore spaces are further reduced and pore water is expulsed from within the flocs and interparticle spaces (Toorman 1999). The resulting smaller and stronger aggregates together with the coarse sand and silt particles form a more compact bed with lower permeability. Primary consolidation is considered complete when excess water pressure has fully dissipated. During secondary compression the particles and flocs tend to rotate and assume more stable configuration at an almost constant volume and water content (Mitchell and Soga 2005). The mechanism of secondary compression involves sliding at interparticle contacts, expulsion of water from microfabric elements, and rearrangement of adsorbed water molecules and cations into different positions. This phenomenon of structural change at constant effective stress is referred to as thixotropy and in the investigated tailings/bentonite beds, it has probably caused the observed small shear strength increase with time of consolidation.

The stable configuration sought by the particles during secondary compression is a function of the magnitude of the effective stress and the water content, that is, the higher the effective stress and water content, the greater the particle rearrangement during secondary compression (Zreik et al. 1997). Unlike bentonite, kaolinite particles are inert and behave as a sandy material forming a deposit with lower void ratio and water content. Furthermore, due to the high permeability of these beds, the rate of water content decrease during primary consolidation is much more remarkable than in the tailings/bentonite beds. Thus, at a low effective stress of approximately the same magnitude, the void ratio and, correspondingly, the water content of the tailings/kaolinite beds is lower than that of the tailings/bentonite beds and hence, little or no particle rearrangement occurs in the former during secondary compression.

*5.3.4.4. Comparative evaluation of drained and partially drained shear strength results*

The results from the drained and partially drained shear strength testing of mixed mine tailings/clay beds, consolidated for 3 and 12 days, are summarized in Table 5.3. The drained and partially drained shear strengths are expressed in terms of $\phi'$ and $\phi_T$, respectively.

| Sample ID | 3 days | | 12 days | |
|---|---|---|---|---|
| | $\phi'$ (°) | $\phi_T$ (°) | $\phi'$ (°) | $\phi_T$ (°) |
| T1 | 40.4 | 23.3 | 40.8 | 23.8 |
| M2 | 39.6 | 21.2 | 40.4 | 22.1 |
| M3 | 38.5 | 19.3 | 39.7 | 20.0 |
| M4 | 37.3 | 17.4 | 38.8 | 18.0 |
| M5 | 35.2 | 15.2 | 37.3 | 17.3 |

**Table 5.3.** Effective and total friction angles for beds prepared from mine tailings/clay mixtures with various composition, consolidated for 3 or 12 days.

During rapid tilting, the beds probably experienced different degree of drainage due to their varying permeability, and, as such, the partially drained strength results were not strictly obtained under the same drainage conditions. However, they can still serve to illustrate the effect of tilting rate and partial drainage on the shear strength of the beds. As expected for a normally consolidated soil, the drained shear strength was higher than the partially drained over the entire stress range for all tested tailings/clay beds. This was due to the positive excess pore pressures generated during rapid shearing in the Tilting Tank and causing a reduction in the normal effective stress. The total friction angle, $\phi_T$, was lower than the effective friction angle, $\phi'$, with the difference between $\phi_T$ and $\phi'$ decreasing in the order M5>M4>M3>M2>T1. It is believed that, in the M5 beds, drainage was minimal and therefore, shearing occurred under nearly undrained conditions. No dissipation of excess pore pressure was evident in this bed, unlike in the mixed tailings/kaolinite beds which all experienced some degree of drainage. Thus, the excess pore water pressure in the M5 bed built up rapidly with the onset of tilting and reached a higher value than in the M2 and T1 beds, for example. As a consequence of the rapid excess PWP generation and lack of pressure dissipation through drainage, the M5 bed failed at a lower angle of tilting than the T1, M2, M3 and M4 beds. In contrast, drainage at the bed surface reduced the net excess PWP in the tailings/kaolinite beds and, as a result, they failed at higher angles of tilting. The increase in the angle of tilting at failure in the order M4<M3<M2<T1 in the tailings/kaolinite beds followed the increase in the degree of drainage within these beds, i.e. from lowest in the M4 beds to highest in the T1 beds.

A detailed investigation of the water content and density distribution in the deposited mixed tailings/clay beds is currently underway. Further research efforts will also focus on measuring the undrained shear strength of the beds. It is expected that the results would provide additional insight into the effect of drainage on the shear strength of the mixed mine tailings/clay beds in the entire range of drainage conditions, i.e., from fully drained to completely undrained.

## 5.4. Summary and Conclusions

Artificial mine tailings/clay mixtures were prepared in the laboratory by adding kaolinite or bentonite clay to hard rock mine tailings. The total clay content of the obtained samples varied from 4% in the original mine tailings to 16%, with the upper boundary corresponding to the maximum clay percentage found in most tailings in Canada. The mixtures were used in the preparation of slurries with high concentration of solids (50% by volume), from which mine tailings/clay beds with final thickness between 1 and 11 cm were sedimented. The beds were allowed to consolidate under self weight for a minimum of 3 days, which period was sufficient to complete their primary consolidation. Thus, the obtained normally consolidated beds were tested in a specially built Tilting Tank where the excess pore water pressure, generated as a result of tilting, was monitored using pressure transducers. The transducers were positioned in a vertical array at three elevations: near the surface, in the middle and close to the bottom of the beds. An average slow titling speed of 0.07°/min was applied to obtain a measure of the drained shear strength of the beds, while rapid tilting at 1.61°/min was adopted to simulate partially drained shearing conditions. The main findings of the research are summarized below:

- During shearing, all tailings/kaolinite beds experienced some degree of pore water pressure dissipation through drainage from the bed surface, the magnitude of which depended on the clay content of the bed, i.e., the higher the clay content the lower the degree of drainage. In contrast, the excess pore water pressure distribution within tailings/bentonite beds was relatively uniform, indicating that minimum or no pressure dissipation occurred in these beds.
- In all beds during slow tilting, the excess pore water pressure at each monitored horizon remained at least an order of magnitude lower than the respective normal effective stress. Failure of the beds occurred when the shear stress at a given depth exceeded the shear strength of the bed at the same depth.
- Rapid titling of the beds resulted in the generation of excess pore water pressure which, at a given elevation, was of the same order of magnitude as the normal effective stress and thus, affected the shear strength of the beds. Slope failure was triggered when the excess pore water pressure became equal to the normal effective stress at a given elevation in the bed.

- During failure, the soil mixture showed complete loss of integrity. The failure plane was parallel to the bottom of the tank and located at 0.4 to 2.5 cm from the bed surface.
- Liner drained residual strength envelopes of tested mixtures were successfully defined at a vertical stress range from 0.03 to approximately 0.18 kPa. The drained residual friction angle of the beds, $\phi'$, generally decreased with increasing clay content in the mixtures, but bentonite was much more effective in reducing $\phi'$ than kaolinite. The partially drained (total stress) failure envelopes obtained for the tested mixtures were also linear within the tested stress range with zero cohesion intercept.
- For beds of the same composition and age, the total friction angle, $\phi_T$, was determined to be lower than $\phi'$, which was attributed to the higher excess pore pressure generated within the beds during rapid tilting in comparison with that induced in response of slow tilting. Experimental results demonstrated little variation of both $\phi'$ and $\phi_T$ with bed age in the tailings/kaolinite beds, whereas increasing the time for consolidation from 3 to 12 days, resulted in 2.1° degrees gain in frictional resistance in the tailings/bentonite beds.

## 5.5. Acknowledgements

This work was supported by funding from the Natural Sciences and Engineering Research Council of Canada (NSERC) in the form of an Individual Discovery Grant awarded to E.K. Yanful and a postgraduate scholarship awarded to Rozalina Dimitrova.

## 5.6. References

Agar GE (1991) Flotation of chalcopyrite, pentlandite, pyrrhotite ores. International Journal of Mineral Processing, 33:1-19.

Al-Shayea NA (2001) The combined effect of clay and moisture content of the behavior of remolded unsaturated soils. Engineering Geology, 62:319-342.

Amaratunga LM, Yaschyshyn DN (1997) Development of a high modulus paste fill using fine gold mill tailings. Geotechnical and Geological Engineering, 15:205-219.

ASTM, Standard D 4253-00 (2006) Standard test methods for maximum index density and unit weight of soils using a vibratory table. American Society for Testing and Materials, Philadelphia, Pasadena, USA.

Aubertin M, Ricard JF, Chapuis RP (1998) A predictive model for the water retention curve: application to tailings from hard-rock mines. Canadian Geotechnical Journal, 35:55-69.

Baroid Industrial Drilling Products (2011) Accessible at: http://www.baroididp.com/public_idp/products-apps/pubsdata/Data_Sheets/I_Z/QUIK-GEL.pdf, last accessed: February 2011.

Bell FG (1999) Geological hazards: their assessment, avoidance, and mitigation. E & FN Spon Press, London, UK.

Benzaazoua M, Belem T, Bussière B (2002) Chemical factors that influence the performance of mine sulphidic paste backfill. Cement and Concrete Research, 32:1133-1144.

Benzaazoua M, Bussière B, Kongolo M, McLaughlin J, Marion P (2000) Environmental desulphurization of four Canadian mine tailings using froth flotation. International Journal of Mineral Processing, 60:57-74.

Benzaazoua M, Marion P, Picqet I, Bussière B (2004) The use of pastefill as a solidification and stabilization process for the control of acid mine drainage. Minerals Engineering, 17:233-243.

Bois D, Poirier P, Benzaazoua M, Bussière B (2004) A feasibility study on the use of desulphurized tailings to control acid mine drainage. In: Proceedings of 36th Annual Meeting of the Canadian Mineral Processors, Paper No 23, Canadian Mineral Processors, Ottawa, Canada.

Darley HCH, Gray GR (1988) Composition and properties of drilling and completion fluids, 5th edn. Butterworth-Heinemann, Woburn, Massachusetts, USA.

Demers I, Bussière B, Mbonimpa M, Benzaazoua M (2009) Oxygen diffusion and consumption in low-sulphide tailings covers. Canadian Geotechnical Journal, 46:454-469.

Di Maio C, Santoli L, Schiavone P (2004) Volume change behaviour of clays: the influence of mineral composition, pore fluid composition and stress state. Mechanics of Materials, 36:435-451.

Fahey M, Newson TA (1997) Aspects of the geotechnics of mining wastes and tailings dams. In: Environmental geotechnics: Proceedings of the 1st Australia-New Zealand Conference Geoenvironment '97, A.A. Balkema, Rotterdam, The Netherlands, pp. 115-134.

Fall M, Cèlestin JC, Han FS (2009) Stability of bentonite-paste tailings mixtures as engineering barrier material for mine waste containment facilities. Minerals Engineering, 22:840-848.

Fang HY, Daniels J (2006) Introductory Geotechnical Engineering: An Environmental Perspective. Taylor & Francis, New York, USA.

Holeman JN (1965) Clay Minerals. Technical Release No. 28, Soil Conservation Service, Engineering Division, US Department of Agriculture, Washington, DC, USA.

Holtz R, Kovacs W (1981) An introduction to geotechnical engineering. Prentice-Hall Inc., Englewood Cliffs, New Jersey, USA.

Imai G (1981) Experimental studies on sedimentation mechanism and sediment formation of clay materials. Soils and Foundations, 21(1):7-20.

Ishihara K, Troncoso J, Kawase Y, Takahashi Y (1980) Cyclic strength characteristics of tailings materials. Soils and Foundations, 20(4):127-142.

Jacobs W, van Kesteren WGM, Winterwerp JC (2007) Permeability and consolidation of sediment mixtures as function of sand content and clay mineralogy. International Journal of Sediment Research, 22(3):180-187.

Jewell RJ (1998) An introduction to tailings. In: Case studies on Tailings Management. International Council on Metals and the Environment, Ottawa, Canada, pp. 7-8.

Kenney TC (1967) The influence of mineralogical composition on the residual strength of natural soils. In: Proceedings of the Geotechnical Conference on Shear Strength Properties of Natural Soils and Rocks, Oslo, Norway, Vol. I, pp. 123–129.

Kuerbis R, Negussey D, Vaid YP (1988) Effect of gradation and fines content on the undrained response of sand. In: Van Zyl, D.J.A., Vick, S.G., (Eds.), Hydraulic Fill

Structures, Geotechnical Special Publication No. 21, American Society of Civil Engineers (ASCE), New York, USA, pp. 330–345.

Lambe T, Whitman R (1969) Soil mechanics. John Wiley & Sons, New York, USA.

Lupini JF, Skinner AE, Vaughan PR (1981) The drained residual strength of the cohesive soils. Géotechnique, 31(2):181-213.

McGregor RG, Blowes DW, Jambor JL, Robertson WD (1998) Mobilization and attenuation of heavy metals within a nickel mine tailings impoundment near Sudbury, Ontario, Canada. Environmental Geology, 36(3/4):305-319.

Mesri G, Olson RE (1971) Mechanisms controlling the permeability of clays. Clays and Clay Minerals, 19:151-158.

Mesri G, Shahien M (2003) Residual shear strength mobilized in first-time slope failures. Journal of Geotechnical and Geoenvironmental Engineering, 129(1):12-31.

Mitchell JK, Soga K (2005) Fundamentals of Soil Behavior, 3rd edn. John Wiley & Sons Inc., Hoboken, New Jersey, USA.

Mittal H, Morgenstern N (1975) Parameters for the design of tailings dams. Canadian Geotechnical Journal, 12:235-261.

Ouangrawa M, Molson J, Aubertin M, Bussière B (2009) Reactive transport modelling of mine tailings columns with capillarity-induced high water saturation for preventing sulfide oxidation. Applied Geochemistry, 24:1312–1323.

Penman AD (1998) The need for dam safety. In: Case studies on Tailings Management. International Council on Metals and the Environment, Ottawa, Canada, pp. 5-6.

Pettibone H, Kealy C (1971) Engineering properties of mine tailings. Journal of the Soil Mechanics and Foundations Division, 97(SM9):1207-1225.

Rankine KJ, Sivakugan N, Cowling R (2006) Emplaced geotechnical characteristics of hydraulic fills in a number of Australian mines. Geotechnical and Geological Engineering, 24:1-14.

Raudkivi AJ (1998) Loose Boundary Hydraulics. A.A. Balkema, Rotterdam, The Netherlands.

Rodríguez R (2006) Hydrogeotechnical characterization of a metallurgical waste. Canadian Geotechnical Journal, 43:1042-1060.

Salgado R, Bandini P, Karim A (2000) Shear strength and stiffness of silty sand. Journal of Geotechnical and Geoenvironmental Engineering, 126(5):451-462.

Shaw SC, Groat LA, Jambor JL, Blowes DW, Hanton-Fong CJ, Stuparyk RA (1998) Mineralogical study of base metal tailings with various sulfide contents, oxidized in laboratory columns and field lysimeters. Environmental Geology, 33(2/3):209-217.

Skempton AW (1985) Residual strength of clays in landslides, folded strata and the laboratory. Géotechnique, 35(1):3-18.

Stark TD, Choi H, McCone S (2005) Drained shear strength parameters for analysis of landslides. Journal of Geotechnical and Geoenvironmental Engineering, 131(5):575-588.

Stark TD, Eid HT (1994) Drained Residual Strength of Cohesive Soils. Journal of Geotechnical Engineering, 120(5):856-871.

Tiwari B, Marui H (2005) A new method for the correlation of residual shear strength of the soil with mineralogical composition. Journal of Geotechnical and Geoenvironmental Engineering, 131(9):1139-1150.

Toorman EA (1999) Sedimentation and self-weight consolidation: constitutive equations and numerical modelling. Gèotechnique, 49(6):709-726.

Wijewickreme D, Sanin MV, Greenaway GR (2005) Cyclic shear response of fine-grained mine tailings. Canadian Geotechnical Journal, 42: 1408–1421.

Wilson GW, Miskolczi J, Dagenais A, Levesque I, Smith Q, Lanteigne L, Hulett L, Landriault D (2006) The application of blended waste rock and tailings for cover systems in mine waste management. In: Proceedings of the 7$^{th}$ International Conference on Acid Rock Drainage (ICARD), American Society of Mining and Reclamation (ASMR), Lexington, USA, pp. 2424-2438.

Zreik DA, Germaine JT, Ladd CC (1997) Undrained strength of ultra-weak cohesive soils: relationship between water content and effective stress. Soils and Foundations, 37(3):117-128.

# CHAPTER 6. RELATIONSHIP BETWEEN EROSIONAL AND MECHANICAL STRENGTH OF MINE TAILINGS AND MINE TAILINGS/CLAY MIXTURES

## 6.1. Introduction

The movement of sedimented soil or rock particles from one location to be deposited at another is termed erosion, and it may result from the movement of water, wind or ice (Dyer 1986). From the erosivity point of view, sediments may be loosely classified as: i) noncohesive; and ii) cohesive (Raudkivi 1998). Noncohesive sediments are those that are composed of discrete particles, the erosion of which depends on particle properties, e.g., shape, size, and density, as well as on the relative position of the particle in the sediment matrix (Mitchener and Torfs 1996; Van Ledden et al. 2004). Cohesive sediments are those for which resistance to erosion depends on the particle size, mineralogy, but also on the strength of the cohesive bonds between particles (Berlamont et al. 1993). The resisting force due to cohesion may far outweigh the influence of the individual particle characteristics. In addition to sediment characteristics, the conditions necessary to initiate erosion are also a function of the fluid properties (e.g., chemistry, density and viscosity) and the flow conditions (average velocity or intensity of turbulent stresses) (Miller et al. 1977). The consolidation and time-related history of the sediment bed is also important (Parchure and Mehta 1985; Mehta et al. 1989; Berlamont et al. 1993). For instance, a cohesive sedimentary deposit may be soft, partially consolidated with very high water content, or a more dense settled bed. Therefore, a density profile of the sediment bed and the pore pressure and effective stress distribution within the bed must be known in order to reliably estimate the erosional strength or resistance of the bed to erosion (Berlamont et al. 1993). Whereas in cohesive sediments, groups of grains are eroded as units, in noncohesive sediments erosion occurs by entraining individual particles. Annandale (1995) introduced an erodibility index to characterize the ability of noncohesive sediments to resist erosion and suggested a correlation between the erodibility index and the rate of energy dissipation of flowing water, from which the critical threshold to initiate erosion of sediment can be predicted. The critical threshold for sediment bed erosion is, in essence, a reflection of the force exerted by the water flowing over a sediment bed that, if exceeded, will put in motion or entrain the grains of the bed. When particle motion is incipient, the bed shear stress attains its critical value and is referred to as critical bed shear stress or critical threshold for erosion, $\tau_c$, which can be estimated if the fluid and sediment properties are known (White 1970; Miller et al. 1977; Annandale 1995; Berlamont et al. 1993).

Near the critical value of the bed shear stress, the motion of grains in any small area of the sediment bed occurs in gusts whose incidence increases as the mean shear stress increases (ASCE 2006). Because of the intermittency with which particles are entrained into the flow, the detection and interpretation of the “critical” condition is highly subjective. Furthermore, determining the erosion of cohesive sediments is even more difficult than that of noncohesive sediments. As the grains of the latter are larger, the erosion process can be easily determined even visually. In contrast, the cohesive sediment particles are often invisible to the naked eye and erosion is determined by either measuring the accumulation of suspended particulate matter in the eroding fluid or by investigating the critical erosion shear stress of the sediment bed, $\tau_c$. Lavelle and Mofjeld (1987) reviewed results of previous studies and suggested that particle movement and transport occurred even below the commonly accepted threshold values. Mantz (1980) concluded that the critical threshold should be selected to correspond to some arbitrary small value of transport, which could be used to denote a point of significant erosion.

Sediment beds can exhibit either relatively uniform properties over depth below bed surface, or be stratified with respect to geotechnical property variations with depth (Parchure and Mehta 1985). While the former are created by remoulding previously formed beds, the latter are formed by allowing suspended sediments to deposit under low flow velocity conditions. After deposition from suspension cohesive and noncohesive sediment beds undergo consolidation, which is accompanied by expulsion of interstitial pore water from the sediment matrix, and results in a more closely packed sediment of greater density and lower water content (Mitchener and Torfs 1996; Roberts et al. 1998). Because of density and particle size variations, the erosion resistance of a vertically stratified bed increases with depth and is characterized by erosion steps, in which the erosion rate is dependent on the consolidation characteristics and strength of the layer being eroded (Mitchener and Torfs 1996; Amos et al. 1996, 1997; Parchure and Mehta 1985; Tolhurst et al. 2000; Maa and Kim 2002). Thus, the erodibility of a stratified sediment bed can be best represented by a series of multiple $\tau_c$ values defined for each layer below the surface of the bed.

Various conceptual models and mathematical formulations have been developed for the description and modelling of the erosion processes in cohesive and noncohesive sediments, separately, but there are only a few that deal with mixed sediments (e.g., Mitchener and Torfs 1996; Houwing 1999; van Ledden et al. 2004). However, often natural sediments and mine tailings are mixtures of sand and mud and the erosional properties of combined sand/mud sediments are required in order to model their erosion behaviour (Torfs et al. 1996; Panagiotopoulos et al. 1997; Le Hir et al. 2008). In the literature and hereinafter, the size fraction with particle diameter less than 0.063 mm, comprising silt and clay, is referred to as mud. A strong dependence of the strength of mixed sediment beds on the sand/mud ratio has been reported by several researchers (e.g., Houwing 1999; Mitchener and Torfs 1996; Panagiotopoulos et al. 1997; van Ledden et al. 2004; Le Hir et al. 2008). Houwing (1999) found that when the mud content of the substratum was low (below 20% mud by weight), the erosion rates were high and the eroded fraction of the sediment bed was composed mainly of sand. In contrast, when the mud content was high (above 20% by weight) the erosion rates decreased substantially and erosion of both the mud and sand fractions was found. Mitchener and Torfs (1996) conducted tests with artificially produced sand/mud mixtures and reported that the critical erosion threshold for a noncohesive sand bed increased when mud was added. Although the authors referred to the additives as "mud", they were actually kaolinite and montmorillonite clays. The maximum erosion resistance was recorded when the sand fraction of the mixed sediment beds was 50 to 70% (by weight).

For sandy sediments, Fukuda and Lick (1980) reported that at a constant value of the applied shear stress and water content, an increase in the clay content of the bulk sediment led to a corresponding decrease in the entrainment rate. Lick et al. (2004) performed experiments with mixtures of uniformly-sized quartz particles and 2% added bentonite and found that bentonite greatly decreased the erosion rates, with the effect being most pronounced for particle diameters between 0.1 and 0.4 mm. The authors found that the erosional behaviour of mixed sediment beds was strongly dependent on the bed formation history, and in particular, on the existence of discrete layers with variable properties within the bed. The work of Panagiotopoulos et al. (1997) confirmed that adding up to 30% cohesive material (mud) to sandy beds generally increased the erosion threshold of sandy deposits under both steady and oscillatory flow. The trend was reported to be valid up to 11-14% clay mineral content (by weight). Panagiotopoulos et al. (1997) hypothesized that for higher than 14% clay content, the sand particles were no longer in contact with each other and the erodibility of the sand/mud mixture was controlled by the clay fraction only. Van Ledden et al. (2004) proposed a new conceptual framework for the erosion of mud/sand mixtures and classified sediment beds into six bed types with different characteristics with respect to network structure and erosion behaviour (cohesive or noncohesive). They concluded that because only the clay particles within the mud fraction exhibit cohesive properties, it is the clay content, and not the mud content, which determines the transition between noncohesive and cohesive behaviour of sediment beds. A clear relationship between the critical stress for erosion of mixed sediments and the mud volume fraction was reported by Le Hir et al. (2008), but they did not find a definitive correlation between $\tau_c$ and the clay fraction.

Although there is abundant literature on the erodibility of natural sediments, studies dealing with erosion of mine tailings, in particular, are relatively sparse. Yanful and Catalan (2002) investigated the wind-induced resuspension of mine tailings using published semi-empirical predictive methods and validated the predictions with field measurements. The results were used to determine a minimum depth of the water cover needed to prevent tailings erosion and resuspension. Mian et al. (2007) defined a relationship between the rate of erosion and the excess shear stress (bed shear stress above the critical threshold for erosion) for mine tailings and suggested the applicability of a power law relationship between the erosion rate and excess shear stress normalized by $\tau_c$. Mian and Yanful (2003) noted, however, that further investigation was required to quantitatively describe the effects of cohesion, self-consolidation, flocculation, fall velocity, tailings pond hydrology and water balance on the resuspension of mine tailings. Although the above studies initiated the evaluation of the erosion behaviour of mine tailings, many questions still remain unanswered. For example, it is presently unclear whether the existing relationships that estimate the critical stress for erosion, $\tau_c$, from the bulk properties (e.g., bulk density, water content, shear strength) of sediments can be successfully applied to mine tailings as well. Since the bulk properties can be determined relatively easily using existing engineering standards (Roberts et al. 1998; Berlamont et al. 1993), it would be useful if mine tailings' resistance to erosion and transport could be predicted from knowledge of these properties. The present work investigates the possibility of correlating the mechanical strength of mine tailings with their erosion resistance and, in particular, with the critical shear stress (threshold) for erosion. The purpose of developing such correlation for a range of mine tailings and mine tailings/clay mixtures was to: (i) attempt to provide empirical methods to predict the erosion resistance of a mixture from its known mechanical (undrained) strength; (ii) improve the fundamental understanding of the effect of clay content and mineralogy on the erosional strength of mine tailings; and (iii) establish a basis for comparing the erosion resistance of tailings of different compositions. The results could be used to develop a predictive model to describe the erosion behaviour of mine tailings. Improving erosion prediction models based on erosion threshold values is a matter of great environmental importance (Fukuda and Lick 1980; Torfs et al. 1996; Panagiotopoulos et al. 1997; Reddi and Bonala 1997; Maa and Kim 2002). Due to their large specific surface and high sorption potential, the fine fraction of tailings tends to preferentially absorb many contaminants.

## 6.2. Testing Materials and Procedures

### *6.2.1. Tailings beds preparation*

The source material (i.e., mine tailings) used in the present study was received from the Clarabelle Copper Mine, Sudbury, Ontario. Its mineralogical composition was previously characterized by Shaw et al. (1998) and McGregor et al. (1998) as consisting of pentlandite, chalcopyrite, pyrrhotite, quartz, feldspar, chlorite, biotite, amphibole, carbonates plus minor pyroxene, apatite, magnetite, ilmenite, marcasite, galena and pyrite. These reported studies (Shaw et al. 1998; McGregor et al. 1998) indicated that the predominant clay minerals in the Sudbury mine tailings were chlorite and biotite, which according to Skempton's activity classification (Skempton 1953) are both considered inactive (activity less than 0.75). The mine tailings were mixed with various amounts of dry kaolin (Fisher Scientific Chemical) or bentonite powder (Baroid Quick-Gel Fast Mixing High Viscosity Bentonite) to obtain four artificial tailings/clay mixtures with varying amount of clay but constant sand/silt ratio. The primary clay minerals present in the selected kaolin and bentonite additives were kaolinite and Na-montmorillonite, respectively. The composition and some index properties of the tailings (denoted T) and artificial tailings/clay mixtures (denoted M) are summarized in Table 5.2 (Chapter 5). Figure 5.1 (Chapter 5) shows the grain size distribution curves of the mine tailings and the mixtures used in the present study. In Figure 5.1, the lower boundary of the family of curves represents that of the pure mine tailings (T1), which have the lowest content of clay-size particles (i.e., 4%). The upper boundary, M4, is the grain size curve of the mixture with the highest clay content (16%). The shaded area between the T1 and M4 curves represents the grain size distributions of mixtures with intermediate clay contents, ranging from 8 to 16% (Table 5.2).

Kaolinite, with its low plasticity, activity and cohesion, exhibits similar physico-chemical properties to those of chlorite (Mitchell and Soga 2005), the dominant clay mineral present in the pure mine tailings. Kaolinite was selected as an additive because it was the least likely to affect the chemistry of the pore-water solution during the experiments and thus, provided an opportunity to study in isolation the effect of increasing the percentage of clay fraction of the mixtures. On the other hand, bentonite, of all clay minerals, has the highest effect on physico-chemical and hence geotechnical properties of the soils, i.e., on their shear strength, compressibility, void ratio, and hydraulic conductivity (Di Maio et al. 2004). It was chosen as a second additive in order to investigate the effect of clay mineralogy on the engineering properties and erosion resistance of the tailings.

Distilled water was added to the tailings/clay mixtures to obtain slurries with 16% (by volume) concentration of solids. The slurries were thoroughly mixed with an electrical mixer (ARROW 1750) for about ten minutes after which they were poured into cylindrical glass containers with a diameter of 14.2 cm where they were left to consolidate under self-weight for three days. Since the slurry concentration was kept constant, slurries with different initial heights were used to obtain mine tailings/clay deposits with varying final thicknesses (between 4 and 10 cm). The selected slurry concentration (i.e., 16 % by volume) is considered moderate, and researchers (e.g., Davies 1968) have shown that deposits obtained through sedimentation from slurries with moderate concentration comprise two portions: a relatively homogeneous thicker lower layer of uniformly distributed coarse particles, and a capping layer of fines. Indeed, visual inspection of the obtained tailings/clay beds confirmed the presence of a 0.5 to 1.0cm-thick capping layer on top of a coarser bottom layer. During the experimental cycle, the laboratory temperature was kept constant at 22°±1°C.

### *6.2.2. Undrained shear strength testing*

Immediately prior to each test the water above the deposited tailings/clay beds was pumped out using a mini pump and the remaining water film was removed by absorption with paper towels. Undrained shear strength measurements were performed using the Automated fall cone device, previously described in Chapter 3, Section 3.2, Subsection 3.2.2, at depth intervals of 1 cm within the beds. The Automated fall cone device utilizes cones having apex angles of 60° and 90°, which are positioned at the surface of the specimen and then allowed to penetrate under their own weight for a period of 5 s. The undrained shear strength, $c_u$, is calculated from the depth of penetration, $d$ and the cone weight, $W$, using the following relationship (Hansbo 1957):

$$c_u = \frac{KW}{d^2} \tag{6.1}$$

where $K$ is the cone factor (i.e., an empirical constant that varies with the cone angle), $W$ is the cone weight, and $d$ is the depth of cone penetration.

Water content measurements were also performed at each horizon to obtain a water content-depth profile within the tested beds. More details about the testing procedure and equipment used in the undrained strength experiments can be found in Chapter 3, Section 3.2.

## 6.3. Results and Discussion

The undrained shear strength of deposited tailings/kaolinite beds with final thicknesses of 4, 7 and 10 cm, prepared from the M2, M3 and M4 mixtures was measured and compared to the strength of T1 beds (original mine tailings) of the same thickness. By varying the percentage of clay but keeping the clay mineralogy constant, the authors aimed to gain an insight into the effect of clay content on the undrained shear strength and erosion resistance of the mine tailings. Tailings/bentonite beds with final thickness of 7 cm were prepared through sedimentation and tested to investigate the effect of clay mineralogy (at constant percentage of added clay) on the mechanical and erosional strength of the mine tailings.

### *6.3.1. Water content distribution*

Figures 6.1a and b present the variation of the water content (and void ratio) with depth below the surface of deposited tailings and tailings/kaolinite beds prepared from the T1, M2, M3 and M4 mixtures. The beds were consolidated for 3 days prior to testing and had a final thickness of either 4 cm or 7 cm.

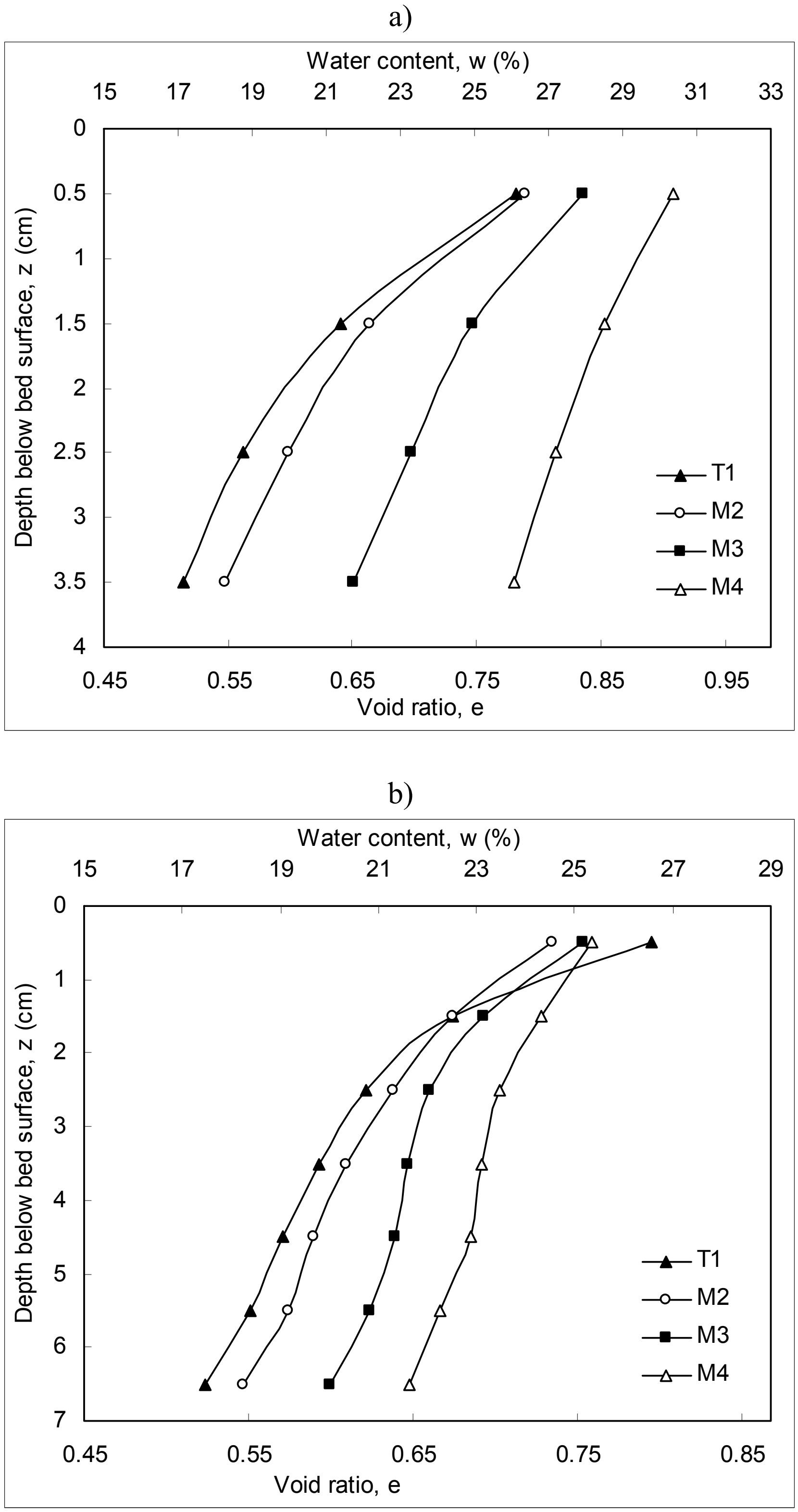


**Figure 6.1.** Water content profiles of beds with final thickness of: (a) 4 cm; and (b) 7 cm prepared from various tailings/kaolinite mixtures and consolidated for 3 days.

Figures 6.1a and b show that the water content in the tested beds increases with increasing clay content, i.e., it is lowest in the T1 beds with 4% clay content and highest in the M4 beds with 16% clay content. This can be expected since the water in the soils is almost entirely associated with the clay-size fraction and thus, increasing the clay content of the mixtures would also increase their water content (Mitchell and Soga 2005). The T1 beds exhibited the lowest void ratio, i.e., between 0.51 and 0.79 at corresponding water contents of 17.1% and 26.6%, whereas the highest void ratio was recorded for the M4 beds, i.e., between 0.64 and 0.90 at water contents of 21.6% and 30.4%. Generally the void ratio increased with increasing clay content of the mixtures in the order T1<M2<M3<M4. The determined range of void ratios compare well with those reported in the literature for similar soils. For instance, Aubertin et al. (1998) measured void ratios between 0.5 and 1.0 for low plasticity silt tailings with 4-6% clay content. For mine tailings with grain size distribution similar to those used in the present study, Rankine et al. (2006) calculated void ratios between 0.61 and 0.96 at corresponding water contents between 17.2 and 33.8%. From the examination of Figures 6.1a and b, it can be seen that in all beds the water content measured in the top layer is higher than the expected, based on the shape of the plots. This observation confirms the hypothesis that there exists a capping layer on top of all beds, which differs in composition from the rest of the deposit. For instance, the capping layer contains a higher percentage of finer clay particles that are capable of binding larger amounts of water and increasing the distance between the coarse sand particles, leading to a higher overall void ratio for the layer. The most significant variation between the water content within the capping layer and the rest of the bed was observed in the T1 bed and became less pronounced in the other beds in the order T1>M2>M3>M4. The authors believe that in the T1 bed, due to its high permeability, the water content measurements within the capping layer were affected by some upward drainage from the deeper subsurface layers. With increasing clay content, the permeability of the mixed beds decreased, thus reducing the effect of upward drainage on the water content of the capping layer.

The effect of clay mineralogy on the void ratio and water content of the deposited mixed beds can be seen when beds prepared from mixtures with the same clay content but with different clay mineralogy (kaolinite versus bentonite) are compared. Figure 6.2 shows such a comparison between 7-cm thick beds prepared from M2 and M5 mixtures and consolidated for 3 days.

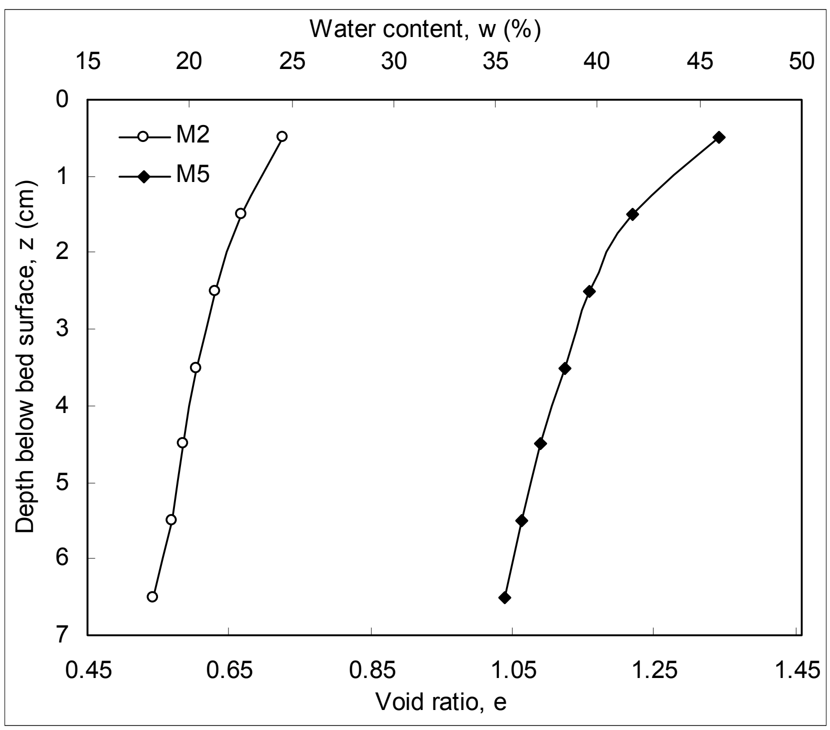


**Figure 6.2.** Water content profiles of 7-cm thick beds prepared from M2 and M5 mixtures and consolidated for 3 days.

Figure 6.2 shows that at the same percentage of added clay (4% increase in the original clay content to a total of 8%), the water content of the tailings/bentonite bed (M5) is nearly twice that of tailings/kaolinite bed (M2). This could be explained with the following hypothesis. When the added clay is highly expansive, as is the case with bentonite, large amounts of water are absorbed as interlayer water, which is effectively immobilized within the soil matrix leading to high water content and void ratio of the tailings/clay deposit. Furthermore, as discussed in Subsection 5.3.2.1 (Chapter 5, Section 5.3) the utilized Baroid Quick-Gel Fast Mixing High Viscosity Bentonite exhibited a tendency to flocculate even when the initial slurries were prepared with distilled water. This flocculation was attributed to the presence of soluble salts in the Baroid Quick-Gel capable of imparting flocculation even in fresh water suspensions. As a result, the tailings/bentonite deposits (M5) had more open flocculated fabric in comparison with the tailings/kaolinite beds (M2, M3 and M4).

The variation of vertical effective stress with water content (and void ratio) in beds with final thicknesses of 4 and 7 cm prepared from tailings/clay mixtures and consolidated for 3 days is shown in Figures 6.3a and b. As mentioned previously, only tailings/bentonite beds with final thicknesses of 7 cm were tested during the experimental program and hence, M5 data are absent from Figure 6.3a.

a)

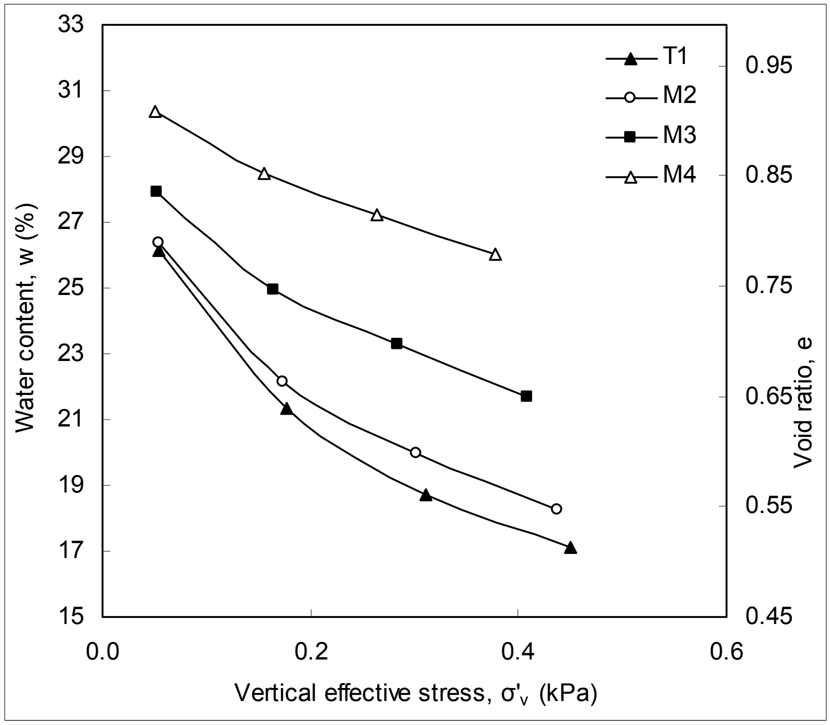


b)

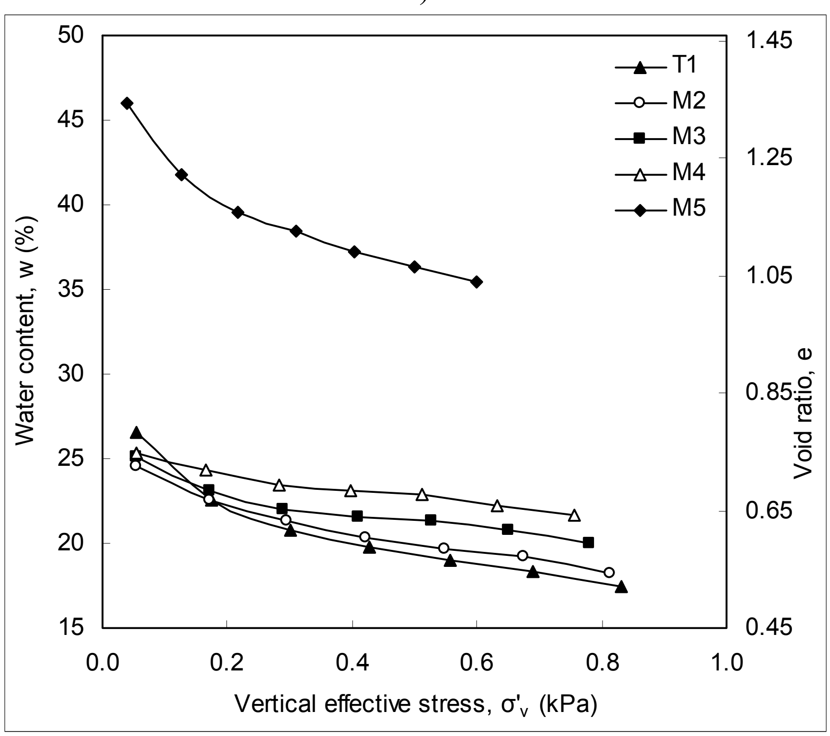


**Figure 6.3.** Vertical effective stress versus water content in beds with final thickness of: (a) 4 cm; and (b) 7 cm prepared from various mixtures and consolidated for 3 days.

Two important assumptions were made when computing the vertical effective stress ($\sigma'_v$) in the tested beds. First, it was assumed that excess pore water pressure (PWP) that developed during the fall cone testing were negligible and thus, at any given point of the tailings beds the PWP was equal to the hydrostatic pressure at that point. The second assumption was that the soil was fully saturated and remained so throughout the test. The equipment used (Automated fall cone device) did not allow measuring the excess PWP at each test point and thus, the accuracy of the first assumption could not be verified experimentally. Measures were put in place, however, to ensure that full saturation of the tested beds was maintained throughout each test. For instance, the fall cone testing at each horizon was performed as rapidly as possible (took only 5-10 minutes); also, between tests the exposed surface of the soil was always covered with damp paper towel to preserve its water content.

Presented data show that the vertical effective stress, $\sigma'_v$ increases as the void ratio and water content decrease (Figures 6.3a and b). Recalling that the latter two properties decrease with depth below bed surface (Figures 6.1a, b and Figure 6.2), these results imply that $\sigma'_v$ increases with depth as expected. Also, at a given water content (and void ratio) $\sigma'_v$ increases with clay content in the T1, M2, M3 and M4 beds, and is greatest in the M5 beds, which exhibit the highest overall water content and void ratio.

### 6.3.2. Undrained shear strength

The undrained shear strength, $c_u$, implicitly accounts for the pore pressure generated by the rapidly applied shear stress during the fall cone testing. The greatest challenge during the shear strength testing using the Automated fall cone device was to ensure that undrained conditions were always maintained and the measured bed shear strength was indeed undrained. Feng (2002) noted that when the liquid limit of a soil decreases to below 30%, the permeability of the soil becomes relatively high, but nevertheless, in the fall cone test it is still an undrained condition during fast rate of loading (i.e., 5 seconds). The present authors believe, however, that extra care should be taken to ensure that no drainage occurred during the fall cone testing. The decision to prepare the deposited tailings/clay beds from slurries with moderate concentrations was made in an effort to minimize drainage through the beds' surface by means of a capping layer with lower permeability formed on the top of the deposit. Umehara et al. (1985) concluded that a thin layer of fines located near the surface of the deposit prevented drainage from the underlying sandy layers and ensured almost undrained conditions during cyclic loading.

During our previous research we demonstrated that the primary consolidation of all mixed tailings/clay beds was complete within 3 days and thus, it was assumed that the excess pore water pressure within the beds was zero at the beginning of each shear strength test (Chapter 5, Section 5.3, Subsection 5.3.2.1). Figures 6.4a and b present the variation of the undrained shear strength, $c_u$, with depth below surface within tailings (T1) and tailings/kaolinite beds (M2, M3 and M4) with final thicknesses of 4 and 7 cm and consolidated for 3 days.

a)

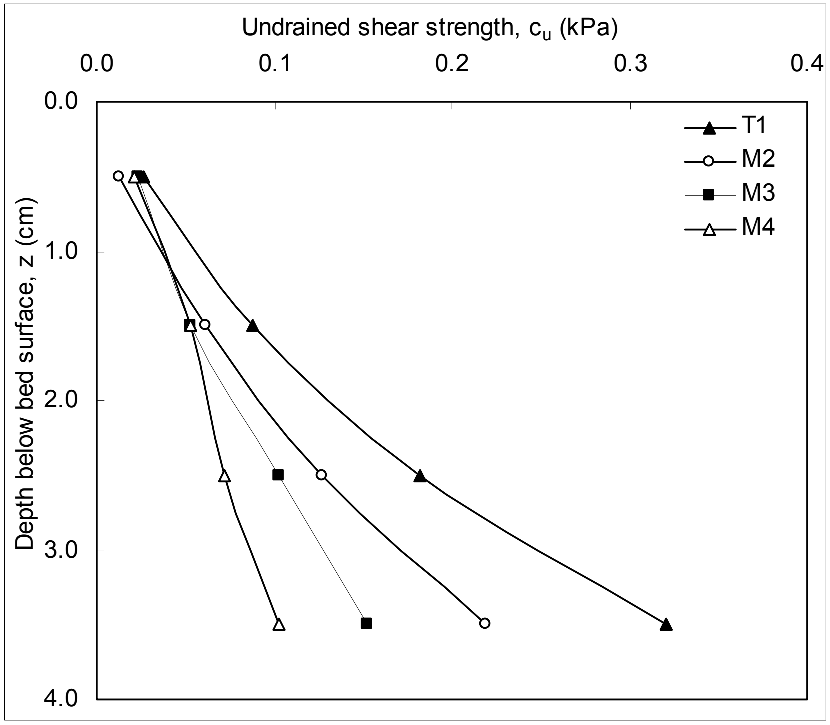


b)

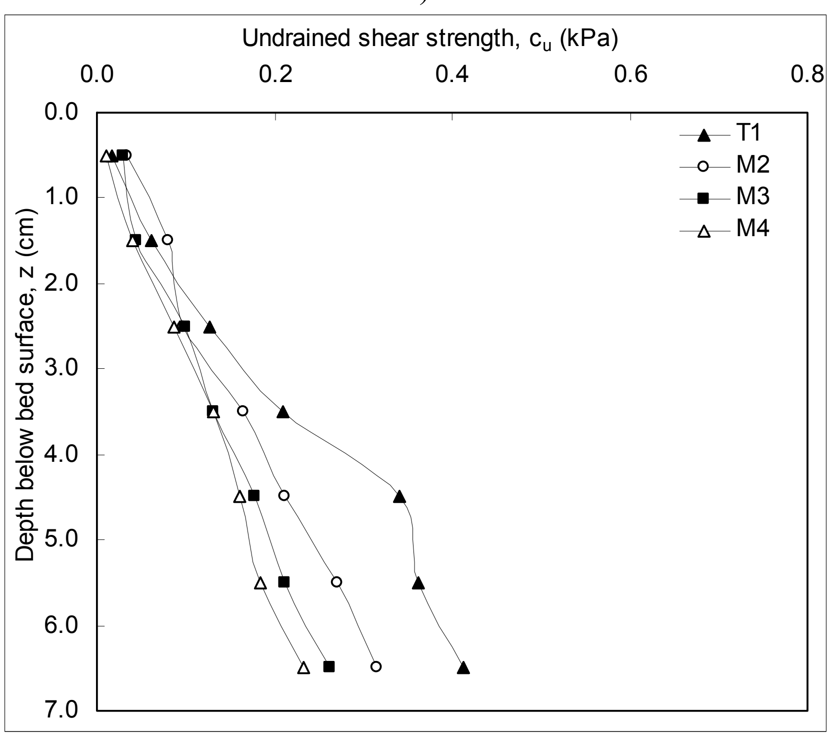


**Figure 6.4.** Undrained shear strength profiles of beds with final thickness of: (a) 4 cm; and (b) 7 cm prepared from various mixtures and consolidated for 3 days.

From Figures 6.4a and b it can be seen that $c_u$ increases with depth below surface in all tested tailings/kaolinite beds, which can be attributed to the corresponding water content decrease (Figures 6.1a and b) and effective stress increase with depth (Figures 6.3a and b). At a particular depth the largest $c_u$ was generally observed in the beds with lowest clay content (T1), whereas the lowest $c_u$ was recorded in those with highest clay content (M4).

The effect of clay mineralogy on the undrained shear strength of mine tailing/clay beds is illustrated in Figure 6.5, where the $c_u$-profiles obtained for beds with the same percentage of added clay (4%) but different clay minerals (i.e., kaolinite versus bentonite) are compared.

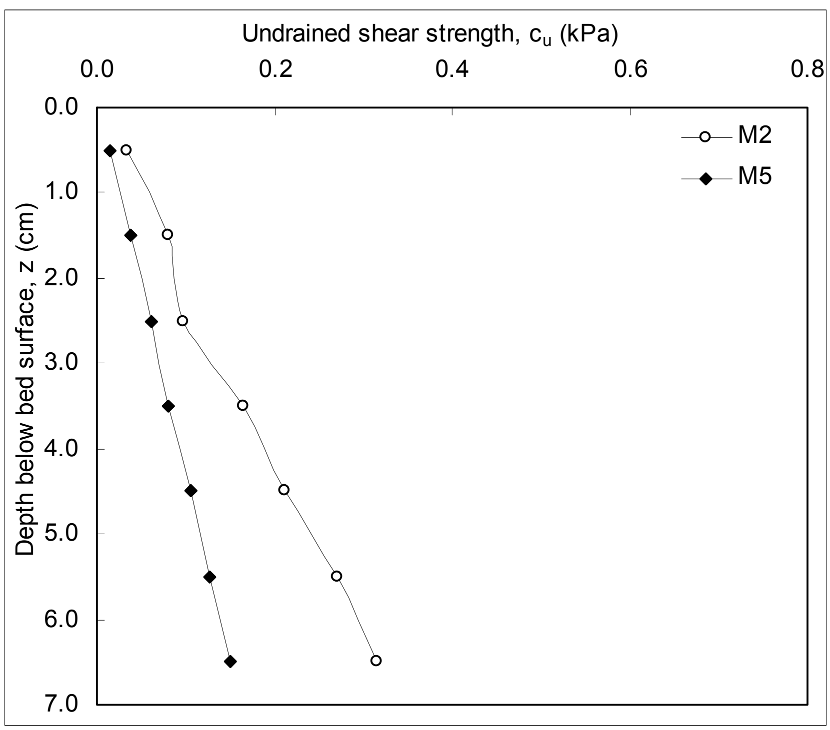


**Figure 6.5.** Undrained shear strength profiles of beds with 7 cm final thickness prepared from M2 and M5 mixtures and consolidated for 3 days.

Referring to Figure 6.5, it can be seen that adding bentonite to the mine tailings brought about a significant decrease in the undrained shear strength of the mixture. This was attributed to the higher void ratio and water content of the M5 bed in comparison to the M2 bed (Figure 6.2). From Figures 6.4a, b and Figure 6.5, it can be concluded that adding either kaolinite or bentonite to the original mine tailings resulted in lowering the undrained shear strength of the mixture, but adding bentonite caused a more substantial increase in the water content of the beds and as a direct consequence, a shear strength reduction of much greater magnitude than kaolinite.

The undrained shear strength, $c_u$, is often normalized by the vertical effective stress, $\sigma'_v$, as a means to estimate the strength increase with depth within a deposit. Figures 6.6a and b present the relationship between the undrained shear strength, $c_u$ and vertical effective stress, $\sigma'_v$ for mine tailings/clay beds, consolidated for 3 days. Figure 6.6a presents only the results for beds with final thickness of 7 cm, whereas the combined plots in Figure 6.6b contain data from undrained shear strength testing of beds of all thicknesses (i.e., 4, 7 and 10 cm).

a)

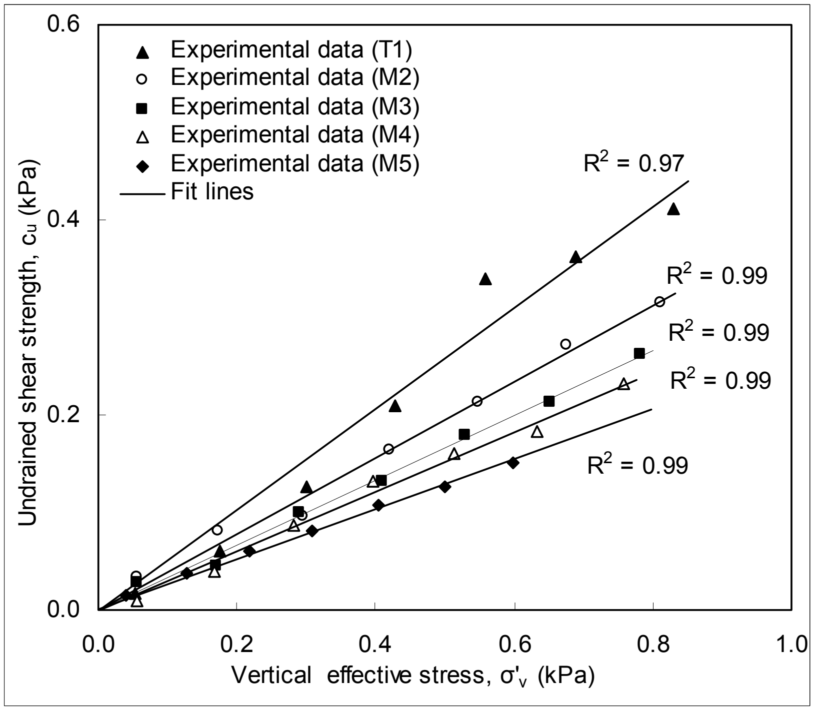


b)

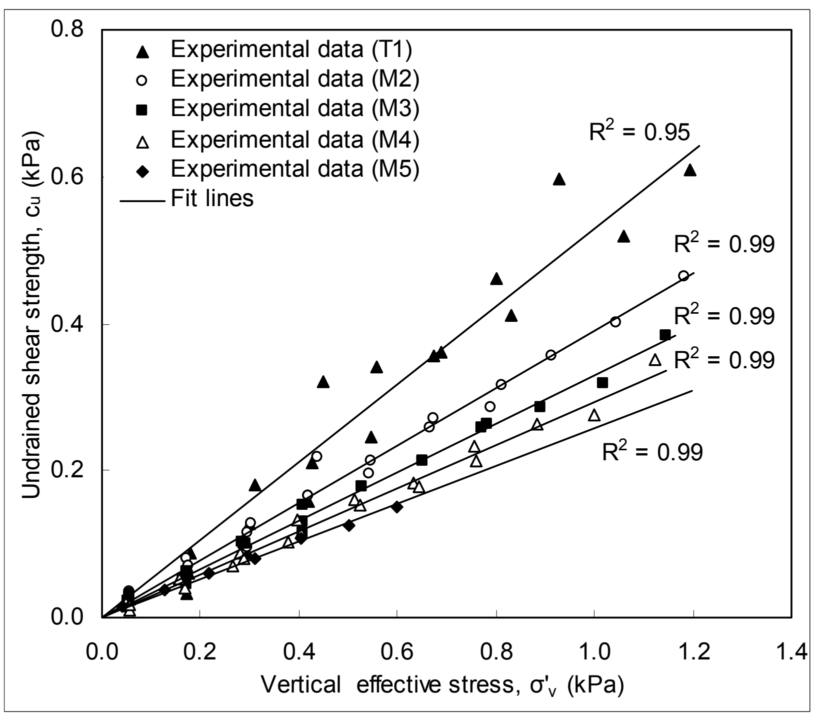


**Figure 6.6.** Undrained shear strength versus vertical effective stress for beds with final thickness of: (a) 7 cm; and (b) 4, 7 and 10 cm prepared from various mixtures and consolidated for 3 days.

Straight lines passing though the origin with *R*-squared values of 0.95 and higher were used to successfully fit the experimental results. Referring to Figures 6.6a and b, at the same magnitude of the vertical effective stress the undrained shear strength, $c_u$, decreases with increasing clay content in the T1, M2, M3 and M4 beds. The undrained shear strength, $c_u$, of the tailings/bentonite beds (M5) is always lower than that of the tailings (T1) and tailings/kaolinite beds (M2, M3 and M4). This trend is consistent with the water content variation measured in these beds at the same magnitude of the effective stress. The authors propose the following hypothesis to explain the observed $c_u$ decrease with increasing clay content of the mixtures. When the fines content is increased incrementally, the intergranular contacts between coarse particles are reduced, which leads to loss of frictional resistance and lower $c_u$-values in the deposited beds. The effect of clay to reduce the friction between sand grains and hence, to facilitate shearing, was also noted by Carraro et al. (2009).

Some earlier publications (e.g., Ladd and Foott 1974; Mesri 1975; Bromwell and Raden 1979) have shown that for natural clays the normalized strength ratio $c_u / \sigma'_v$ is independent of the magnitude of the effective consolidation stress, and for normally consolidated material (OCR=1.0) it is close to 0.20. Vick (1990), however, noted that a ratio of $c_u / \sigma'_v = 0.20$ does not apply in a strict sense to mine tailings and may only be considered as a conservative lower-bound estimate of the undrained shear strength of some types of normally consolidated slimes.

Thevanayagam (1998) pointed out that the intergranular void ratio, $e_{sk}$, which is the void ratio of the sand-grain-matrix, has an important control on the undrained shear strength of silty sand soils. The intergranular void ratio, $e_{sk}$, is considered to be an index of active coarser-granular frictional contacts within the soil matrix that sustain the normal and shear forces, and it can be determined from:

$$e_{sk} = (e + f_c)/(1 - f_c) \qquad (6.2)$$

where $f_c$ is the silt fraction of silty sand (by weight), and $e$ is the overall void ratio of the silty sand.

Thevanayagam (1998) introduced the term “host sand” (HS) to denote the sand fraction of the silty sand. This author observed that when $e_{sk}$ of the silty sand was in the vicinity of or exceeded $e_{\max,HS}$, the undrained shear strength, $c_u$, became dependent on the initial effective confining stress. Furthermore, at all investigated initial confining stresses, the undrained shear strength normalized with respect to the initial consolidation stress, $c_u / \sigma'_{v0}$, decreased with increasing percentage of fines (kaolinite) in the tested sand/kaolinite mixtures (Thevanayagam 1998). In the present study, all tested beds were normally consolidated and hence $\sigma'_v = \sigma'_{v0}$. The maximum void ratio of the tailings sand, i.e., the host sand, was $e_{\max,TS} = 1.01$, and was determined following ASTM standard D4253-00 (ASTM 2006a) on the sand fraction of the original tailings (i.e., the fraction greater than 0.075 mm). The intergranular void ratio of the tested whole tailings and tailings/clay mixtures, $e_{sk}$, was calculated from Eq. (6.2), and with $e = e_{\min}$ for each soil it was found to vary between 1.43 and 1.83. The minimum void ratio, $e_{\min}$, was determined following ASTM standard D4254-00 (ASTM 2006b). Since even when $e = e_{\min}$ was used in the calculations, for all tested soils $e_{sk}$ exceeded $e_{\max,TS}$, it was concluded that the quantity of fines (silt and clay) was sufficient to fully occupy the voids between the sand particles and they were floating within the fines matrix.

As evident from Figures 6.1 to 6.3, the void ratio, $e$, of the mixtures with similar clay mineralogy (T1, M2, M3 and M4) increased with increasing clay content, whereas the normalized undrained shear strength ratio, $c_u / \sigma'_v$, decreased with increasing clay content in the order T1>M2>M3>M4 (Figures 6.6a and b), which was consistent with the results of Thevanayagam (1998).

Other researchers (e.g., Sharma and Bora 2003, Trauner et al. 2005) have shown that the fall cone test yields a linear relationship between the logarithm of the undrained shear strength, $c_u$, and the logarithm of water content of the tested samples. Figure 6.7 shows log-log plots of the undrained shear strength, $c_u$, versus the water content for 7 cm-thick beds prepared from various mixtures and consolidated for 3 days. For easier reading of the plots, the horizontal axis in Figure 6.7 only shows a selected portion instead of a full log cycle (i.e., from 1 to 100).

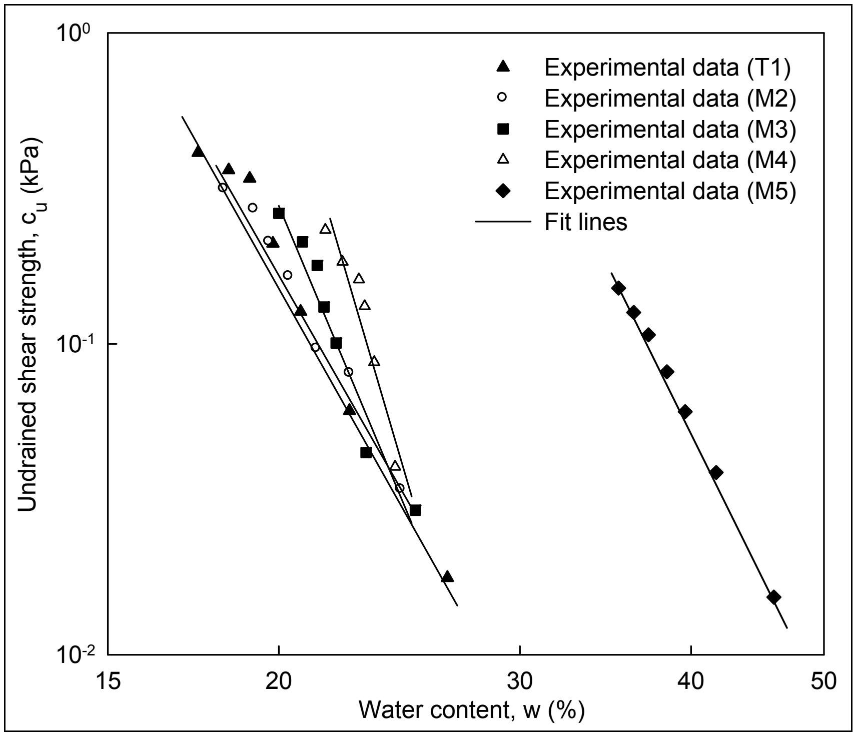


**Figure 6.7.** Undrained shear strength versus water content for 7 cm-thick beds prepared from various mixtures and consolidated for 3 days.

The experimental data in Figure 6.7 were fitted with straight lines with the following general equation:

$$\log(c_u) = m + n \log(w) \tag{6.3}$$

The coefficients *m* and *n* in Eq. (6.3) were determined by regression analysis and their values along with the correlation coefficients, *R*, for the studied mine tailings/clay mixtures are summarized in Table 6.1. The correlation coefficients, *R*, of the proposed linear relationship for the different tests were high (0.91 and greater) and dependent on the composition of the mixtures.

| Material | $m$ | $n$ | $R$ |
|---|---|---|---|
| T1 | 9.7453 | -8.0699 | 0.98 |
| M2 | 9.2498 | -7.6869 | 0.98 |
| M3 | 13.3000 | -10.6350 | 0.96 |
| M4 | 25.8860 | -29.725 | 0.91 |
| M5 | 12.905 | -8.8433 | 0.99 |

**Table 6.1.** Coefficient values in Eq. (6.3).

As can be seen from Figure 6.7, $c_u$ decreases with increasing water content in all studied beds. Furthermore, at the same value of the water content, $c_u$ appears to generally increase with increasing clay content of the beds in the order T1<M2<M3<M4 (Figure 6.7). The authors found that when the water content/undrained shear strength fit line for the M5 bed (Figure 6.7) was extrapolated to a lower water content (i.e, between 15% and 29%) it yielded a $c_u$-value for this bed higher than the $c_u$-values of the tailings (T1) and tailings/kaolinite beds (M2, M3 and M4). The extrapolation was not shown in Figure 6.7 for easier reading of the plots. A possible explanation for the observed dependence of $c_u$ on the water content is given below. The undrained shear strength, $c_u$, is strongly affected by the intergrain water in the soil, while it remains unaffected by the interlayer water in swelling clay minerals, i.e., montmorillonite (Trauner et al. 2005). The intergrain water, in turn, consists of free pore water and water adsorbed on the external surfaces of clay particles. Thus, the total quantity of adsorbed water increases with increasing clay fraction of the tailing/clay mixtures and with increasing specific surface of the clay minerals. Since Na-montmorillonite (major constituent of bentonite) has the highest specific surface of all clay minerals, i.e., 50 to 120 $m^2/g$ (Mitchell and Soga 2005), it is expected that the tailings/bentonite mixture will correspondingly exhibit

the highest water content. The experimental results confirm this hypothesis. Similar results were reported by Trauner et al. (2005) who investigated the relationship between the water content and the undrained shear strength of various sand/kaolinite and sand/Ca-montmorillonite mixtures. The authors found that at the same water content, $c_u$ of the sand/kaolinite mixtures increased with increasing the percentage of kaolinite, but remained lower than the $c_u$ of the sand/ montmorillonite mixtures with the same sand/clay ratio. Trauner et al. (2005) concluded that the relationship between water content and undrained shear strength was non-linear and dependent primarily on the soil composition and, in particular, on the quantity and mineralogy of the clay fraction.

### *6.3.3. Estimation of the critical shear stress for erosion*

The critical shear stress (threshold) for erosion, $\tau_c$, of the mixed mine tailings/clay beds was estimated using the available and widely accepted formulations listed below. The results of the water content (Figures 6.1a, b and 6.2) measurements for each bed were used as input parameters in the estimation of $\tau_c$.

#### *6.3.3.1. Shields (1936) formulation for noncohesive sediments*

One of the first reliable methods for prediction of $\tau_c$ for noncohesive sediments was proposed by Shields (1936). He used the results of his own experiments as well as those of several other workers in flumes with fully-developed turbulent flows and artificially flattened beds of noncohesive sediments, and introduced a dimensionless shear stress relationship in the following form:

$$\tau_* = \frac{\tau_0}{(\rho_s - \rho)gD} \tag{6.4}$$

where $D$ is taken as the mean size of the sediment (i.e., $D_{50}$), $\tau_0$ is the bed shear stress, $\rho$ and $\rho_s$ are the density of fluid and sediment, respectively, $g$ is the acceleration of gravity, $\tau_*$ is the dimensionless shear stress. On the Shields (1936) diagram (Figure 6.8), the dimensionless shear stress, $\tau_*$, is plotted versus the dimensionless boundary Reynolds number, $R_{e*}$, given by:

$$R_{e*} = \frac{u_* D}{\nu} \tag{6.5}$$

where $u_*$ is the shear velocity, and $\nu$ is the kinematic viscosity of the fluid.

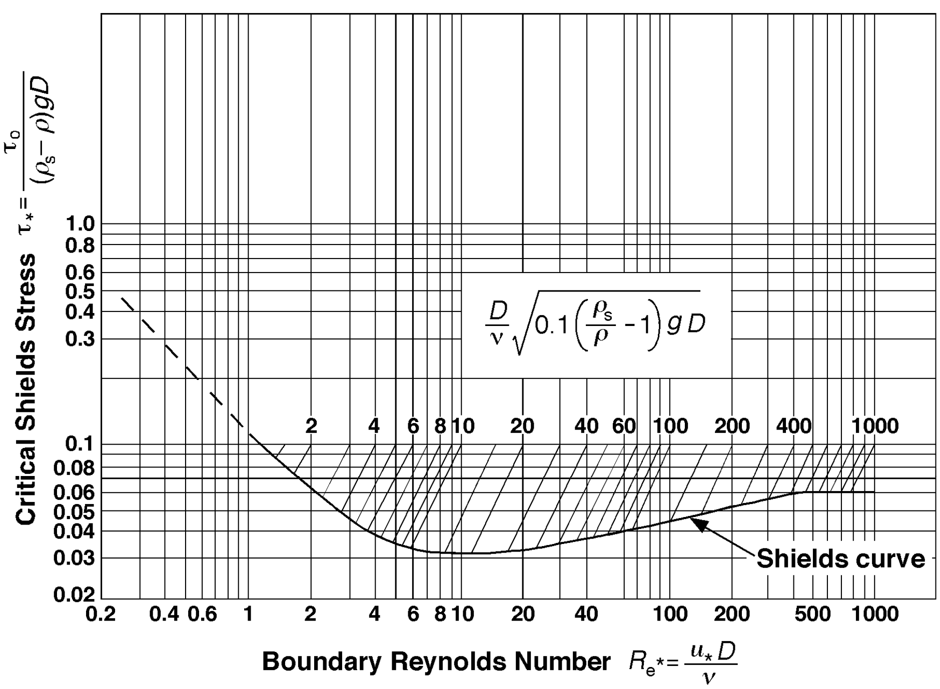


**Figure 6.8.** The Shields diagram.

Eq. (6.4) contains the functional representation of the dimensionless shear stress, $\tau_*$, commonly referred to as the Shields entrainment function. When this function represents the critical (threshold) condition for sediment motion, it is denoted by $\tau_{*c}$ and is called Shields criterion. If the applied bed shear stress corresponds to a point above the Shields curve (Figure 6.8), erosion of particles will occur. Inversely, if the point falls below the curve, the flow will be unable to entrain particles from the bed.

The auxiliary scale in the Shields diagram (Figure 6.8) with lines with positive slopes of 2.0 was included by the American Society of Civil Engineers (ASCE 2006) to facilitate the calculations of $\tau_c$ when the sediment and fluid properties are known. To find $\tau_*$, the value of the parameter $\frac{D}{\nu}\sqrt{0.1\left(\frac{\rho_s}{\rho}-1\right)gD}$ was calculated and this value was located on the auxiliary scale. A line was then drawn through this point parallel to the inclined lines and the value of $\tau_*$ was read at the intersection with the Shields curve from which $\tau_0 = \tau_c$ was calculated.

*6.3.3.2. Amos et al. (1997) formulation for sediments with varying sand/silt/clay fractions*

Amos et al. (1997) identified strong and consistent positive correlation between erosion threshold and wet bulk density of the sediment bed, in the following form:

$$\tau_c = 7.0\times10^{-4}\,\rho_b - 0.47 \qquad (6.6)$$

where $\tau_c$ is the critical shear stress for erosion (erosion threshold) in Pa, and $\rho_b$ is the wet bulk density of sediment bed in kg/m$^3$. According to the authors, the correlation is valid for wet bulk densities from 1000 < $\rho_b$ < 2000 kg/m$^3$ and for sediments with varying sand/silt/clay fractions.

*6.3.3.3. Mitchener and Torfs (1996) formulation for sand/mud mixtures*

For artificially produced mixed (sand/mud) beds, Mitchener and Torfs (1996) proposed an exponential relationship between $\tau_c$ and the sediment bulk density, which takes the form:

$$\tau_c = 0.015(\rho_b - 1000)^{0.73} \tag{6.7}$$

where $\tau_c$ is the critical shear stress for erosion (erosion threshold) in N/m$^2$, and $\rho_b$ is the wet bulk density of the sediment bed in kg/m$^3$.

The theoretical predictions of $\tau_c$ for the investigated beds, based on the above formulations are summarized in Table 6.2.

| Bed characteristics | | | | Shields (1936) | Amos et al. (1997) | Mitchener and Torfs (1996) |
|---|---|---|---|---|---|---|
| Composition | Void ratio, $e$ | Water content, $w$ (%) | Wet bulk density, $\rho_b$ (kg/m$^3$) | $\tau_c$ (Pa) | $\tau_c$ (Pa) | $\tau_c$ (Pa) |
| T1 | 0.52-0.79 | 17.5-26.6 | 2102-2300 | 0.10-0.12 | 1.00-1.14 | 2.50-2.81 |
| M2 | 0.55-0.73 | 18.4-24.6 | 2133-2267 | 0.10-0.11 | 1.02-1.12 | 2.54-2.76 |
| M3 | 0.59-0.74 | 20.0-25.2 | 2117-2224 | 0.09-0.10 | 1.01-1.09 | 2.52-2.69 |
| M4 | 0.64-0.75 | 21.6-25.3 | 2111-2185 | 0.09 | 1.00-1.06 | 2.51-2.63 |
| M5 | 1.03-1.34 | 35.4-46.0 | 1814-1937 | 0.07-0.09 | 0.80-0.89 | 2.00-2.22 |

**Table 6.2.** Estimated values of the critical shear stress for erosion of beds prepared from various tailings/clay mixtures and consolidated for 3 days.

Obtained estimated values of the critical shear stress for erosion, $\tau_c$, were compared with the results from erosion experiments on mine tailings and sand/silt/clay mixtures reported in the literature. For instance, Davé et al. (2003) performed flume experiments to determine the erosion characteristics of hard rock mine tailings deposited under water. The critical shear stress measured for the total mill tailings ($D_{50}$ = 0.15 mm) was 0.16 Pa and it was found to be independent of the particle size distribution, method of deposition, and time for consolidation of the tailings bed. Furthermore, the tailings were observed to behave like a noncohesive material, similar to fine sand and thus, it was concluded that their erosion threshold, $\tau_c$, could be well predicted using the Shields curve and general relationships for noncohesive materials (Davé et al. 2003). Critical shear stress values of 0.12 to 0.17 Pa were reported by Yanful and Catalan (2002) from filed observations of resuspension of base-metal tailings containing 10 - 20% kaolinite. Samad and Yanful (2005) measured a critical shear stress value of 0.09 Pa for gold mine tailings (8 - 10% illite, and 5 - 10% chlorite) in erosion flume experiments. Mian and Yanful

(2003) studied the erosion behaviour of tailings from three sites and concluded that the similar milling process at each site produced tailings of similar nature, characterised by relatively uniformly-sized angular particles that eroded at a similar $\tau_c$. Based on the above studies, the authors of the present paper concluded that the critical stress for erosion of mine tailings (T1) and tailings/kaolinite mixtures (M2, M3 and M4) was best predicted by the Shields (1936) formulation for noncohesive sediments. The Shields (1936) formulation yielded values of $\tau_c$ (Table 6.2) closest to those reported in the literature for mine tailings of similar gradation and composition (i.e., clay content and mineralogy). In contrast, for the same mixtures (T1, M2, M3 and M4) the formulations of Amos et al. (1997) and Mitchener and Torfs (1996) predicted values of $\tau_c$ an order of magnitude higher that those measured in filed and laboratory erosion experiments on mine tailings.

The effect of adding bentonite on the erosion resistance of sand was studied by Mitchener and Torfs (1996), who reported a value of $\tau_c$ of 0.6 Pa for sand with 5% added bentonite. For uniform-size quartz particles ($D_{50}$ = 0.10 mm) with 2% added bentonite, Lick et al. (2004) measured $\tau_c$ within the rage from 0.6 to 0.7 Pa. A comparison between the experimental results reported in the above studies and the predictions of the three formulations summarized in Table 6.2, shows that for the M5 beds Amos et al. (1997) formulation yields a value of $\tau_c$ closest to the measured in the laboratory for similar soils. In contrast, Shields (1936) formulation underpredicts, while Mitchener and Torfs (1996) overpedicts the erosion resistance of the mine tailings/bentonite mixtures (M5).

The variation of the critical shear stress for erosion, $\tau_c$, with depth below surface and wet bulk density in 7 cm-thick mine tailings and tailings/clay beds of various composition is shown in Figures 6.9a and b. The $\tau_c$-values for the tailings and tailings/kaolinite beds (T1, M2, M3 and M4) were obtained using the Shields (1936) diagram (Figure 6.8), whereas those for the tailings/bentonite bed (M5) were calculated from Amos et al. (1997) formulation (Eq. 6.6).

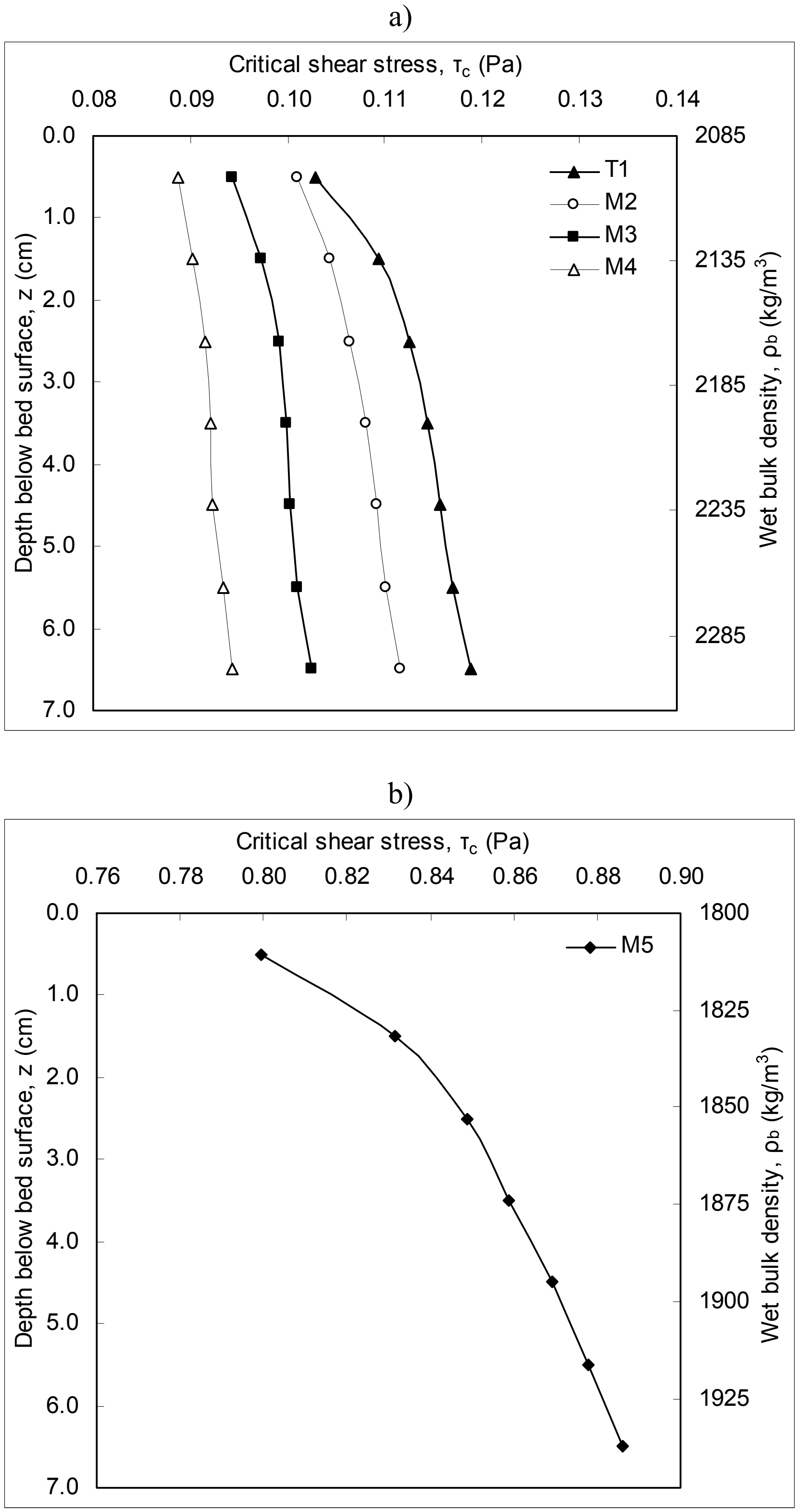


**Figure 6.9.** Variation of the critical shear stress for erosion with depth and wet bulk density for 7 cm-thick beds prepared from: (a) T1, M2, M3 and M4; and (b) M5 mixtures.

From Figures 6.9a and b, it can be seen that in all beds the critical shear stress for erosion (and respectively, the erosion resistance) increases with depth below bed surface and with wet bulk density, which is agreement with the results reported in the literature (e.g., Mitchener and Torfs 1996; Amos et al. 1992, 1997). Lick et al. (2004) noted that at higher densities (and greater depths), the particles within the bed are more closely packed and as a result, less exposed to the fluid flow. Accordingly, the drag and lift forces acting on each individual particle are smaller and the critical shear stress for erosion, $\tau_c$, is higher.

Figures 6.10a and b show the variation of the critical stress for erosion, $\tau_c$, with the water content for 7 cm-thick tailings and tailings/clay beds consolidated for 3 days.

a)

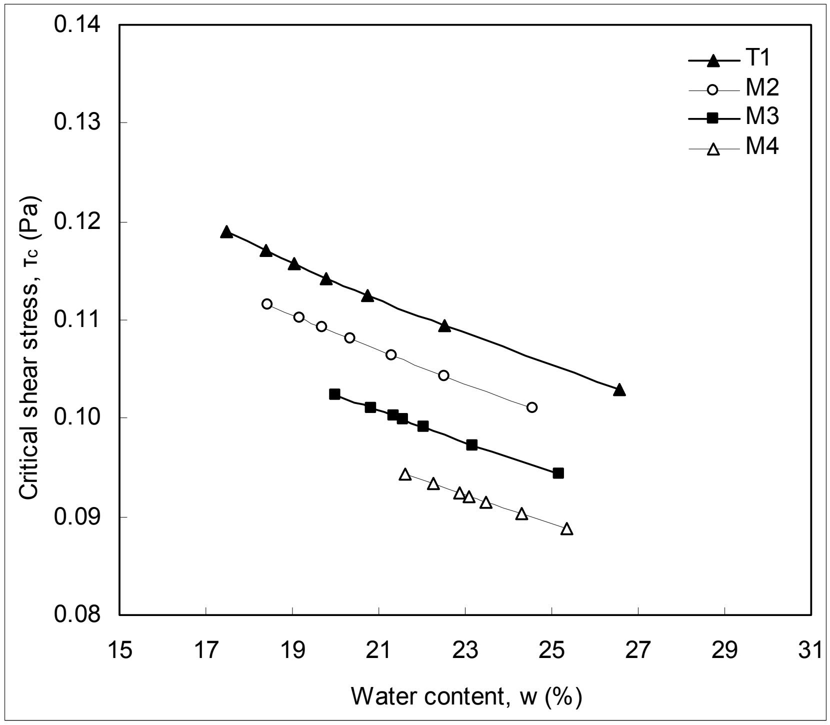


b)

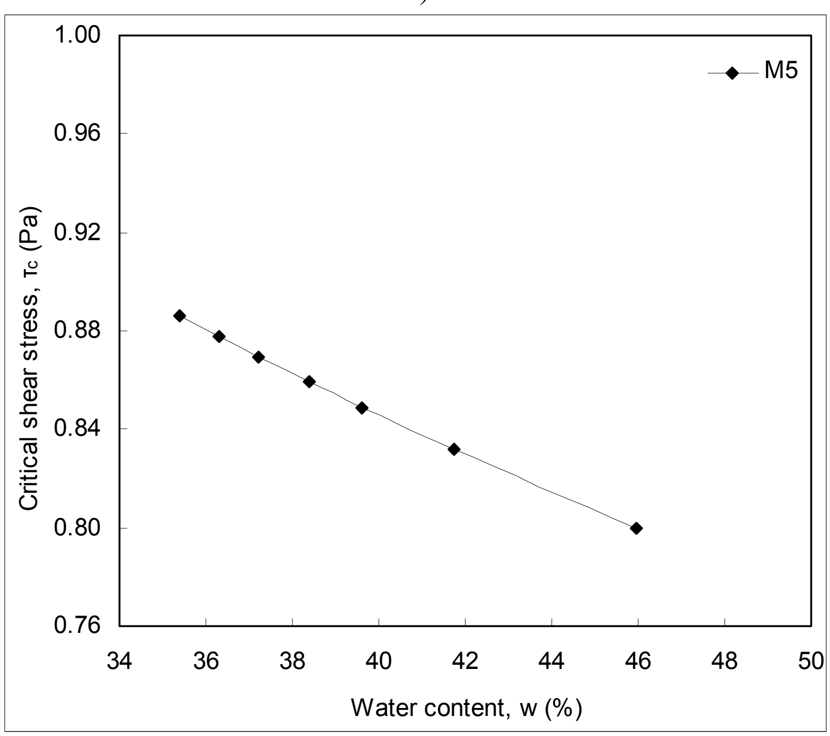


**Figure 6.10.** Variation of the critical shear stress for erosion with water content for 7 cm-thick beds prepared from: (a) T1, M2, M3 and M4; and (b) M5 mixtures.

As evident from Figures 6.10a and b, in all investigated beds $\tau_c$ decreases with increasing water content. The immediate conclusion that can be drawn from these results is that, at a given value of the applied bed shear stress, the bed layers with higher water content will also exhibit higher rate of erosion. Maa et al. (1998) also observed an increase in erosion rate that closely matched the increase in the water content of the cohesive bottom sediments in the Baltimore Harbor. Aberle et al. (2004) reported an increase in erosion resistance with a decrease in the sediment water content and with an increase in dry bulk density. They emphasised that for sand/mud mixtures, the composition of the bed material plays an important role in erosion resistance, in addition to the bulk dry density and water content. Grissinger (1966) found that the effect of water content on the erosion resistance of cohesive soils varied depending upon the dominant clay mineral and upon the orientation of the clay particles in the soil. For the studied tailings and tailings/clay mixtures, the relationship between $\tau_c$ and water content was found to be nonlinear and dependent on the composition of the mixtures, i.e., on the clay content and clay mineralogy (Figures 6.10a and b). Similar observations were made by Fukuda and Lick (1980), who found that a linear increase in sediment water content results in logarithmic increase in the entrainment rate of the sediment.

### *6.3.4. Relationship between the undrained shear strength and the critical threshold for erosion*

To investigate the relationship between the critical shear stress for erosion, $\tau_c$, and the undrained shear strength, $c_u$, for the tested tailings and tailings/clay mixtures, the fall cone experimental results were plotted versus estimated $\tau_c$-values as shown in Figures 6.11a and b.

a)

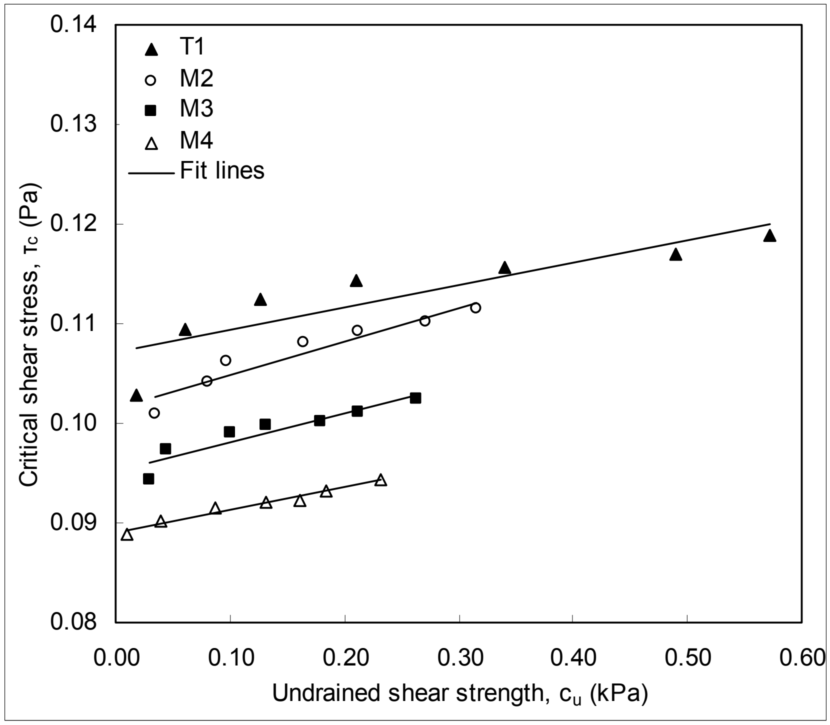


b)

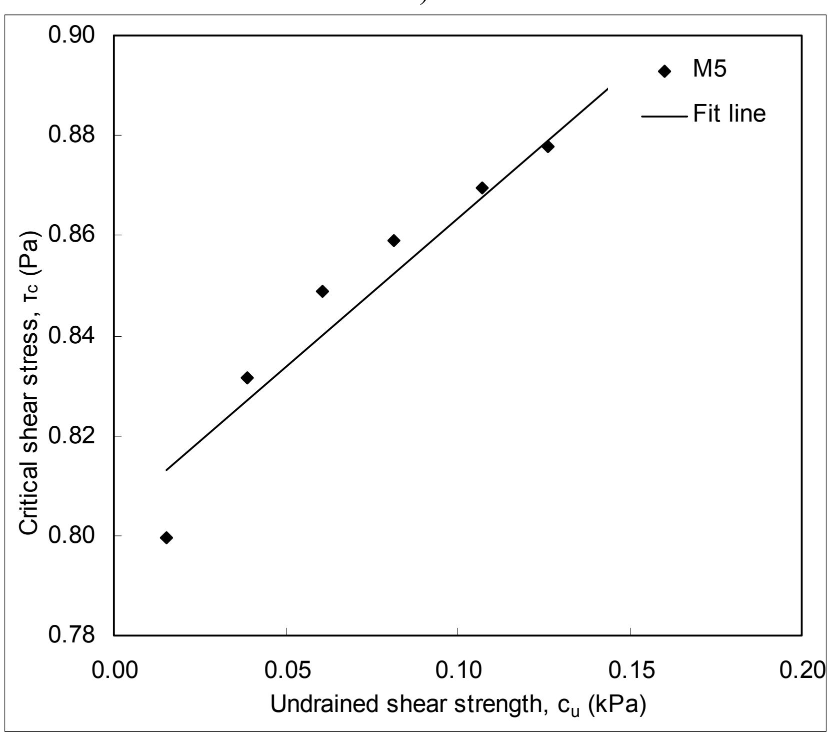


**Figure 6.11.** Critical shear stress for erosion versus undrained shear strength for 7 cm-thick beds prepared from: (a) T1, M2, M3 and M4; and (b) M5 mixtures.

It appeared that the relationship between $\tau_c$ and $c_u$ was linear and given by the following equation:

$$\tau_c = a + b c_u \qquad (6.8)$$

where $\tau_c$ is the critical shear stress for erosion (erosion threshold) in Pa, and $c_u$ is the undrained shear strength in kPa. The coefficients *a* and *b* in Eq. (6.8) were found to be dependent on bed composition. They were calculated by regression analysis and shown along with the correlation coefficients, *R*, in Table 6.3.

| Material | *a* | *b* | *R* |
|---|---|---|---|
| T1 | 0.1071 | 0.0224 | 0.78 |
| M2 | 0.1016 | 0.0336 | 0.91 |
| M3 | 0.0952 | 0.0291 | 0.87 |
| M4 | 0.0890 | 0.0228 | 0.97 |
| M5 | 0.8042 | 0.5923 | 0.93 |

**Table 6.3.** Coefficient values in Eq. (6.8).

Linear correlation between the undrained shear strength (vane) and the critical stress for erosion has also been identified by Amos et al. (1996). They noted that the three orders of magnitude difference between $\tau_c$ and $c_u$ was due to the fact that the former is governed by the strength of the individual bonds between the sediment particles, whereas the latter is provided by the strength of the entire sediment structure. Zreik et al. (1998) elaborated that the undrained shear strength measured using the fall cone method was a macrostructural strength, whereas the resistance against erosion by flowing water, i.e., the erosional strength, was a microstructural strength.

The effect of composition (percentage and mineralogy of the clay fraction) on the erosion resistance of tailings/clay mixtures can be accurately evaluated only if the investigated beds are compared at the same water content. For this purpose, the undrained shear strength of all beds was recalculated using the linear relationship between the logarithm of undrained shear strength and the logarithm of the water content (Eq. 6.3) and the coefficient values given in Table 6.1. For the tailings and tailings/kaolinite beds, the new $c_u$ values were obtained at 0.5% intervals for water contents ranging from 21.5% to 24.5% and plotted versus $\tau_c$ determined from the Shields (1936) diagram (Figure 6.8) as shown in Figure 6.12a. To illustrate the effect of the clay mineralogy, while keeping the percentage of added clay constant, the $c_u$ versus $\tau_c$ plots for the tailings/kaolinite (M2) and tailings/bentonite (M5) beds were compared to those for T1 beds (Figure 6.12b). The new $c_u$ data points in Figure 6.12b were calculated from Eq. (6.3) at 2% intervals for water contents between 38% and 50%. The $\tau_c$-values for the M2 beds (Figure 6.12b) were obtained using the Shields (1936) diagram (Figure 6.8), whereas those for the M5 beds were estimated from Amos et al. (1997) formulation (Eq. 6.6).

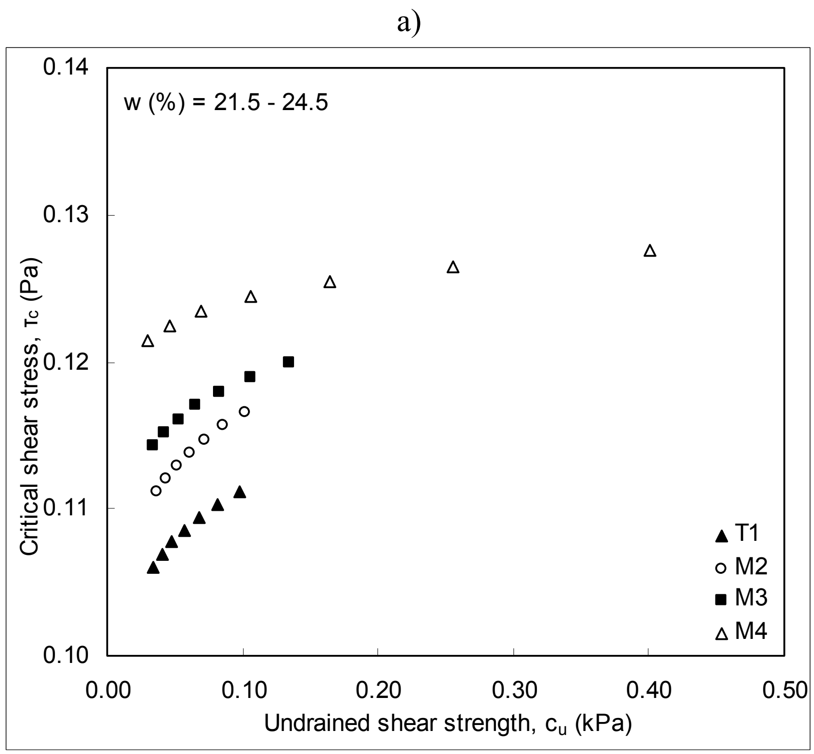


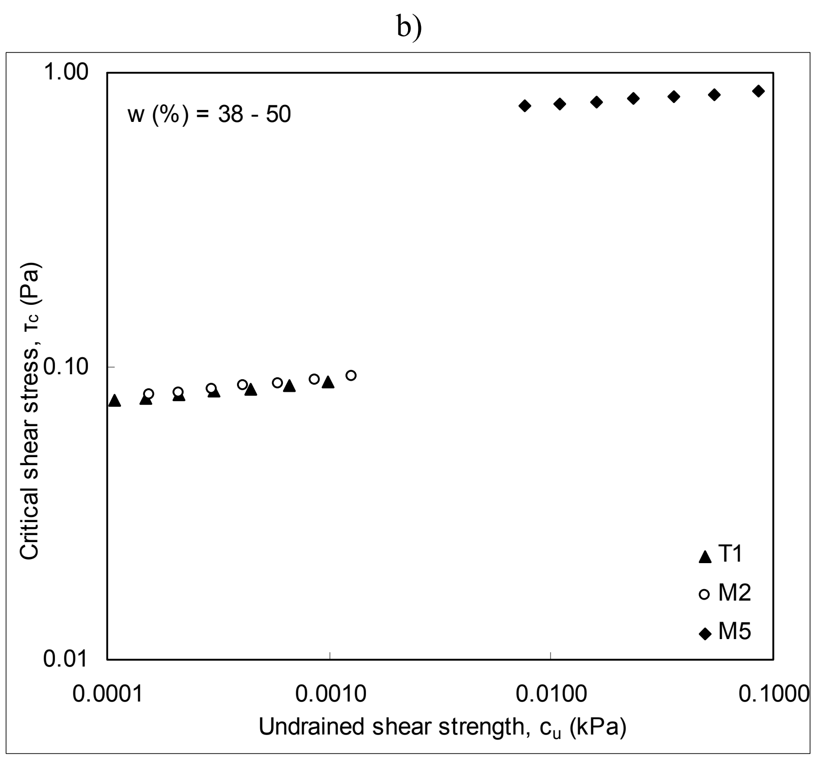


**Figure 6.12.** Critical shear stress for erosion versus recalculated at the same water content values undrained shear strength for 7 cm-thick beds prepared from: (a) T1, M2, M3 and M4; and (b) M5 mixtures.

As can be seen from Figure 6.12a, when the tailings (T1) and tailings/kaolinite beds (M2, M3 and M4) are compared at the same water content, it appears that at a given undrained shear strength, the critical shear stress for erosion increases with increasing kaolinite content in the mixtures in the order T1<M2<M3<M4. Adding 4% kaolinite (M2) or 4% bentonite (M5) to the tailings, both resulted in an overall increase in their erosion resistance, however the effect of adding bentonite was much more pronounced than that of kaolinite (Figure 6.12b). For instance, when compared to the T1 bed, the M2 bed (4% kaolinite) exhibited an increase in $\tau_c$ of 0.1 Pa, whereas for the M5 bed (4% bentonite) the increase in $\tau_c$ was nearly an order of magnitude (Figure 6.12b). Obtained results correlate well with those reported by Mitchener and Torfs (1996) who found that the erosion resistance of a sandy bed increased with adding clay, but the rate of increase varied for the different types of cohesive material. Mitchener and Torfs (1996) proposed the hypothesis that the increased erosion resistance of mixed sand/mud sediments above a given mud percentage was due to the smoothing of the sand surface in the presence of mud, and to the fine mud particles forming a network structure around the sand grains, thus increasing the cohesiveness of the mixture. Kamphius and Hall (1983) and Kamphius (1990) demonstrated that the capability of a cohesive soil to resist erosion increased with clay content and plasticity index, which can explain why in the present study, the erosion resistance of the more plastic M5 mixture was found to be greater than that of the nonplastic T1, M2, M3 and M4 mixtures. Grissinger (1966) reported that adding sodium montmorillonite to a silt loam soil greatly improved the resistance of the mixture to erosion by flowing water. Lick and McNeil (2001) and Lick et al. (2004) attributed the observed increased erosion resistance of quartz/clay mixtures with adding

bentonite to an additional force (different than the cohesive force) due to the binding of quartz particles by bentonite coatings formed on their surface.

## 6.4. Summary and Conclusions

Artificial mine tailings/kaolinite and mine tailings/bentonite mixtures with varying percentage of the clay-size fraction but with constant sand/silt ratio were prepared in the laboratory. Distilled water was added to the mixtures to obtain slurries with moderate concentration (16% by volume), from which deposited beds with final thicknesses between 4 and 10 cm were obtained by sedimentation. The beds comprised two portions: a lower layer of uniformly distributed coarse particles, and a capping layer of fines. This bed configuration was sought because the lower permeability of the capping layer was believed to minimize drainage from the beds during testing and thus, ensure that undrained conditions are maintained. The undrained shear strength of beds, consolidated for 3 days prior to each experiment, was obtained using the Automated fall cone device at depth intervals of 1 cm within the beds. Water content profiles of the tested beds were also developed by making water content measurements at each horizon where undrained shear strength testing was performed. The critical shear stress (threshold) for erosion of the mixed tailings/clay beds was estimated using the Shields (1936) diagram for the tailings and tailings/kaolinite beds, and Amos et al. (1997) formulation for the tailings/bentonite beds. The main findings of the study are summarized below:

- In all tested beds, the water content and the void ratio decreased with depth below the bed surface. At the same percentage of added clay, the effect of bentonite on both quantities was much more pronounced than that of kaolinite.

- The undrained shear strength increased with depth in all tested beds, which was attributed to the corresponding water content decrease and effective stress increase. At a given depth, the largest undrained strength was observed in pure tailings beds and decreased with clay content increase in the tailings/kaolinite beds. The smallest undrained strength was recorded in the tailings/bentonite beds.
- The critical shear stress for erosion of the mine tailings and mine tailings/kaolinite mixtures was estimated using the Shields (1936) diagram, which yielded values of $\tau_c$ closest to the reported in the literature for soils of the same composition and gradation. For the mine tailings/bentonite mixtures, the formulation proposed by Amos et al. (1997) was found to predict $\tau_c$-values that best reflected the published laboratory results. Thus, the critical shear stress for erosion of the tailings/kaolinite mixtures was estimated to vary between 0.09 and 0.12 Pa, whereas that for tailings/bentonite mixtures was in the range 0.80 to 0.89 Pa.
- In all beds, the critical shear stress for erosion increased with depth below bed surface in response to density and undrained shear strength increase.
- The relationship between the undrained shear strength and the erosion resistance, expressed by the critical threshold for erosion, was found to be linear. The parameters of the linear function depended on bed composition, and in particular, on the percentage and mineralogy of the clay-size fraction.
- The three orders of magnitude difference between the undrained shear strength and the critical stress for erosion was attributed to the different measuring techniques employed in the shear and erosional strength measurements, whereby the former

measured macrostructural strength whereas the latter measured microstructural strength.

## 6.5. Acknowledgements

This work was supported by funding from the Natural Sciences and Engineering Research Council of Canada (NSERC) in the form of an Individual Discovery Grant awarded to E.K. Yanful and a postgraduate scholarship awarded to R.S. Dimitrova.

## 6.6. References

Aberle J, Nikora V, Walters R (2004) Effects of bed material properties on cohesive sediment erosion. Marine Geology, 207:83-93.

ASTM, Standard D 4253-00 (2006a) Standard test methods for maximum index density and unit weight of soils using a vibratory table. American Society for Testing and Materials, Philadelphia, Pasadena, USA.

ASTM, Standard D 4254-00 (2006b) Standard test methods for minimum index density and unit weight of soils and calculation of relative density. American Society for Testing and Materials, Philadelphia, Pasadena, USA.

American Society of Civil Engineers (2006) Sedimentation Engineering, Vito A. Vanoni (ed.), ASCE Task Committee for the preparation of the Manual on Sedimentation, Sedimentation Committee, Hydraulics Division, ASCE Manuals and Reports on Engineering Practice N54, Reston, Virginia, USA.

Amos CL, Christian HA, Grant J, Paterson DM (1992) A comparison of in situ and laboratory methods to measure mudflat erodibility. In: Proceedings of the 2nd International Conference on Hydraulic and Environmental Modelling of Coastal, Estuarine and River Waters. Falconer RA, Chandler-White SN, Liu SQ (eds.), Vol. 1, pp. 325-336.

Amos CL, Feeney T, Sutherland TF, Luternauer JL (1997) The stability of fine-grained sediments from the Fraser River delta. Estuarine, Coastal and Shelf Science, 45:507–524.

Amos CL, Sutherland TF, Zevenhuizen J (1996) The stability of sublittoral, fine-grained sediments in a subarctic estuary. Sedimentology, 43:1-19.

Annandale GW (1995) Erodibility. Journal of Hydraulic Research, 33(4):471-494.

Aubertin M, Ricard JF, Chapuis RP (1998) A predictive model for the water retention curve: application to tailings from hard-rock mines. Canadian Geotechnical Journal, 35: 55-69.

Berlamont J, Ockenden M, Toorman E, Winterwerp J (1993) The characterisation of cohesive sediment properties. Coastal Engineering, 21:105-128.

Bromwell LG, Raden DJ (1979) Disposal of phosphate mining wastes. In: Current Geotechnical Practice in Mine Waste Disposal, Committee on Embankment Dams and Slopes of Geotechnical Engineering Division, American Society of Civil Engineers, New York, USA, pp. 88-112.

Carraro JAH, Prezzi M, Salgado R (2009) Shear strength and stiffness of sands containing plastic or nonplastic fines. Journal of Geotechnical and Geoenvironmental Engineering, 135(9):1167–1178.

Davé NK, Krishnappan BG, Davies M, Reid I, Lanteigne L (2003) Erosion characteristics of underwater deposited mine tailings. Open presentations, Mining and the Environment International Conference, Laurentian University, Sudbury, Ontario, 25–28 May 2003.

Davies R (1968) The experimental study of the differential settling of particles in suspension at high concentrations. Powder Technology, 2(1):43-51.

Di Maio C, Santoli L, Schiavone P (2004) Volume change behavior of clays: the influence of mineral composition, pore fluid composition and stress state. Mechanics of Materials, 36: 435–451.

Dyer KR (1986) Coastal and estuarine sediment dynamics. John Wiley & Sons Ltd., Chichester, UK.

Feng TW (2002) Discussion of "Percussion and cone methods of determining the liquid limit of soils: Controlling mechanisms." by A. Sridharan and K. Prakash. Geotechnical Testing Journal, 25(1):104-105.

Fukuda MK, Lick W (1980) The entrainment of cohesive sediments in freshwater. Journal of Geophysical Research, 85(C5):2813–2824.

Grissinger EH (1966) Resistance of selected clay systems to erosion by water. Water Resources Research, 2(1):131-138.

Hansbo S (1957) A new approach to determination of the shear strength of clay by the fall cone test. In: Proceedings of the Royal Swedish Geotechnical Institute, Stockholm, Sweden, Publication No.14, pp. 7-47.

Houwing EJ (1999) Determination of the critical erosion threshold of cohesive sediments on intertidal mudflats along the Dutch Wadden Sea Coast. Estuarine, Coastal and Shelf Science, 49: 545–555.

Kamphius JW (1990) Influence of Sand or Gravel on the Erosion of Cohesive Sediment. Journal of Hydraulic Research, 28(1): 43-53.

Kamphuis JW, Hall KR (1983) Cohesive Material Erosion by Unidirectional Current. Journal of Hydraulic Engineering, 109(1): 49- 61.

Ladd CC, Foott R (1974) New design procedure for stability of soft clays. ASCE Journal of the Geotechnical Engineering Division, 100(GT7):763-786.

Lavelle JW, Mofjeld HO (1987) Do critical stresses for incipient motion and erosion really exist. Journal of Hydraulic Engineering, 113(3):370-385.

Le Hir P, Cann P, Waeles B, Jestin H (2008) Erodibility of natural sediments: experiments on sand/mud mixtures fro laboratory and field erosion tests. In:

Proceedings in Marine Science, Sediment and Ecohydraulics – INTERCOH 2005, Vol. 9, pp. 137-153.

Lick W, Jin L, Gailani J (2004) Initiation of movement of quartz particles. Journal of Hydraulic Engineering, 130(8):755-761.

Lick W, McNeil J (2001) Effects of sediment bulk properties on erosion rates. The Science of the Total Environment, 266:41-48.

Maa JPY, Kim SC (2002) A constant erosion rate model for fine sediment in the York River, Virginia. Environmental Fluid Mechanics, 1(4):345-360.

Maa JPY, Sanford L, Halka JP (1998) Sediment resuspension characteristics in Baltimore Harbor, Maryland. Marine Geology, 146:137-145.

Mantz PA (1980) Low sediment transport rates over flat beds. ASCE Journal of the Hydraulics Division, 106:1173-1190.

McGregor RG, Blowes DW, Jambor JL, Robertson WD (1998) Mobilization and attenuation of heavy metals within a nickel mine tailings impoundment near Sudbury, Ontario, Canada. Environmental Geology, 36(3/4):305-319.

Mehta AJ, Hayter EJ, Parker ER, Krone RB, Teeter AM (1989) Cohesive Sediment Transport I: Process Description. Journal of Hydraulic Engineering, 115(8):076-1093.

Mesri G (1975) Discussion of "New design procedure for stability of soft clays." by Ladd CC and Foott R. ASCE Journal of the Geotechnical Engineering Division, 101( NGT4):409-412.

Mian MH, Yanful EK (2003) Tailings erosion and resuspension in two mine tailings ponds due to wind waves. Advances in Environmental Research, 7(4):745-765.

Mian MH, Yanful EK, Martinuzzi R (2007) Measuring the onset of mine tailings erosion. Canadian Geotechnical Journal, 44(4):473-489.

Miller MC, McCave IN, Komar PD (1977) Threshold of sediment motion under unidirectional currents. Sedimentology, 24:507-527.

Mitchell JK, Soga K (2005) Fundamentals of Soil Behavior, 3rd edn, John Wiley & Sons Inc., Hoboken, New Jersey, USA.

Mitchener H, Torfs H (1996) Erosion of mud/sand mixtures. Coastal Engineering, 29:1-25.

Panagiotopoulos I, Voulgaris G, Collins MB (1997) The influence of clay on the threshold of movement of fine sandy beds. Coastal Engineering, 32:19-43.

Parchure TM, Mehta AJ (1985) Erosion of soft cohesive sediment deposits. ASCE Journal of Hydraulic Engineering, 111(10):1308-1326.

Rankine KJ, Sivakugan N, Cowling R (2006). Emplaced geotechnical characteristics of hydraulic fills in a number of Australian mines. Geotechnical and Geological Engineering, 24(1):1-14.

Raudkivi AJ (1998) Loose Boundary Hydraulics. A.A. Balkema, Rotterdam, The Netherlands.

Reddi LN, Bonala MVS (1997) Critical shear stress and its relationship with cohesion for sand-kaolinite mixtures. Canadian Geotechnical Journal, 34:26-33.

Roberts J, Jepsen R, Gotthard D, Lick W (1998) Effects of particle size and bulk density on erosion of quartz particles. Journal of Hydraulic Engineering, 124(12):1261-1267.

Samad MA, Yanful EK (2005) A design approach for selecting the optimum water cover depth for subaqueous disposal of sulfide mine tailings. Canadian Geotechnical Journal, 42:207-228.

Sharma B, Bora PK (2003) Plastic limit, liquid limit and undrained shear strength of soil - reappraisal. Journal of Geotechnical and Geoenvironmental Engineering, 129(8):774–777.

Shaw SC, Groat LA, Jambor JL, Blowes DW, Hanton-Fong CJ, Stuparyk RA (1998) Mineralogical study of base metal tailings with various sulfide contents, oxidized in laboratory columns and field lysimeters. Environmental Geology, 33(2/3):209-217.

Shields A (1936) Anwendung der Aehnlichkeitsmechanik und der turbulenzforschung auf die Geschiebebewegung. Mitteilungen Preussischen Versuchsanstalt fur Wasserbau und Schiffbau, Berlin, 26. English translation: Application of Similarity Principles and Turbulence Research to Bed-load Movement. W.M. Keck Laboratory of Hydraulics and Water Resources, California Institute of Technology, Report 167, pp. 43.

Skempton AW (1953) The colloidal activity of clays. In: Proceedings of the 3rd International Coference on Soil Mechanics and Foundation Engineering, Zurich, Vol. I, pp. 57-61.

Thevanayagam S (1998) Effect of fines and confining stress on undrained shear strength of silty sands. Journal of Geotechnical and Geoenvironmental Engineering, 124(6):479-491.

Tolhurst TJ, Black KS, Paterson DM, Mitchener HJ, Termaat GR, Shayler SA (2000) A comparison and measurement standardisation of four in situ devices for determining the erosion shear stress of intertidal sediments. Continental Shelf Research, 20:1397-1418.

Torfs H, Mitchener H, Huysentruyt H, Toorman E (1996) Settling and consolidation of sand/mud mixtures. Coastal engineering, 29:27-45.

Trauner L, Dolinar B, Mišič M. (2005) Relationship between the undrained shear strength, water content, and mineralogical properties of fine-grained soils. International Journal of Geomechanics, 5(4): 350–355.

Umehara Y, Zen K, Hamada K (1985) Evaluation of soil liquefaction potentials in partially drained conditions, Soils and Foundations, 25(2):57-72.

Van Ledden M, van Kesteren WGM, Winterwerp JC (2004) A conceptual framework for the erosion behaviour of sand–mud mixtures. Continental Shelf Research, 24:1–11.

Vick SG (1990) Planning, analysis, and design of tailings dams. 2nd edn. BiTech Publishers, Vancouver, B.C., Canada.

White SJ (1970) Plane bed thresholds of fine-grained sediments. Nature, 228:152-153.

Yanful EK, Catalan LJJ (2002) Predicted and Field-Measured Resuspension of Flooded Mine Tailings. Journal of Environmental Engineering, 128(4):341-351.

Zreik DA, Krishnappan BG, Germaine JT, Madsen OS, Ladd CC (1998) Erosional and mechanical strengths of deposited cohesive sediments. Journal of Hydraulic Engineering, 124(11):1076-1085.

# CHAPTER 7. SUMMARY AND CONCLUSIONS

A comprehensive characterization of mine tailings and mine tailings/clay mixtures for engineering purposes was undertaken. The drainage conditions and stress range relevant to those in the tailings management facilities were considered and simulated as closely as possible in the laboratory environment. The main findings of the research are summarized below.

- In the laboratory prepared tailings/water slurries with moderate to high concentration of solids, tailings particles settled in the conditions of hindered settling. Performed calculations proved that wall effect had negligible influence on the settling velocity of the particles in the slurries. Sedimentation and consolidation experiments with and without pore pressure measurements demonstrated that the primary consolidation of pure tailings was complete in approximately one hour and all excess pore water pressure generated during sedimentation was fully dissipated at the end of this period. No measurable volume changes occurred in the deposited tailings beds during secondary compression.
- The sedimentation of tailings beds from slurries with moderate concentration resulted in formation of deposits comprising two portions: i) a relatively ungraded thick bottom layer, and ii) a thin capping layer of fines. The latter layer suppressed drainage through the bed surface, and along with the rapid rate of load application, ensured that truly undrained conditions were maintained during the fall cone testing. When the beds were sedimented from slurries with high concentration of solids (50% by volume) obtained deposits were relatively homogeneous with minimum property variation with depth.

- Undrained shear strength profiles with depth within the tailings deposits were obtained using an automated fall cone device at depth intervals of 1 cm. It was believed that undrained friction as opposed to undrained cohesion provided the main contribution to the measured undrained shear strength during fall cone testing. Obtained results showed that the undrained shear strength increased, whereas the water content decreased with depth within the tailings beds. In the effective stress range below 1.2 kPa and for water contents between 17% and 27%, the measured undrained shear strength varied between 0.01 and 0.98 kPa, with the lower strength values measured at the bed surface and the high values associated with greater depths within the deposits. The test results demonstrated that the primary factor controlling the undrained shear strength within the tailings beds was the vertical effective stress, whereas the water content had measurable but secondary effect.
- Drained and partially drained shearing conditions were simulated by varying the rate of loading in a specially built Tilting Tank. The excess pore water pressure (PWP) measurements indicated that when the tilting rate was rapid (1.61°/min), measurable excess PWP built up within the deposited beds, and because volume changes were not prevented, bed failure occurred under partially drained conditions. When the rate of loading was sufficiently slow (i.e., 0.07°/min), the excess PWP remained an order of magnitude lower than the normal effective stress at the respective depths and thus, the shearing was under drained conditions.
- Failure of the bed slope within the Tilting Tank always occurred along a failure plane parallel to the bottom of the Tank, located at 0.4 to 1.5 cm from the surface of the deposit. At failure, the structure of the soil mass above the failure plane was

completely destroyed and liquefied tailings propagated like a dense liquid to the bottom of the Tank. Observed flow-like behaviour of tailings during failure was attributed to the rapid generation of excess PWP at a given horizon within the bed, which at some point, became equal to the normal effective stress at this horizon.

- Linear drained (effective) and partially drained (total) shear strength envelopes with zero cohesion intercept were defined over the normal stress range of 0 to approximately 1 kPa, which was much lower than the stresses utilized in conventional geotechnical testing equipment. The effective friction angle, $\phi'$, of the pure tailings was found to be between 40.4° and 40.8° for beds consolidated for 3 and 12 days, respectively. The total friction angle, $\phi_T$, was always lower than $\phi'$ and ranged from 23.3° to 23.8°.
- The effect of clay content and clay mineralogy on the engineering properties of mine tailings was investigated by testing artificial mine tailings/clay mixtures. The mixtures were prepared in the laboratory by adding kaolinite or bentonite to the original hard-rock mine tailings. As the water in soils is entirely associated with the clay-size fraction, increasing the clay content of the mixtures produced a corresponding increase in their liquid limit, $w_L$. Adding up to 12% kaolinite to pure mine tailings did not result in development of plasticity, whereas addition of only 4% bentonite gave the tailings/bentonite mixtures some low but measurable plasticity.
- The mixed tailings/clay deposits obtained through sedimentation from slurries with high concentration were relatively ungraded. The void ratio, $e$, of the beds generally increased with increasing clay content of the mixtures, but at the same percentage of added clay, bentonite, due to its expansive character, produced deposits with void

ratios twice as high as kaolinite. Time for primary consolidation varied depending on the quantity of added clay and clay mineralogy; that is, for the tailings/kaolinite mixtures it increased with increasing percentage of clay, but remained shorter in comparison to the tailings/bentonite mixtures. This variation was attributed to the effect of clay on the properties of the mixtures, whereby kaolinite only slightly reduced the permeability of the original tailings, whereas addition of bentonite brought about a significant reduction in their hydraulic conductivity.

- During shearing, the tailings/kaolinite beds experienced some degree of pore water pressure dissipation through drainage from the surface, which increased with decreasing kaolinite content of the beds. In contrast, adding bentonite to tailings significantly reduced the permeability of the deposits and thus, suppressed pore water dissipation during shearing. As a result, excess PWP distribution within the tailings/bentonite beds was relatively uniform.
- Similarly to the pure tailings, drained and partially drained shear strength testing in the Tilting Tank was performed on mixed tailings/clay beds. During slow tilting the excess PWP at each monitored horizon within the mixed beds remained at least an order of magnitude lower than the respective normal effective stress at the same horizon. Failure under drained conditions occurred when the shear stress exceeded the shear strength of the bed at a given depth. Shear-induced excess pore water pressure during rapid tilting of mixed beds was comparable with the normal effective stress at the respective elevations within the beds, and thus it affected their shear strength. Full loss of strength and disintegrative failure was triggered when the excess pore pressure became equal to the normal effective stress at a given depth

within the beds. The failure plane in the mixed beds was parallel to the bottom of the Tank, but located deeper than that in the pure tailings beds, i.e., at 0.4 to 2.5 cm from the bed surface.

- Linear drained and partially drained strength envelopes of the tested mixtures with zero cohesion intercept were defined. It was observed that both drained (effective), $\phi'$, and partially drained (total), $\phi_T$, friction angles decreased with increasing clay content in the mixtures, but bentonite was much more effective in reducing $\phi'$ and $\phi_T$ than kaolinite. By comparing the intergranular (or skeleton) void ratio of the whole tailings with the maximum void ratio of the tailings sand (coarse fraction only), it was determined that the quantity of fine material in the original tailings was sufficient to fully occupy the void spaces between the sand particles and they were essentially floating within the fines matrix. Adding clay to the tailings further increased the distance between the sand grains, which was manifested in a corresponding decrease in the frictional resistance of the mixtures and reduced shear strength. The excess PWP induced in the mixed beds during rapid tilting lead to earlier slope failure in comparison to slow tilting, and respectively $\phi_T$ remained always lower than $\phi'$.
- Varying the time for consolidation of the deposits of pure tailings did not seem to lead to a measurable mechanical strength gain which was attributed to a lack of thixotropic effects in the coarse grained and noncohesive mine tailings. Similarly, in the tailings/kaolinite mixtures, increasing bed age did not bring any measurable strength gain. Increasing the time for consolidation of tailings/bentonite beds from 3 to 12 days, however, resulted in 2.1° degrees gain in frictional resistance, which was

interpreted as evidence of some thixotropic rearrangement of soil structure in these deposits during secondary compression.

- Mixed tailings/clay beds were also deposited from slurries with moderate concentration to obtain ungraded deposits capped with a layer of fines. It was found that in the beds consolidated for 3 days the water content and void ratio decreased whereas the undrained shear strength and effective stress increased with depth below bed surface. At a given depth, the highest undrained strength was observed in pure tailings beds. In the tailings/kaolinite beds the undrained shear strength decreased with kaolinite content, but remained higher than the tailings/bentonite beds, which exhibited the lowest measured strength. The relationship between the logarithm of the undrained shear strength and logarithm of the water content of the tested mixtures was found to be linear with parameters varying with the composition of the mixtures.
- The resistance against erosion of the tailings/clay mixtures, expressed through their critical stress for erosion, was estimated using existing formulations for noncohesive sediments and sediment mixtures. A comparison of obtained results with erosion threshold values published in the literature demonstrated that for the pure mine tailings and tailings/kaolinite mixtures the Shields (1936) diagram best predicted the erosion resistance. In contrast, for the tailings/bentonite mixtures the formulation proposed by Amos et al. (1997) yielded values of the critical shear stress for erosion that were closest to the published laboratory results on mine tailings. Thus, the critical shear stress for erosion of the tailings/kaolinite mixtures was estimated to vary between 0.09 and 0.12 Pa, whereas that for tailings/bentonite mixtures was in the range of 0.80 to 0.89 Pa.

- As a direct consequence of the density and undrained shear strength increase with depth recorded in all tested beds, the critical shear stress for erosion also increased with depth. A linear relationship was established between the undrained shear strength and the critical shear stress for erosion, the parameters of which depended on the composition of the bed, and more specifically, on the percentage and mineralogy of the clay fraction. It was hypothesized that the undrained shear strength of the mixtures was a measure of the macrostructural strength, whereas the erosion resistance was a measure of their microstructural strength. The difference in the measuring techniques was proposed as an explanation for the observed three orders of magnitude difference between undrained shear and erosional strength of the mixtures.

The outcome of the research described in the present thesis provided better understanding of the fundamental nature of mine tailings and their properties relevant to engineering applications. It should be noted, however, that the selected tailings material ($D_{50}$ = 0.12 mm) appears coarser compared to tailings from other sources. However, such coarse tailings are representative of the material stored at the Sudbury tailings area and are not unusual for copper and nickel tailings, in general. Therefore, although the results of our study may not apply to finer cohesive tailings, they still provide useful information for many sites that store coarser hard-rock tailings or for applications that involve tailings sands. The investigation of the strength behaviour and failure modes of mine tailings in the ultra low stress range and under various degrees of drainage provides key parameters (e.g., drained and undrained shear strength, void ratio, specific gravity, plasticity parameters, water content) for the existing slope stability models for tailings embankments. A better understanding of the sedimentation, self-weight consolidation and erosion processes as related to mine tailings deposited under water is expected to improve the accuracy of erosion and transport predictive models. For instance, capturing the variation of geotechnical properties with depth within the deposits reflects the fact that erosion of such deposits occurs in discrete steps and layers and thus, the properties of each individual layer are required for accurate modelling of the erosion process. The validity of the research is extended to incorporate tailings/clay mixtures with varying percentage and mineralogy of the clay fraction. The experimental methods proposed to measure the extremely low mechanical strength of deposited mixed tailings/clay beds in their structured state closely simulating the conditions in the tailings pond had not been applied to tailings deposits previously. Test results can facilitate the interpretation of the behaviour of other saturated tailings or tailings/clay mixtures. Correlation of mechanical strength of mine tailings and mixtures with their erosional resistance expressed with the critical shear stress for erosion serves a number of purposes: i) provides an empirical formulation to predict the erosion resistance of tailings deposits with various compositions from knowledge of their mechanical (undrained) strength; (ii) improves the understanding of the effect of clay content and mineralogy on the erosional strength of mine tailings; and (iii) helps establish a basis for comparison of the erosion resistance of tailings deposits of various composition. To be able to predict the erosional strength of mine tailings under water is a matter of a great environmental importance as tailings erosion and resuspension into the water column could compromise suspended solids discharge criteria, and increase the overall sulphide oxidation, thus creating conditions for formation of acid mine drainage.

# CHAPTER 8. RECOMMENDATIONS FOR FURTHER RESEARCH

The research work presented in this thesis, a1though comprehensive in its development, leaves room for further improvement before a predictive erosion model can be developed for mine tailings under environmental loading. Further research efforts can focus on the following topics:

- The engineering properties of cohesive mine tailings containing an appreciable (greater than 50%) amount of fines need to be investigated and the fundamental differences between the mechanical and erosional behaviour of noncohesive and cohesive tailings need to be outlined. The effect of clay mineralogy on the tailings characteristics can be further studied by using other clay minerals as additives.
- Additional experimental work on sedimentation of mine tailings from suspensions with low concentration of solids and property variation in the resulting highly graded tailings deposits would complement the present study that dealt with suspensions of moderate or high concentrations. The effect of particle gradation with depth on the erosional strength and mode of erosion of sedimented tailings deposits should also be investigated.
- The automated fall cone device utilized in the present research would greatly benefit from a pore pressure transducer mounted at the tip of the cone as it would provide an indication of the excess pore water pressure that develops within the soil at the time of failure as well as additional reassurance that soil failure occurs under truly undrained conditions.
- The proposed linear relationship between undrained shear and erosional strength of mine tailings needs to be validated with comprehensive laboratory experiments that

encompass both cohesive and noncohesive mine tailings. The possibility to estimate the critical stress for erosion of mine tailings and tailings/clay mixtures from other geotechnical properties, such as density or water content, should also be thoroughly investigated.

- All tested beds in the present study were self-weight consolidated and as such, were relatively loose and with high void ratio and water content. It would be interesting to study the strength behaviour of deposits that have been preconsolidated to various pressures and identify any differences that solely are due to the degree of consolidation.

# APPENDIX A

This appendix contains additional information pertinent to Chapter 3 of the thesis. It includes the results of undrained shear strength testing using the Automated fall cone device on tailings beds consolidated for 6, 18 and 46 days.

a)

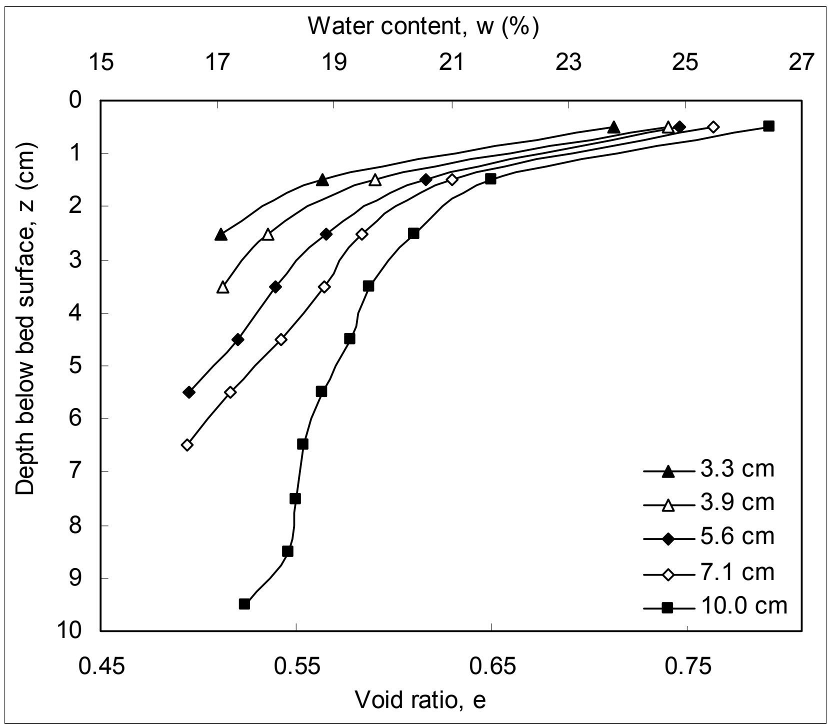

b)

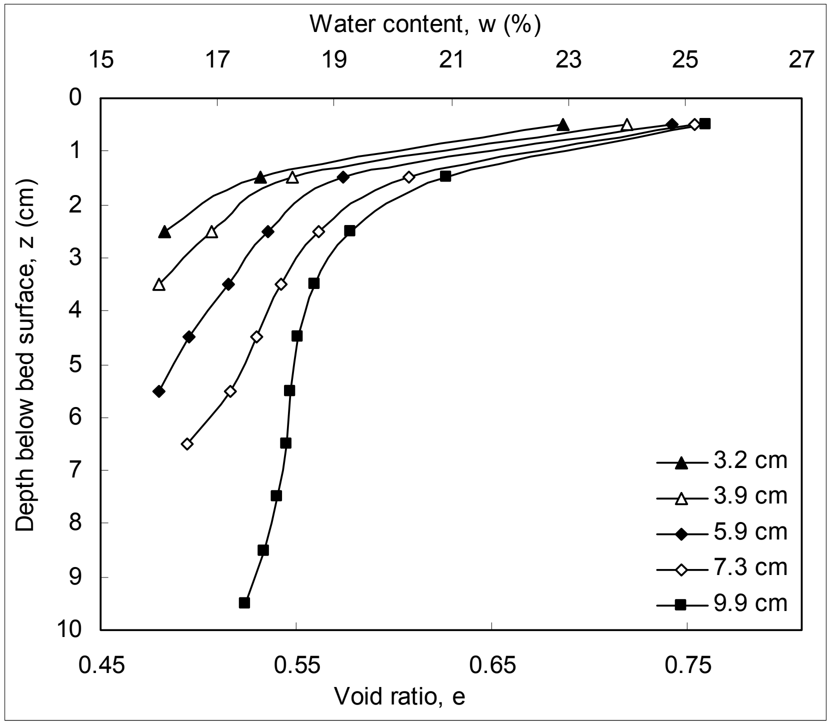


c)

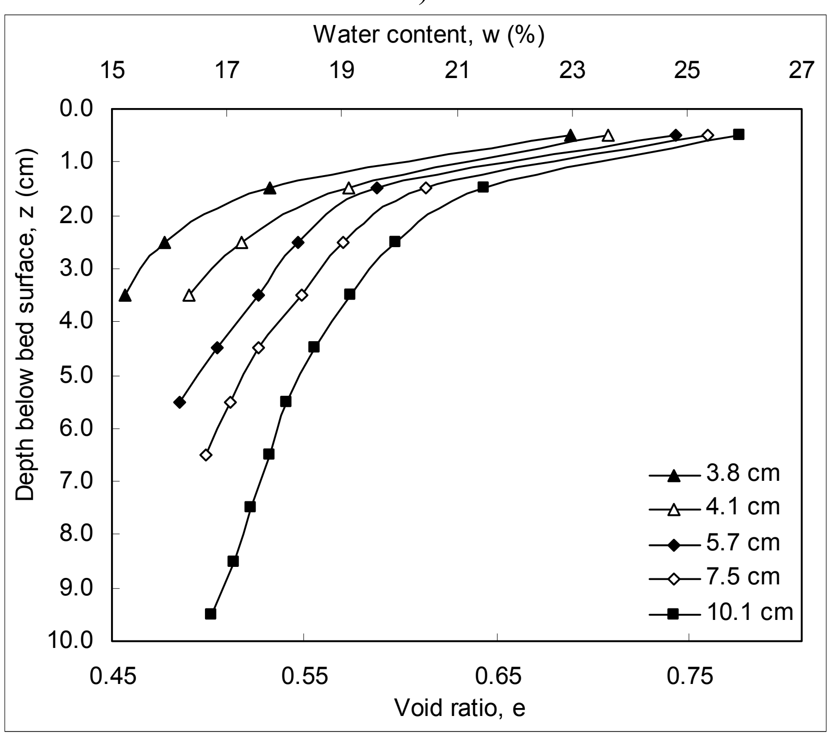


**Figure A.1.** Water content profiles of mine tailings beds with different thicknesses consolidated for: (a) 6 days; (b) 18 days; and (c) 46 days.

a)

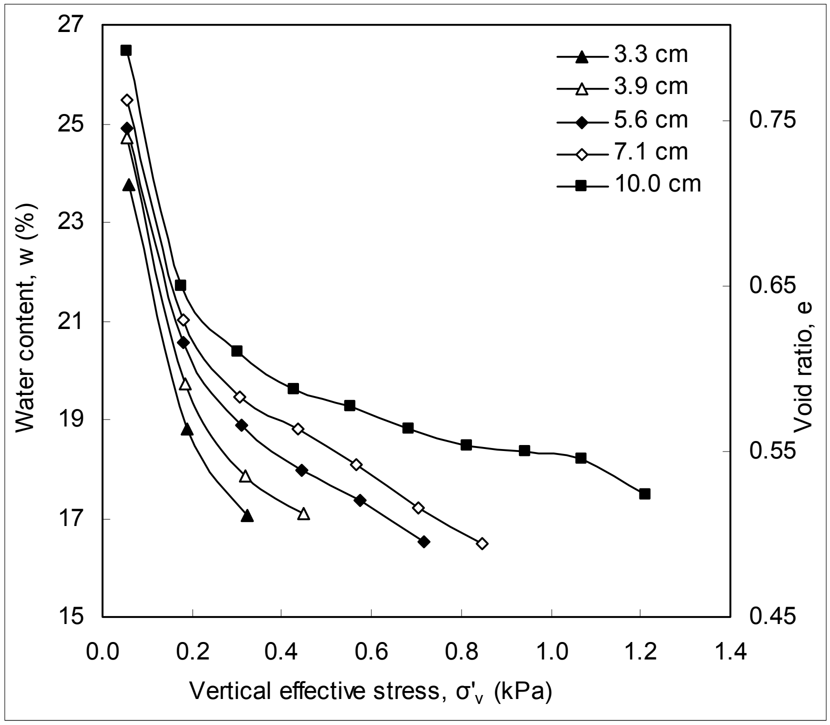

27
25
23
21
19
17
15
0.75
0.65
0.55
0.45
0.0
0.2
0.4
0.6
0.8
1.0
1.2
1.4
3.3 cm
3.9 cm
5.6 cm
7.1 cm
10.0 cm
Water content, w (%)
Void ratio, e
Vertical effective stress, σ'v (kPa)


b)

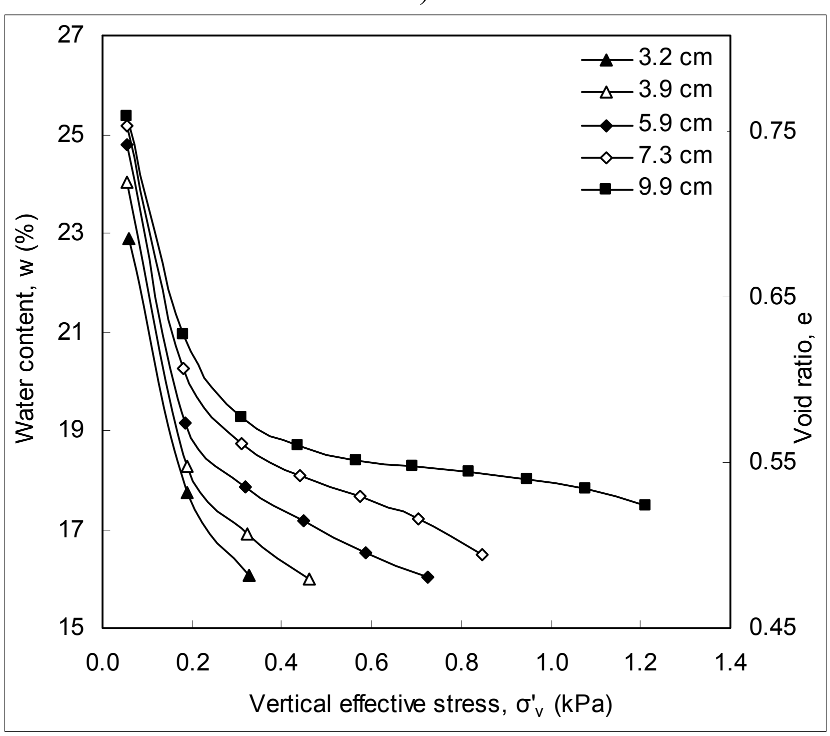

27
25
23
21
19
17
15
0.75
0.65
0.55
0.45
0.0
0.2
0.4
0.6
0.8
1.0
1.2
1.4
3.2 cm
3.9 cm
5.9 cm
7.3 cm
9.9 cm
Water content, w (%)
Void ratio, e
Vertical effective stress, σ'v (kPa)

c)

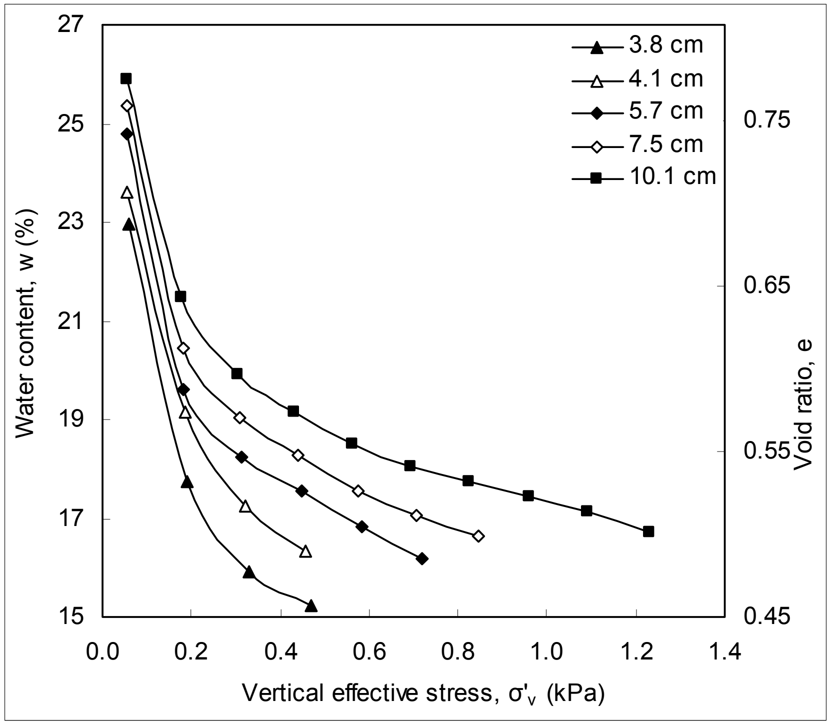


**Figure A.2.** Variation of vertical effective stress with water content for mine tailings beds with different thicknesses consolidated for: (a) 6 days; (b) 18 days; and (c) 46 days.

a)

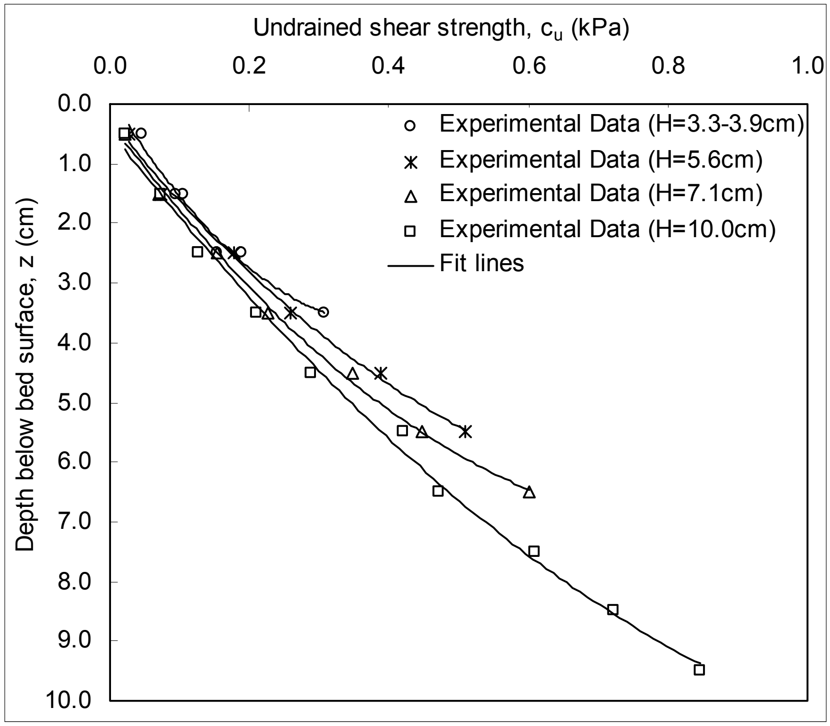

Undrained shear strength, $c_u$ (kPa)
0.0
0.2
0.4
0.6
0.8
1.0
Depth below bed surface, z (cm)
0.0
1.0
2.0
3.0
4.0
5.0
6.0
7.0
8.0
9.0
10.0
Experimental Data (H=3.3-3.9cm)
Experimental Data (H=5.6cm)
Experimental Data (H=7.1cm)
Experimental Data (H=10.0cm)
Fit lines


b)

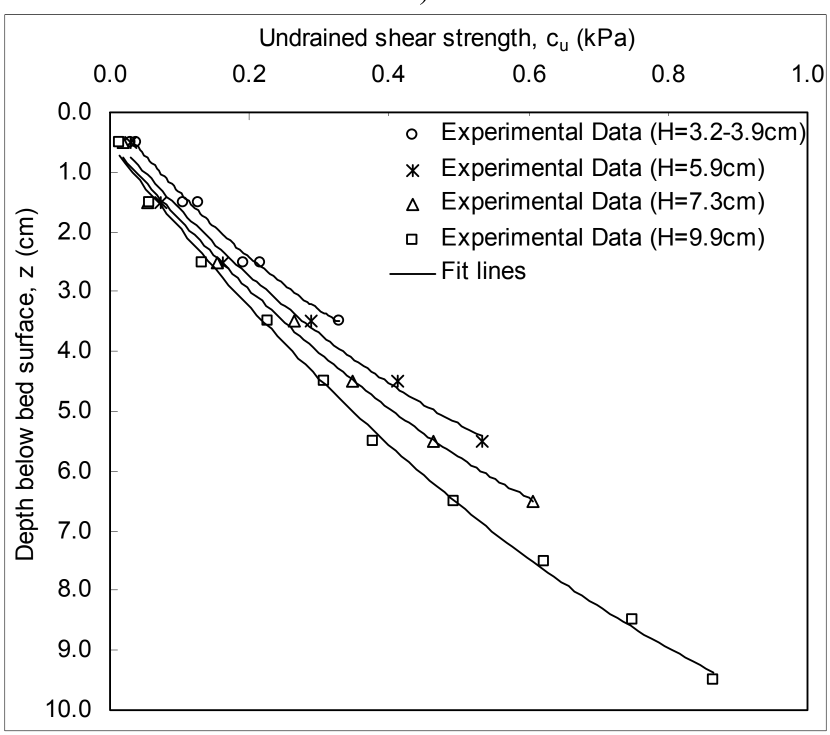

Undrained shear strength, $c_u$ (kPa)
0.0
0.2
0.4
0.6
0.8
1.0
Depth below bed surface, z (cm)
0.0
1.0
2.0
3.0
4.0
5.0
6.0
7.0
8.0
9.0
10.0
Experimental Data (H=3.2-3.9cm)
Experimental Data (H=5.9cm)
Experimental Data (H=7.3cm)
Experimental Data (H=9.9cm)
Fit lines

c)

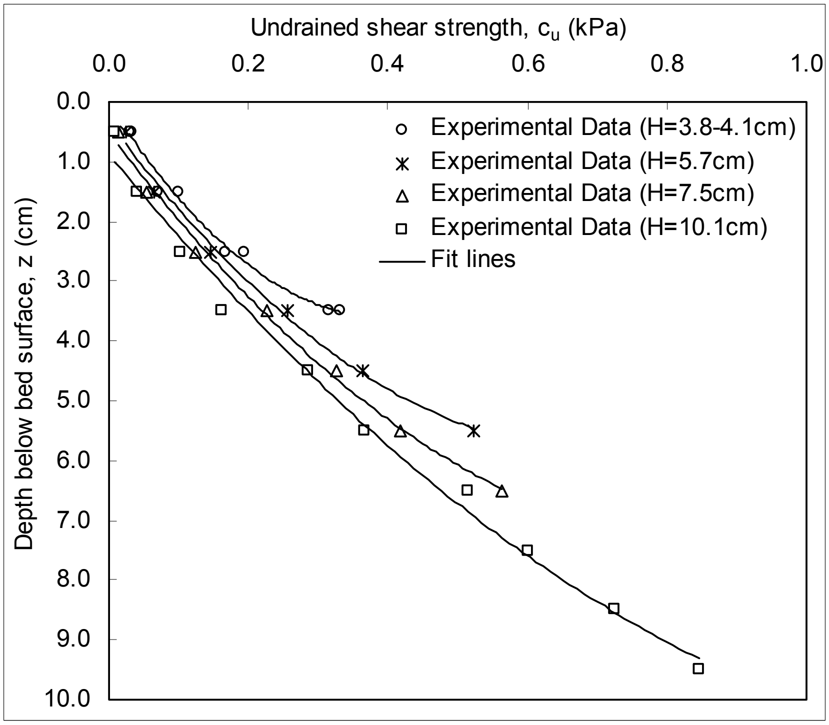


**Figure A.3.** Undrained shear strength profiles of mine tailings beds with different thicknesses consolidated for: (a) 6 days; (b) 18 days; and (c) 46 days.

a)

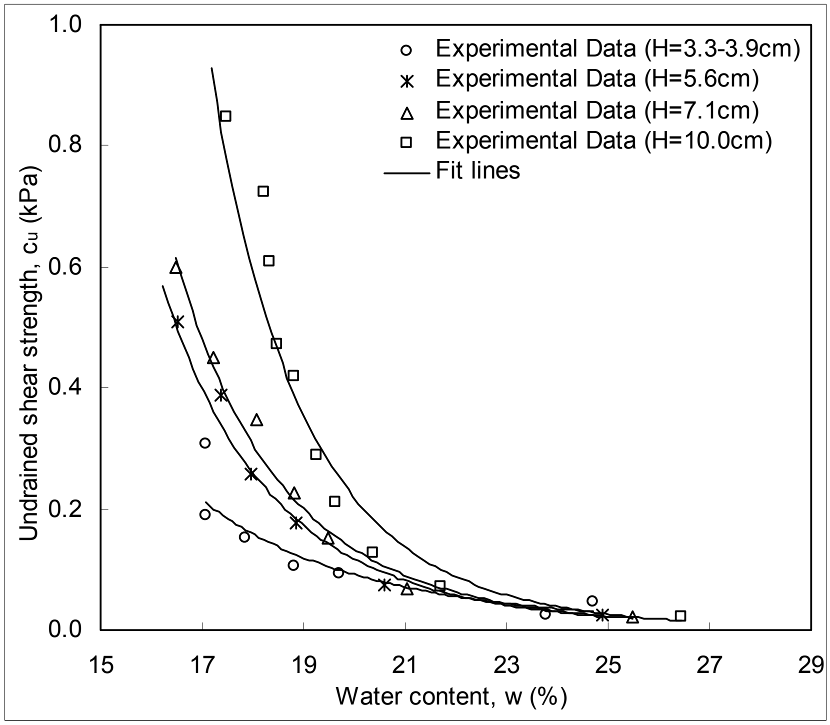

Experimental Data (H=3.3-3.9cm)
Experimental Data (H=5.6cm)
Experimental Data (H=7.1cm)
Experimental Data (H=10.0cm)
Fit lines
Undrained shear strength, cu (kPa)
Water content, w (%)
1.0
0.8
0.6
0.4
0.2
0.0
15
17
19
21
23
25
27
29


b)

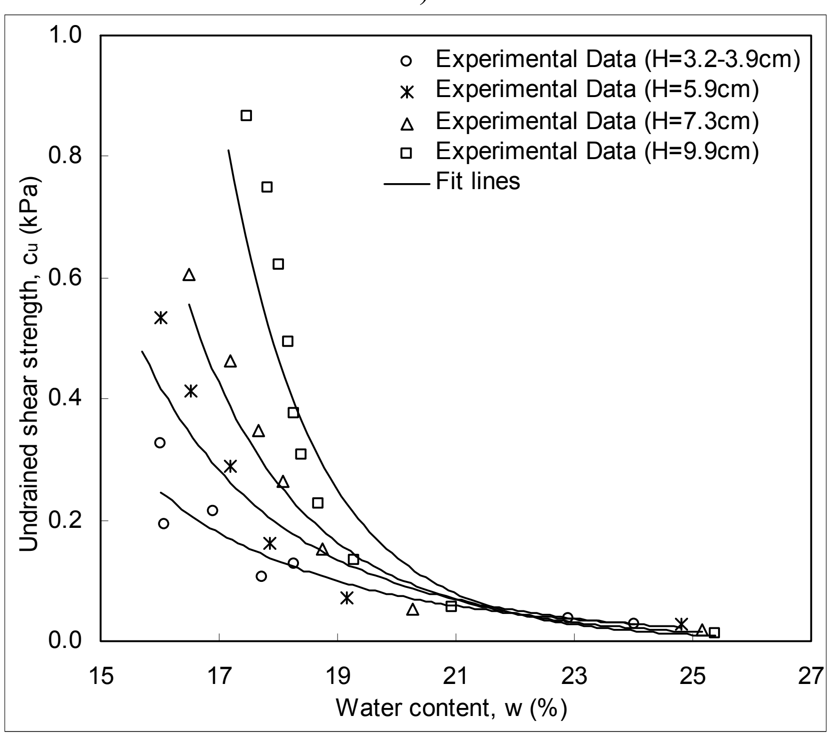

Experimental Data (H=3.2-3.9cm)
Experimental Data (H=5.9cm)
Experimental Data (H=7.3cm)
Experimental Data (H=9.9cm)
Fit lines
Undrained shear strength, cu (kPa)
Water content, w (%)
1.0
0.8
0.6
0.4
0.2
0.0
15
17
19
21
23
25
27

c)

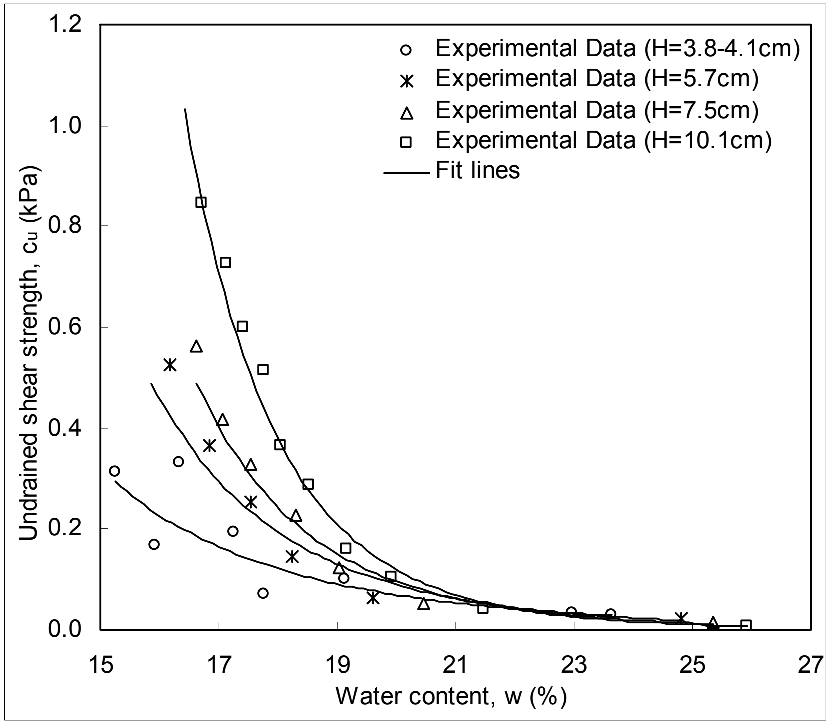


**Figure A.4.** Variation of undrained shear strength with water content for mine tailings beds with different thicknesses consolidated for: (a) 6 days; (b) 18 days; and (c) 46 days.

a)

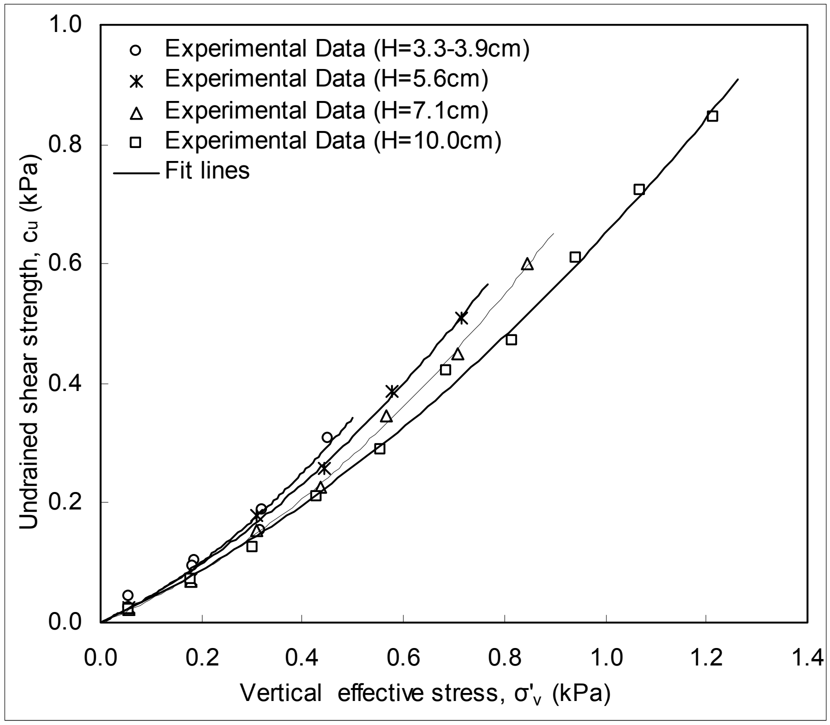
Experimental Data (H=3.3-3.9cm)
Experimental Data (H=5.6cm)
Experimental Data (H=7.1cm)
Experimental Data (H=10.0cm)
Fit lines
Undrained shear strength, cu (kPa)
Vertical effective stress, σ'v (kPa)
0.0
0.2
0.4
0.6
0.8
1.0
1.2
1.4

b)

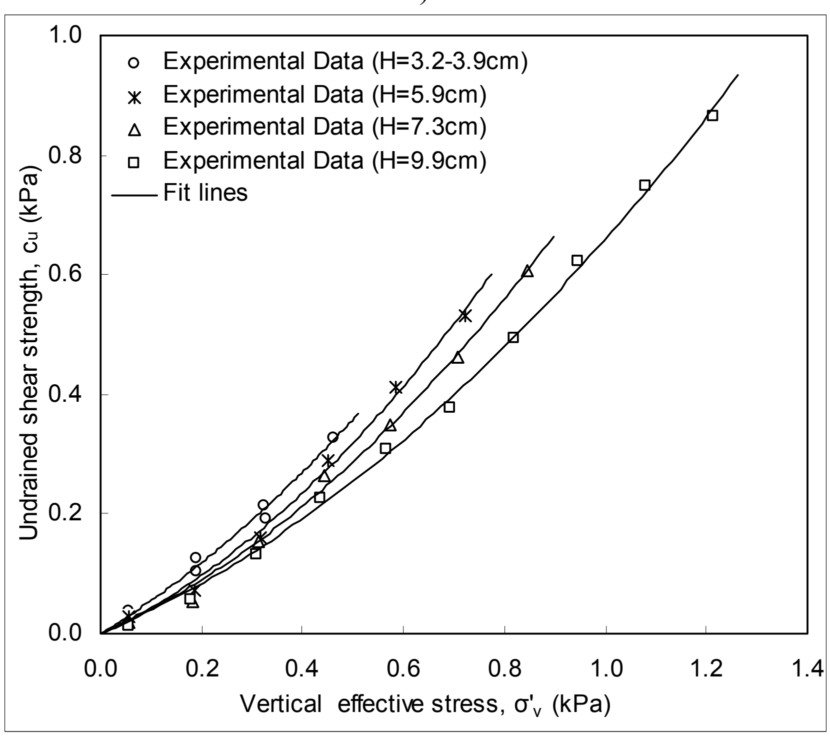
Experimental Data (H=3.2-3.9cm)
Experimental Data (H=5.9cm)
Experimental Data (H=7.3cm)
Experimental Data (H=9.9cm)
Fit lines
Undrained shear strength, cu (kPa)
Vertical effective stress, σ'v (kPa)
0.0
0.2
0.4
0.6
0.8
1.0
1.2
1.4

c)

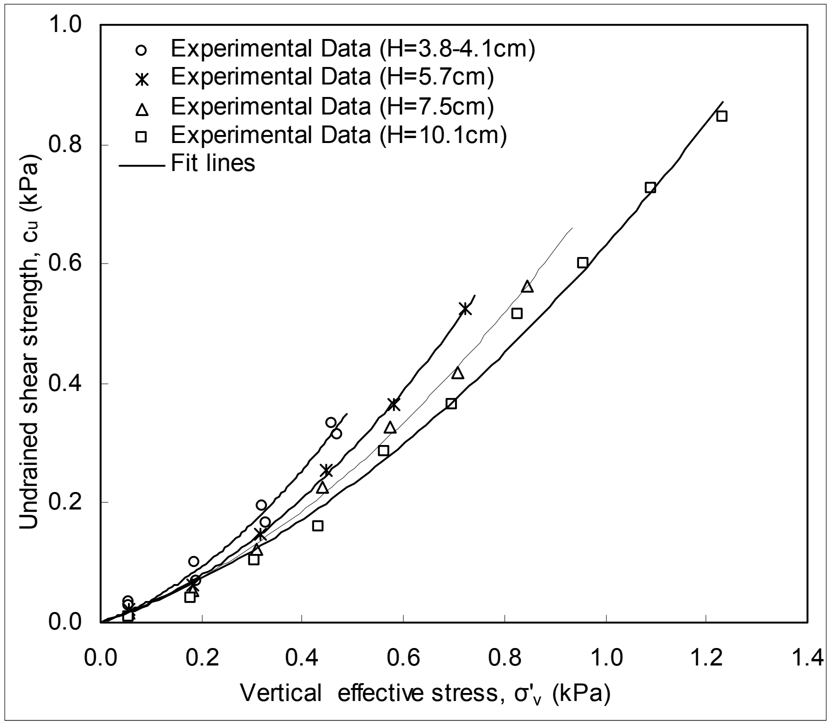


**Figure A.5.** Undrained shear strength versus vertical effective stress for mine tailings beds with different thicknesses consolidated for: (a) 6 days; (b) 18 days; and (c) 46 days.

a)

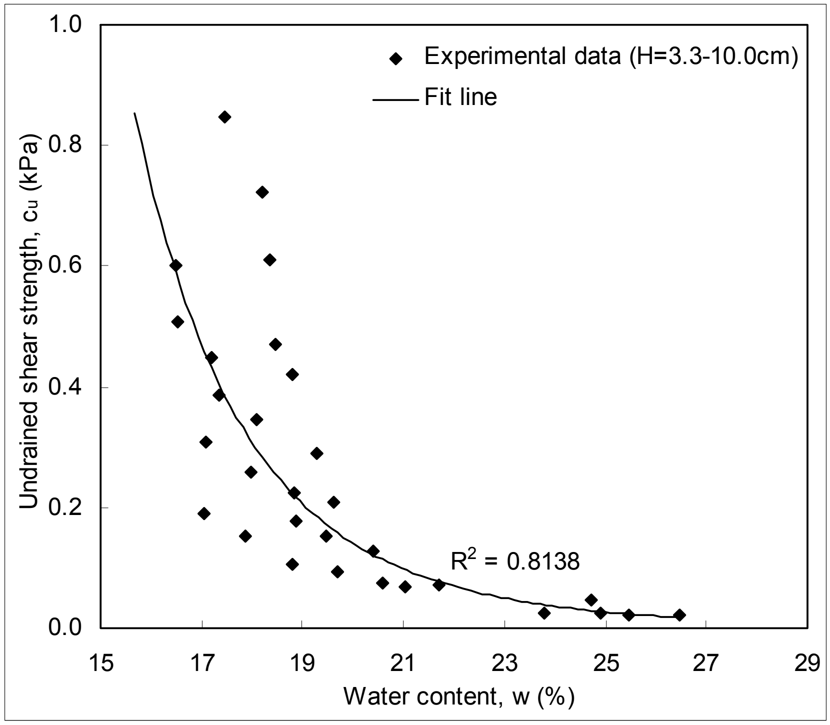

1.0
0.8
0.6
0.4
0.2
0.0
Undrained shear strength, cu (kPa)
Experimental data (H=3.3-10.0cm)
Fit line
R2 = 0.8138
15
17
19
21
23
25
27
29
Water content, w (%)


b)

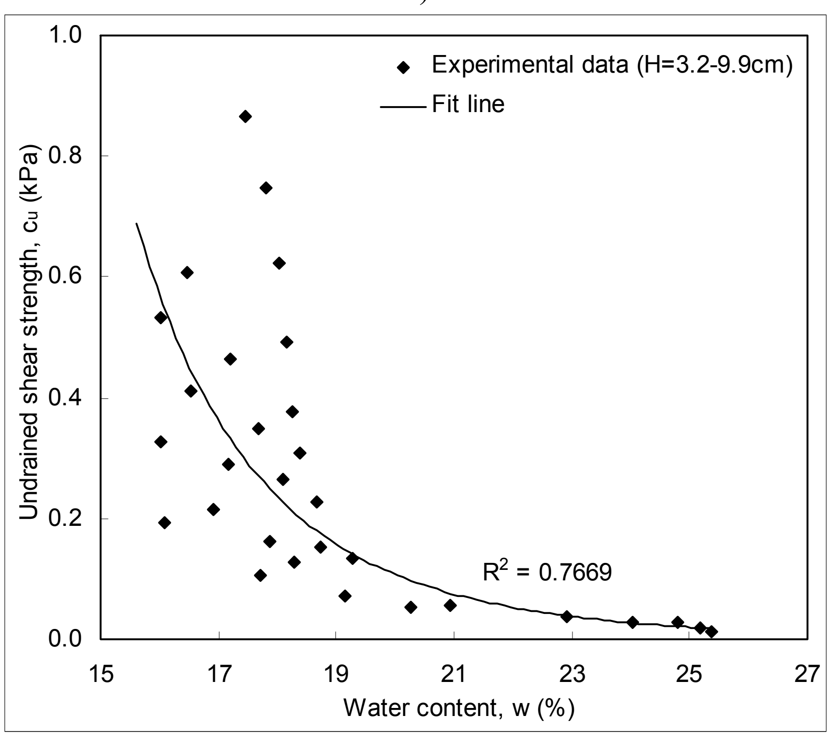

1.0
0.8
0.6
0.4
0.2
0.0
Undrained shear strength, cu (kPa)
Experimental data (H=3.2-9.9cm)
Fit line
R2 = 0.7669
15
17
19
21
23
25
27
Water content, w (%)

c)

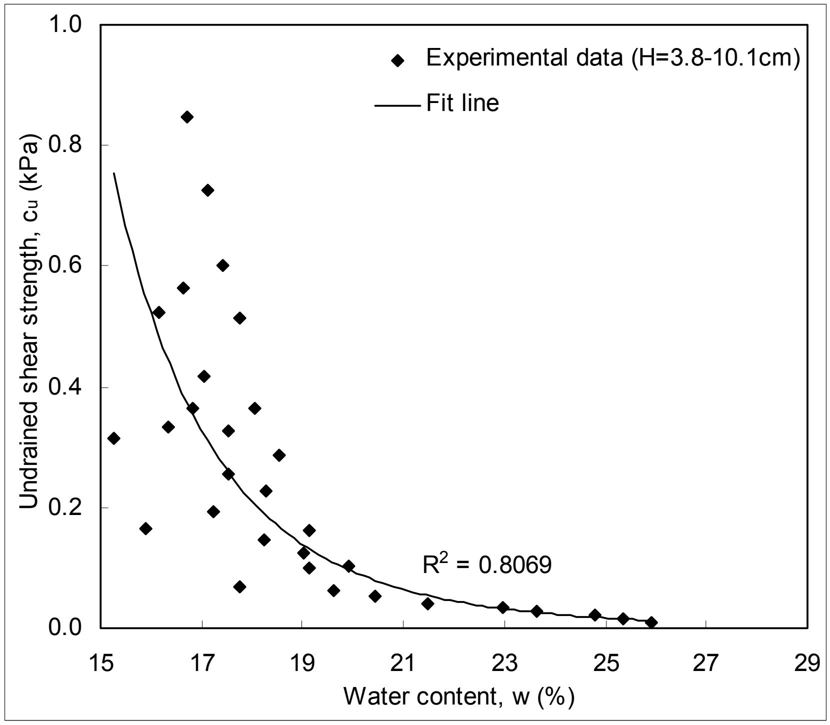


**Figure A.6.** Variation of undrained shear strength with water content for mine tailings beds consolidated for: (a) 6 days; (b) 18 days; and (c) 46 days.

a)

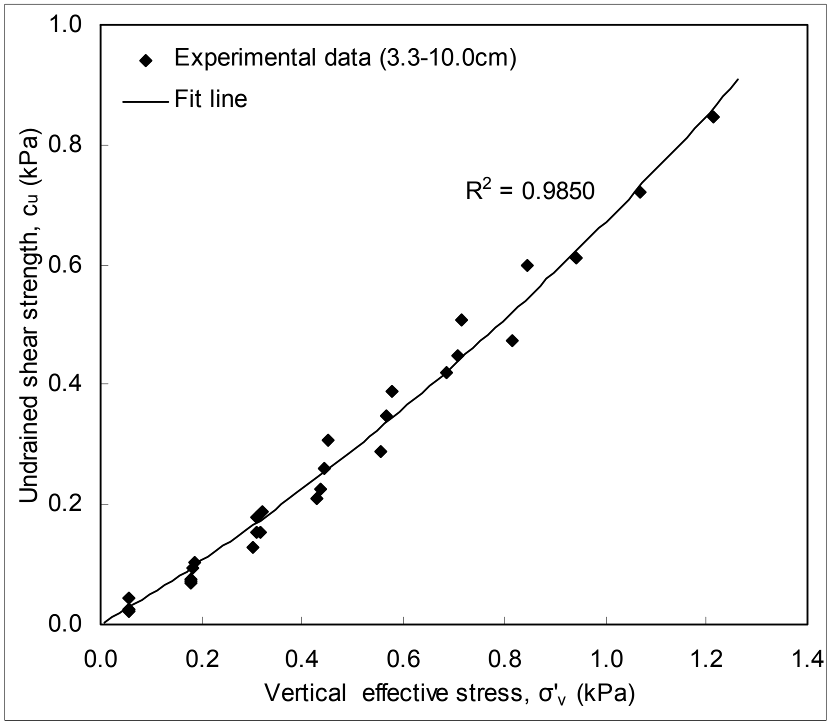
Experimental data (3.3-10.0cm)
Fit line
$R^2$ = 0.9850
Undrained shear strength, $c_u$ (kPa)
Vertical effective stress, $\sigma'_v$ (kPa)
0.0
0.2
0.4
0.6
0.8
1.0
1.2
1.4

b)

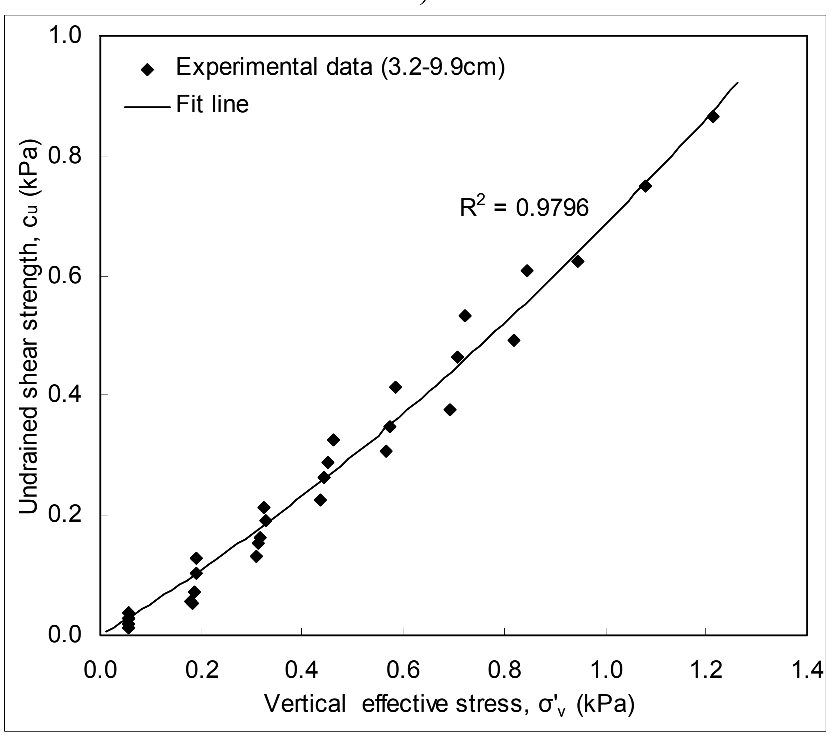
Experimental data (3.2-9.9cm)
Fit line
$R^2$ = 0.9796
Undrained shear strength, $c_u$ (kPa)
Vertical effective stress, $\sigma'_v$ (kPa)
0.0
0.2
0.4
0.6
0.8
1.0
1.2
1.4

c)

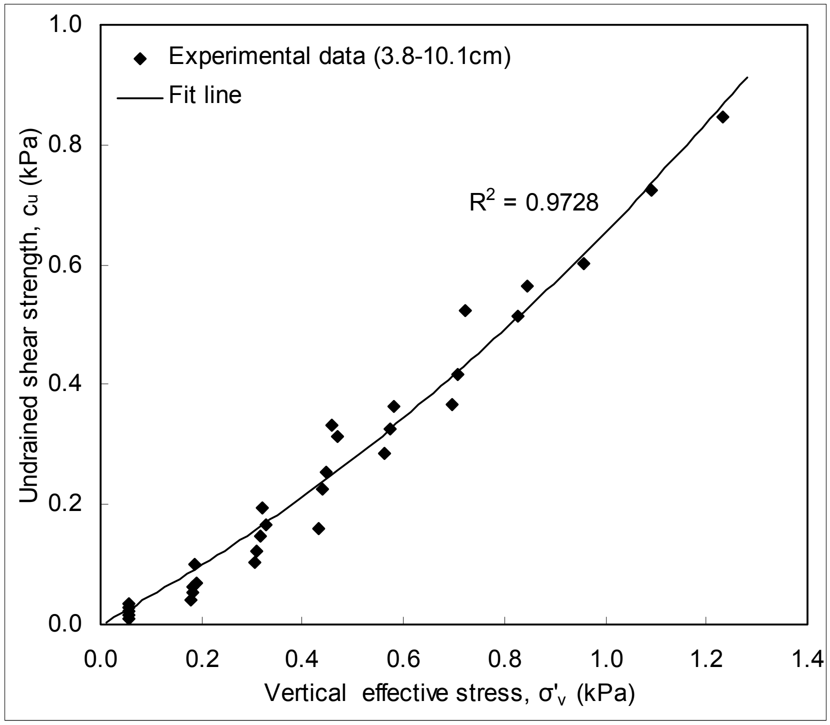


**Figure A.7.** Variation of undrained shear strength with vertical effective stress for mine tailings beds consolidated for: (a) 6 days; (b) 18 days; and (c) 46 days.

# APPENDIX B

This appendix contains additional information pertinent to Chapter 4 of the thesis. It includes photos of the Tilting Tank, the results of drained and partially shear strength testing using the Tilting Tank on tailings beds consolidated for 6, 18 and 46 days. Drained (effective) and partially drained (total) failure envelopes were determined and shown in the figures that follow.

a)

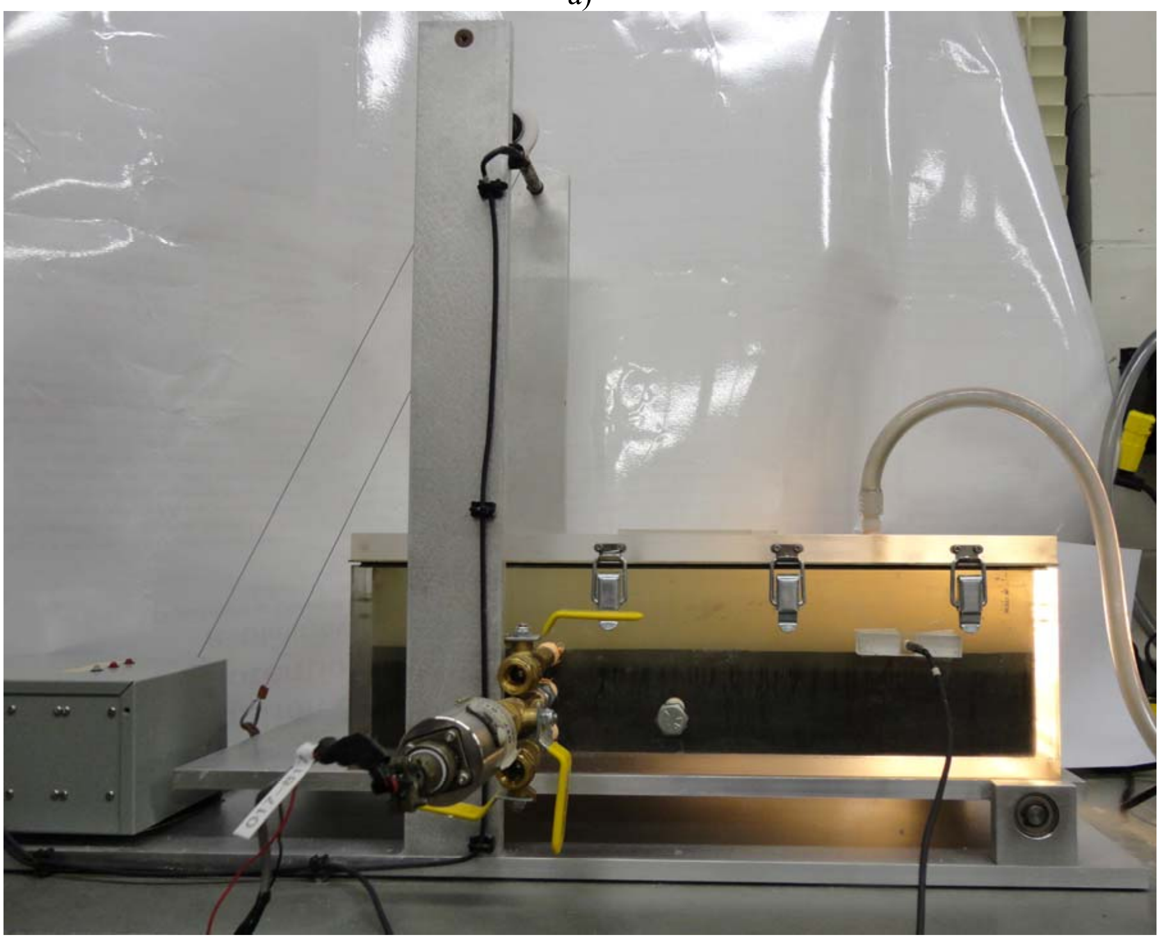

b)

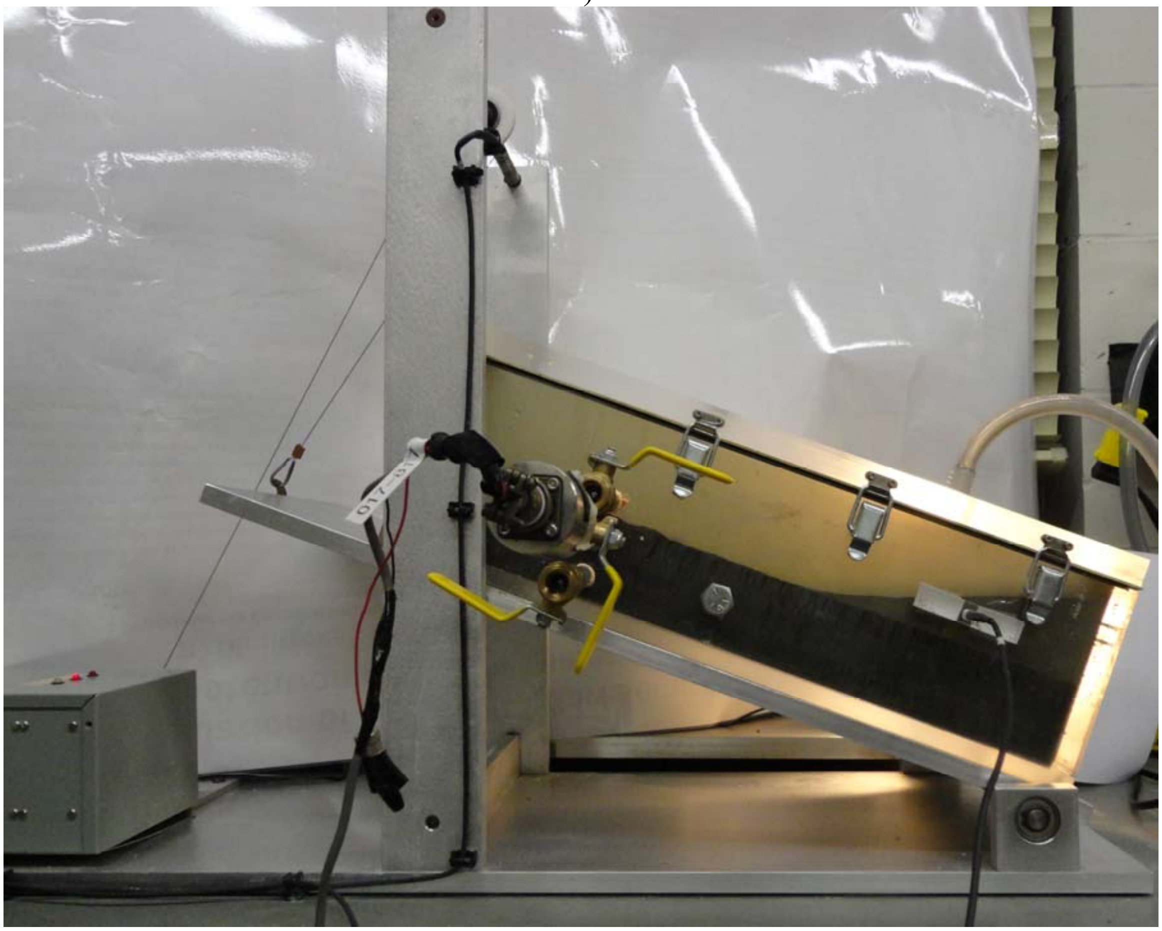

**Figure B.1.** The tilting Tank: (a) Photo of the experimental setup before tilting; (b) Photo of the experimental setup at bed failure.

a)

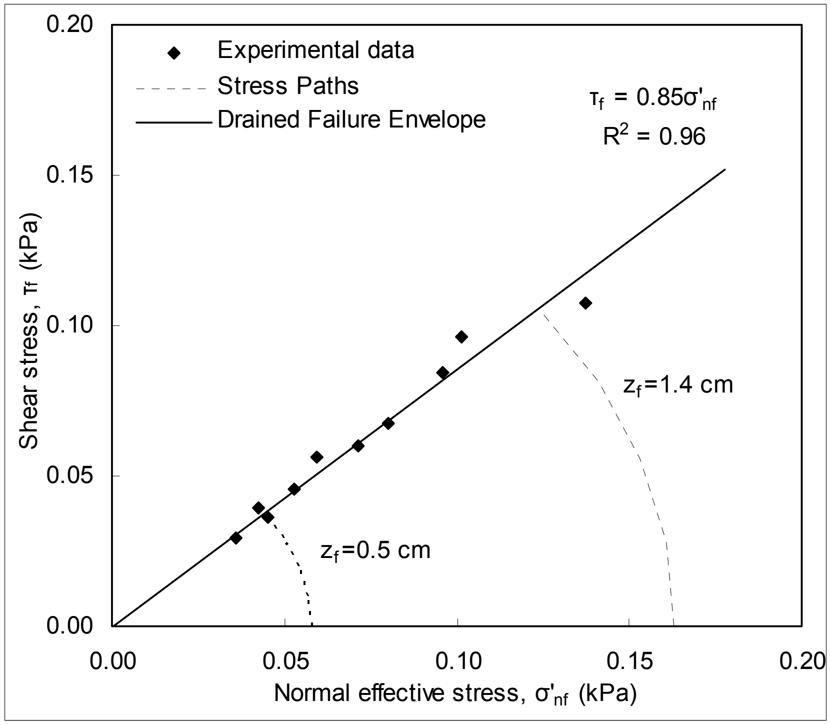

Experimental data
Stress Paths
Drained Failure Envelope
τf = 0.85σ'nf
R2 = 0.96
zf=1.4 cm
zf=0.5 cm
Shear stress, τf (kPa)
Normal effective stress, σ'nf (kPa)
0.00
0.05
0.10
0.15
0.20


b)

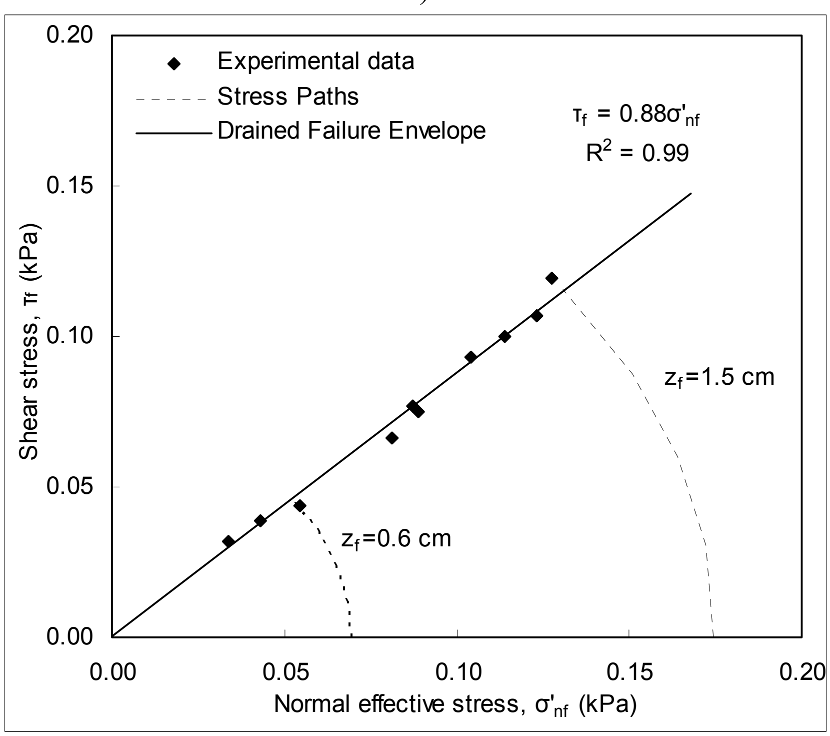

Experimental data
Stress Paths
Drained Failure Envelope
τf = 0.88σ'nf
R2 = 0.99
zf=1.5 cm
zf=0.6 cm
Shear stress, τf (kPa)
Normal effective stress, σ'nf (kPa)
0.00
0.05
0.10
0.15
0.20

c)

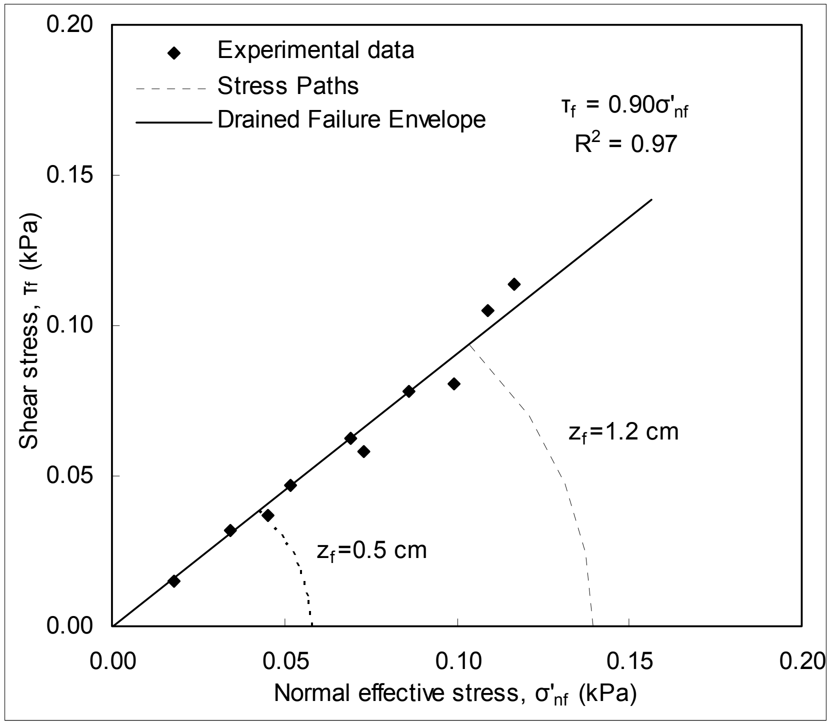


**Figure B.2.** Drained failure envelope and effective stress paths for tailings beds of various thicknesses consolidated for: (a) 6 days; (b) 18 days; and (c) 46 days.

a)

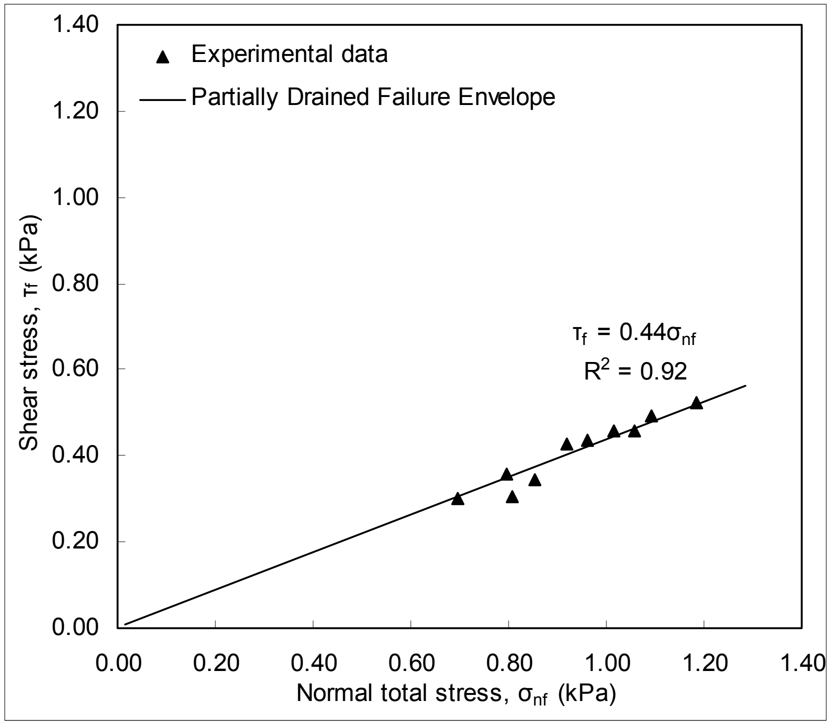

Experimental data
Partially Drained Failure Envelope
$\tau_f$ = 0.44$\sigma_{nf}$
$R^2$ = 0.92
Shear stress, $\tau_f$ (kPa)
Normal total stress, $\sigma_{nf}$ (kPa)
0.00
0.20
0.40
0.60
0.80
1.00
1.20
1.40


b)

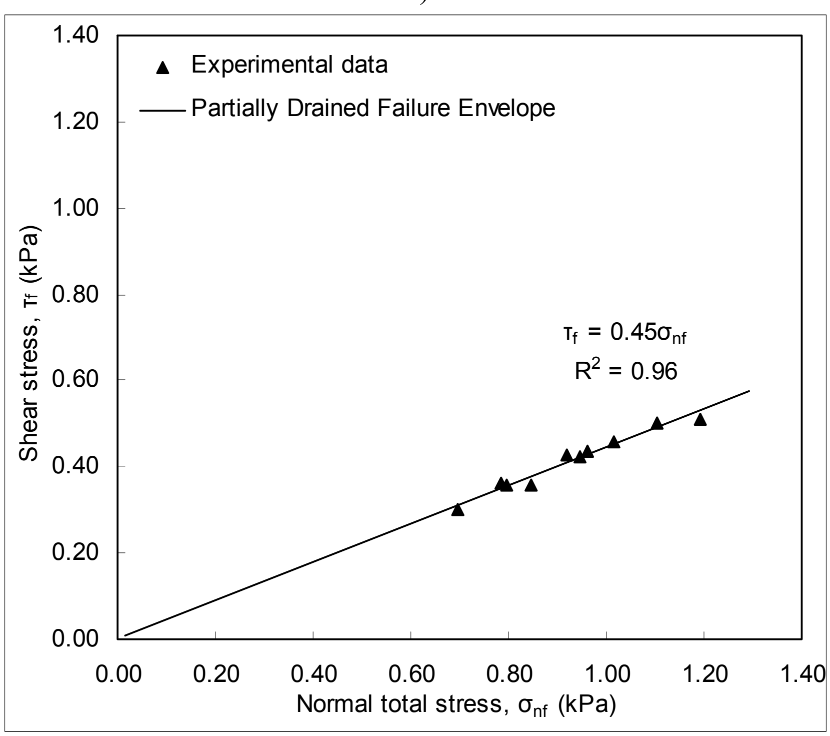

Experimental data
Partially Drained Failure Envelope
$\tau_f$ = 0.45$\sigma_{nf}$
$R^2$ = 0.96
Shear stress, $\tau_f$ (kPa)
Normal total stress, $\sigma_{nf}$ (kPa)
0.00
0.20
0.40
0.60
0.80
1.00
1.20
1.40

c)

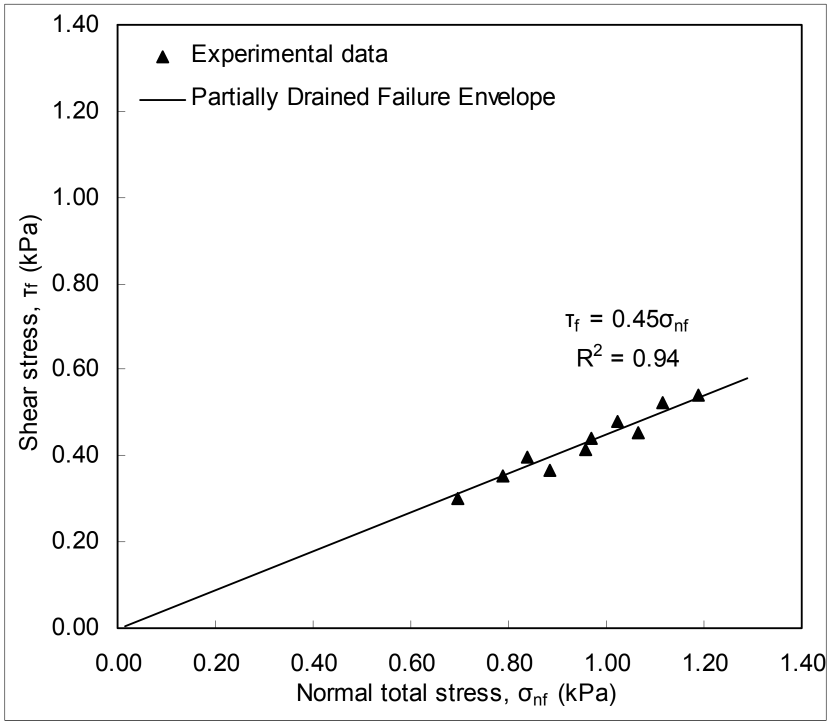


**Figure B.3.** Partially drained failure envelope for tailings beds of various thicknesses consolidated for: (a) 6 days; (b) 18 days; and (c) 46 days.

a)

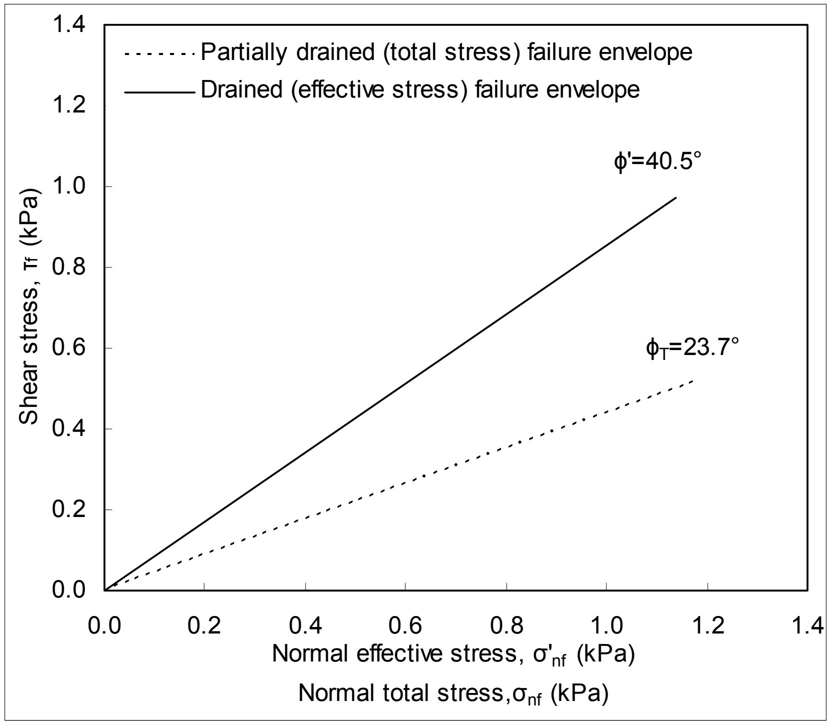

1.4
1.2
1.0
0.8
0.6
0.4
0.2
0.0
Partially drained (total stress) failure envelope
Drained (effective stress) failure envelope
ϕ'=40.5°
ϕT=23.7°
Shear stress, τf (kPa)
0.0
0.2
0.4
0.6
0.8
1.0
1.2
1.4
Normal effective stress, σ'nf (kPa)
Normal total stress,σnf (kPa)


b)

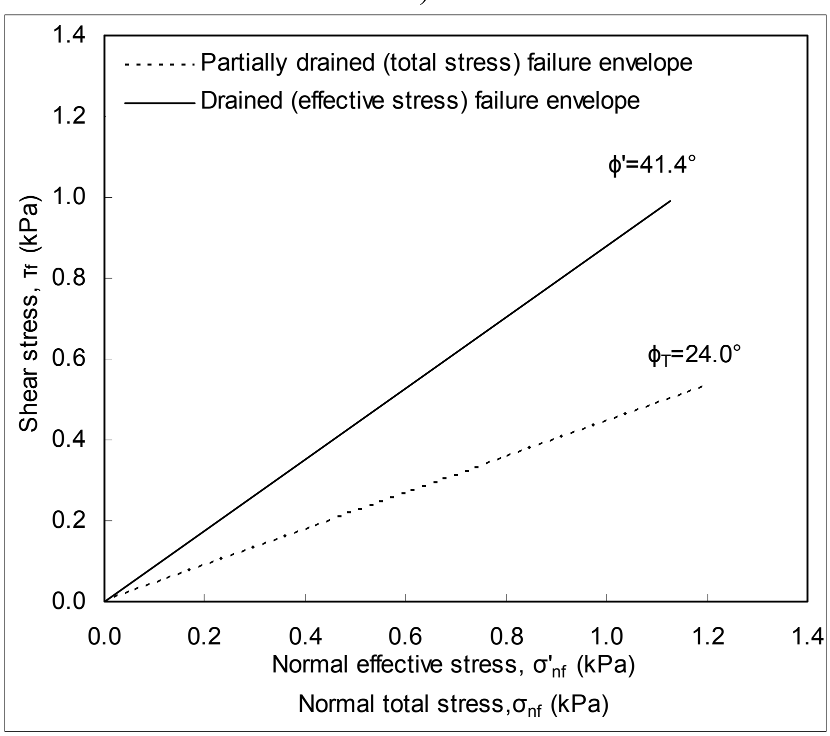

1.4
1.2
1.0
0.8
0.6
0.4
0.2
0.0
Partially drained (total stress) failure envelope
Drained (effective stress) failure envelope
ϕ'=41.4°
ϕT=24.0°
Shear stress, τf (kPa)
0.0
0.2
0.4
0.6
0.8
1.0
1.2
1.4
Normal effective stress, σ'nf (kPa)
Normal total stress,σnf (kPa)

c)

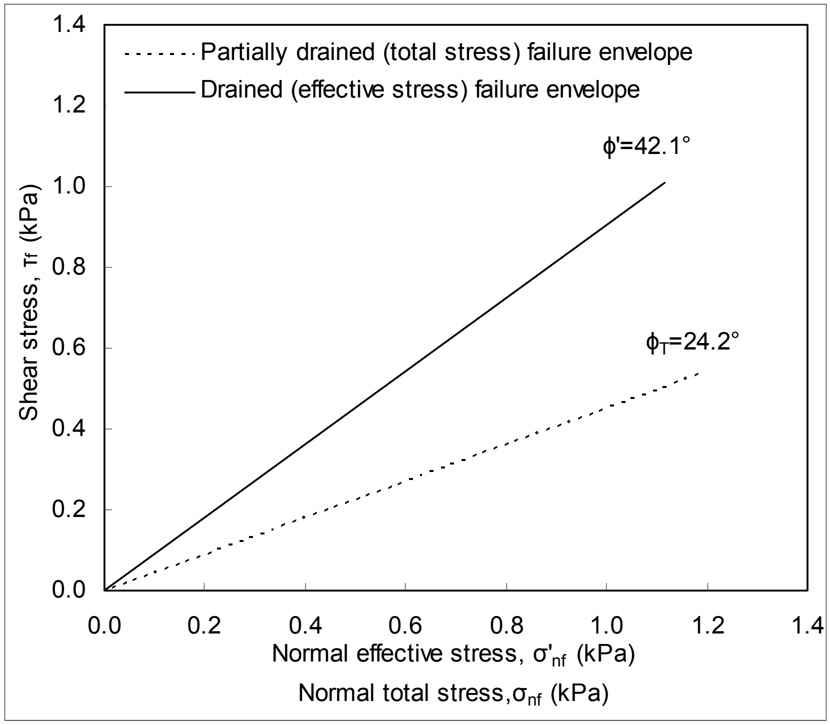


**Figure B.4.** Comparison between drained and partially drained shear strength for tailings beds consolidated for: (a) 6 days; (b) 18 days; and (c) 46 days.

# APPENDIX C

This appendix contains additional information pertinent to Chapter 5 of the thesis. It includes the results of drained and partially shear strength testing using the Tilting Tank on tailings and tailings/clay mixed beds consolidated for 12 days. These tests were performed without pore pressure measurements. Drained (effective) and partially drained (total) failure envelopes were determined and shown in the figures that follow.

a)

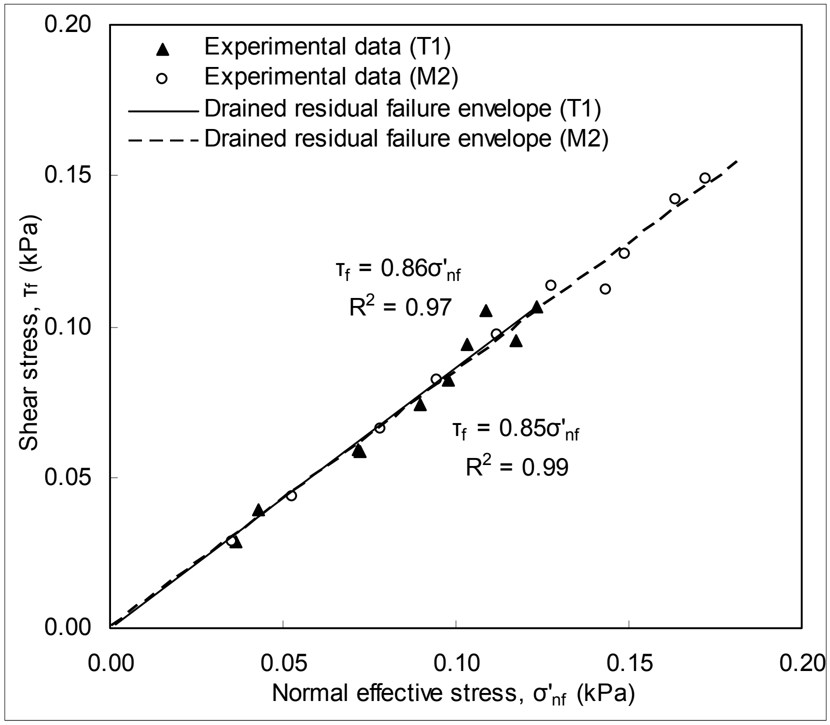


b)

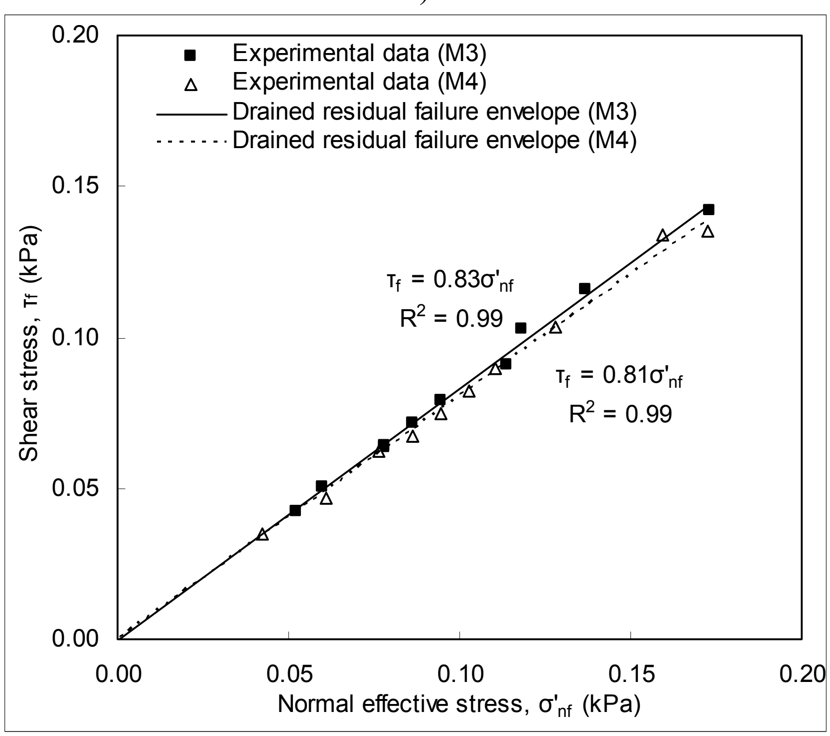


**Figure C.1.** Drained failure envelopes for beds prepared from: (a) T1 and M2, and (b) M3 and M4 mixtures and consolidated for 12 days.

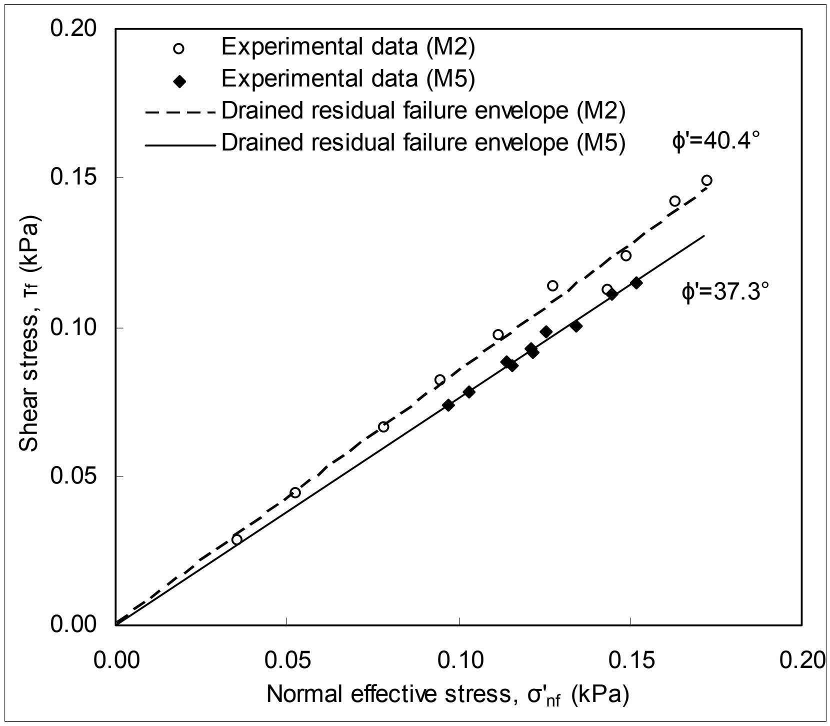


**Figure C.2.** Drained failure envelopes for beds prepared from M2 and M5 mixtures and consolidated for 12 days.

a)

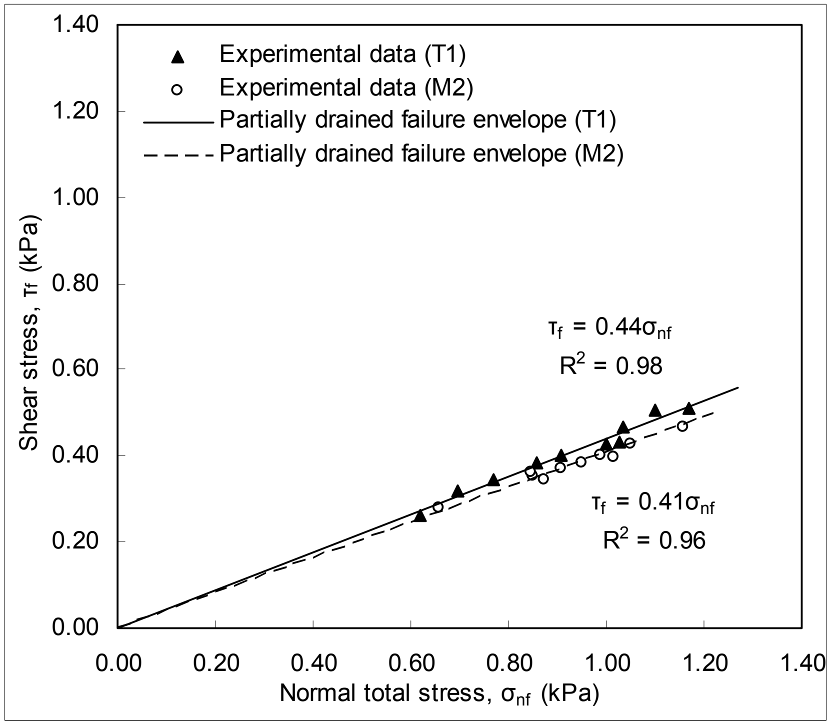


b)

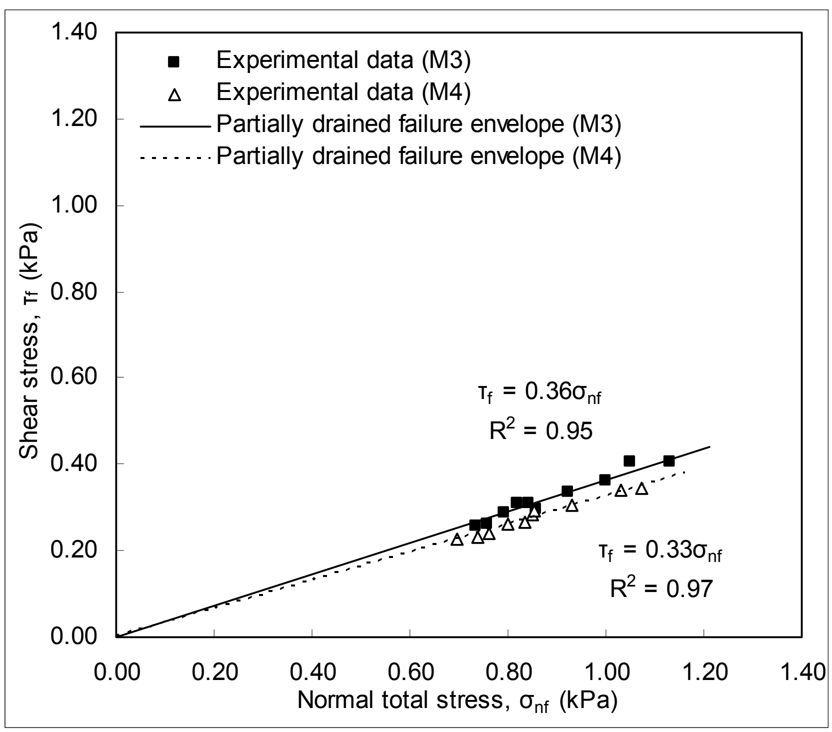


**Figure C.3**. Partially drained failure envelopes for beds prepared from: (a) T1 and M2, and (b) M3 and M4 mixtures and consolidated for 12 days.

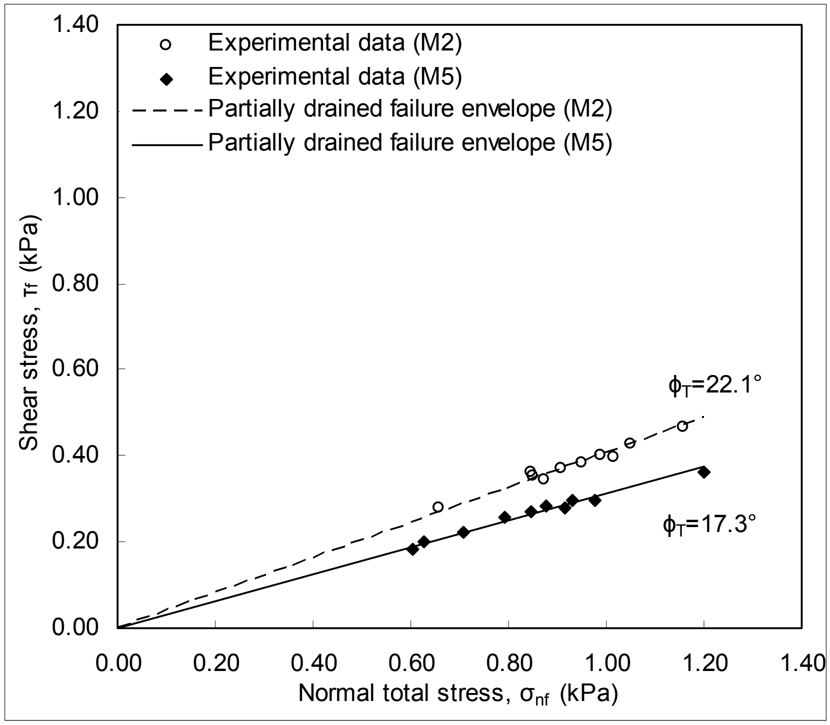


**Figure C.4.** Partially drained failure envelopes for beds prepared from M2 and M5 mixtures and consolidated for 12 days.

# APPENDIX D

This appendix contains additional information pertinent to Chapter 6 of the thesis. It includes the results of water content measurements and undrained shear strength testing using the Automated fall cone device on tailings and tailings/clay mixed beds consolidated for 3 or 12 days.

a)

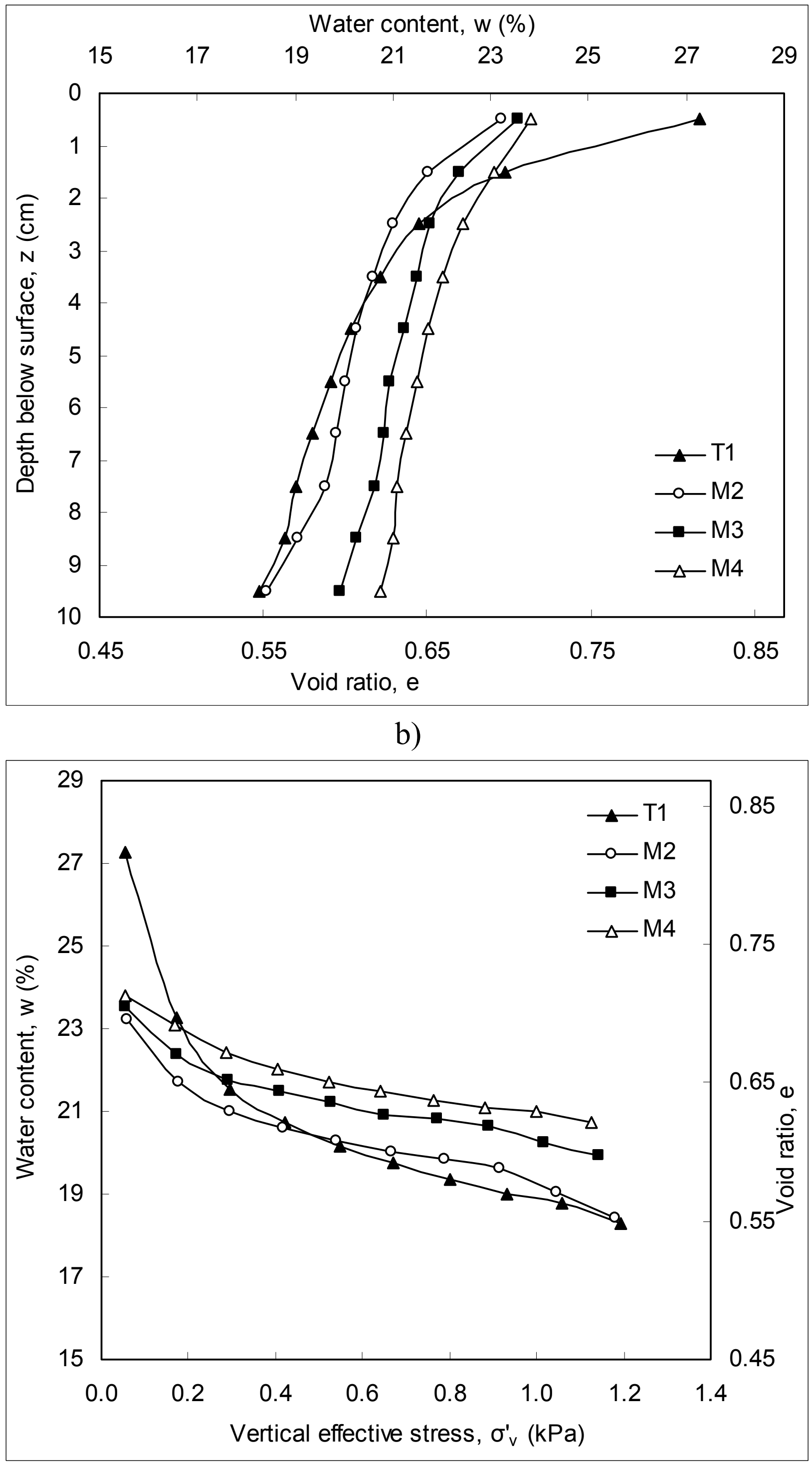


**Figure D.1.** Variation of water content with: (a) depth below bed surface; and (b) vertical effective stress in beds with final thickness of 10 cm prepared from various mixtures and consolidated for 3 days.

a)

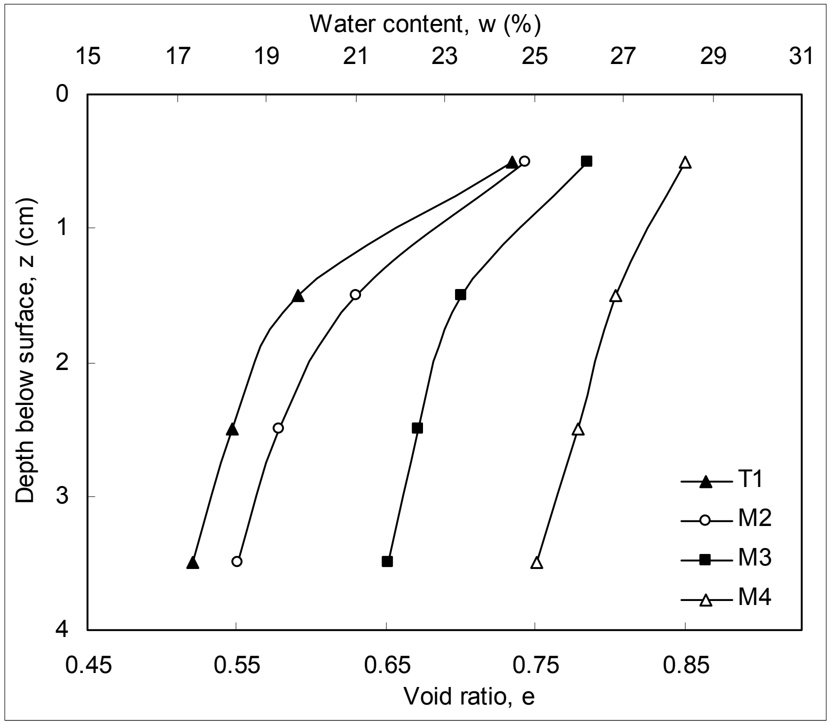
Water content, w (%)
15
17
19
21
23
25
27
29
31
0
1
2
3
4
Depth below surface, z (cm)
T1
M2
M3
M4
0.45
0.55
0.65
0.75
0.85
Void ratio, e

b)

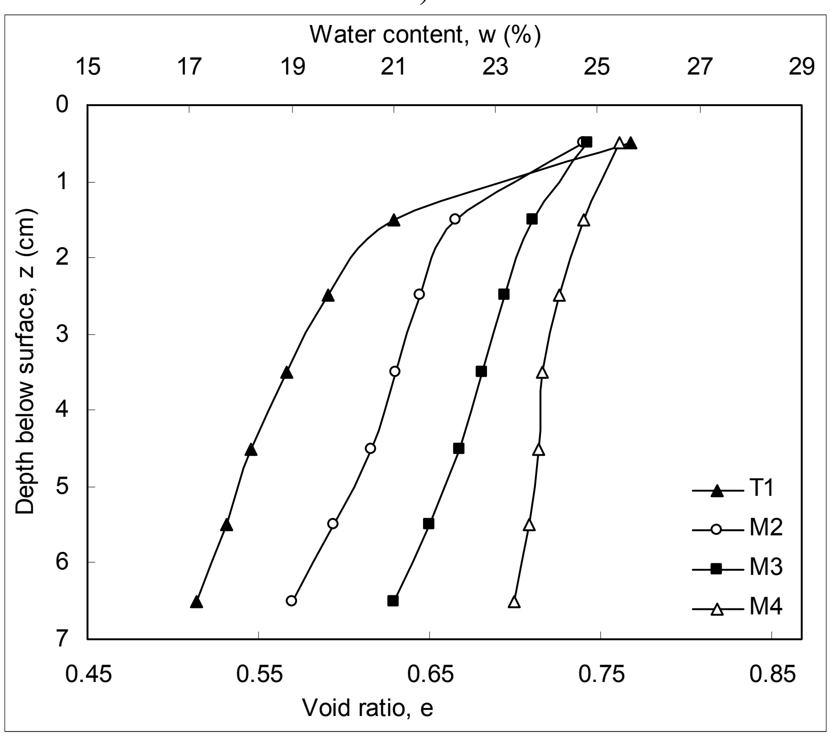
Water content, w (%)
15
17
19
21
23
25
27
29
0
1
2
3
4
5
6
7
Depth below surface, z (cm)
T1
M2
M3
M4
0.45
0.55
0.65
0.75
0.85
Void ratio, e

c)

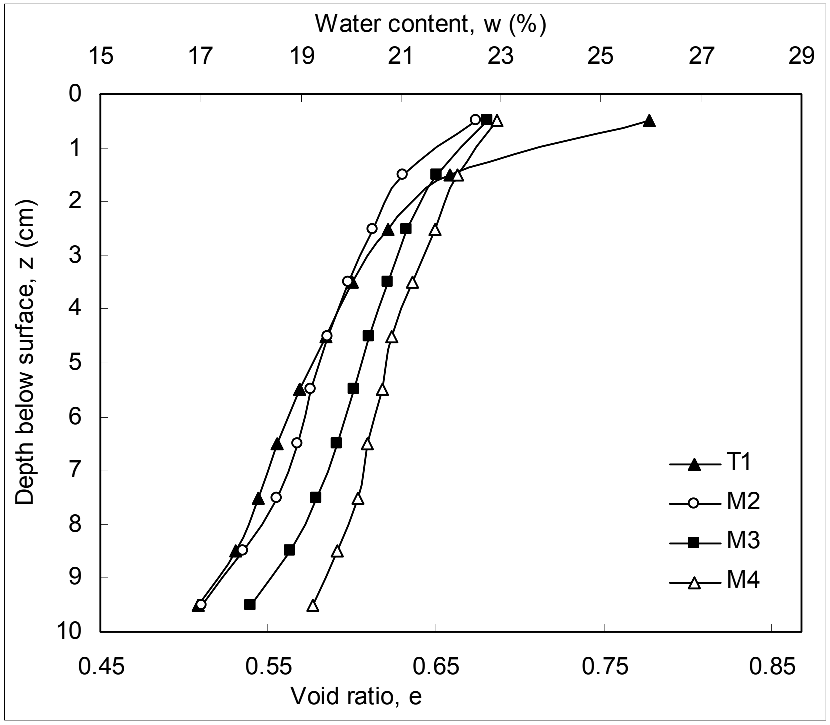


**Figure D.2.** Water content profiles of beds with final thickness of: (a) 4 cm; (b) 7 cm; and (c) 10 cm prepared from various tailings/kaolinite mixtures and consolidated for 12 days.

a)

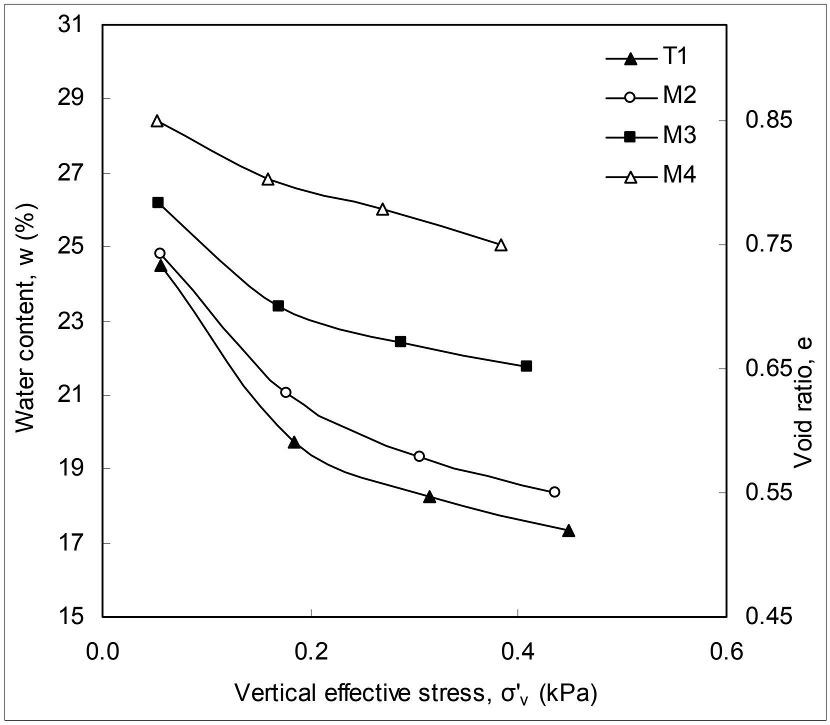

T1
M2
M3
M4
Water content, w (%)
Void ratio, e
Vertical effective stress, σ'v (kPa)
31
29
27
25
23
21
19
17
15
0.85
0.75
0.65
0.55
0.45
0.0
0.2
0.4
0.6


b)

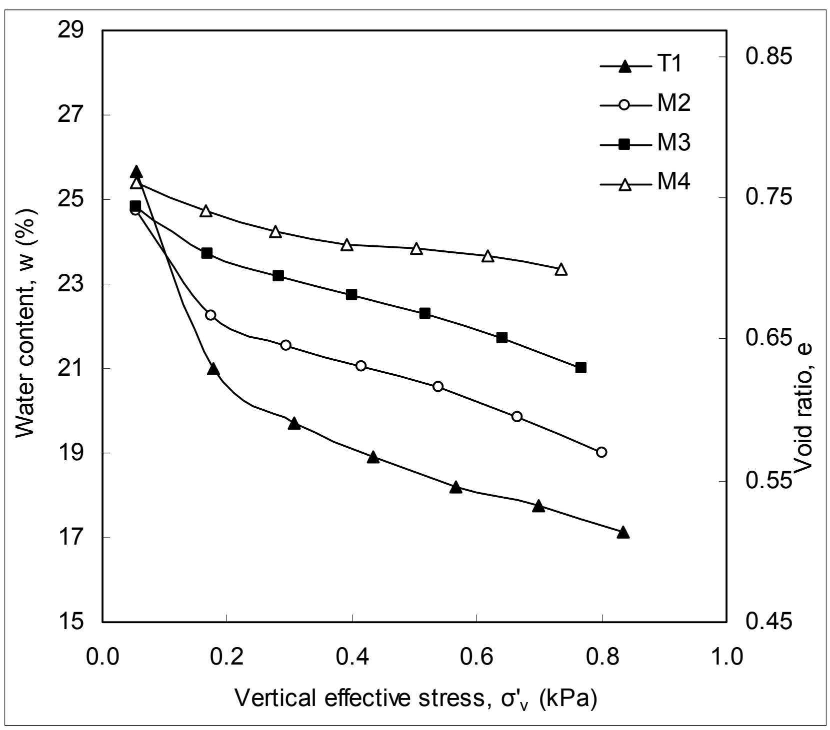

T1
M2
M3
M4
Water content, w (%)
Void ratio, e
Vertical effective stress, σ'v (kPa)
29
27
25
23
21
19
17
15
0.85
0.75
0.65
0.55
0.45
0.0
0.2
0.4
0.6
0.8
1.0

c)

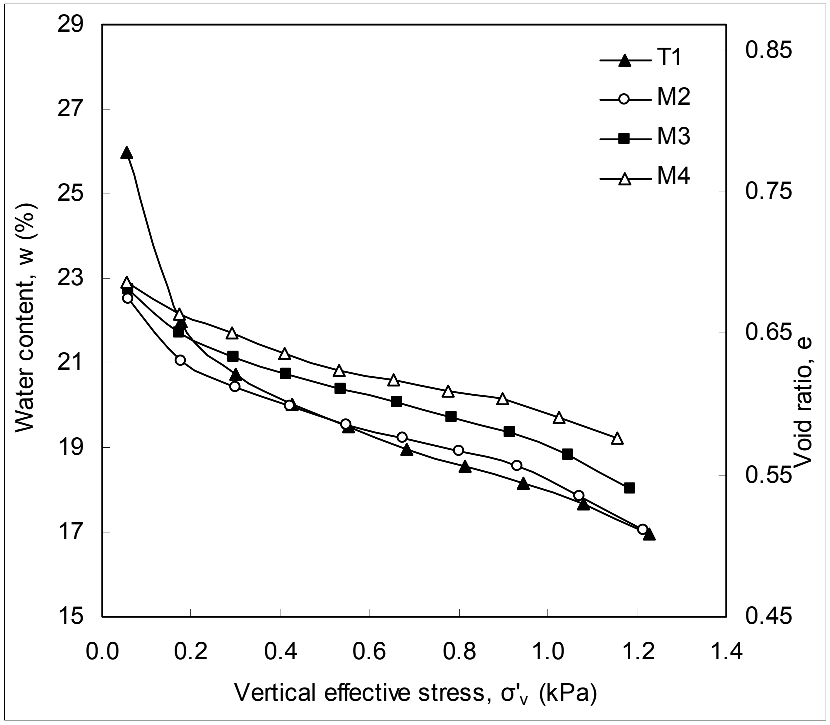


**Figure D.3.** Vertical effective stress versus water content in beds with final thickness of: (a) 4 cm; (b) 7 cm; and (c) 10 cm prepared from various mixtures and consolidated for 12 days.

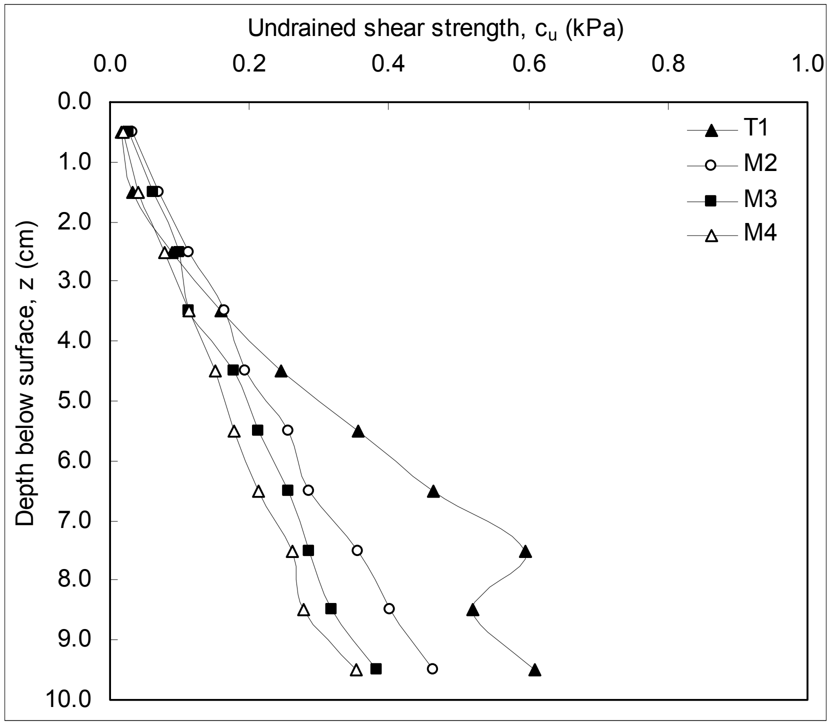


**Figure D.4.** Undrained shear strength profiles of beds with final thickness of 10 cm prepared from various mixtures and consolidated for 3 days.

a)

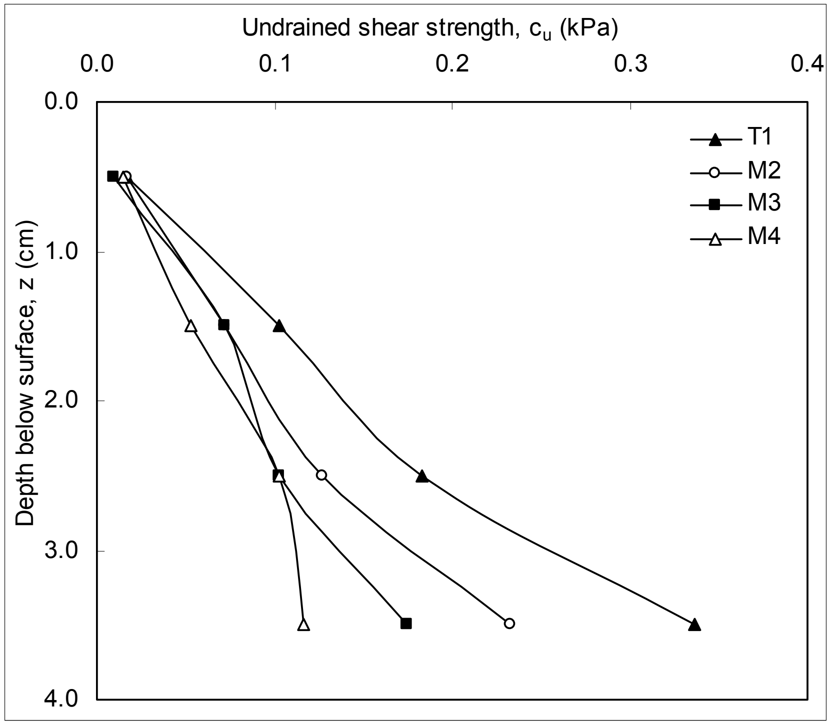
Undrained shear strength, $c_u$ (kPa)
0.0
0.1
0.2
0.3
0.4
Depth below surface, z (cm)
0.0
1.0
2.0
3.0
4.0
T1
M2
M3
M4

b)

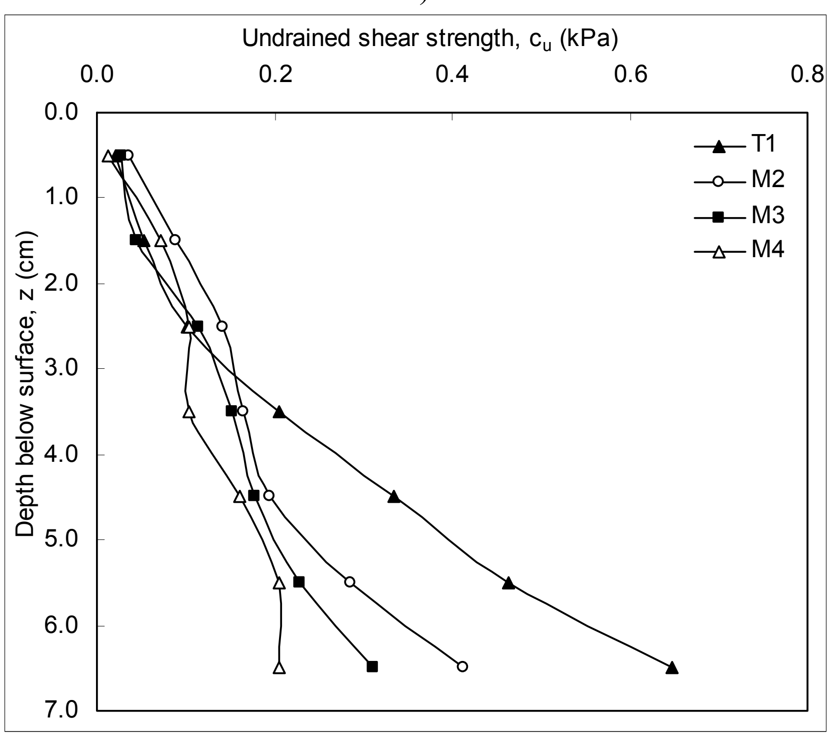
Undrained shear strength, $c_u$ (kPa)
0.0
0.2
0.4
0.6
0.8
Depth below surface, z (cm)
0.0
1.0
2.0
3.0
4.0
5.0
6.0
7.0
T1
M2
M3
M4

c)

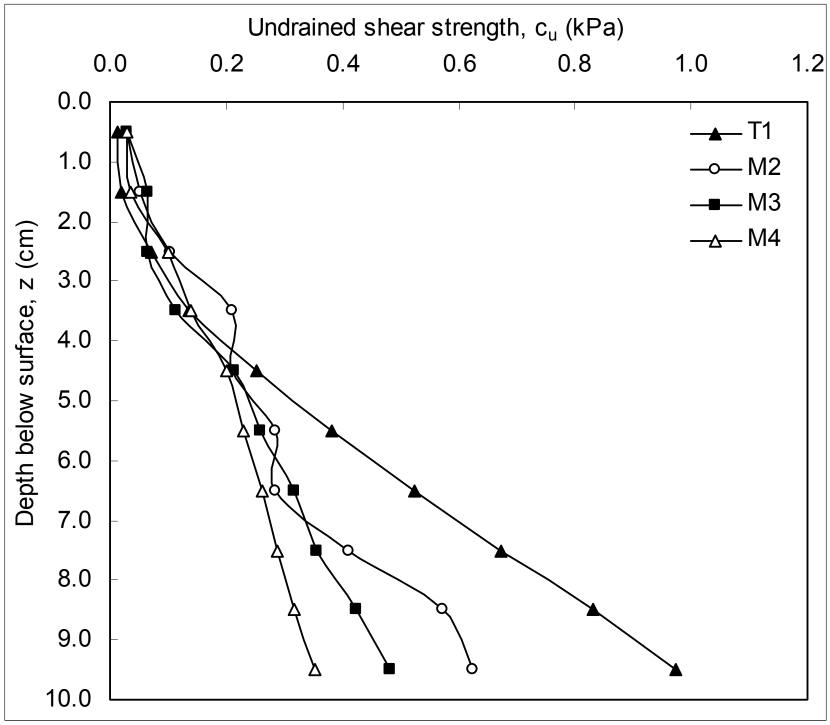


**Figure D.5.** Undrained shear strength profiles of beds with final thickness of: (a) 4 cm; (b) 7 cm; and (c) 10 cm prepared from various mixtures and consolidated for 12 days.

a)

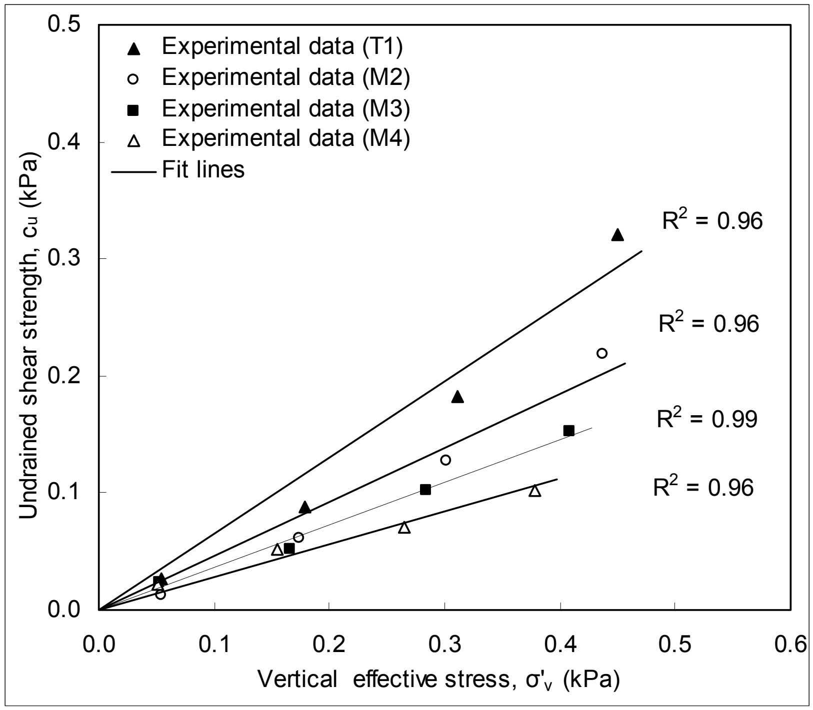


b)

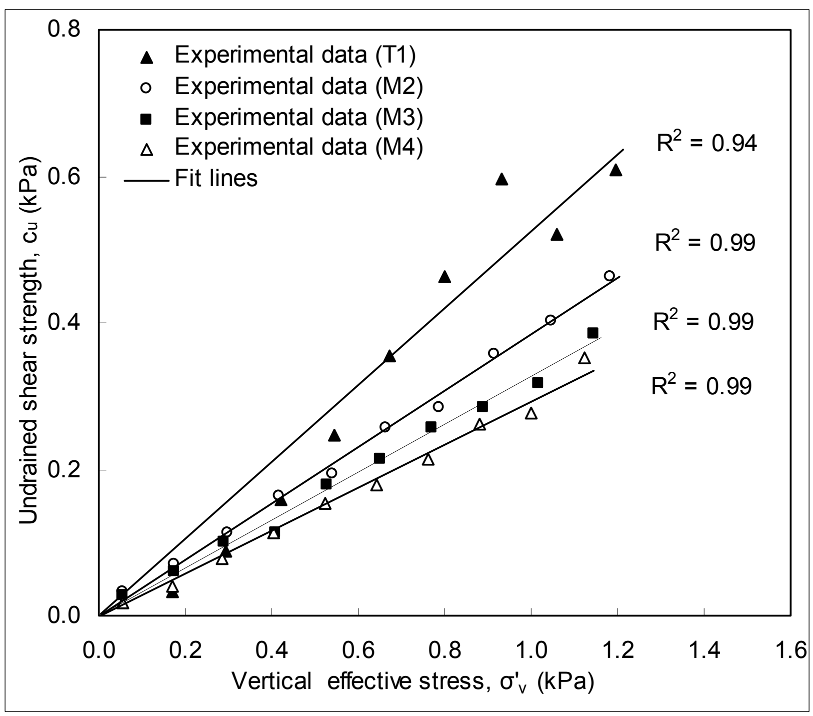


**Figure D.6.** Undrained shear strength versus vertical effective stress for beds with final thickness of: (a) 4 cm; and (b) 10 cm prepared from various mixtures and consolidated for 3 days.

a)

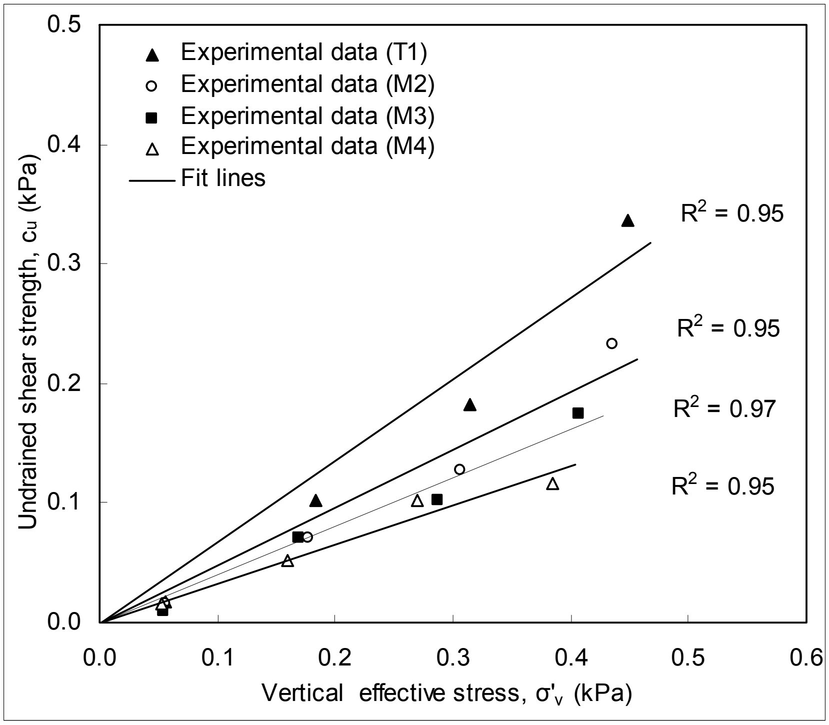

0.5
0.4
0.3
0.2
0.1
0.0
Undrained shear strength, cu (kPa)
Experimental data (T1)
Experimental data (M2)
Experimental data (M3)
Experimental data (M4)
Fit lines
$R^2$ = 0.95
$R^2$ = 0.95
$R^2$ = 0.97
$R^2$ = 0.95
0.0
0.1
0.2
0.3
0.4
0.5
0.6
Vertical effective stress, σ'v (kPa)


b)

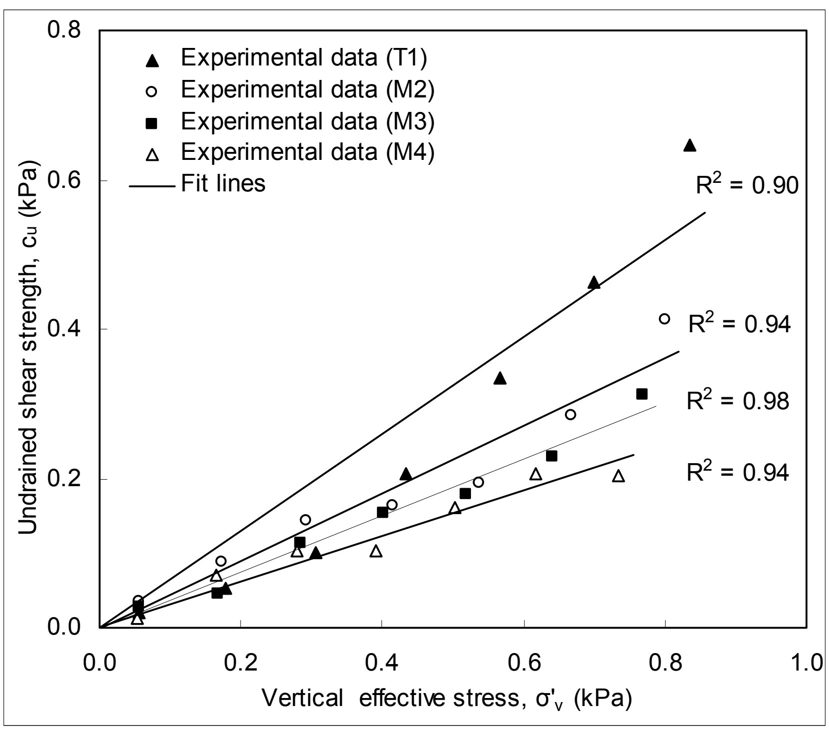

0.8
0.6
0.4
0.2
0.0
Undrained shear strength, cu (kPa)
Experimental data (T1)
Experimental data (M2)
Experimental data (M3)
Experimental data (M4)
Fit lines
$R^2$ = 0.90
$R^2$ = 0.94
$R^2$ = 0.98
$R^2$ = 0.94
0.0
0.2
0.4
0.6
0.8
1.0
Vertical effective stress, σ'v (kPa)

c)

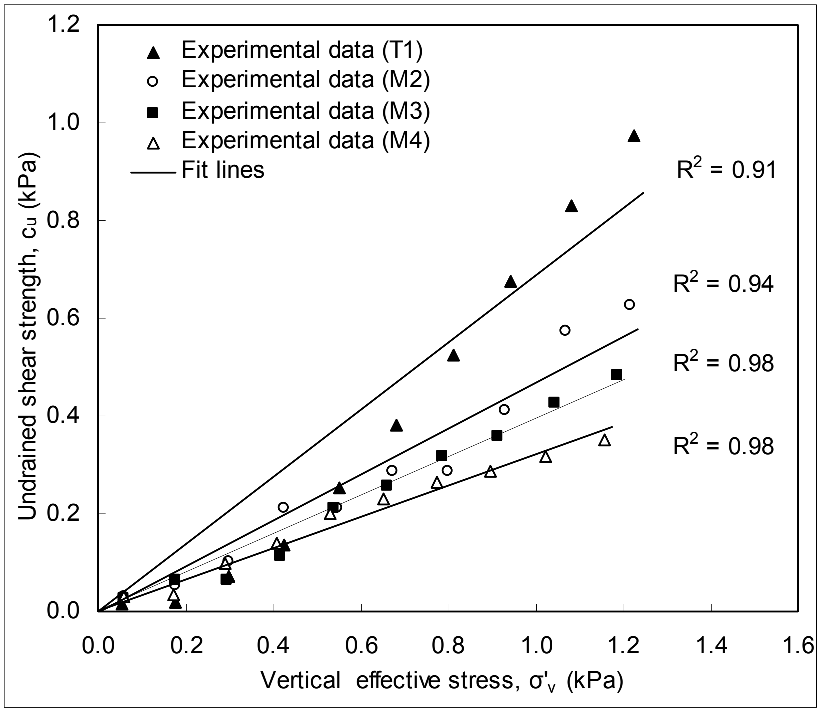


d)

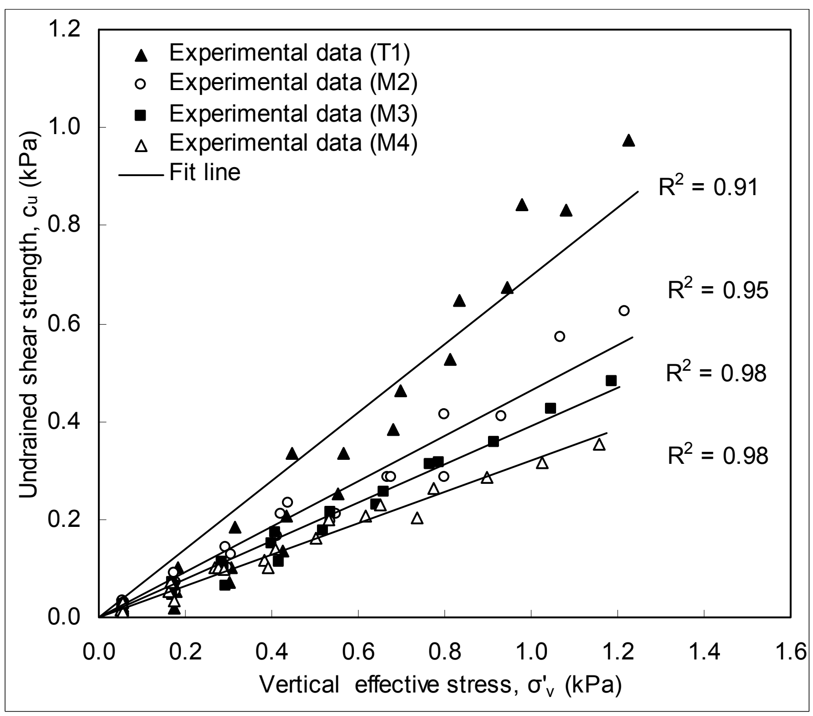


**Figure D.7.** Undrained shear strength versus vertical effective stress for beds with final thickness of: (a) 4 cm; (b) 7 cm; (c) 10 cm; and (d) 4, 7 and 10 cm prepared from various mixtures and consolidated for 12 days.

a)

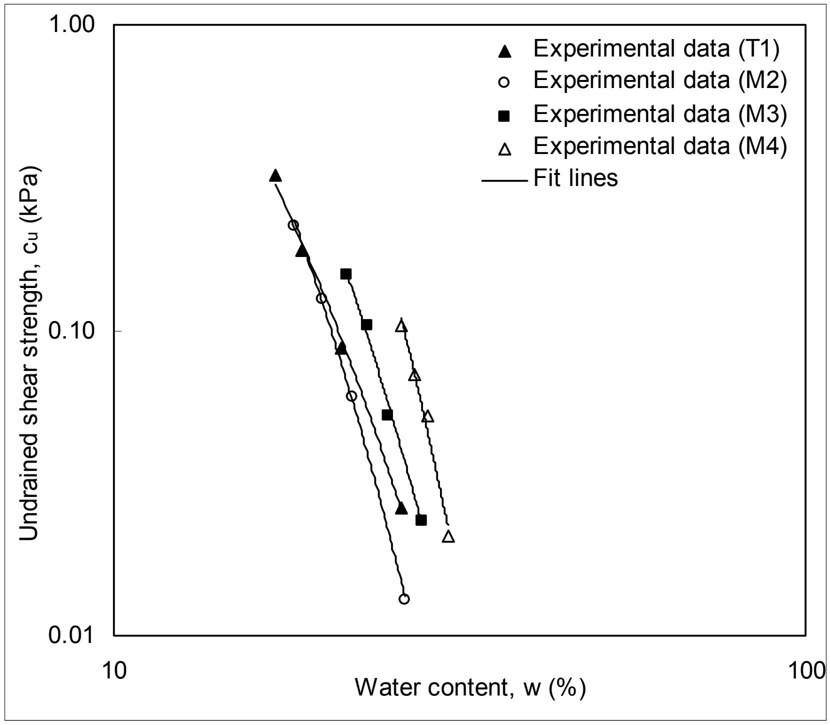


b)

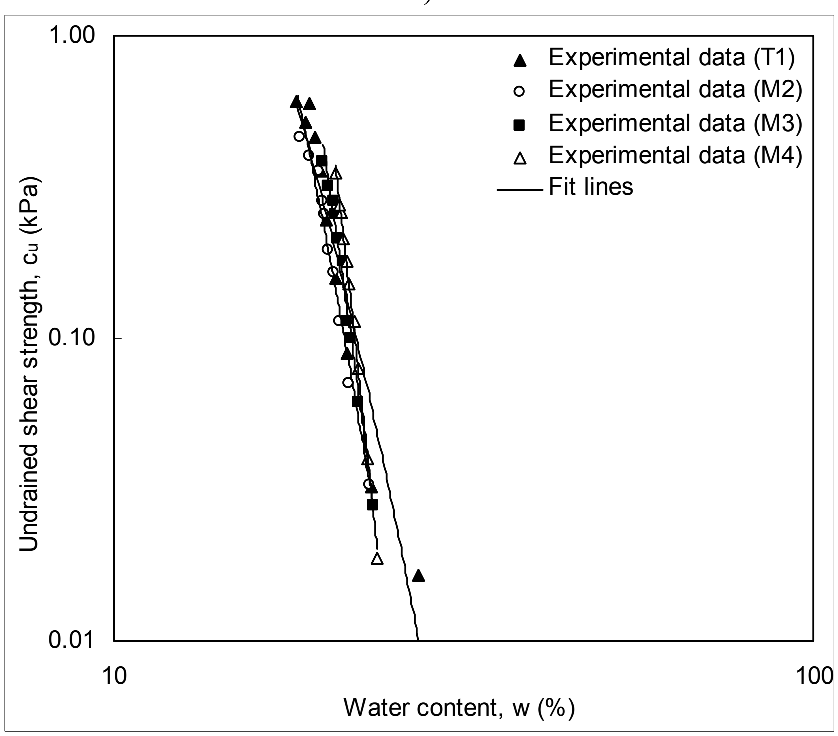


**Figure D.8.** Undrained shear strength versus water content for beds with final thickness of: (a) 4 cm; and (b) 10 cm prepared from various mixtures and consolidated for 3 days.

a)

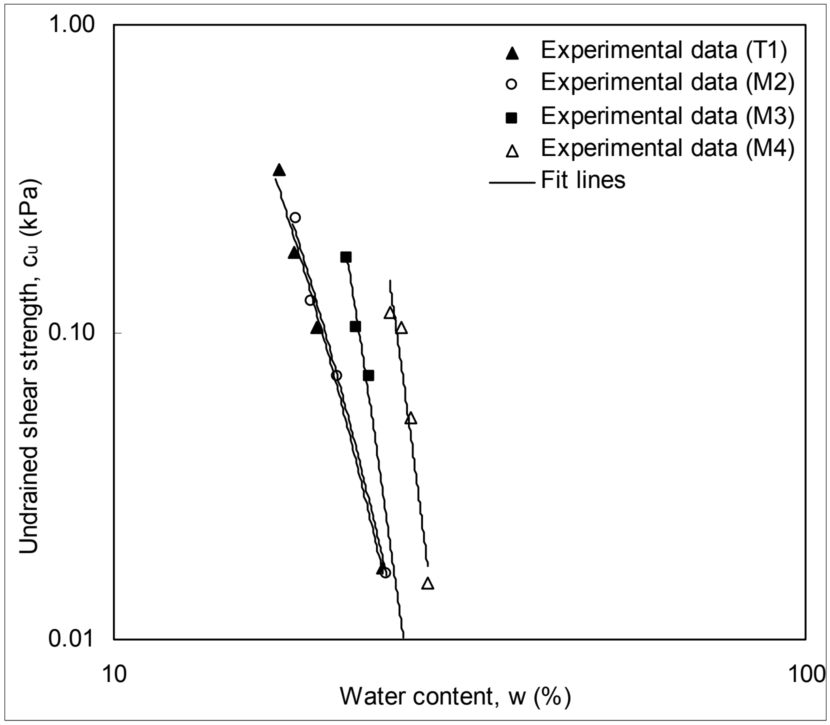

1.00
0.10
0.01
10
100
Undrained shear strength, cu (kPa)
Water content, w (%)
Experimental data (T1)
Experimental data (M2)
Experimental data (M3)
Experimental data (M4)
Fit lines


b)

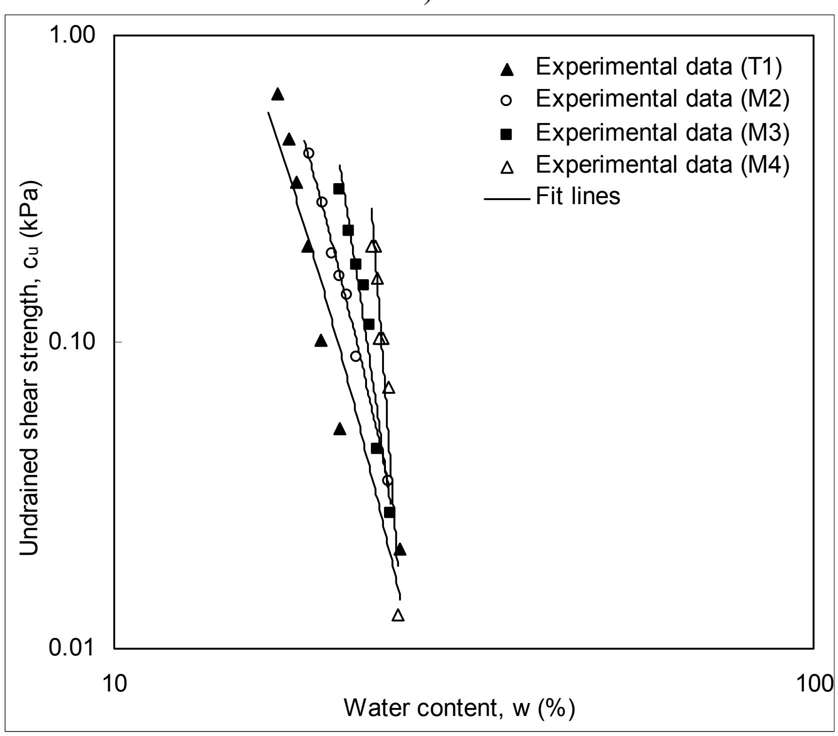

1.00
0.10
0.01
10
100
Undrained shear strength, cu (kPa)
Water content, w (%)
Experimental data (T1)
Experimental data (M2)
Experimental data (M3)
Experimental data (M4)
Fit lines

c)

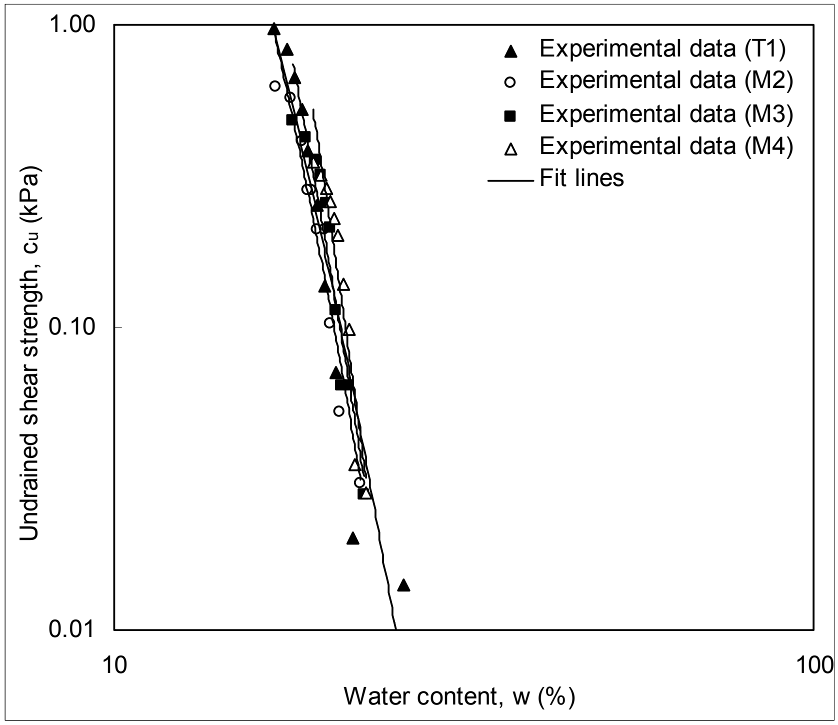


**Figure D.9.** Undrained shear strength versus water content for beds with final thickness of: (a) 4 cm; (b) 7 cm; and (c) 10 cm prepared from various mixtures and consolidated for 12 days.

# CURRICULIM VITAE

## EDUCATION

| | |
|---|---|
| May 2007 – Present | University of Western Ontario, London, Ontario<br>**Ph.D. Candidate (Civil and Environmental Engineering)**<br>Thesis: Geotechnique, physico-chemical behaviour and a new erosion model for mine tailings under environmental loading. |
| 2005 – 2007 | Lakehead University, Thunder Bay, Ontario<br>**M.Sc.Eng. Environmental Engineering**<br>Thesis: Evaluation of GaN and InGaN semiconductors as potentiometric anion selective electrodes. |
| 1991 – 1993 | University of architecture and civil engineering, Sofia, Bulgaria<br>**M.Sc.Eng. Hydrotechnical Engineering**<br>Thesis: Project for an underground pressure pipeline. |
| 1988 – 1991 | University of architecture and civil engineering, Sofia, Bulgaria<br>**B.Sc.Eng. Civil Engineering**<br>Thesis: Project for a municipal road. |

## PROFESSIONAL EXPERIENCE

| | |
|---|---|
| September 2007 - Present | University of Western Ontario, London, Ontario<br>**Course Instructor/Graduate Teaching Assistant** |
| 2005 – 2007 | Lakehead University, Thunder Bay, Ontario<br>**Graduate Teaching Assistant** |
| 1999 – 2004 | IDP Education Australia Limited, Sofia, Bulgaria<br>**Business Analyst** |
| 1995 - 1999 | The UK Know How Fund, Sofia, Bulgaria<br>**Assistant to the Social Security Adviser** |
| 1993 – 1995 | Kremikovtzi Steel Mill Corporation, Sofia, Bulgaria<br>**Engineer/ Process Designer** |

**SCHOLARSHIPS & AWARDS**

- Ontario Graduate Scholarship, May 2010-Present
- Bickell Graduate Scholarship in Mining, May 2009.
- NSERC Postgraduate Scholarship PGS D3, University of Western Ontario, 2007-2010.
- Western Graduate Research Scholarship, University of Western Ontario, May 2007-Present.
- Western Engineering Graduate Entrance Scholarship, University of Western Ontario, 2007.
- Faculty Research Scholarship, Lakehead University, 2005-2006.
- Best Poster Presentation Award, Canadian Section of the Electrochemical Society, Fall Symposium, Thunder Bay, Ontario, September 2006.
- Bombardier Incorporated Transportation Equipment Group Graduate Scholarship, Lakehead University, 2005.
- Ontario Graduate Summer Fellowship, Lakehead University, 2006.
- Lakehead University Graduate Scholarship, Lakehead University, 2005.
- Special Entrance Award, Lakehead University, 2005.

**PUBLICATIONS & CONFERENCE PRESENTATIONS**

- R. Dimitrova, L. Catalan, D. Alexandrov, A. Chen (2007) Evaluation of GaN and $In_{0.2}Ga_{0.8}N$ semiconductors as potentiometric anion selective electrodes. *Electroanalysis*. Vol.19 (17), pp.1799-1806.
- R. Dimitrova, L. Catalan, D. Alexandrov, A. Chen (2008) Impedance study of GaN and $In_{0.2}Ga_{0.8}N$ semiconductor anion selective electrodes. *Electroanalysis*. Vol.20 (7), pp.789-796.
- R. Dimitrova, L. Catalan, D. Alexandrov, A. Chen, *Evaluation of GaN and $In_{0.2}Ga_{0.8}N$ semiconductors as potentiometric anion selective electrodes*, 29 Sept 2006, Fall Symposium of the Canadian Section of the Electrochemical Society, Thunder Bay, Ontario, First Place award winning Poster Presentation (also presented orally).
- R. Dimitrova, E.K. Yanful, *Factors affecting the drained strength of deposited mine tailings beds in the very low stress range,* Geo2010 63rd Canadian Geotechnical Conference & 6th Canadian Permafrost Conference, September 12-16, 2010.
- R. Dimitrova, E.K. Yanful (2011) Undrained strength of deposited mine tailings beds: effect of water content,

effective stress and time of consolidation, *Geotechnical and Geological Engineering*. Vol.29(5), pp.935-951.